Moisture Movement and Mould Management in Straw Bale Walls for a Cold Climate

by

Nicholas Rangco Bronsema

A thesis
presented to the University of Waterloo
in fulfilment of the
thesis requirement for the degree of
Master of Applied Science
in
Civil Engineering

Waterloo, Ontario, Canada, 2010

Author's Declaration

I hereby declare that I am the sole author of this thesis. This is a true copy of the thesis, including any required final revisions, as accepted by my examiners.

I understand that my thesis may be made electronically available to the public.

Abstract

There is a growing interest in straw bale construction for its low embodied energy and insulation value. Early studies of its structural behaviour and fire resistance have shown it to be a viable alternative to traditional building techniques. However, the biggest remaining obstacle to widespread acceptance is the moisture behaviour within the straw bale walls, especially as it concerns mould growth. The uncertainty of this behaviour leads to the hesitation of building officials and insurance providers to freely accept straw bale construction. Therefore, this study investigates the moisture, temperature and mould growth in straw bale walls, through a combination of analysis, dynamic modeling and field studies. A study of mould is presented along with the current methods available for predicting mould growth.

Moisture is the primary controllable factor to mould growth in buildings. Therefore, an understanding of moisture accumulation within straw bale walls is necessary to provide a safe design that precludes mould growth. This study compiles the current state of knowledge of the hygrothermal properties of the materials used in straw bale walls. Then a parametric steady-state analysis is conducted to show the expected behaviour of vapour diffusion and the effects of the material properties.

Two 14”thick x 6’ wide x 8’ high straw bale test walls were constructed: one was rendered with a typical cement-lime plaster and the other with a clay plaster. Temperature and moisture were monitored throughout the walls for over a year. These test walls provide more information on the macro behaviour of the walls to both vapour diffusion and, more importantly, rain.

Hygrothermal computer modeling was conducted and compared to the test data to assess its accuracy. Thermal modeling was successful, while moisture modeling was found to be more difficult due to a lack of accurate rain data. With better climate data it is expected that accurate hygrothermal modeling of straw bale walls is possible.

The result of this work is a general starting point for more detailed studies of the hygrothermal behaviour of straw bale walls with the ultimate goal of assessing the mould risk for various construction techniques and locations.

Acknowledgements

Many hands make for light work, especially when they are the generous hands of my fellow students, Aaron, Rachel, Brian, Jeung, Ivan and Peter. I greatly appreciated their presence and help in this endeavor. I would like to thank Keith Dietrich for his time and expertise in plastering the straw bale walls; and Ben Polley of Harvest Homes who so graciously donated the materials for the plasters. I would like to thank John Straube for his expertise in building science and the many humorous anecdotes, both of which helped me throughout my studies.

Dedication

This thesis is dedicated to my wife, Melodie, and the rest of my family. They have endured my being a student for so long and have encouraged me all the way. I've appreciated all the support and love they gave me through the whole process. God bless you all.

Table of Contents

List of Figures

List of Tables

1 Introduction

1.1 Background

Increasing concerns about occupant health and damage to the environment have led to changes in the residential construction field. Considerations of the impact of building materials themselves on health and the environment has led to a growing interest in materials that require minimal processing and are thus more "natural", that is closer to the raw materials and with little embodied energy. Straw bales are one such material, used for walls in residential construction, and touted as an environmentally-friendly alternative to standard construction materials. However, the material and its construction method do not have the history or scientific research of more standard techniques and therefore many questions about its safety and durability have surfaced. This has led to difficulties in receiving building permits and insurance for straw bale homes, which in turn slows the growth of the technique.

As the history of the technique increases a better understanding and wider acceptance has developed. This comes in part from case studies on existing homes that alert builders to problematic and failed techniques and highlight durable construction methods; however, this is a slow process. To increase the rate of acceptance it is better to conduct specific research on various aspects, such as structure, fire, and moisture. There have been numerous studies on the structural performance of plastered straw bale walls (King, 2006). In addition, fire testing has been conducted to show the more than adequate performance of straw bale walls when plastered (Theis, 2006). However, a concern for moisture related problems remains.

There have been case studies on moisture related mold and damage in straw bale walls, but many of these only find moisture problems common to all building techniques, such as window leaks and high interior humidities. Other studies have reported some effects due to driving rain, but details are limited. (Jolly, 2000; CMHC, 2000; Straube and Schumacher, 2003; Wihan, 2007) Therefore, a complete understanding of moisture within a straw bale wall is lacking. This leaves straw bale home owners with unanswered questions about the long-term state of their walls. Testing of straw bale walls in response to specific moisture loads could improve our understanding and develop best practices for moisture control in straw bale walls. This will ensure that by employing proper construction rotting will not occur and thus increase the durability of the houses. It will also assure builders, owners and building inspectors of the performance of the straw bale walls in relation to moisture.

1.2 Objectives

Developing a complete understanding of moisture and straw bale walls will require numerous studies as moisture has various sources and transport mechanisms. Specific testing to date has focused on plaster moisture properties and straw thermal conductivity. These have provided enough data to formulate a simple understanding of the hygrothermal performance of the wall assembly, but various assumptions are still required and no data exists to confirm this behaviour in detail. Therefore, the objectives of this study are to first compile the relevant research on material properties and existing case studies as a bibliography for future work. Secondly, to monitor the hygrothermal behaviour of full-scale wall assemblies to achieve a better understanding of the behaviour of the wall system as a whole and provide insights into areas that are most critical for future work. Lastly, to provide a general comparison between the use of cement-lime plaster and earthen plaster and their effects on the hygorthermal behaviour of plastered strawbale walls.

1.3 Approach

The study will begin with the compilation of existing research on the relevant material properties for hygrothermal analysis of straw bale walls. From this literature review a summary of the current state of material properties will be developed for future reference. This data will also aid in developing computer models of the full-scale test walls.

The one-dimensional steady state conditions in straw bale walls with various plaster permeances will be calculated. This analysis will provide a rough comparison between expected behaviour of walls using different plasters.

Two common strawbale wall assemblies being constructed in Ontario will be tested, with the primary difference between them being the type of plaster used. One wall will be finished with cement-lime plaster the other with earthen plaster. These walls will be exposed to ambient weather conditions at the University of Waterloo. Full instrumentation for moisture and temperature will be installed through the height and width of the wall. Review of the data will provide a real-world comparison between cement-lime plastered walls and earthen plastered walls. In addition, the data will be used to assess the validity of a computer model and better the understanding of the hygrothermal behaviour of the wall assembly as a whole.

A dynamic computer model will then be developed and compared with the measured data to assess the accuracy of the hygrothermal behaviour of straw bale walls. This model

will also provide insight into areas where further material property testing would be required.

2 Straw Bale Construction Background

2.1 Straw Bales

In cereal agriculture the goal is to produce grain from a crop, such as corn, wheat, and rice. These are staples to human diets around the world and make up the largest agricultural crop type at 2.3 billion metric tons per year in 2004 ("Agriculture", n.d.). Harvesting of grains begins after the plant has died and is sufficiently dry. The process is to cut the stalk of the plant in order to remove it from the ground (reaping), separate the grain from the stalk (threshing) and then remove the chaff from the collected grain (winnowing). Left over stalk and leaves become straw and typically amount to 0.7 to 1.7 times the weight of grain collected (Helwig et al, 2002). Annual straw production in North America alone is about 140 million tons (Wilson, 1995).

Straw plays an important role in maintaining the health of the soil in which it was grown. Leaving stubble or tilling straw into the soil helps reduce erosion and rejuvenate organic matter in the soil. The amount of straw required for these functions is determined based upon the current health of the soil and is at the discretion of the individual farmer. In healthy soils there is potential to remove up to 80% of all straw residue while maintaining sustainable farming practices (Helwig et al, 2002) Thus, there is a substantial amount of straw that is considered waste to grain farmers unless it can be sold for other uses.

Traditionally, straw has been used for fuel, bedding (both human and animal), earth brick fiber reinforcing, thatched roofs, and as part of an animal diet. The nutrient value of straw is very low so its use as food is limited. Where it is used as animal feed, it is used primarily to supplement the regular diet of animals in cold climates in order to provide them with extra energy. It should be made clear that straw is not hay. Hay is a dried grass or legume that contains much more nutritive value than straw and is used as animal feed. There is often confusion between the two because they are both baled for storage and thus appear similar to the untrained eye. Straw continues to have numerous uses, including the traditional ones although techniques may have changed. Some modern uses for straw are as a biomass fuel in power plants (Nikolaisen, 1998), a speculative source for producing biofuels (Mordant, 2009), as fiber in the manufacturing of paper ("Canadian magazine makes history", 2008), in strawboard (Southam, 1997), and straw bale homes.

Straw is typically packed into bales of various shapes and sizes that reduce the bulk size by 4 to 8 times (Larmour, 1992). This produces a range of bale densities that are

typically between 90 to 140 kg/m^3, but sometimes as low as 40kg/m^3 and as high as 200kg/m^3 (Nikolaisen, 1998). Originally, bales were small to allow for ease of manual handling, but with increased use of equipment, larger bales could be accommodated. Common rectangular bales are either two-string (36x46x91cm / 14x18x36") or three-string (40x61x122cm / 16x24x48"), so called for the number of strings of twine that hold the bale together, see Figure 1; these are the bales most often used in straw bale home construction. Round bales vary from 1.2-1.8m (4-6ft) in diameter. There are also jumbo sizes of rectangular and round bales for use as biomass fuel.

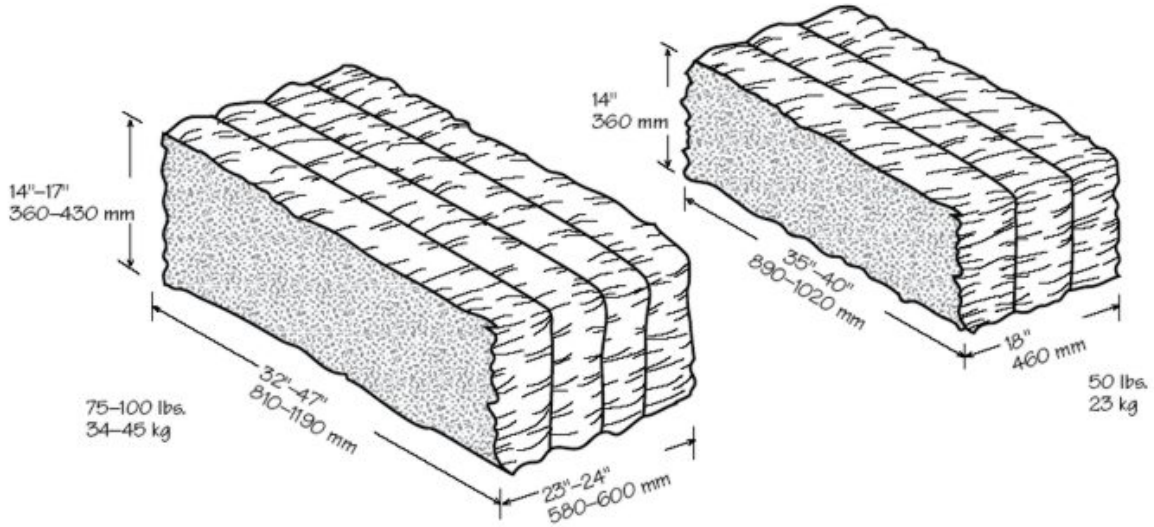

Figure 1. Common rectangular bale sizes (Wilson, 1995).

2.2 History of Straw Bale Houses

The original intent for baling straw and hay was to facilitate easier transport and storage for use and sale, but their use in buildings started almost immediately with their development. European settlers arriving in the Sand Hills in northwestern Nebraska. during the late 1800's had limited building resources (Hammet, 1998). Sod, which was a typical building material at the time, was of poor quality due to the sandy soil or was otherwise valued for cropland. Timber was another common building material, but there was very little natural supply. Therefore, with the advent of horse-powered balers the settlers found a temporary construction material until they could gather or import more of the traditional materials. However, they soon found that straw construction was suitable and durable and there was no need to construct with more traditional materials. The oldest known building that still remains is the Burke house in the town of Alliance, Nebraska, which was built in 1903 and is shown below (King, 2006).

Figure 2. Burke house in Alliance, Nebraska (King, 2006).

Straw bale construction became less frequent as more traditional materials became more readily available. However, there has been a revival of straw bale construction in the past years. The desire for straw bale construction is largely driven by its perceived environmental benefits. The material has low embodied energy and good insulating value, thus reducing the carbon footprint of the building that it produces. The interest in straw bale buildings is continuing to grow as environmental concerns grow and research proves the ability of the technique. There are a number of current books about straw bale construction (Steen, Steen & Bainbridge, 1994; Lacinski & Bergeron, 2000; Magwood, Mack & Therrien, 2005; King, 2006). These show common methods of working with straw and common building details. These methods and details have been developed through research of existing buildings and experimentation. The basic techniques have been refined through practice and structural testing and will likely endure.

2.3 Benefits and Drawbacks

The primary benefit of straw bale construction over more common methods is the low embodied energy of the material. It is sourced from an agricultural waste product and thus is often not harvested directly for any other purpose. Second, there is little processing of the straw, the only mechanization is in baling, assuming the cutting of the stalk from the ground is part of the grain harvest. Third, straw is a rapidly renewable resource. It can be shown that only a few acres of land is sufficient to provide the straw for a modest home every year. Lastly, if the material is sourced locally there is minimal transportation to the building location. All of these result in reduced green house gas emissions in resource extraction, processing, and transportation to the site when compared with other materials, such as wood framing and fiberglass insulation. There is also little resource extraction (none with sustainable farming practises).

Straw bale construction also benefits human health. Unlike many modern building products there are no manufactured chemicals in straw bale walls. Various chemicals from building products have been related to human ailments and Sick Building Syndrome. Pesticide residue may be found in straw bales, but is usually minimal as pesticides are typically applied early to wheat and rice crops and have sufficient time to be washed away. This can be completely eliminated by the use of organic straw.

Another great benefit of straw construction is its insulating value. Strawbales are less insulating on a per unit thickness basis than modern insulations, but are installed at much greater thickness, thereby resulting in better performance. High insulation values is often one of strawbale walls' most touted benefits (Lacinski & Bergeron, 2000; Steen et al., 1994), however, it should be noted that similar insulation values can be obtained with wood framing, but such highly insulated wood walls will tend to cost more and the production of the insulating materials will have a greater environmental impact. For these reasons the insulating value in relation to the cost and environmental impact is good for straw bales. The benefit of higher insulating values is reduced heating and cooling loads on the building that will result in lower energy consumption for space conditioning and smaller heating and cooling equipment. As a result there will be fewer greenhouse gas and other pollutant emissions. Occupant comfort is also improved.

Straw bale construction is not common and so most have little understanding of its performance and the previous mentioned benefits. Often people believe it will not perform structurally, or it will be easy to burn, or it is more enticing to pests. This has caused difficulties in obtaining permits and insurance. However, all of these aspects have been tested and research shows the opposite is true in each of these cases. Structurally, straw bale buildings can fair quite well, often performing better in seismic zones than wood framed buildings (King, 2006). Plastered strawbale walls pass fire testing easily and have higher resistance ratings than typical construction (Theis, 2006). Straw itself is not the most suitable food for pests as it lacks nutritional value, in addition the density of the bales and continuity of the plaster prevent pests from easily entering the walls (Magwood, Mack, & Therrien, 2005). The true remaining issue is of the durability of the straw itself where moisture is concerned.

2.4 Structure

Basic construction consists of stacking straw bales like bricks to form the core of the wall and then applying plaster on both sides of the stacked bales. Although this appears straightforward, there are numerous variations which can be used. Bales are typically

stacked in running bond, but other layouts are used depending on the framing within the wall. The length of the bale is always oriented parallel with the wall but it may be stacked either on edge (narrow edge facing down) or flat (wide edge facing down). The stacked bales may or may not be pinned or tied together; this depends on the structure and the builder's preference, but more commonly pinning is not used. There are three primary plaster binders: cement, lime, and clay. A multitude of plaster mixtures can be developed from these binders by varying the proportions of binder, aggregate, fibers, and admixtures. Plastering techniques vary but often the plaster is placed in several layers with the final texture being applied as a skim coat.

Straw bales can be used as a load bearing component in a building or simply as infill. Older simpler designs used load-bearing construction in which the roof rafters are supported directly by the straw bale walls. This was done to eliminate the timber required to frame the walls. More recently straw bales have been used as a wall material that infills between a timber frame construction. There are numerous variations for straw bale infill. One of the simplest and most similar to load-bearing construction is to wrap a building in straw bales: the entire structure is surrounded by straw bale walls. This provides continuous straw bale walls with no framing in the walls, except for openings. Other construction is more similar to modern stick framing. Framing members are built up from standard lumber to span the width of the wall and straw is placed in between the framing members. This type of construction uses the insulation benefits of straw, but does not considerably reduce the use of lumber, if at all.

Load bearing construction would be the preferred approach, as it reduces the use of wood, and requires simpler, easier to build details; however, it is only practical in the driest climates. During construction loadbearing walls must be built before a roof can provide protection. Therefore, there exists a considerable period of time when the bales could be damaged by the weather. It is possible to cover the bales with temporary shelter, such as tarps, although concentrated wetting still often occurs at laps and tears in the tarp. However, tarping adds to the cost of the home due to the materials required and the time required to set up and take down the shelter. As well, this may increase the time for construction by the added task of setting up and taking down the shelter. Given these drawbacks infill construction is currently used in the majority of North American straw bale buildings.

There are numerous structural details in straw bale construction that do not require mentioning here. These can be found in other papers and books, with a good summary of the current state of the art in "Design of Straw Bale Buildings" by Bruce King (2006).

These details address load bearing capacity of the walls, shear load resistance, earthquake resistance and other related topics.

2.5 Moisture Control

In addition to designing for structural stability it is necessary to provide durability, which impacts the future performance of the building. Poor durability may cause safety concerns for the occupants and will increase the lifecycle costs of the building. In straw bale buildings the largest concern for durability is rotting of the straw. This occurs as a result of high moisture levels in the straw, which may be caused by various sources: interior and exterior humidity, driving rain, splash back, ground moisture and plumbing leaks. Each of these has its own considerations as explained below and details have been developed to control their effects. However, as their remains some uncertainty over moisture behaviour in straw bale walls these details may change as a better understanding is reached through experience and research. Most important will be the detailing at discontinuities in the straw, such as windows, and guidelines for plaster moisture properties.

2.5.1 Rain

Rain is the greatest short term source of moisture, besides major plumbing leaks, and in wet climates is the dominant source of moisture. Various strategies are employed to control rain wetting on building walls. These vary from completely eliminating rainfall from striking the wall to providing increased drying ability so that rain entering the wall may dry out. Experience has shown that attempting to build a perfectly waterproof outer plaster does not work and can, in fact, be disastrous.

The first strategy used is large roof overhangs to limit the amount of rain that strikes the walls, this is generally recommended for all straw bale construction; however, it may not be practical for certain designs such as at gable ends or two story walls. Therefore, other strategies are desired to control rain as overhangs can limit the usefulness of straw bale walls.

Another strategy that would provide a very good level of protection from rain is a rain-screen, which is the most common strategy in standard residential construction. This is essentially a rain shedding layer placed over the plastered straw bale wall with an air gap in between. This layer's sole function is to drastically reduce the quantity of rain striking the straw bale wall, while allowing ventilation of the straw bale plaster so as not to reduce the drying potential of the straw bale wall. The simplest example is wood siding

applied to furring strips on the plastered straw bale wall. This is an effective strategy for very wet climates, but would add considerable cost and material to the building, which may be able to resist rain wetting without the rain-screen.

A plastered straw bale wall itself has some resistance to rain wetting. The primary concern is water that penetrates the plaster and wets the straw. The fact that the plaster gets wet is not significant. There are two idealized rain control strategies to prevent the wetting of the straw (Straube & Burnett, 2005), both of which are not practical on their own in straw bale construction; however, straw bale walls can utilize a marriage of these two strategies.

First, the plaster on the straw bale walls acts in a similar way to a mass wall, historic masonry for example, in which there is enough moisture storage capacity that rain water will never penetrate. However, there are no expectations that the plaster would be able to store all the rain that it absorbs as this requires too thick of a layer for substantial rain events. Nonetheless this type of behaviour works during light rainfalls and short duration rainfalls.

Another type of rain control strategy is the 'perfect barrier.' This is the most idealized and least practical in all construction in that it assumes that all the rain will be shed from the wall and none will penetrate or absorb. This is theoretically possible for glazing, sheet metals and similar materials, but in all these constructions there exist joints that provide opportunity for rain to penetrate. Therefore, this method cannot practically be relied upon for site built construction. However, the principle can be applied to the plaster in straw bale construction. The difficulty is that plaster is porous and will readily absorb water, whereas nonporous materials are typically used in the 'perfect barrier' strategy. Therefore, it is necessary to reduce the absorption capability of the plaster by applying a surface finish that is either a sealant or water repellant finish. However, the finish needs to allow for outward drying of the wall assembly and therefore, sealants do not work as they tend to limit both liquid and vapor movement, whereas water repellant finishes may reduce liquid movement while not significantly impacting vapor diffusion. Thus, the most realistic approach is a water repellent finish. Even so, there will exist shrinkage cracks throughout the plaster as well as other cracks and joints, all of which provide entry points for water to bypass the plaster and wet the straw, so that a perfect water repellent finish would still not eliminate wetting of the straw.

It is the combination of the water shedding and plaster storage behaviour of the plaster that provides the primary rain control in straw bale construction.

Regardless of how the plaster keeps rain from wetting the straw, it is expected that there will be some wetting, through cracks and similar paths, and therefore, it is just as important to allow for this water to get out of the wall as it is to stop it from getting in. Thus, a vapor permeable plaster is desired to facilitate drying by vapor diffusion of the rain that does penetrate.

2.5.2 Humidity

Despite the importance of rain, interior and exterior humidity can also be important. In cold climates it is the interior humidity during the winter that provides the greatest source of moisture due to vapor diffusion and air leakage. Diffusion is the movement of water vapor in the air from a point of high vapor pressure on the interior to a point of low vapor pressure on the exterior (conditions are reversed in the summer). With a large difference in vapor pressure there can be considerable amounts of vapor movement, depending on the wall assembly permeance. This may not be of great concern except when it leads to high humidities within the wall and more importantly when the vapor condenses to form liquid water as it reaches its dewpoint temperature towards the cold side of the wall.

Vapor movement is controlled by the vapor permeance of the wall materials. In straw bale construction the plaster skins provide the greatest opportunity for vapor control. The increasing tendency is towards more permeable plasters that will allow for increased vapor movement. This may seem counterintuitive considering that the vapor drive due to interior moisture is controlled by a vapor barrier in standard construction; however, of greater concern is the increased ability for drying of other sources of moisture that enter the wall.

More research is needed to assess the potential damage from outward moisture drive during the winter and how much vapor diffusion control is required. There may be a need for some vapor retarding plaster or finish to be applied on the interior, or the moisture storage ability of the straw may great enough to adsorb the excess vapor during the winter and then let it dry during the summer.

2.5.3 Air Leakage

Air leakage can introduce a much higher rate of moisture movement than by diffusion alone. During the winter warm interior moisture laden air may pass through cracks and holes in the plaster and then through the air permeable straw toward the exterior, where it will eventually reach its dewpoint and deposit condensation. This can be a significant source of moisture. Therefore, it is important provide air tight construction. Interior

plaster provides an air barrier, but at the extents of the wall it must be sealed to the framing to ensure there is no air leakage into the wall assembly. A butt joint of the plaster to the framing does not provide a seal as shrinkage of the plaster will cause it to pull away from the framing; however, the resulting space may be caulked. For better continuity a lap joint is used, in which the plaster would be applied over the framing to an extent. A variation of this is to attach a piece of gypsum board behind the framing, over which the plaster is applied. This method essentially continues the plaster behind the framing by means of the gypsum board. Other details can be developed depending on the type of strucuture used and the desired appearance.

2.5.4 Splash-back

Splash-back occurs during rain events as rain strikes and splashes off of the ground and then hits the wall. This is compounded when rain runs directly off of the roof above the wall and falls to the ground directly in front of the wall. Roof run-off is controlled by large overhangs that keep splash-back far enough away from the wall. Eavestroughs can also be used but require maintenance to avoid overflowing and concentrating water. General splash-back is controlled by placing the base of the straw bale wall six to eight inches above grade to prevent rain splash-back and other ground level water from contacting the wall, such as snow. Further, ground cover, such as 1.5” or larger river rock, that limits splash back can also be used.

2.5.5 Ground Moisture

Moisture from the ground will be absorbed into hygroscopic materials such as concrete and plaster through capillary action. This means it is necessary to provide a moisture break somewhere between the ground and the wall. Most often this occurs at the wall and foundation interface. It is a good choice to place the break here rather than between the foundation and the ground as built in moisture in the foundation as well as any imperfections in the moisture break will allow moisture into the wall from the foundation. Locating the moisture break at the foundation-wall intersection is quick and easy to install and is relatively durable. It usually consists of a sheet of polyethylene being placed over the foundation before the wall is erected. In addition a drainage layer is also provided in case of any moisture ingress into the wall as well as any failure of the polyethylene. This provides a small height at the bottom in which liquid water may collect and dry, and it provides a secondary capillary break from the foundation. This usually consists of a layer of coarse gravel.

2.5.6 Discontinuities

Straw bale walls are rarely continuous for their entire length. Residential construction creates a number of openings for windows and doors. Also, the structural framing in straw bale construction causes discontinuities in the straw and/or plaster. These instances require special consideration for moisture control.

Framing of openings usually depends on structural considerations. Sometimes the framing passes through the entire width of the wall but more often with straw bale-infill it is only several inches wide at the location of the window or door. This leaves the corner of the bale exposed at the opening which is usually rounded and then covered with plaster. It is desirable to keep the windows and doors towards the exterior of the wall to increase the temperatures through the wall in the winter so that condensation potential is reduced.

Experience has shown that windows should be expected to leak and thus their rough openings should be framed and flashed so that water will be directed toward the exterior of the wall with a drip edge to keep it from running onto the plaster.

Framing members that are completely within the straw are left bare. However, when plaster contacts the framing members sheet products are used as both capillary breaks and bond breaks. These are typically used in standard construction as a drainage plane to stop liquid water from absorbing into the framing and plywood sheeting. The same idea is used in straw bale construction, such that when plaster is placed against framing members a sheet product is used to act as a drainage plane. However, many builders exempt clay based plasters from this requirement. The understanding is that clay plasters are hydrophilic and readily absorb moisture such that if the underlying wood does get wet it will also dry by absorption into the plaster. Also, clay plasters are more flexible and hence will not crack as readily if in contact with wood elements that expand and contract differentially.

3 Heat and Moisture Physics

In order to determine the moisture levels in straw bale walls and deterioration mechanisms it is necessary to understand the transport mechanisms of both heat and moisture. Moisture transport requires knowledge of heat transfer as some moisture parameters depend upon temperature. Therefore, the three modes of heat transfer (conduction, convection and radiation) are discussed. Then the movement and storage of both water vapor and liquid are presented. Finally, the methods of analysis relevant to this study are outlined to show how the physics of heat and moisture are used.

3.1 Heat Transfer

Heat flows in three modes: conduction, convection, and radiation. Conduction is the transfer of heat by direct molecular contact. This plays the biggest role in heat transfer through solids. Convection is the transfer of heat by the bulk movement of molecules with a change in their heat content. This is an important mode of transfer between solids and gases or liquids. Radiation is the transfer of heat by electromagnetic waves. The waves are emitted from any material above absolute zero with increasing emission at increasing temperatures. Objects of differing temperatures will have a net electromagnetic transfer from the hot to the cold object.

Heat is also absorbed and released when materials change state. This is termed latent heat. This is due to the fact that to change state a material requires a certain amount of energy input or energy withdrawal. This change in energy content occurs at a constant temperature while both states coexist. Once the state has changed then the temperature will also change according to the surrounding conditions. Although, latent heat is not a method of heat transfer, it does require special attention.

3.1.1 Conduction

The equation governing conduction heat transfer is Fourier's Law:

$$\vec{q} = -k \cdot \nabla T \qquad 3.1$$

Where $\vec{q}$ = heat flux (W/m^2),
k = conductivity (W/mK), and
∇T = temperature gradient (K/m).

The conductivity is a measure of how well a material will transfer heat by conduction. Aluminum has a high conductivity whereas fiberglass insulation has a low conductivity.

It may be assumed constant for the range of temperatures experienced in typical building science applications. However, the thermal conductivity does vary with temperature and in extreme conditions this needs to be considered.

In one dimension Fourier's Law becomes

$$q_x = -k_x \frac{dT}{dx} \qquad 3.2$$

For many building applications the one dimensional heat transfer through a material of a given thickness (l) with constant conductivity (k) is desired and so Fourier's Law can be simplified to

$$q = -\frac{k}{l}\Delta T \qquad 3.3$$

The value k/l has been termed the conductance, C (W/m^{2}K). Also, the inverse of the conductance is the thermal resistance, R (m^{2}K/W), often called the 'R-value'. Therefore, the equation can be simplified again to the following forms

$$q = -C\Delta T = -\frac{1}{R}\Delta T \qquad 3.4$$

3.1.2 Convection

Convective heat transfer is the transfer of energy by bulk movement of a fluid, in addition to conductive heat transfer mechanisms. Therefore, it is more complex than conductive heat transfer alone. Usually, this method of heat transfer is discussed for the movement of energy between a solid and a fluid, although heat transfer within a fluid would also fall under this category. Because of the complexity of fluid mechanics various simplified heat transfer coefficients have been developed for many common situations. Thus, it is different from conductive heat transfer in that empirical coefficients are used rather than fundamental thermal properties.

The basic equation stem's from Newton's Law of Cooling (O'Sullivan, 1990). When a hot object was allowed to cool to air temperature, Newton found that it approached the temperature of the air at an exponentially decaying rate. He found that the instantaneous heat flux was proportional to the temperature difference and he developed the following equation:

$$q = h_c\left(T_s - T_\infty\right) \qquad 3.5$$

Where q = heat flux (W/m^2),
h_c = convective heat transfer coefficient (W/m^{2}K),
T_s = temperature of the object (K or ^{o}C), and
T_∞ = temperature of the surroundings (K or ^{o}C).

Coefficients have been developed for both laminar and turbulent natural convection and forced convection. Natural convection is the flow of material due to the density differences that develop from variations in temperature. Forced convection is when air flow is induced by an outside force, a fan for example. Air flow is also categorized into laminar or turbulent depending on the flow regime. Typically forced convection is turbulent, while the temperature gradient in natural convection determines the flow regime. Air flow increases for high temperature differences and turbulent convection develops, whereas low temperature differences lead to laminar convection.

Some of the convective heat transfer coefficients that are pertinent to building science are described below (Straube & Burnett, 2005).

Natural laminar convection from vertical surfaces:

$$h_c = 1.87 \cdot \Delta T^{0.32} \cdot H^{-0.05}, \text{OR} \qquad 3.6$$

$$h_c = 1.42 \cdot \left(\frac{\Delta T}{L}\right)^{0.25} \qquad 3.7$$

Where T is temperature (K), H is the wall height (m), and L is four times the area divided by the perimeter (m).

Natural laminar convection from horizontal surfaces:

A: against buoyancy (eg. Heat flow up from cold surface, heat flow down from hot surface)

$$h_c = 0.59 \cdot \left(\frac{\Delta T}{L}\right)^{0.25} \qquad 3.8$$

B: with buoyancy (eg heat flow up to cold surface, heat flow down to hot surface)

$$h_c = 1.32 \cdot \left(\frac{\Delta T}{L} \right)^{0.25} \qquad 3.9$$

Natural turbulent convection from horizontal surfaces (eg heat flow up from hot roof):

$$h_c = 1.52 \cdot \Delta T^{0.33} \qquad 3.10$$

Natural turbulent convection from vertical surfaces (eg heat flow away from hot wall):

$$h_c = 1.31 \cdot \Delta T^{0.33} \qquad 3.11$$

Forced convection depends primarily on the velocity of the moving fluid. For air flow over plates the heat transfer coefficients can be calculated by the following:

$$h_c = 5.6 + 3.9 \cdot V \quad \text{for V} = 1 \text{ to } 5 \text{ m/s} \qquad 3.12$$

$$h_c = 7.2 \cdot V^{0.78} \quad \text{for V} = 5 \text{ to } 30 \text{ m/s} \qquad 3.13$$

These coefficients are not overly precise. Variations in surface texture, nearby protrusions, and microclimate factors will all affect the convective coefficient. This is not of great concern in most building science applications, as the forced convection provides little overall resistance to heat transfer. It may be a factor in low insulation cases, such as windows and uninsulated walls. Therefore, these coefficients will give good estimates of the heat transfer for the different conditions for most building science applications. There are other equations that have been developed for more specific conditions and these may be consulted on an individual basis as needed.

In this thesis convection plays a role at the wall surfaces. Radiative heat transfer also occurs at this location and therefore a combined coefficient is used, termed the surface film coefficient. This surface film coefficient takes into account all modes of heat transfer between the surface of the wall and the air it is contact with. For interior walls the equivalent conductance is assumed to be 8.3 W/m^2K. Exterior film coefficients will vary with wind speed and temperature and so for winter the value may be taken as 34 W/m^2K for a wind speed of 6.7m/s and 23 W/m^2K in the summer with a wind speed of 3.4m/s. For average conditions a value of 20 W/m^2K may be assumed. (Straube & Burnett, 2005)

In addition to convective heat transfer between a fluid and a solid, there exists the potential for bulk convective heat transfer within a fluid. In building science this often

occurs as heat flow that accompanies air flow through the building enclosure. If there exists an air leak in the wall and a certain mass flow rate of air passes through the leak the heat that accompanies that air is described by the following equation:

$$q = c_o \Delta T \frac{dm}{dt} = c_o \Delta T \rho \frac{dV}{dt} \qquad 3.14$$

Where q = mass heat flow (W),
c_o = specific heat capacity of air (1000 J/kgK at 20°C),
ΔT = temperature difference between the interior and exterior (K or °C),
dm/dt = mass flow rate of air (kg/s), and
dV/dt = volumetric flow rate of air (m^3/s).

In any wall there is potential for convective heat flow to circulate through air gaps in the construction (Brown et al, 1993) and within air permeable insulations (Dyrbol, Svendsen, & Elmroth, 2002). There are some references to this occurrence in straw bale construction although it is not well documented (Stone, 2003; Rissanen & Viljanen, 1998). Study of this topic is beyond the scope of this thesis but may be of interest in the future as these convective circuits result in an undesirable reduction in the overall R-value of the wall.

3.1.3 Radiation

Radiation heat transfer is a complicated process. The net radiation exchange between two surfaces is the net heat transfer, which is of interest. This depends on the temperatures of the two surfaces as well as their emissivity and geometry. The temperature determines the total possible amount of radiation that may be emitted by the surface and the emissivity tells what fraction of that total amount is actually emitted. The geometry is used to determine how much of what is emitted strikes the surface of interest, in the case of two exchanging surfaces, how much strikes the other surface.

The maximum amount of radiation that can be emitted at a given temperature is termed "black body radiation" as by definition a theorectical body that emits all wavelengths perfectly is called "black". This amount is described by the Stefan-Boltzmann equation

$$q = \sigma \cdot T^4 \qquad 3.15$$

Where q = rate of emission (W/m^2),
T = absolute temperature of surface (K), and
σ = Stefan-Boltzmann constant = 5.67×10^{-8} W/m^2K^4.

There are very few objects that behave as true black bodies. Most surfaces do not emit all wavelengths perfectly but have preferences for particular wavelengths. The ratio of the actual amount of radiation emitted at a particular wavelength (λ) to that of a black body is the emissivity at that particular wavelength for that material, ε_λ. The emissivity does vary with wavelength; however, it is possible to take an average emissivity for a range of wavelengths. This is useful in building science as radiation heat transfer can be broken into two categories: solar radiation and terrestrial radiation.

Solar radiation (short-wave radiation) is that which occurs between the wavelengths of 0.1 to 5 μm and terrestrial radiation (long-wave radiation) occurs between the wavelengths of 5-100μm. The division of short and long-wave radiation is due to the temperatures of the materials that emit thermal radiation at those wavelengths. The surface of the sun is roughly 5800K and thus emits radiation at a shorter wavelength than common terrestrial objects that vary in temperature from about 223-353K. Often the short-wave emissivity for materials is not quoted as they do not reach the temperature of the sun, but rather they absorb solar radiation and thus the absorptivity is quoted. But for long-wave radiation the emissivity is given, even though it will also absorb long-wave radiation at this level. However, the absorptivity is equal to the emissivity for any specific wavelength as stated in Kirchoff's Law (ASHRAE, 2005). This equality is for a particular wavelength but may be extended to an average value for a range of wavelengths. Therefore, most instances of a material's absorptivity refer to short-wave absorptivity and references to emissivity are to long-wave emissivity.

Net radiation exchange between objects is complicated by the geometry. This is due to the fact that radiation is emitted in all directions from a surface but not in equal amounts. Therefore, the amount of radiation that strikes the surface of interest depends strongly on geometry. This is accounted for by the view factor (F_A). It is also complicated by the emissivities of the materials, as some radiation will be reflected back to the original surface. This dependence is put into the emissivity factor (F_E). This is important in most applications of radiation heat exchange, however there are a few common cases in building science for which this can be simplified. The first case is a small object emitting to a large space, in this case the view factor is 1 for the small object to the large space. The equation is then

$$q_{1\to 2} = F_A \cdot F_E \cdot \sigma \cdot \left(T_1^4 - T_2^4\right) = (1) \cdot (\varepsilon_1) \cdot \sigma \cdot \left(T_1^4 - T_2^4\right) \qquad 3.16$$

Where q = net radiation from small object (1) to large space (2) (W/m^2),
T_1 = absolute temperature of small object (K),
T_2 = absolute temperature of large space (K),

ε_1 = emissivity of small object, and

σ = Stefan-Boltzmann constant = 5.67 x 10^{-8} W/m^2K^4.

Another common situation is heat exchange between two parallel surfaces in close proximity. This is applicable to small air voids within walls and windows. Again the view factor is 1, but the emissivity factor is

$$F_E = \frac{1}{\frac{1}{\varepsilon_1} + \frac{1}{\varepsilon_2} - 1} \qquad 3.17$$

3.2 Moisture Physics

Water transport is an important topic in building science as most durability-related issues depend upon exceeding a threshold moisture level in the affected materials. Water is most often thought of in its liquid form, but it is the only substance that is regularly found naturally in all three states (solid, liquid, and gas). It is essential to life and is commonly called the universal solvent. It pervades nature in many ways: It is found in living matter, it is in the atmosphere, and it is adsorbed to surfaces. The study of moisture movement in building science requires the knowledge of how water is transported within a given state and how it changes from one state to another. There are many relationships that have been developed to explain moisture movement and while they provide an adequate description for the most part, there is still more to be learned in this field.

Liquid water is experienced in buildings in numerous ways. It falls in the form of rain on the building enclosure, it passes through the building in pipes for various services, it may form as a result of condensation of water vapor, and it may also be in ponds and fountains. This is the water that we usually see. Its movement is described by fluid dynamics and is a large field of study ranging from groundwater to rivers to highly specialized applications. In building science the flow of liquid water is not usually addressed, as it does not occur under normal conditions except at the surface of the enclosure. Instead, how liquid water is absorbed into materials is of great interest, this topic is addressed later in the section on capillarity and absorption.

3.2.1 Water Vapor

Water vapor exists in air at most normal conditions in buildings. The amount of water vapor depends on a variety of conditions and is described in a couple of ways. First, it can be most directly described by the total vapor pressure. Second, it can be defined by

its relative humidity, which is the ratio of how much water vapor is in the air to the maximum amount of water vapor that can be held. The maximum amount is termed the saturation vapor pressure; if any more water vapor is added to the air there will form condensate so that the total amount of vapor will not increase. The saturation vapor pressure varies with temperature as warmer air can hold more water vapor. This relationship is expressed in the following approximate equation:

$$P_{ws} = 1000 \cdot e^{\left(52.58 - \frac{6790.5}{T} - 5.028 \ln T\right)} \quad \text{[Pa], T in K} \qquad 3.18$$

Alternately

$$P_{ws} = 611.2 \cdot e^{\left(\frac{17.67t}{t+243.5}\right)} \quad \text{[Pa], t in } ^{o}\text{C} \qquad 3.19$$

When this value is known, the relative humidity (RH or Φ) can then be calculated as the ratio of the actual vapor pressure (P_w) to the saturated vapor pressure (P_{ws}).

$$RH = \phi = \frac{P_w}{P_{ws}} \qquad 3.20$$

Relative humidity often has more relevance in building science than does the actual vapor pressure. When the RH reaches 100% condensation will occur. Condensation is a common source of moisture problems in buildings caused by moisture transported by diffusion of vapor or leakage of warm humid interior air towards cold surfaces within the enclosure. To assess the danger of condensation, the dewpoint temperature can be used. This is the temperature for which the vapor pressure of interest reaches the saturation pressure. It can be found by rearranging the previous equation used to find the saturation vapor pressure.

$$t_d = \frac{4030}{18.689 - \ln\left(\frac{P_w}{133}\right)} - 235 \quad [^{o}\text{C}], P_w \text{ in Pa} \qquad 3.21$$

Condensation most often is supported by vapor transported along with bulk air transport. When the air moves past a surface below the dewpoint temperature it will deposit condensate. This can lead to large amounts of condensation due to the large mass of air that can pass by the surface, as compared to condensation as a result of diffusion.

These two methods of vapor transport are analogous to the heat transfer modes of conduction and convection. Diffusion is the movement of individual molecules from areas of higher concentration to lower concentration. The movement of the molecules is limited by the material separating the concentration difference. In a near vacuum there is little to stop the movement of vapor molecules, whereas a sheet of metal has no pores or openings and hence will not allow vapor through. Most other materials are between these two extreme cases. Porous materials will allow vapor to pass but at a slower rate than through free air. Vapor transport by diffusion is described by the following equation:

$$\frac{dw}{d\theta} = -\overline{\mu} \cdot \nabla P_w \qquad 3.22$$

Where w = moisture content of the air (ng/m^3),
θ = temporal variable (s),
μ = average vapor permeability (ng/Pa·m·s), and
P_w = vapor pressure (Pa).

This equation is often simplified to one dimension for diffusion through walls.

$$\frac{dw_x}{d\theta} = -\overline{\mu}\frac{dP_x}{dx} \qquad 3.23$$

For discrete layers of thickness, l, of constant permeability, $\overline{\mu}$, this simplifies further:

$$q_v = \frac{-\overline{\mu}}{l}\Delta P \qquad 3.24$$

Vapor Permeance, M (ng/Pa m^2 s), is defined just as thermal conductance was for heat transfer. Similarly the Vapor Resistance, R_v (Pa m^2 s/ng) is the reciprocal of the vapor permeance. These relations are described by the following equation:

$$M = \frac{\overline{\mu}}{l} = \frac{1}{R_v} \qquad 3.25$$

Then the diffusion process can be expressed

$$q_v = M\Delta P = \frac{1}{R_v}\Delta P \quad [\text{ng/m}^2\text{s}] \qquad 3.26$$

Accurate determination of the vapor permeability is not easy. It is a slow process and requires long test durations. Also, the permeability has been found to vary with the

moisture content of the material and may also vary with temperature (Galbraith, Guo, & McLean, 2000). For these reasons it is often desirable to measure the vapor permeability under conditions that best represent the situation under consideration. However, often test results follow standard guidelines regardless of the application of the material.

Bulk transport of vapor is the movement of water vapor with a mass of air. It is described in the following way (Straube & Burnett, 2005)

$$m_w = W \rho_{air} Q_{air} \qquad 3.27$$

Where m_w = mass flow of water vapor (kg/s),
W = humidity ratio (kg water vapor to kg of air),
ρ_{air} = air density (kg/m^3), and
Q_{air} = volumetric flow rate of the air (m^3/s).

3.2.2 Adsorption

Some water vapor in the air attaches to the surfaces of solids, this phenomenon is called adsorption. Generally, the amount of adsorbed water increases with relative humidity. Also, lower temperatures allow more water to be adsorbed than higher temperatures; however, there is very little variation over the range of temperatures normally experienced and so, in building science temperature is often neglected and the adsorption curve with respect to RH becomes the sorption isotherm. The actual amount of water adsorbed will depend upon the material under question and is reported in percent moisture content, usually dry basis. Examples of sorption isotherms for several materials are given in Figure 3.

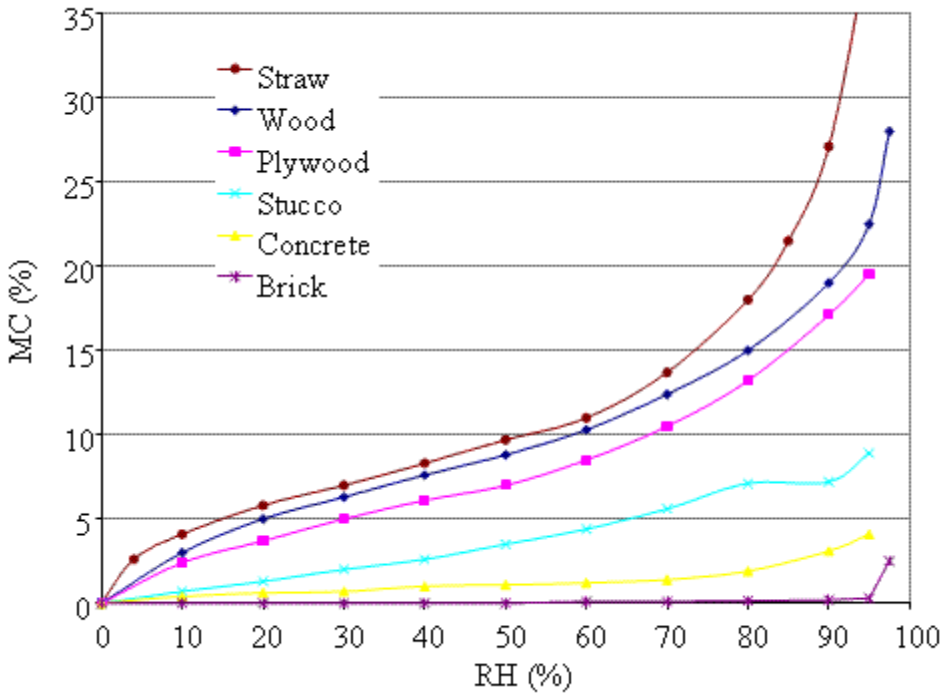

Figure 3. Sorption isotherm of various materials (Straube & Burnett, 2005).

Dry basis (*db*) moisture content is the ratio of the mass of water to the mass of dry solid as a percentage, it is found by first weighing the wet sample and then drying it in an oven until the mass no longer drops. The difference in the masses is the mass of water. The other moisture content measurement that can be reported is the wet basis (*wb*) which is the ratio of the mass of the water to the total mass of the wet sample (water and dry solid). These relationships are shown in the following equations, note the relationship between the dry basis and the wet basis measurement, this allows for easy conversion between the readings.

$$MC_{db} = \frac{m_w}{m_s} \times 100\% \qquad 3.28$$

$$MC_{wb} = \frac{m_w}{m_{tot}} \times 100\% = \frac{m_w}{m_w + m_s} \times 100\% \qquad 3.29$$

$$MC_{db} = \frac{MC_{wb}}{1 - MC_{wb}} \qquad 3.30$$

$$MC_{wb} = \frac{MC_{db}}{1 + MC_{db}} \qquad 3.31$$

Where MC_{db} = dry basis moisture content,
MC_{wb} = wet basis moisture content,
m_w = mass of water,
m_s = mass of solid, and
m_{tot} = total mass (water + solid).

3.2.3 Capillarity and Absorption

When a glass tube of sufficiently small diameter is inserted into a water bath there is a noted rise of water within the tube, this is referred to as capillarity. The height to which the water rises increases with decreasing tube diameter. Also, the rate at which equilibrium is reached is slower with decreasing diameter due to increased resistance to flow as well as the higher height which must be reached to achieve equilibrium. The reason for the absorption of the water is due to the surface tension of water and is described by the following equation (Washburn, 1921).

$$P_{cap} = h\rho g = \frac{-2\sigma\cos\theta}{r}, \text{or rearranging} \qquad 3.32$$

$$h = \frac{-2\sigma\cos\theta}{r\rho g} \qquad 3.33$$

Where P_{cap} = capillary pressure (Pa),
H = height of water column above the free surface (m),
σ = surface tension of water (N/m),
θ = contact angle between water surface and pore (Rad),
r = pore radius (m),
ρ = density of water (kg/m^3), and

g = acceleration due to gravity = 9.81N/m^2.

Another effect of the capillary suction is the reduction of the vapor pressure above the water surface. This is due to the curvature of the surface and is described by the Kelvin equation which can be rearranged to provide the RH for which a given pore radius will experience capillary condensation as below

$$RH = e^{\left(\frac{-2\sigma\cos\theta}{r\rho R_{wv}T}\right)} \qquad 3.34$$

Where R_{wv} is the water vapor gas constant and the other terms are as before.

Often, the analogy of a glass tube is used for simplicity; however, in reality porous materials are not made up of parallel tubes of various diameters but an interconnected grid of pore spaces of various sizes. Therefore, for practical use the water uptake test is the most widely used method to assess the capability of a material to absorb water. In this test it is found that the rate of absorption follows linearly with the root of time and therefore the results are given in the units kg/m^{2}s$^{1/2}$.

3.3 Heat and Moisture Analysis

One dimensional analysis of heat and moisture transport consists of a single layer or series of layers that divide specified boundary conditions. For buildings it is the building envelope that separates the interior and exterior conditions. These conditions are defined by the temperature, relative humidity (or vapor pressure), thermal radiation, and driving rain. The building envelope is broken into layers that represent the different materials that make up its construction.

Often, steady state calculations can provide a reasonable estimate of conditions that may be experienced within an enclosure. This is performed following a few simple rules that are based on thermal conduction and vapor diffusion. First, the total thermal and vapor resistance of the assembly is the sum of the respective resistances of the layers and second, the ratio of the temperature and vapor pressure change over a given layer to the total change over the assembly is equal to the ratio of the respective resistance of that layer to the total resistance. These are summarized in the following equations:

$$R_{(T or v)tot} = R_1 + R_2 + ... + R_n = \sum_{i=1}^{n} R_i \qquad 3.35$$

$$\Delta T_i = \frac{R_{T,i}}{R_{T,tot}} \Delta T_{tot} \qquad 3.36$$

$$\Delta P_i = \frac{R_{v,i}}{R_{v,tot}} \Delta P_{tot} \qquad 3.37$$

Where $R_{T,i}$ = thermal resistance of layer i,
$R_{v,i}$ = vapor resistance of layer i,
$R_{(T or v),tot}$ = total thermal or vapor resistance of assembly,
ΔT_i = temperature drop over layer i,
ΔP_i = vapor pressure drop over layer i, and
ΔT_{tot}, ΔP_{tot} = temperature and vapor pressure difference over assembly.

The application of these principles is usually done through a spreadsheet that produces a table showing the temperature profile and vapor pressure profile through the assembly. Special considerations need to be made for the occurrences of vapor pressure beyond that of saturation, which is not physically possible. In such instances it is necessary to impose the limit of the saturation vapor pressure and assume that the boundary has a relative humidity of 100%. The analysis is then divided into two parts that can follow the earlier guiding principles, but now with one common boundary at 100%RH. For a more detailed explanation of this form of analysis refer to Ch. 6 – Water Vapor Transport in *Building Science for Building Enclosures* (Straube & Burnett, 2005).

Steady state analysis does not capture diurnal effects of solar radiation or outdoor temperature fluctuations which may have a significant impact on temperatures in the wall and vapor movement. In addition, the impact of rain events and moisture storage in the straw requires dynamic analysis. For these reasons, a computer model will be used to perform dynamic one-dimensional analysis. WUFI4 Pro® is a software program developed to compute dynamic heat and moisture transfer in a one-dimensional assembly.

One-dimensional analysis will suffice for this thesis as it is a study of solid straw bale walls with no doors, windows or other discontinuities. Therefore, the interior and exterior boundary conditions are parallel and the wall assembly has the same cross section at all points. These properties create one-dimensional heat and moisture transport. An exception to this case is at the top and bottom of the wall where

discontinuties do exist and heat and moisture may move in two dimensions. However, the focus of the numerical modeling will be at the mid-height of the wall, which is far enough removed from the top and bottom so that one-dimensional behaviour exists. Another limit to the one-dimensional analysis is the potential for vertical movement of moisture within the wall and thermal convective loops in the straw. These will affect the overall behaviour of the wall but are expected to have a relatively small impact.

4 Mold and Decay

Mold, mildew, decay, rot and various other terms all describe some result of fungal growth. Fungi belong to their own biological kingdom with an estimate of more than 1.5 million species and 64,000 formally described (Gow & Gadd, 1995). With so many species there are many different variations of fungi, and hence the various terms to describe them. However, they are all classified as fungi due to the following characteristics: they are multicellular eukaryotes, rely on organic sources of carbon for growth, use carbon compounds for energy and externally digest and then absorb carbon compounds. These characteristics differentiate fungi from the other biological kingdoms (plantae, animalia, protista and monera).

Being eukaryotic means their cells are bound by a membrane with a complex structure that includes a nucleus. Plants, animals, and protists are also eukaryotes and are differentiated from the monera kingdom, whose cells do not contain a nucleus (prokaryotes). They are also multicellular, which differentiates them from simpler organisms in the protist kingdom, such as algae and protozoa. Although, fungi may appear similar to plants, they in fact grow in a manner more like animals. Plants grow through photosynthesis, deriving carbon from the atmosphere and energy from the sun, animals and fungi use carbon for both growth and energy deriving it from organic sources. However, fungi differ from animals in digestion. Animals ingest food sources and digest them internally, whereas fungi externally digest food sources and then absorb the digested carbon compounds. The differentiation between fungi and the other kingdoms is shown in Table 1.

Fungi perform three roles in an ecosystem: pathogen, symbiont, and saprobe. Most fungi are saprobes, decomposing organic matter to contribute to the nutrient cycle. Some are symbionts that grow alongside plants for their mutual benefit. Others are pathogens or parasites to plants or animals.

In ecosystems, fungi are indispensible; however, in buildings they have no value: Buildings are made to endure whereas fungi cause decomposition. In addition, pathogenic fungi, although generally rare, generate health concerns for building occupants.

Biological Kingdom	Nucleus	Complex Cellular Organization	Organic Carbon for Growth	Externally Digest
Fungi	Yes	Yes	Yes	Yes
Animalia	Yes	Yes	Yes	No
Plantae	Yes	Yes	No	-
Protista	Yes	No	-	-
Monera	No	-	-	-

Table 1. Differentiating Fungi from other biological kingdoms.

4.1 Cellular Organization

Cellular organization of fungi starts with hyphae, which are small tubelike cells, see Figure 4. These grow to form an interconnected hyphal system called a mycelium. The mycelium often grows within the substrate. Thus, the only visible sign of the fungus is the deterioration it causes on the substrate. Hence, the terms decay and rot are used that reference the appearance of the substrate as opposed to the fungus itself. Sometimes fungi will grow on the surface and may be visible to the unaided eye, often in the form of mycelial fans, see again Figure 4, this visible appearance of fungi is termed mold and mildew, and references the appearance of the fungus directly.

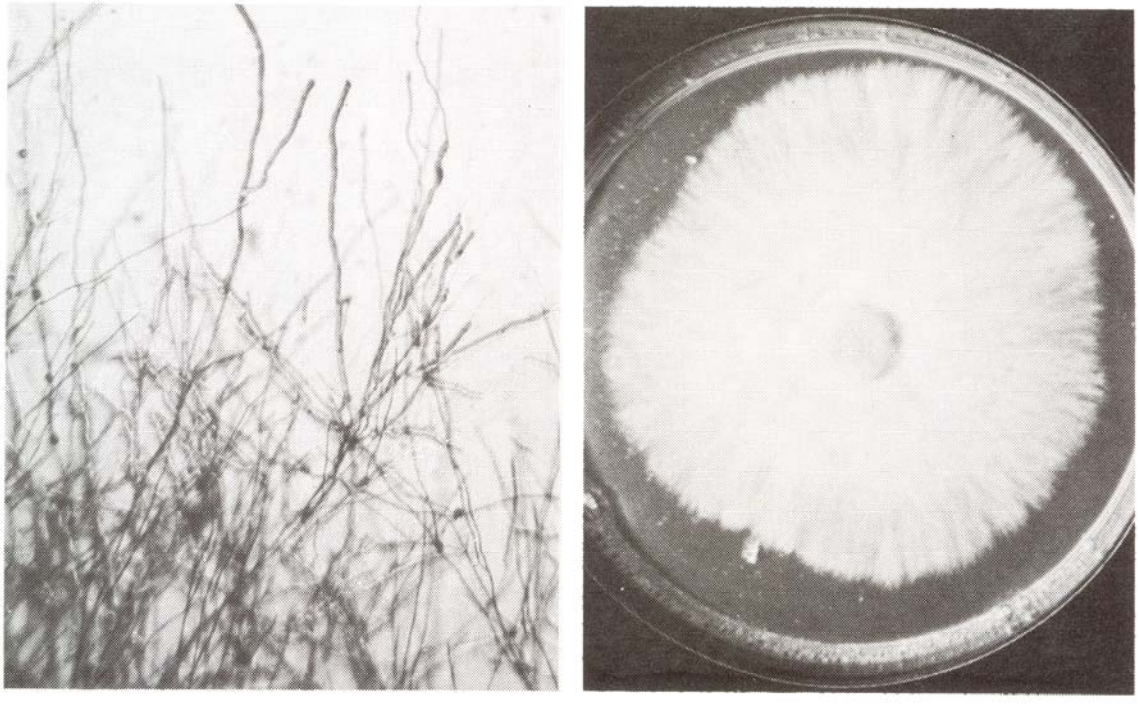

Figure 4. Hyphae (left) and mycelial fan (right) (Coggins, 1980).

Sporophores eventually produce and release fungal spores, which are their primary means of reproduction. The sporophores take various forms and are the principal criteria to classifying fungi. Some sporophores are part of fruiting bodies such as mushrooms and puffballs, but many fungi do not develop these bodies and their sporophores are not visible to the naked eye.

Fungal spores are often forcibly ejected from the sporophore to be carried by air currents, but may also be transported by insects and other motive creatures. The transport of the spore is important for the spread of the fungus as the mycelium has limited capability of growing over regions of unsuitable substrate. When a spore reaches a suitable substrate it will germinate to form a hypha and develop another fungal colony (Gow & Gadd, 1995). Due to the large number of spores produced and their capability for transport they exist in almost all locations and therefore fungal growth will certainly occur on all suitable substrates (Zabel, 1992).

Yeast are a particular type of fungi that do not develop the previously discussed hyphae and mycelial system. Instead they exist as single cells and produce a bud that separates into a daughter cell for reproduction. This system is more economical in usage of resources and can resist greater changes in osmotic pressure. However, yeast are not capable of moving across substrates, except as air currents or animals may move them. There exist some fungi that are able to switch between hyphal growth or yeast-like growth.

4.2 Requirements for Germination and Growth

There are two stages of growth in fungi. The first is spore germination and the second is the growth of the resulting hyphae. The needs for growth vary slightly between the two stages; however, the basic requirements for both are the following (Zabel & Morrell, 1992):

1. Free or unbound water,
2. Favorable temperature,
3. Atmospheric oxygen,
4. Digestable carbon compounds / suitable substrate, and
5. No toxic compounds present.

Fungal growth will not occur with any one component missing (Black, 2006).

Germination results in a germ tube developing from the spore. The germ tube must reach suitable conditions for growth as the spore contains little nutrients to support its own growth. Germ tubes may grow towards amino acids, water, volatile compounds, etc. depending upon the species. (Gow & Gadd, 1995)

Hyphae grow at the tip and elongate. Existing hyphae adhere to the substrate and transport materials for growth to the hyphal tip through protoplasmic streaming. Therefore, the tip may pass over regions not condusive to growth by relying on previously developed hyphae. Growth at the tip of the hypha is effective for penetrating the substrate and enables fungi to grow into a substrate. Some fungal hyphae can grow away from the substrate and move through gas phases. In general, hyphae grow away from each other, which results in the mycelial fan appearance, however, other tropisms are difficult to study and there is a general skepticism as to the occurrence of response to external stimuli.

Higher fungi (Ascomycetes, Deuteromycetes, Basidiomycetes) develop fruiting bodies and cross links between radiating strands of hyphae, called hyphal fusion. Also, they have many cross walls or septa. These fungi are thus called septate-reticulate. Lower fungi (Oomycetes, Zygomycets) lack fruiting bodies and the cross linking between radiating hyphae and have fewer septas, with multiple nuclei within the compartments between septa. Therefore, they have been called filamentous-coenocytic.

Lower fungi appear to be capable of hyphal septation and fusion. Though the simpler form is all that is adequate for their life and spending energy and resources on septa and fusion would only be a waste. Lower fungi can develop a septum to cut off damaged or old parts of the mycelium. This may take up to 20 minutes, whereas higher fungi have already developed septa, of which their pores can just be sealed to close off the damaged area. Higher fungi may reconnect past the damaged compartment through hyphal fusion and reestablish protoplasmic continuity. When lower fungi cut off old or damaged regions that branch is then disconnected from the previous growth, since no interconnections occur with other hypha, this may result in an original mycelium breaking into several disconnected regions. (Gow & Gadd, 1995)

4.2.1 Water

Water serves the following four general purposes:

1. Reactant in hydrolysis,

2. Diffusion medium for enzymes and solubilized substrate molecules,
3. Solvent or medium for life systems, and
4. Capillary swelling agent.

Water is critical for the germination of spores. Only a few fungi are able to germinate at low humidities. Water is unique for this requirement as even deuterium oxide, heavy water, does not suffice. The concentration of water required for growth depends on the species. This has been extensively studied for different fungi by placing incubating spores at controlled humidities, either by liquid water solutions or gaseous water control. (Gottlieb, 1978)

The water needs to be "free water" to allow the movement of solutes. Although water is adsorbed to solids from vapor in the air, it is likely not until the fiber saturation point that it becomes available to mould growth.(Zabel & Morrell, 1992; Morris, 2002). This is about 30%MC in wood and 39% in rice straw (Summers et al, 2002). The water activity required for germination is generally lower than that required for sustained growth of the mycelium, by around 2%RH (Grant, 1989; Adan, 1994). Likewise, the water activity required for sustained growth is less than that required for sporulation (Adan, 1994). Therefore, increasing water activity is required for further growth stages.

As the growth of mould converts carbohydrates into water through respiration, the substrate may continue to be moistened simply by the mould itself. Theoretically, the decomposition of 1.0g of cellulose will result in 0.555g of water (Griffin, 1977). Therefore, it is easier to stop mould growth from starting on a clean substrate than it is to stop it from continuing on an already inoculated substrate (Morris, 2002).

Desiccating fungi will likely not kill it but may cause it to go into dormancy and or cut off sections that are facing unfavourable growth. Desiccation cannot be relied upon to kill wood rotting fungus (Findlay, 1950) and likely will not kill other fungi as well.

4.2.2 Hydrogen Ion Concentration

Fungi generally have their optimum germination at pH levels of 5-8 with few species preferring alkaline conditions. However, growth can occur at both acidic and alkaline conditions, with some fungi able to germinate at pH as low as 1.6 and as high as 11.1 (Adan,1994).

4.2.3 Time

Spores remain dormant until favorable conditions initiate germination, thus they are in a state of exogenous dormancy. In order to survive periods of dormancy spores have low rates of metabolism, lack of cytological activities, and sometimes thick protective walls. Although the rate of metabolism is slow, internal energy sources and other necessary compounds are eventually consumed and the spore will no longer be able to germinate. This length of time varies with the species and may be several years.

When favorable conditions are found there is still time required before a spore will germinate due to some form of constitutive dormancy. The exact nature of this delay varies with fungal species, but one explanation is common: There is an inhibiting chemical that resides within the spore, which requires sufficient moisture and time so as to diffuse out of the cell until its concentration is no longer limiting (Gottlieb, 1978). The main purpose is to ensure that spores do not germinate until after dispersal (Chitarra, 2003). As well, there may be a period of maturity wherein the spore is not able to germinate under any conditions (Cochrane, 1974). Another postulate is that the DNA helix is distorted when dehydrated, which stops germination and growth (Adan, 1994). Often, only the time to germination is reported for a given set of conditions without further examination or explanation.

4.2.4 Temperature

Temperature affects the biochemical reactions in fungi that lead to growth. High temperatures increase the rate of reactions while low temperatures slow them. As germination and growth is primarily an enzymatic process it is the effect of temperature on the proteins involved that limit or promote germination. There is a range of temperatures within which growth will occur, the low end between 0-10^{o}C and the upper end around 34-36^{o}C. There are some fungi that are cryophilic and have a lowered range, while some are thermophilic and have increased limits, with maxima up to 40-50^{o}C. Other fungi are thermoduric and have a larger overall range of temperatures favorable to growth. The temperature range is also dependent on time. At longer incubation periods the low end temperature may decrease (Gottlieb, 1978).

Minimum, optimum, and maximum temperatures are reported for different fungi, these are termed the cardinal temperatures. The optimum temperature for each fungi are the most reliable of these as it does not often change with other factors. There is usually a sharp decrease in germination from the optimum to the maximum temperature. This is likely due to the exceedance of the critical temperature for one of the essential reactions

that causes it to become damaging. In a study of 80 species the average optimum temperature is 26°C, with a normal distribution between 15°C and 40°C (Gottlieb, 1978).

Temperatures below the range for growth are most often not lethal, unless slow crystallization is possible. However, temperatures above the acceptable range are usually lethal. A study on heat sterilization of green southern pine was conducted by Chidester in 1937 (Zabel & Morrell, 1992). He found the minimum temperature to kill all fungi in the greenwood was 66°C and it took 75min to do so. Table 2 shows some of the other times required to kill the fungi at higher temperatures.

Temperature (°C)	Time (min)
65.6	75
76.7	30
82.2	20
93.3	10
100	5

Table 2. Time until fungi are killed at various temperatures (Zabel & Morrell, 1992).

However, other tests have shown some fungi to remain viable at temperatures above 65°C for 8 to 72 hours. Still, another test showed that temperatures 50°C and above were enough to kill fungi. (Zabel & Morrell, 1992) The temperature to kill spores in 30 minutes is 60-65°C, lower than for developed fungi, but there are some heat resistant ascospores (Adan, 1994).

The cardinal temperatures for mycelial growth are similar to those for incubation but generally have a wider range.

4.2.5 Oxygen

Most fungi require free oxygen for respiration, in order to produce energy. The equation of respiration of sucrose is

$$C_6H_{12}O_6 + 6O_2 \rightarrow 6CO_2 + 6H_2O + energy \quad (\Delta G^o - 686 kcal/mol)$$

In this process oxygen is used as a proton and electron acceptor, which ends up in the formation of water. There are some fungi that can use other radicals as electron acceptors and are therefore able to use anaerobic respiration and do not require oxygen. Yeast can

obtain energy directly from chemical compounds through fermentation and also do not require oxygen.

Normal atmospheric concentration of oxygen is sufficient for fungal growth (21%). Reduction of growth occurs only at very low oxygen levels (<2%).

Carbon dioxide also has an effect on fungal growth. Some fungi may require small amounts of CO_2 for growth (0.05%). But high levels of CO_2 are toxic to fungi, and also contribute to higher substrate acidity levels. Respiration of fungi in confined spaces may result in a significant reduction of O_2 and an increase of CO_2 that may result in slowed or stopped growth. (Zabel & Morrell, 1992)

4.2.6 Substrate

Some spores contain all the nutrients required to start germination, but to continue growth requires nutrient supplies from the substrate. The needs that the substrate fills are

1. Carbon compounds for energy through oxidation,
2. Metabolites for growth and development, and
3. Vitamins, nitrogen, minor elements.

Many fungi are able to degrade cellulose, but only a few thousand species of fungi are wood-inhabiting and able to break down and use the cellulose-hemicellulose-lignin complex that makes up the wood cell wall (Zabel & Morrell, 1992)

Toxic Substances

Some substances are toxic to fungi and inhibit growth. This effect is the basis for mold and rot resistant lumber products. This subject is not pertinent to this study and thus is not investigated.

4.3 Measuring Growth

Fungal growth is measured in several ways. The primary method is visual inspection. Fungal spores can be monitored under a microscope and germination is said to have begun when a germ tube reaches a specified length. The number of spores that have already germinated at a given time can be counted and the percentage germination found. Also, mycelial growth can be measured as the radial growth of the mycelial fan when

grown in ideal conditions such that a circular mycelial fan develops. Another visual method indicates only the percentage of surface covered, this can be analyzed under a microscope or with the naked eye, the ability to detect small growth being possible with the microscope only.

Other techniques for quantifying fungal growth are to measure secondary effects. For example, CO_2 evolution and O_2 consumption can be measured in controlled vessels to assess fungal growth rates.

4.4 Predicting Growth

Fungi are used in a variety of ways in numerous industries. The optimization of mold growth depending on different control factors is often studied. In building science the effects of relative humidity and temperature are of primary concern for the growth of fungi on building materials. There have been attempts to develop relationships between these factors and the growth of mold on specific building materials, most notably wood. However, there will always be limitations to the models as there are a multitude of factors that ultimately affect the growth of fungi. But it is a beneficial effort for ecological building materials, such as straw, that have a high propensity for mold growth. The prediction of mold growth will aid in design, with more accurate predictions leading to a larger range of acceptable designs.

4.4.1 Lowest Isopleth

A static model will give the latent period required for a given set of conditions before germination occurs. This will provide the upper time limit for exposure at the tested conditions on the tested material.

The most basic prediction ability is to state at what combination of temperature and humidity mold will grow. However, some fungi are capable of growing at low humidities, although it takes a long time before germination begins. For example, mold was noticed on locust beans after 861 days at 65% RH, but only 35 days at 75%RH (Snow, 1944). Therefore, a time frame is required that represents a realistic length of time for constant conditions in buildings. Maybe this means a year, a season, or just a few weeks. In any event a certain limit needs to be selected for which it is safe to say that mold growth will never occur at that given condition. Afterwards, a chart can be developed by testing at various combinations of temperature and humidity, with a boundary line between conditions that support growth and those that don't. Therefore, by

this method it is required to stay outside of the region that supports growth. Often, this is quite limiting and short durations in that range will not lead to mold growth.

For example, the minimum RH for A. versicolor is 79% on 2% malt extract agar at 25°C and 83% at 12°C, the duration of the test was 21 days (25°c) and 42 days (12°C) although the time to growth was not given (Grant, 1989). Grant states that a limit of 80%RH will stop mould growth on building materials. This common 80%RH limit is based on a 3 week time period and 25°C temperature (Adan, 1994). Tests are usually conducted between 20-30°C so that temperature is not a limiting factor. The common limit for wood is 80%RH or 20%MC (Zabel & Morrell, 1992), although others us 16%MC as the safe level.

Waite (1949) tested the duration to first noticeable mould on cured hay. His results (Table 3 and Table 4) show that 70%RH or 12.9%MC is the limiting humidity at 20°C. However, it took 200 days to develop mold at this condition. A more realistic limit is 75% (19 days).

RH (%)	MC (%)	Days to develop mould
70	12.9	c. 200
75	15.7	19
80	18.2	6
82	20.4	4
84	22.5	3
85	21.6	4
86	23.8	3
88	27.6	2
90	28.0	2

Table 3. Incidence of mould growth on cured hay during storage at 19-20°C (Waite, 1949).

	75% RH		85% RH	
Temp. of Storage (^{o}C)	Mould Growth	Equilibrium moisture content (%)	Mould Growth	Equilibrium moisture content (%)
6	None up to 200 days	15.4	Growth after 120 days	22.1
15	None up to 200 days	15.0	Growth after 2 days	20.3
20	Growth after 6 days	15.0	Growth after 2 days	20.0
25	Growth after 28 days	14.8	Growth after 2 days	20.2

Table 4. The effect of temperature on mould growth on cured hay and absolute humidity at 75 and 85% RH (Waite, 1949).

Summers et al (2002) tested degradation of rice straw and noted a marked increase above 39%MC_{db}, which corresponds to an equilibrium RH of 93-97%. Above 40%MC and up to 150%MC the loss of straw mass was 0.5-2% per day which is 50-200 times more than rates below this level (0.0003%/day at 14%MC and 0.003%/day at 28% MC). Therefore, from Waite and Summers it appears that mould may grow on straw above 70%RH but significant growth will not occur until near 90%RH.

4.4.2 Categorizing Mould Species

Mould species vary in their required conditions for growth, some are hydrophilic others xerophilic, some cryophilic others thermophilic. Also, many moulds are not toxigenic and so may not have as great a requirement for control as those that are detrimental to human health. The most precise model will have specifics for all species of mould. However, such a model requires too much information due to the enormous number of species. Of course the types of mould spores present are not known during design. It is better to assume all moulds are likely to grow and for ease of calculation to group them into categories of similar behavior, and hopefully few enough categories result in minimized computation.

Grant (1989) studied moulds found in British residential locations and produced a table showing a general sequence of mould species that will grow (Table 5). Notice early colonizers are various aspergillus or penicillium moulds; these are the most common residential moulds. Cladiosporium are also a common mould and are seen as secondary colonizers. Stachybotrys and chaetomium are natural moulds of straw and hay and other cellulosic materials (Nielsen, 2002). Stachybotrys Atra is seen as a tertiary colonizer in Grant's study. The higher wood decay type fungi will occur after initial mould

development as they are initially limited by mould that quickly overgrows the substrate (Morris, 2002).

A_w level in substrate	Species of moulds colonising substrates at:	
	12°C	25°C
<0·80	*A. repens*	*A. repens*
	P. brevicompactum	*A. versicolor*
(Primary	*P. chrysogenum*	*P. brevicompactum*
colonisers)	*P. spinulosum*	*P. chrysogenum*
		P. nigricans
		P. spinulosum
0·80–0·90	*A. versicolor*	*Alt. alternata*
	Aur. pullulans	*Aur. pullulans*
(Secondary	*C. cladosporioides*	*C. cladosporioides*
colonisers)	*C. sphaerospermum*	*C. sphaerospermum*
	G. pannorum	*F. moniliforme*
	M. plumbeus	*G. pannorum*
	P. nigricans	*U. chartarum*
	U. chartarum	*U. consortiale*
>0·90	*Alt. alternata*	*M. plumbeus*
	F. moniliforme	*Ph. herbarum*
(Tertiary	*Ph. herbarum*	*S. brinkmannii*
colonisers)	*S. brinkmannii*	*St. atra*
	St. atra	
	U. consortiale	

Table 5. Suggested sequence of fungal colonization from Grant (1989).

Clarke et al (1999) after investigating 250 references on mould growth developed a chart based on 6 categories of mould, from highly xerophilic to highly hydrophilic (Figure 5). Sedlbauer categorized moulds based upon health risk to humans: highly pathogenic (Class A), pathogenic over long exposures or allergenic (Class B), and not detrimental to human health (Class C). He found a differentiation between the lower boundary for growth of Class A and the other classes but the moulds in Class B and C behaved similarly enough to incorporate into one grouping (Figure 6). For the most conservative estimate the lowest possible isopleths should be used to cover all species of mould that have been encountered in buildings.

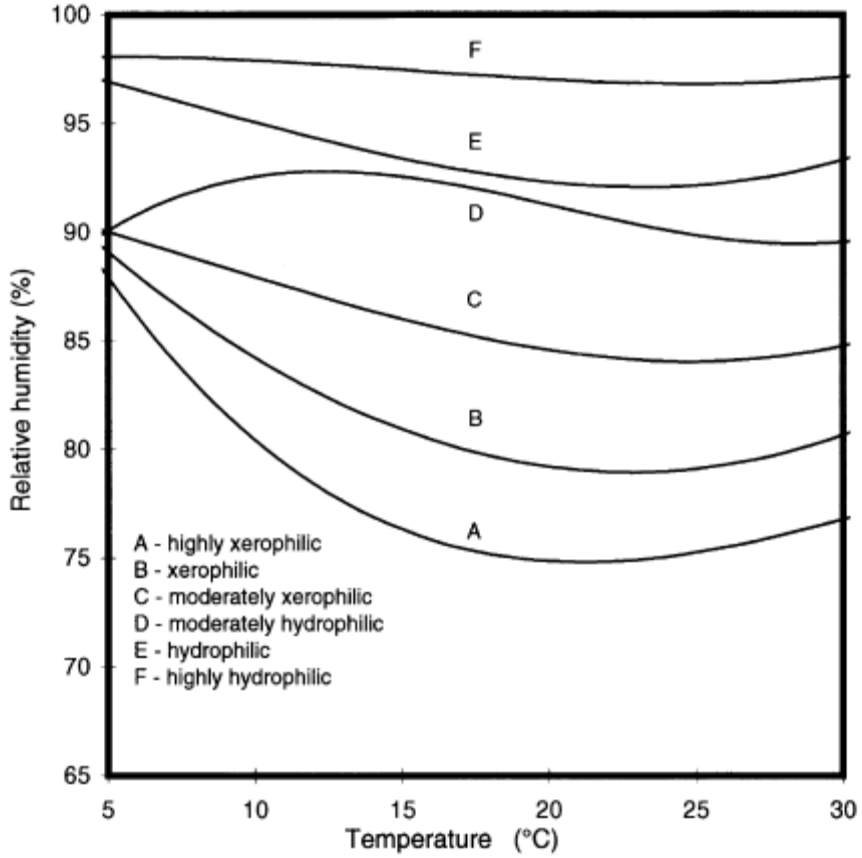

Figure 5. Limiting growth curves for six mould growth categories from Clarke et al. (1999).

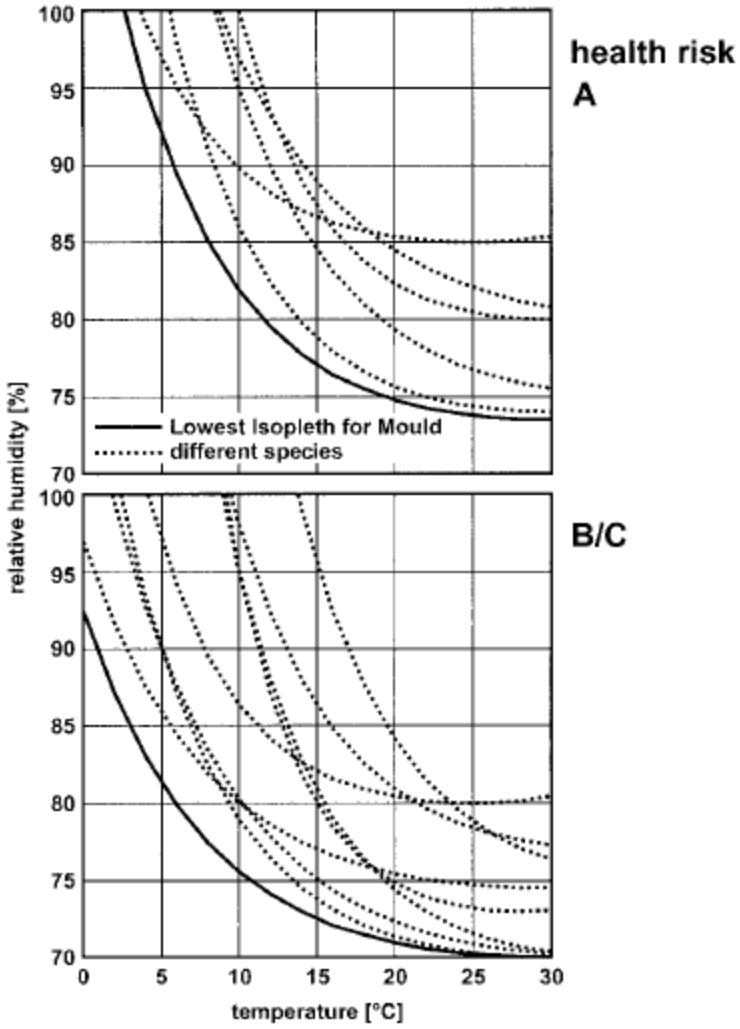

Figure 6. Sedlbauer hazard classes lowest isopleths (2002).

4.4.3 Substrate

To develop a general curve it is necessary to categorize materials based on their suitability as a substrate for fungal growth. It would be more precise to determine parameters for each material, however, it is more practical and convenient to develop classes of materials. This will provide a built in safety factor, as well as cover a wider dataset from testing of various materials.

The substrate provides nutrients to the mould. This is a basic requirement for growth. A perfect substrate has all the required nutrients with no toxic substances. Therefore, it is not limiting to growth. Other materials will be low or lack a required substance and thus limit growth. Yet materials that are inorganic will never support growth, unless they are covered with organic material. Sedlbauer (2002) recognized four categories of substrates

shown in Table 6. He used these categories to develop different isopleths for each category, shown in Figure 7.

Substrate category 0:	Optimal biologic culture medium.
Substrate category I:	Biologically recyclable building materials like wall paper, paper facings on gypsum board, building materials made of biologically degradable raw materials, material for permanent caulking.
Substrate category II:	Building materials with porous structure such as renderings, mineral building materials, certain wood species as well as insulation material not covered by I.
Substrate category III:	Building materials that are neither biodegradable nor contain any nutrients.

Table 6. Substrate categories from Sedlbauer (2002).

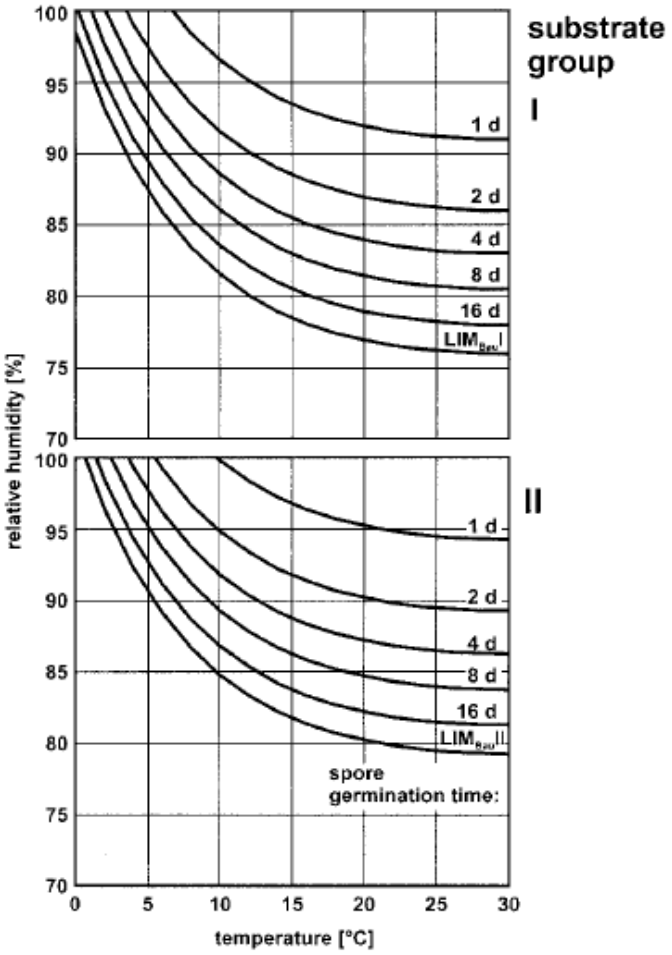

Figure 7. Isopleth curves for spore germination from Sedlbauer (2002). Isopleth system for substrate group I on top and group II on bottom.

4.4.4 Time to Germination

To include the concept of time to germination for static conditions the boundary line on the chart can be adjusted for different time frames. Sedlbauer (2002) references work by Smith and Hill (1982) who developed isopleths for different fungal species. Beyond just giving conditions and time to germination he also provided charts with growth rates of the mycelium at various conditions, two examples are shown in Figure 8.

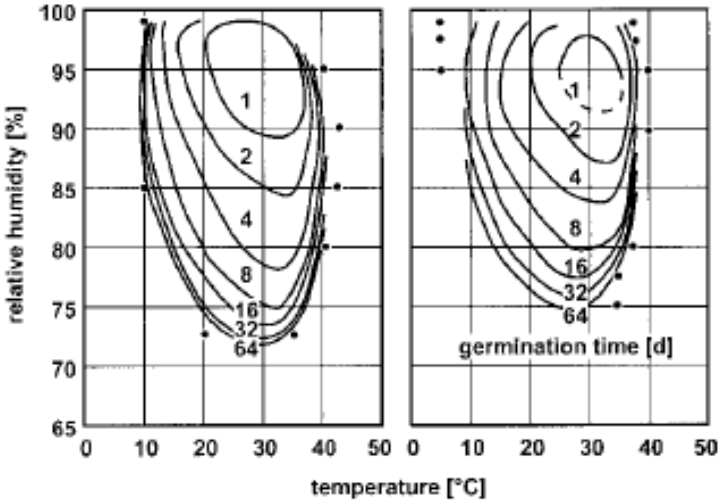

Figure 8. Isopleth for mould spores of Aspergillus restrictus (left) and Aspergillus versicolor (right) (Sedlbauer, 2002).

4.4.5 Mycelium Growth Rate

Beyond spore germination is mycelium growth. A small amount of growth is typically not a problem and initially occurs at the microscopic level. The rate of growth will depend upon various factors, but most of all temperature and humidity. It may be more favourable to allow small amounts of growth in any mould prediction model, as long term durability is not affected by short duration fungal growth, but by sustained growth.

4.4.6 Dynamic Hygrothermal Conditions

The previous conditions for growth have all assumed a steady condition until germination, or during mycelial growth, and that is how they are tested. However, in reality the temperature and humidity fluctuate, often quite drastically, so that the steady conditions will never be realized and can only be used in steady state modeling which will overpredict mould growth. In addition, decay of mould can be accounted for during unfavourable conditions, although there appears little work on this aspect, instead studies concentrate on how long a colony can remain viable under stressful conditions, but often do not state how much of the previous growth remains viable. This will impact the growth rate of the mould as it continues from a dormant state. This is due to the growth rate often reported in mm/day and therefore the total growth in mm^2/day depends upon the perimeter of growth. If the perimeter of growth is reduced during unfavourable conditions the total growth that resumes will be less than if the perimeter is assumed to continue.

The dynamic conditions can be modeled with software similar to WUFI® during design, or they can be measured directly in testing.

4.4.7 Using the Lowest Isopleth for Mould

The simplest prediction method would use the lowest isopleth for mould (LIM). For each hour of data the conditions are assessed for potential for mould growth based on temperature and humidity. If the conditions are above the lowest isopleth then a count is added to the total time above the threshold. When the total time above the threshold is greater than the steady state time to germination, the risk of mould growth is assumed. However, this does not account for variations in time to germination at different conditions. For example, high humidities will cause more rapid growth whereas lower humidities will have prolonged dormancy. Instead, this method assumes a single time to germination for all conditions above the threshold. For conservative estimates, the lowest time to germination is assumed. This time is quite short and therefore it is often assumed that once conditions have reached those for which germination is possible the risk of mould is assumed, whereas mold growth may not occur.

Clarke (1999) used this method. He modeled a building to collect data for the surface conditions on the walls and superimposed the data onto mould growth curves, see

Figure 9. He deduced that growth in all categories occurred as there was data in all categories and this was in agreement with the mycological samples collected. The curves used are the lowest isopleths for various categories of molds as explained earlier. Clarke does state the model is unable to predict the mould growth over prolonged periods of time due to the steady state nature of the mould growth curves that were used.

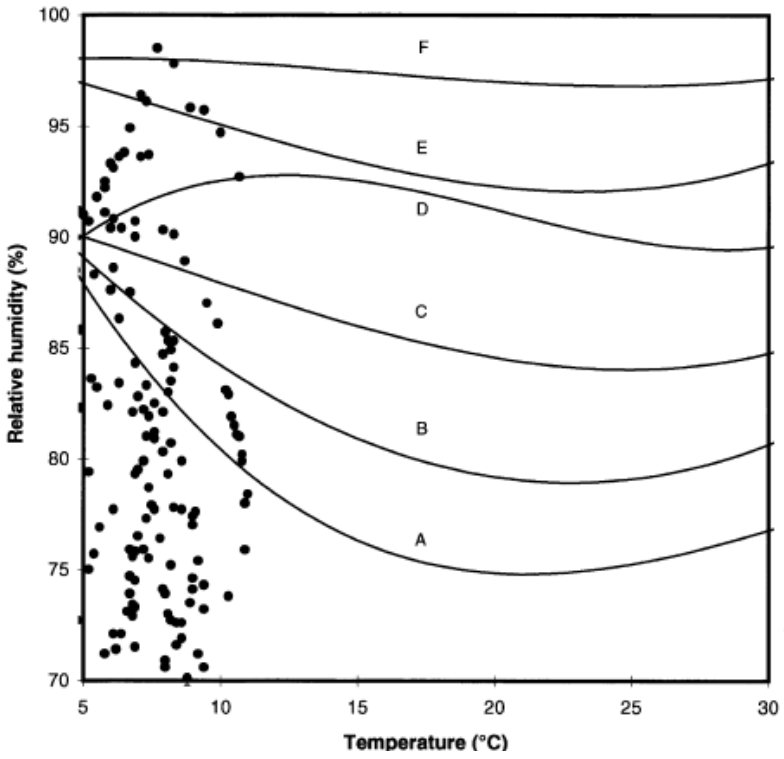

Figure 9. Results from Clarke's model (1999) using lowest isopleths.

4.4.8 Using Multiple Isopleths

Moon (2003) showed a method that uses the developed isopleths to predict mould growth for transient conditions. His method is similar to using the cumulative time above the lowest isopleth, however he also incorporates increasing risk categories (each with its own isopleths). For each category the cumulative time in that range is monitored. When the time in any category is beyond the steady state time to germination for that category the growth of mould is assumed. The accumulated time is for any condition that is within the given risk category. Thus any count within the highest risk category also adds a count to all the risk categories below it. See Figure 10 and Table 7 for an example of this method.

One drawback is the lack of ability to account for dry periods. Moon reset the cumulative times to zero when unfavourable conditions were met, as shown in day 10 of his example: the conditions were not favourable and so the times were reset, therefore on day 11 when conditions were favourable there was no risk indicated. However, this does not represent the behavior of molds. As Adan (1994) has shown, periods of dry conditions will stop the immediate growth but does not kill the mould, also time to germination does not require constant wet conditions, but the accumulation of wet

conditions. The effect of the dry periods will likely increase the required time at favourable conditions to achieve germination, however further studies are required to assess this effect and thus the steady state time to germination is used. However, Moon does state that once germination is reached the risk of mould growth is always present.

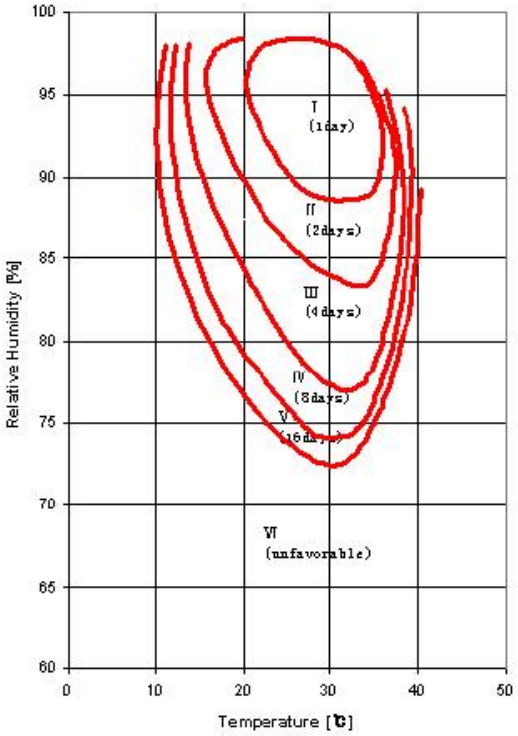

Figure 10. Moon (2003) mold germination graph with risk groups. Time to germination is given for each risk category, which is controlled by the temperature and relative humidity conditions.

Day	Surface		Group	Accu. exposure time	Req. exposure time	Mold growth risk	
	Temp	RH					
1	20	70	VI	-	-	x	x
2	25	80	III	1	4	x	x
3	23	85	III	2	4	x	x
4	26	90	II	1	2	x	x
			III	3	4	x	
5	30	95	I	1	1	o	o
			II	2	2	o	
			III	4	4	o	
6	22	85	III	5	4	o	o
7	18	97	II	1	2	x	o
			III	6	4	o	
8	25	80	III	7	4	o	o
9	18	97	II	1	2	x	o
			III	8	4	o	
10	20	70	VI	-	-	x	x
11	25	80	III	1	4	x	x
12	18	97	II	1	2	x	x
			III	2	4	x	

Table 7. Example from Moon (2003) of the application of his method.

4.4.9 Fluctuating Conditions

Adan (1994) tested the effects of fluctuating humidity on the growth of moulds. He varied the RH between a dry level (either 10, 33, 58, or 85%) and a wet level (97%RH). The fraction of time spent at the high level he termed the "Time of Wetness" (TOW), which also had a certain frequency. He was studying the fungal defacement of interior finishes, which would be well modeled by this system. Typically the interior can be assumed to remain relatively constant and wet locations, such as a bathroom, will see regular intervals of wetting to high levels. However, towards the exterior of the wall the conditions vary much more considerably: there are seasonal, diurnal, and even hourly variations that depend upon the local climate, weather, and immediate conditions at the wall.

The frequency did not greatly affect the growth rate at a given TOW except at very high frequencies, where the growth rate increased considerably.

TOW of 0.33 showed no growth while TOW of 0.66 required 2-3 weeks before germination (with a dry condition of 58%) compared to 2-3 days for the steady state condition of 97%. The growth rate was also reduced by about 40%. However, the total growth did approach that of the steady state conditions.

If the growth rate was only dependent on RH and remained unaffected by fluctuations, then during the wet periods the mould would grow at the same rate, and during the dry periods it would not grow. However, due to the nature of moulds they do not instantly start growing as soon as favourable conditions are encountered. So it is expected that rather than simply taking a ratio of the growth rate or time to germination based upon the TOW, that a slower growth rate and longer time to germination would occur. This is what was found in Adan's testing.

A dry level of 85% showed a reduction of 20% in growth rate (for TOW=0.5), a level of 58% showed a 60% reduction with lower humidities only reducing the growth rate minimally below this level.

4.4.10 Viitanen Model for Growth on Wood

Viitanen (1999) developed a model for predicting mould growth on wood materials. Specifically, pine and spruce which were used to develop the model. Viitanen uses the following scale for mould growth:

0 No growth
1 Some growth detected only with microscopy
2 Moderate growth detected with microscopy (coverage more than 10%)
3 Some growth detected visually
4 Visually detected coverage more than 10%
5 Visually detected coverage more than 50%
6 Visually detected coverage 100%

Originally the scale was used to allow for easy visual inspection method to quantify mold growth. In the model, it is possible to have non-integer values.

The minimum relative humidity for mould growth is given by the following equation and shown in Figure 11. For all temperature greater than 20^{o}C the minimum RH is assumed to be 80%.

$$RH_{crit} = \begin{Bmatrix} -0.00267T^3 + 0.160T^2 - 3.13T + 100.0 \quad for T \le 20^o C \\ 80.0 \quad when T > 20^o C \end{Bmatrix} \qquad 4.1$$

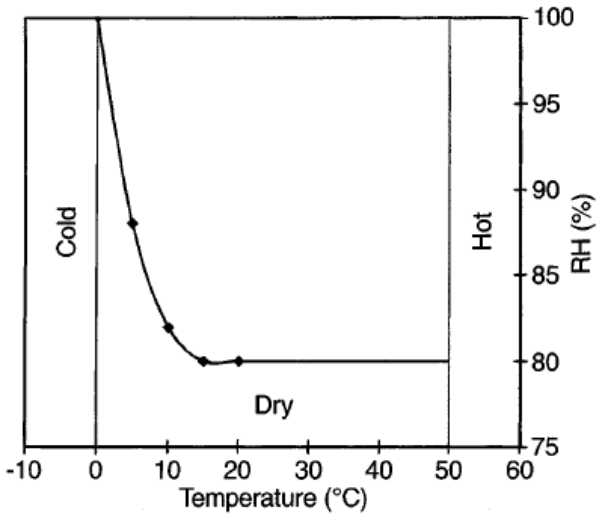

Figure 11. Minimum relative humidity for mould growth (Viitanen, 1999).

Viitanen also assumes that only a microscopic amount of mould growth will occur at the minimum relative humidity with total growth increasing for increasing humidities, until at 100% RH full coverage is expected. He models this with the following equation:

$$M_{\max} = 1 + 7\frac{RH_{crit} - RH}{RH_{crit} - 100} - 2\left(\frac{RH_{crit} - RH}{RH_{crit} - 100}\right)^2 \qquad 4.2$$

This equation is shown in Figure 12. It may not be representative of true mould behavior as growth will usually continue so long as conditions are favourable; however the rate of growth will change with conditions. Thus, if the RH is low, but still supporting growth, the mycelium will take longer to reach a given mould index than for higher conditions, but it will still likely reach that coverage.

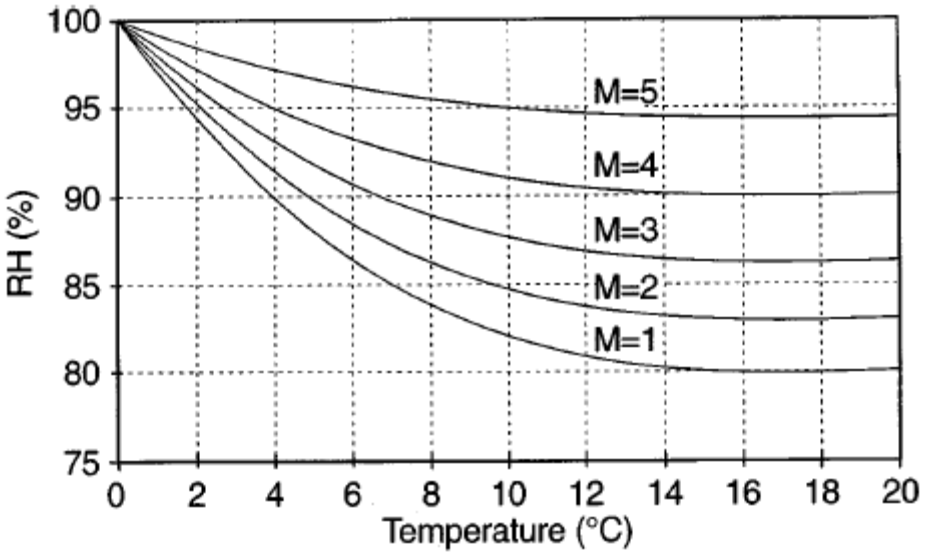

Figure 12. Limiting curves for maximum growth conditions (Viitanen, 1999).

Viitanen had previously developed a regression equation for the time to initiation of mould growth (M=1), t_m, and the time to first appearance (M=3), t_v, in weeks. These are given in the following equations:

$$t_m = \exp(-0.68 \ln T - 13.9 \ln RH + 0.14W - 0.33SQ + 66.02) \qquad 4.3$$

$$t_v = \exp(-0.74 \ln T - 12.72 \ln RH + 0.06W + 61.50) \qquad 4.4$$

Assuming the mould index, M, increases linearly with time results in the following differential equation for the growth of mould based on the times measured to germination and visible growth. t_m is used for growth up to a mould index of 1 and a combination of t_m and t_v is used for growth beyond a mould index of 1, this is controlled with the k_1 factor. The effect is that the change in mould index is linear with respect to time up to germination at the rate defined by t_m. After growth starts the rate changes to that found by the time to go from M=1 to M=3, which is t_v-t_m. Therefore, the rate to germination is $M_{germination}/t_{germination} = 1/t_m$ and the rate for mould growth is $(M_{visible}-M_{germination})/(t_{visible}-t_{germination}) = 2/(t_v-t_m)$. These times are in weeks, therefore multiply by seven to convert the rate to mould index change per day.

To incorporate the effect of the maximum mould index, M_{max}, given earlier, the factor k_2 was introduced, which limits the growth as it approaches the maximum mould index, at a mould index 1 less than the max the growth rate is reduced by 10%, at 0.5 below the max it is reduced by approximately 30%. Viitanen states that the experiment suggests the model is valid for fluctuating hygrothermal conditions but only if the conditions are

continuously favorable to growth and so does not account for dormancy of moulds during unfavourable conditions. The initial value of M must be known, and for the testing it was assumed to be 0.

$$\frac{dM}{dt} = \frac{k_1 k_2}{7 t_m} \qquad 4.5$$

$$k_1 = \begin{cases} 1 & when M < 1 \\ \dfrac{2}{t_v / t_m - 1} & when M \geq 1 \end{cases} \qquad 4.6$$

$$k_2 = 1 - e^{2.3(M - M_{\max})} \qquad 4.7$$

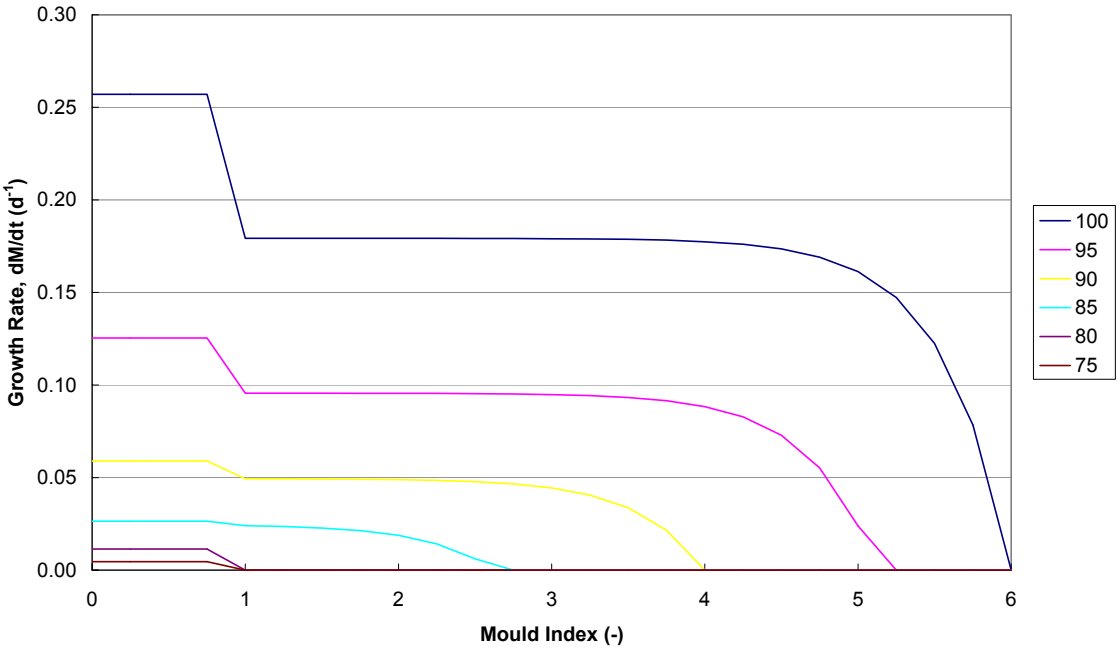

Figure 13. Example of growth rate by Viitanen's model at 20°C for various relative humidities (75-100%).

To account for periods of unfavourable growth a decay rate is used. This rate does not reflect the actual decay of the mould but accounts for the slowed growth response when favourable conditions return. However, the equations are based on a small set of data, do not cover periods longer than 14 days or the effects of temperatures below 0°C. Therefore, this can be used as a rough approximation at best.

$$\frac{dM}{dt} = \begin{cases} -0.032 & when t - t_1 \le 6h \\ 0 & when 6h < t - t_1 \le 24h \\ -0.016 & when t - t_1 > 24h \end{cases} \qquad 4.8$$

This model is based upon limited data and is very specific to the tested materials. It does not account for fundamental mould growth characteristics but is simply a fit to the data collected. Therefore, it should not be expected to predict growth with much certainty in conditions that are much different than those in the test procedure. However, it does give an example of fitting equations to the data to predict mould growth beyond germination.

More testing needs to be done to validate this model and expand it to cover other substrates and moulds. The mould index could also be verified, and it may be more useful to develop a measure of percent area covered or total volume of mold per area as a better scale.

4.4.11 Sedlbauer Model for General Growth

Sedlbauer (2002) created a model that determined the moisture content of a spore and when a certain value is reached it is assumed to germinate. The spores absorb water from the air by the osmotic potential defined by its chemical makeup, this potential depends on the humidity and is described by the moisture retention curve. Sedlbauer used a modified bacteria curve, shown in Figure 14. The value of water content at which spores will germinate was determined from the previous LIM curves. The minimum humidity required for germination would correspond with the required moisture content in the water retention curve.

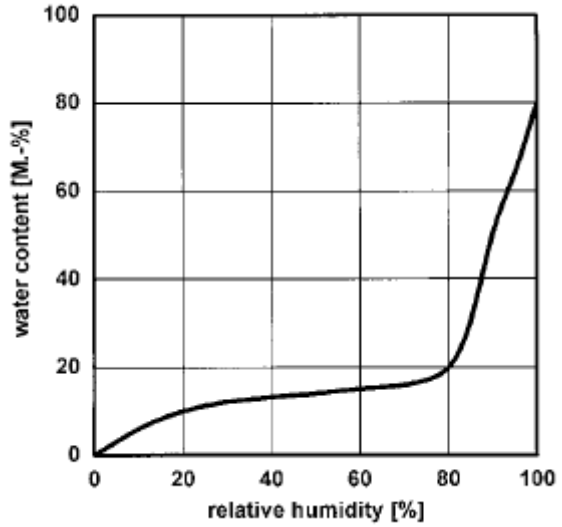

Figure 14. Moisture retention curve of the model spore (Sedlbauer, 2002)

The rate of water absorption will depend upon how quickly water can transfer through the cell wall. Sedlbauer thus gave the pore an equivalent permeability and applied a diffusion equation to the moisture transfer. The permeability was modified so that the model would give the same results as the previous LIM graphs for both substrates I and II to include any effects of the substrate. The resulting permeability is given in Figure 15. Because the values were inferred and not directly measured, Sedlbauer indicates that further testing to derive these values more directly should be conducted.

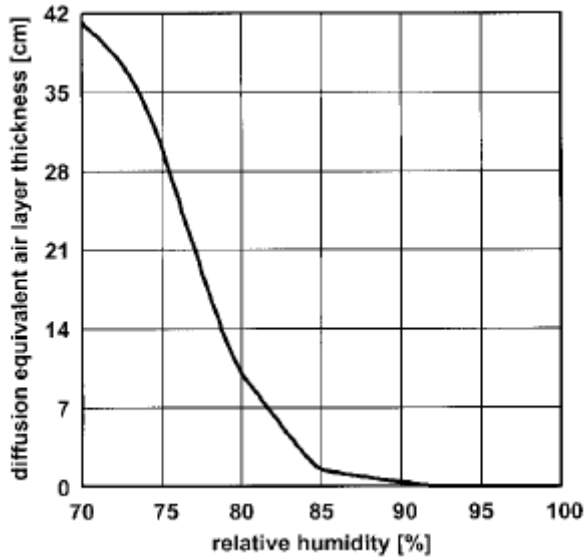

Figure 15. Diffusion of equivalent air layer thickenss of the spore septum (Sedlbauer, 2002).

The spore is then analysed using software such as WUFI to monitor the moisture content of the spore. The spore is modeled in 1-dimension with ambient conditions on both sides, as shown in Figure 16. The spore diameter is about 3μm which is below the capability of the WUFI software, therefore, Sedlbauer converted the diameter to 1cm along with the physical properties.

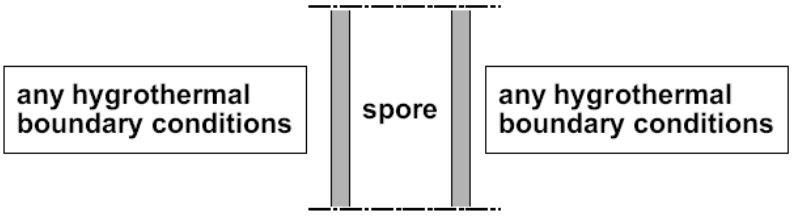

Figure 16. Model diagram from Sedlbauer (2002)

The difficulty with this model is the determination of the moisture parameters of the mould. It would best describe the dormancy compared to other models for the theory of a self-inhibiting agent that needs to be diluted or eliminated before germination can begin. However, growth rate after germination is not included.

4.5 Conclusions

Temperature and humidity are the two factors of mould growth that can be practically controlled in building design. A static limit of 80%RH for all temperatures is overly conservative as it does not include the time to germination, nor does the lowest isopleth for mould. Small fluctuations above these limits are likely not going to lead to mould growth, but cannot be quantified by these methods. Therefore, a more accurate model is desired to provide a wider range of design options.

This will require a dynamic approach to include the time to germination. The simplest dynamic predictor would be to use multiple isopleths in a manner similar to that of Moon (2003) which incorporates the time to germination for various limits of temperature and humidity. However, this method is not capable of predicting the amount of growth nor the effects of dormancy during unfavourable conditions. A complete model will likely be empirically fit to test data such as that by Viitanen (1999), but take into account a larger variety of substrates for wider applicability. Otherwise, further research is required to better understand the relationship between moisture and germination and growth to create a hygrothermal model similar to that of Sedlbauer (2002).

Further work beyond this study is required to refine the existing prediction methods and to confirm their applicability to various substrates.

5 Hygrothermal Properties of Straw Bales and Plaster

Thermal conductivity of straw bales walls has been the most studied hygrothermal property. This was done to aid in presenting the benefits of straw bale construction to garner interest in the technique. Specifically, it was to further establish the environmental benefit of straw bale construction compared to conventional techniques. One benefit of the construction is a higher than average R-value, this reduces energy consumption for heating and air conditioning. In fact a study by CMHC showed an average of 20% less heating energy use for straw bale homes than conventional homes (Gonzalez, 2002). However, this study does not definitively state how much of these savings are from the straw bale wall insulation value. For hygrothermal studies of straw bale walls it is necessary to look at the tests conducted on the thermal conductivity on straw itself as well as tests on the overall resistance of a straw bale wall.

As interest continues in the straw bale industry it is necessary to prove and improve the durability of the construction and hence further hygrothermal properties are required for assessing moisture issues. Straube (2002) conducted a study on the permeance and water uptake of various plasters as a start to the subject, but further testing is still required. In the mean time, it is possible to make reasonable estimates of the hygrothermal properties of the materials in straw bale walls by extrapolating from tests conducted on similar materials. These related studies include those in the agricultural field on straw and grasses, and studies in building science on stucco, plasters, brick, concrete, etc.

5.1 Straw Bales

5.1.1 Thermal Conductivity

The density of typical straw bales ranges from 60 to 160 kg/m^3; however, some machines can produce bales up to 350 kg/m^3. For load bearing applications the straw should be at least 112kg/m^3 (King, 2003), which is specified in the 1995 California straw bale code Article 2(e). The straw used in this study has a dry density of approximately 110kg/m^3.

Similar insulating materials include cellulose fiber, fibrous batts, sugarcane fiber and hemp. Cellulose ranges in density from 37 – 51 kg/m^3 and has a conductivity between 0.039 – 0.046 W/m·K. Batt insulation has a range of conductivities between 0.035 – 0.048 W/m·K (Straube and Burnett, 2005). Hemp insulation ranges from 30 – 70 kg/m^3 with a conductivity of 0.033 – 0.058 W/m·K (Valovirta & Vinha, 2002). A study of the use of sugarcane fiber for insulation yielded a conductivity of 0.047-0.053W/mK for a

density between 100-130 kg/m^3 (Manohar, 2002). Thatch is similar to straw and has a thermal conductivity of 0.070 W/m·K with a density of 240 kg/m^3 (Goodhew, 2005).

Studies have been conducted on different straws of various densities. There have been several types of tests conducted. The most direct test of the thermal conductivity of straw itself is the guarded hot plate test (ASTM C177). Another test method uses a thermal probe inserted into a full scale test specimen and analysis of the temperature rise under a constant power usage (Goodhew, 2004). A third method is a hotbox test performed on a full scale section of a straw bale wall, which may include a single bale or a full wall. This test is the most comprehensive for determining the U-factor of the assembly; it is also possible to find the thermal conductivity of the straw through back-calculations by assuming conductivities for the plaster and surface coefficients. This method gives the best results for the overall R-value of the wall but only approximate results of the conductivity of the straw.

McCabe (1993) is the first widely referenced study on the conductivity of straw. He performed a guarded hot plate test on 133 kg/m^3 wheat straw and found conductivities of 0.054 W/m·K for heat flow perpendicular to the straw, and 0.061 W/m·K for parallel flow (Beck, 2004). Similar studies were conducted by Rissanen (1998), Andersen (2001) and Beck (2004). Rissanen studied flax straw at 35-97 kg/m^3 and found conductivities in the range of 0.039-0.057 W/m·K. Beck studied 80 kg/m^3 barley straw and found a conductivity of 0.041 W/m·K. Andersen studied straw samples at 75kg/m^3 and 90kg/m^3. He found conductivities for flow perpendicular and parallel to the straw of 0.052 W/m·K and 0.057 W/m·K at 75 kg/m^3, and values of 0.056 W/m·K and 0.060 W/m·K at 90 kg/m^3. Tests using the thermal probe technique on unplastered straw have been performed by Acton (1994) and Goodhew (2005). Acton studied 83 kg/m^3 bales and found a conductivity of 0.054 W/m·K (Stone, 2003). Goodhew studied several materials including 60 kg/m^3 straw bales, for which he found a conductivity of 0.067 W/m·K. A summary of these results is given in Table 8.

Study	Density, ρ (kg/m^3)	Thermal Conductivity, λ (W/m·K)	
		Parallel	Perpendicular
McCabe (1993)	133	0.061	0.054
Rissanen (1998)	35-97	0.039-0.057	
Andersen (2001)	75	0.057	0.052
Andersen (2001)	90	0.060	0.056
Beck (2004)	80	0.041	
Acton (1994)	83	0.054	
Goodhew (2005)	60	0.067	
Valovirta[1] (2002)	60	0.047	

1. Valovirta studied loose hemp insulation

Table 8. Summary of straw thermal conductivity from guarded hot plate and thermal probe tests on unplastered samples.

Other testing has been done to determine the overall imperial R-value of a straw bale wall. The first test was conducted by Watts et al. (1995) on an existing straw bale wall by installing numerous thermocouples on the interior and exterior of the wall and applying a heat flux with a hot plate. This study found an overall R-value of 28.4 $^{o}F \cdot ft^2 \cdot hr/Btu$ for an 18.5" wall of unknown straw density (Stone, 2003).

Christian performed two tests at Oak Ridge National Lab, one in 1996 and the other in 1998. The first test was intended as a demonstration to K-12 teachers of measuring thermal conductivities. The teachers helped to apply a stucco exterior and a gypsum board interior. This resulted in notable gaps between these layers and the straw bales. The results gave an R-value of about 17 $^{o}F \cdot ft^2 \cdot hr/Btu$. Due to the low number and the noted deficiencies a second test was conducted to mimic a professionally installed straw bale wall, thus the aid of David Eisenberg, a well known member of the straw bale construction community, was used. The results of the second test showed an R-value of 27.5 $^{o}F \cdot ft^2 \cdot hr/Btu$ for a two-string bale wall with the bales laid flat (Stone, 2003).

Another test was conducted by Stone (1997). He found an R-value of 26 $^{o}F \cdot ft^2 \cdot hr/Btu$ for 3-string bales laid flat and 33 $^{o}F \cdot ft^2 \cdot hr/Btu$ for bales on edge. These results were not taken as the most reliable, as the test was conducted in a frame intended for windows and the gaps around the bales were stuffed with loose straw, as well, the plaster was not allowed

to dry sufficiently before the test was performed. Therefore, convection currents through the loose straw and energy transfer by moisture movement will increase the measured heat transfer.

The last known test was performed by Andersen. He found an R-value for a two-string bale wall to be 27.3 $^{o}F \cdot ft^2 \cdot hr/Btu$ and 29.4 $^{o}F \cdot ft^2 \cdot hr/Btu$ with the bales flat and on edge respectively. A summary of the R-values measured for plastered straw bale walls is given in Table 9.

Study	Bale Type	Bale Orientation	Wall Thickness (in)	Wall Thickness (m)	R-Value ($^{o}F \cdot ft^2 \cdot hr/Btu$)	U-factor (W/m^2K)
Watts (1995)	2-string	flat	18.4	0.467	28.4	0.200
Christian (1996)	2-string	flat	18.5	0.470	17.0	0.334
Christian (1998)	2-string	flat	19	0.483	27.5	0.206
Stone (1997)	3-string	edge	n/a	n/a	33.0	0.172
Stone (1997)	3-string	flat	23	0.584	26.0	0.218
Andersen (2001)	2-string	flat	18.1	0.461	27.3	0.203
Andersen (2001)	2-string	edge	16.4	0.417	29.4	0.196

Table 9. Summary of measured R-values of plastered straw bale walls.

There is a poor correlation between the measured conductivity of straw and the measured R-value of plastered walls. Predicting the U-factor of a plastered straw bale wall using the measured conductivities gives a lower U-factor than is measured. For example, from the study by Andersen the conductivity of straw with heat flow parallel to the grain is 0.057 W/m·K. His plastered sample was 385mm of straw with 76mm of plaster, a total thickness of 465mm. Assuming the conductivity of the plaster of 0.8 W/m·K, the overall U-factor is only 0.15 W/m^2K (R-value of 39 $^{o}F \cdot ft^2 \cdot hr/Btu$) (Andersen, 2001). This is considerably more insulating that the measured U-factor of 0.20 W/m^2K (R-value of 27 $^{o}F \cdot ft^2 \cdot hr/Btu$). Obviously there are other factors that come into play in the full wall assembly. These can be included in a thermal analysis through the use of an effective straw conductivity. This is derived from the measured U-factor and the dimensions of the wall assembly. Assuming a plaster conductivity of 0.8 W/m·K the conductivities are found as shown in Table 10. The conductivity of the plaster does not affect the results very much, unless the plaster is very insulating. However, as the plaster thickness is small and the conductivity of the plaster is an order of magnitude greater than the straw its effect on the calculated straw conductivity is limited to 3% for a straw conductivity of 0.3 W/m·K, which is not a likely case.

Study	Bale Thickness (m)	Bale Thickness (in)	Plaster Thickness (m)	Plaster Thickness (in)	Straw Conductivity (W/mK)
Watts (1995)	0.385	15.2	0.076	3.0	**0.078**
Christian (1996)	0.385	15.2	0.076	3.0	0.133
Christian (1998)	0.385	15.2	0.090	3.5	**0.081**
Stone (1997)	0.470	18.5	0.100	3.9	**0.083**
Stone (1997)	0.580	22.8	0.100	3.9	0.130
Andersen (2001)	0.385	15.2	0.076	3.0	**0.080**
Andersen (2001)	0.365	14.4	0.052	2.0	**0.072**

Table 10. Straw conductivity as computed from wall assembly U-factor.

The measured conductivity of straw is approximately 0.055+/- 0.005 W/m·K. However, the effective conductivity for the straw as determined by measured wall U-factors is about 0.080+/-0.003 W/m·K for flow parallel to the grain, the one value for conductivity perpendicular to the grain is 0.072 W/m·K from Andersen, again showing a better performance. For poor construction as noted in the erroneous tests the conductivity is about 0.13 W/m·K.

This range of values shows the effect that construction technique may have on the insulation value of the straw. Poor technique will result in a large reduction in the effective conductivity, more than doubling it, whereas, current practice provides a conductivity about 45% more than is measured under ideal conditions. This indicates that there may be further refinement to increase the thermal performance of straw bale walls. For current design practice it is advisable to use a conductivity of 0.08 W/m·K to be on the conservative side, also noted by Andersen. Straube and Burnett (2005) have reported a range between 0.06-0.075 W/m·K between the ideal and the effective values. This should be the range of conductivities aimed for in best practice, with perpendicular to grain conductivities between 0.060 and 0.070 W/m·K and parallel to grain between 0.065 and 0.075 W/m·K.

5.1.2 Factors Affecting Straw Conductivity

Details

Plaster intrusion into the bale and bale joints will decrease the effective thickness of the bale insulation. This reduces to overall R-value of the wall, without reducing the conductivity of the straw.

Poor adhesion of the plaster to the bales may result in air gaps between the bale and plaster. Also, gaps may occur where bales do not fit snuggly to the opening and so loose straw is stuffed in. These gaps will result in convective air currents that may increase the heat flow through the wall.

Air Permeability and Convection

Studies have shown the dramatic effect of connected air spaces that bypass insulation in cavities. It was also noted in the first study by ORNL that air gaps were noticeable between the plaster and the straw, which is one reason postulated for a lower R-value in that test. Andersen (2001) mentions that convection within the wall may increase the U-factor by more than 10%, from 0.15 W/m^2K to 0.17 W/m^2K in his study. Although, it is not clear if this is due to convection in air gaps or within the bale itself, it is assumed that this is due to convection within the bale itself as no mention was made of poor construction of the plaster.

Rissanen (1998) found an air permeability of unpacked flax insulation between 1.2-$8.4x10^{-9}m^2$ and packed flax of 0.4-$4.3x10^{-9}m^2$. He states that such a high permeability to air will allow for natural convection within the insulation that can lower the insulating ability. This effect is increased with larger temperature differences through the straw. Rissanen calculated that the heat conductivity would increase by 5-10% for a thickness of 0.2m with 40 kg/m^3 flax insulation and a temperature difference of 40^oC due to convection within the insulation.

Moisture

Vilovirta (2002) found the conductivity for loose hemp fibre insulation to be 0.045 W/m·K at 10^oC and 33%RH, while at 85%RH it increased 20% to 0.055 W/m·K.

Hansen (2001) found an increase in conductivity for insulation materials at high levels of humidity. He found that the most marked increase occurred when condensation occurred at the cold plate of the test apparatus. This occurred for an average RH of 75% and above in some samples. This results in the latent heat of moisture evaporation at the hot plate and condensation at the cold plate reflecting in the overall heat transfer. The effect causes up to a 50% increase in conductivity, and maybe more, although it was noted that a stable condition was not able to be achieved during these tests.

Kehrer et al. (2003) studied the effect of adsorped water on the thermal conductivity of ecological insulations and also found that the effect of the redistribution of vapor in the

insulation causes enthalpy flows that result in increased heat flow measured by the device. They showed that this effect can be cancelled by diurnal fluctations in vapor flow. For a situation of outward vapor drive at night with subsequent daytime solar heating that causes inward vapor drive during the day, the overall effect of the enthalpy flow from the vapor is zero and the average heat flow through the wall is the same as for a dry condition. However, they do not state the effect of prolonged outward vapor drive for a shaded wall that will likely not see inward vapor drive for the winter season. In this case the continual vapor diffusion will add to the total energy lost through the wall, but it should be accounted for separately from the conductivity of the insulation.

Further studies should be undertaken to fully account for this phenomenon, as one of the greatest benefits of straw bale construction is its thermal performance. It would be best to understand all the effects that may reduce this. It is especially important for cold climates and walls of northern exposure. However, it is desirable to keep the moisture content of straw insulation down to prevent molding and therefore the effect may not occur in proper design.

Temperature and Density

Other factors that will affect the conductivity are the temperature, which has an effect on the radiative component of heat transfer through the straw, as well as the density which changes the distribution heat transfer modes through the straw. For example, higher densities increase the conduction mode of transport but decrease the convection and radiation modes. At higher temperatures the radiation mode of heat transfer is increased and so generally the overall conductivity increases as well.

With most insulating materials there is an optimum density for which the lowest conductivity can be achieved. This is a result of minimizing the effects of all three modes of heat transfer. At too low of a density convection and radiation are high and at too high a density conduction is too high, but somewhere in the middle is a balance of all modes and a minimum overall conductivity. For straw bales over 40kg/m^3 it appears that thermal conductivity will increase with increasing density, as shown in Figure 17. An optimum between 0 and 40 kg/m^3 may be found but is below the practical densities for straw bale walls.

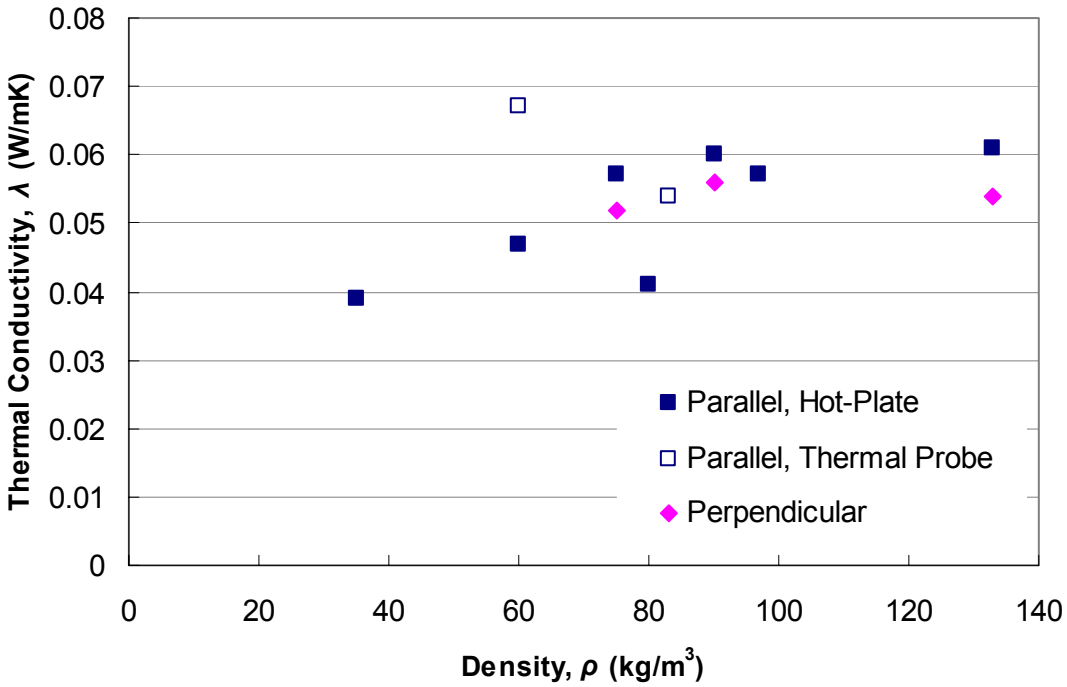

Figure 17. Measured thermal conductivities in relation to density as given in Table 8.

Straw Orientation

The orientation of the straw fibers in the bale also affects the heat transfer. Heat flow parallel with the fibres is generally higher than flow perpendicular to the fibres as seen in McCabe's (1993) and Andersen's (2001) results. It was also seen in Vilovirta's (2002) results on hemp insulation products that the samples with heat flow perpendicular to the grain of the hemp had lower conductivities than the samples with random orientation.

This may be explained by the more tortuous path for heat flow by going perpendicular to the straw. This requires heat flow to pass through more points of contact which reduces the flow, as well as the shorter radiation paths that are available. In addition conduction flows do not travel in straight lines but have to follow the outside of the stem, which produces a longer path, thereby reducing the overall conductance. Whereas, when the heat flow runs parallel to the grain there are more direct conduction routes along the stem, as well as radiation paths through the hollow of the stem.

5.1.3 Vapor Permeability

Some materials for which vapor permeability have been determined, which are similar to straw, are cellulose insulation (ρ = 25-50 kg/m^3, μ = 110-130 ng/Pa·s·m), wood fibreboard (ρ = 340 kg/m^3, μ = 20-60 ng/Pa·s·m), wood-wool cement board (ρ = 400

kg/m^3, μ = 30-40 ng/Pa·s·m) and straw light clay (ρ = 450 kg/m^3, μ = 80 ng/Pa·s·m) (Straube, 2002). Straw bale is less dense than wood fibreboard, wood-wool cement and straw light clay, and therefore it is likely that its permeability will be above 40, 60, and 80 ng/Pa·s·m. However, it is less dense than cellulose insulation and so can be expected to be lower than 110 ng/Pa·s·m. Therefore, Straube has suggested a range of 50-100 ng/Pa·s·m for straw bales.

The most similar material of those shown is straw light clay (SLC). It is essentially the same network of straw fibres as used in a straw bale, however, they have been coated in a clay slip. This results in the fibres being somewhat bonded and the pore spaces reduced, thereby giving SLC a higher density. Thornton (2004) performed a study on SLC. He found permeabilities ranging from 27-60 ng/Pa·s·m for densities from 632-951 kg/m^3. A reference to Minke (2000) gives a range of permeability from 40-82 ng/Pa·s·m, for densities of 450-1250 kg/m^3. There was a good relationship between density and permeability in both studies, with permeability increasing with decreasing density. Therefore, it should be expected that straw with a density range between 60-150 kg/m^3 would have a higher permeability than reported for SLC. So a recommended lower limit for straw is 80 ng/Pa·s·m.

As straw is denser than cellulose insulation it may be expected to be less permeable, although a direct correlation cannot be made due to the difference in the materials. But this would put an upper limit of 120 ng/Pa·s·m. From these values it may be estimated that straw will have a permeability of about 100 ng/Pa·s·m, at the upper end of Straube's estimate.

However, a study on straw samples of densities between 50-80 kg/m^3 showed a wet cup permeability of 144 ng/Pa·s·m for diffusion parallel to the straw grain and 240 ng/Pa·s·m perpendicular to the grain. The uncertainties in the testing procedure result in a potential range of values for parallel and perpendicular from 120-180 ng/Pa·s·m and 180-360 ng/Pa·s·m respectively (Andersen, 2001). These results are considerably higher than estimated. There was also no correlation found between density and permeability over the range of densities tested. From these results it may be expected that straw permeability will be at least 100 ng/Pa·s·m.

The test on straw permeability was conducted at a temperature of 23^{o}C for which the permeability of still air is 198 ng/Pa·s·m at standard atmospheric pressure. Some of the results are obviously greater than the permeability of still air which is not possible for pure vapor diffusion. This was mentioned in the study as they found the results for flow

parallel to the straw were initially greater than that for still air, after applying corrections to the measured values. They suggested that the air speed used in the test (2 m/s) may have induced air flows in the sample, thereby increasing the permeability. Efforts were taken to reduce this effect in the reported results. Yet the values are still high. The diffusion resistance factor for flow parallel to the grain is 1.4 and perpendicular is 0.83. However, as the permeability for still air is the limiting case, the range of diffusion resistance factors for straw will be between 1.0 and 1.4 as found in this testing.

Hansen et al (2001) found similar results for cellulose, flax, and other insulating materials. The average density of the materials tested was about 40 kg/m^3 with a range between 16-85 kg/m^3. He noted that some of the corrected values were near or greater than that for still air. He suggests the corrections may be greater than allowed, but states that a study by Lackey et al (1997) shows a permeability nearly equivalent to that of still air for medium density glass fiber board when approaching 100%RH. The least permeable materials were the most dense at 65 and 85 kg/m^3 and had a permeability of about 105 ng/Pa·s·m. The other samples had values up to and above 200 ng/Pa·s·m. Again the test was conducted at 23^{o}C where the still air permeability is 198 ng/Pa·s·m at standard atmospheric pressure. It is expected that straw bales will exhibit lower permeabilities than the materials tested due to their higher density.

The interesting results of these tests really indicate the varying nature of water transport through hygroscopic materials. As relative humidity increases so does the adsorbed water levels. It has been proposed that it is possible to have a greater permeability than still air through "water canal/water island" effects and surface diffusion of adsorbed moisture. Thus it may be that straw will have a permeability as high as that for still air near 100% RH, which will show up in the wet cup tests, but lower values for lower RH. However, Hansen et al (2001) also conducted dry cup tests for the insulation materials they tested and found the permeabilities to be within 10-15% of the wet cup values. This is much different than the results for oriented strand board (OSB) which has a 30-fold increase in permeance from 20% to 90%RH (Straube & Burnett, 2005).

Based on these tests and suggestions, it is likely that straw bales have a permeability around 100 ng/Pa·s·m. This gives a diffusion resistance factor of 2.0 and it may be as low as 1.0 for low density straw (60kg/m^3).

5.1.4 Sorption Isotherm

Some studies have been conducted on straw and other biological materials for their use as building materials. But, most studies of the sorption isotherm for straws, hays, and

grasses have been conducted in the agricultural field. A review of various studies gives a reasonably precise estimate for the adsorption isotherm for straw bales.

Hedlin (1967) tested the sorption isotherm at 21^{o}C of 5 types of grain straw common to the Canadian prairies at the time. They were thatcher wheat, cypress wheat, garry oats, jubilee barley and redwood flax.

Duggal and Muir (1981) tested the sorption isotherms at 5, 15, 25, and 35^{o}C of straw from Glenlea utilility wheat grown in Manitoba. They fit 6 mathematical models (Henderson, Day-Nelson, Henderson-Thompson, Chung-Pfost, Strohman-Yoerger, and Chen-Clayton) to the data and found the Henderson-Thompson model produced the minimum residual sum of squares. However, the shape of this equation does not follow well the shape of the isotherm at extreme RH; it overpredicts the MC at high RH and underpredicts at low RH. Therefore, only the data results will be used.

Lamond and Graham (1993) reviewed previous testing on grass mixtures and fit four models to the data (Dumont and Park, Henderson, Savoie et al. and Gompertz). They found the more complex double Gompertz equation gave the best result for predicting EMC through all ranges of RH, while simpler models such as the Henderson predict the EMC well through a limited range of RH.

Nilsson et al (2005) studied the adsorption on flax straw, hemp stalks and reed canary grass at temperatures of 5, 15 and 25^{o}C. They compared 5 commonly used equations (modified Henderson, modified Chung-Pfost, modified Halsey, modified Oswin and the modified GAB) to determine which best represented the measured results. They found the Modified Halsey best represented the sorption isotherm for un-retted flax straw, with coefficients A=5.11, B=-0.00846, and C=2.26; it was also best for the reed canary grass with coefficients A=6.63, B=-0.0321, and C=2.72. The modified Oswin model best suited the un-retted hemp isotherm with coefficients A=10.6, B=-0.0229, C=2.96.

Valovirta and Vinha (2002) conducted tests on loose hemp insulation. Their results were stated to be similar to flax insulation tested by Rissanen and Viljanen (1998). Tests on various processed fractions obtained from hemp, flax, and linseed were tested by Kymalainen and Pasila at 21^{o}C (2000).

All the previous test results are shown graphically in Figure 18. An average was fit based on visual inspection. Greater weight was given to Lamond and Hedlin's studies. Sain (1975) and Valovirta's results are noticeably lower than the other studies. Sain's samples were ground to pass a 2mm sieve, while other studies used more raw straw samples, for

example Hedlin cut straw to 64mm samples. The sample size may have some effect, but Waite (1949) found little variance when he tested the effects of sample size of cured hay on the measured adsorped moisture content. His results are shown in Table 11.

Compare the results for straws and grasses with those of other materials in Figure 19.

	Size of sample				
Botanical species	Uncut	2 in.	½ in.	Meal	Mean
Timothy (*Phleum pratense*)	10·6	11·1	10·8	10·3	10·7
Meadow grass (*Poa pratensis*)	10·2	9·9	10·1	9·6	10·0
Yorkshire fog (*Holcus lanatus*)	10·4	10·9	10·4	10·9	10·6
Italian rye (*Lolium italicum*)	10·8	10·4	11·2	10·8	10·6
Mean	10·5	10·6	10·6	10·4	10·5

Table 11. Effect of sample size on moisture content measurements at 60%RH (Waite, 1949).

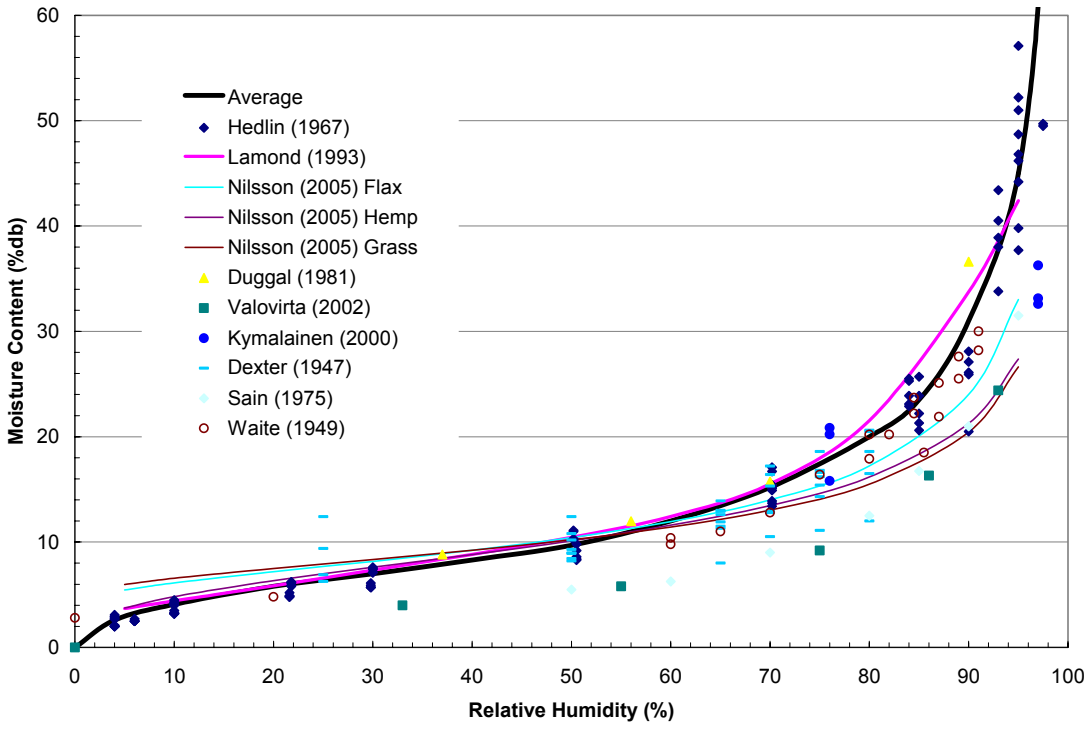

Figure 18. Combined sorption isotherm chart with results at 21°C, except for Valovirta at 25°C and Duggal at 23°C.

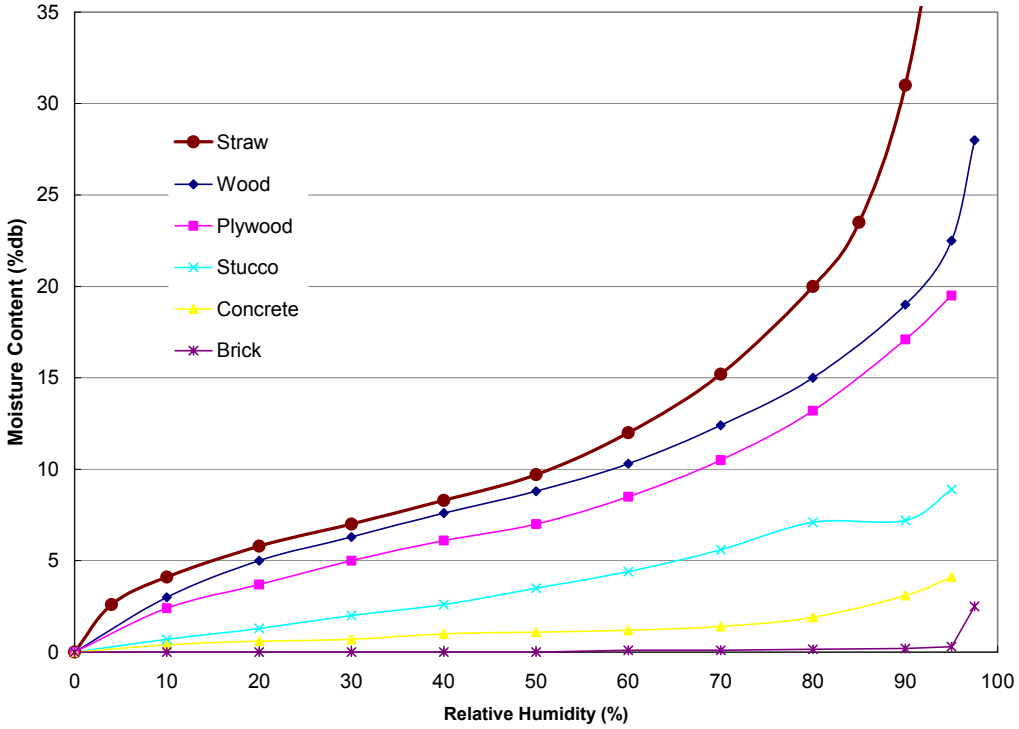

Figure 19. Comparison of sorption isotherms for different building materials from Straube (2002), including straw data from this paper.

It can be seen that straw follows a similar curve to that of wood at lower humidities (0-70%RH). They are both cellulosic in nature and the available surface area per mass is expected to be similar. However, above 80%RH the moisture content in straw increases at a faster rate than for wood. This is due to the larger pores in the bulk straw that continue to adsorb moisture at higher relative humidities (Rissanen, 1998).

The density of the individual cells will be roughly the same for both straw and wood, since they are a similar material, so the resulting difference in bulk density is due to larger pore volume in bulk straw. This results in densities of 80-150 kg/m^3 for straw and 400-700 kg/m^3 for wood. However, it should be noted that these curves are on a mass basis and not by volume. In fact, wood will adsorb more moisture per volume than straw nearly to saturation. At 90% RH wood has 19%MC while straw has 27.1%MC, changing to a volume basis wood has 19%*500kg/m^3= 95kg/m^3 moisture and straw has 27.1%*120kg/m^3 = 33kg/m^3. Near saturation the amount of water wood can adsorb is approximately 35% which results in a volumetric capacity of 175kg/m^3. Straw is able to adsorb up to 150% which results in a volumetric capacity of 180kg/m^3. The saturation value is expected to be higher than wood based on density alone, and the expectation of more pore volume that can be filled.

Variation within temperatures normally experienced by buildings is minimal, especially noted in the study by Nilsson (2005) for flax and hemp. The equation used by Lamond (1993) shows little temperature dependence and Lamond states it can be used over a temperature range of 10-50^{o}C. The variation of adsorption due to temperature differences is within the range of the uncertainty of the average curve, and therefore, does not affect the estimation significantly. But it is generally expected that lower temperatures result in higher adsorption.

Hysteresis is not well documented, but a larger effect is expected at higher RH due to the ink bottle effect in the capillary condensation range and reduced effect at lower RH. Hedlin (1967), gave desorption values shown in Figure 20 compared to adsorption. The difference in adsorbed moisture between adsorption and desorption is not considerable when compared to the uncertainties of the variation between types of straws. Therefore, an acceptable average value can be used to represent both adsorption and desorption.

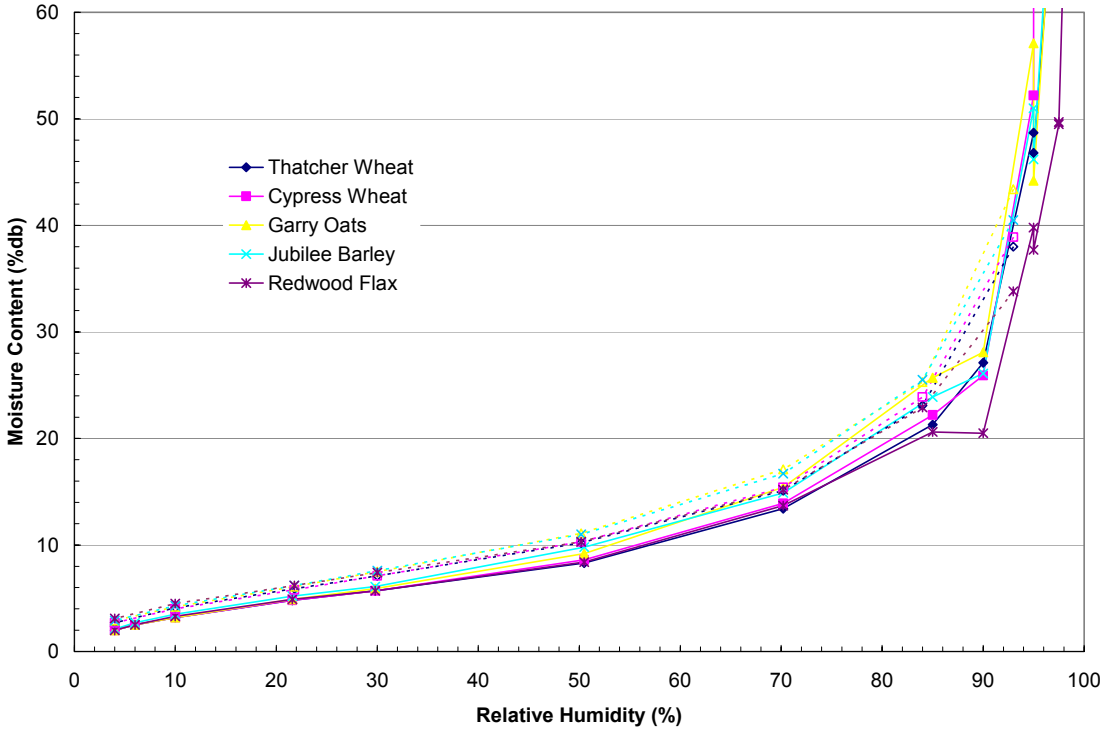

Figure 20. Adsorption-desporption hysteresis for five types of straw, with desorption shown as a dashed line (Hedlin, 1967).

The average curve found here represents a large number of types of straw and grass and therefore is not overly precise but can be used as a representative adsorption curve for these types of materials. The greatest uncertainty is at relative humidities above 80%.

This is due to difficulties in measurement as well as the steepness of the curve which will cause large errors in the results for small errors in testing conditions. Another factor that affects the study of sorption at high humidities is the growth of mold on the samples. Control of this effect was noted in Hedlin's study (1967) and Dexter's data (1947) showed samples with visible mold, Waite (1949) also noted the divergence of measurements due to mold growth.

5.1.5 Water Uptake

There have not been direct measures of water uptake for straw of which the author is aware. However, there have been some related studies on water absorption: loose hemp insulation, straw light clay, and other insulating materials. Results from these studies are tabulated in Table 12 and Table 13. From these range of values an absorption coefficient for straw will likely be between 0.001-0.03 $kg \cdot m^{-2} \cdot s^{-1/2}$, which is a large range and not definitive, but provides a basis for further work.

The walls of the straw stalks will absorb water by capillary action, in a similar manner to wood. Pine has a water absorption coefficient of 0.004 $kg \cdot m^{-2} \cdot s^{-1/2}$ for suction perpendicular to the grain and 0.016 $kg \cdot m^{-2} \cdot s^{-1/2}$ parallel to the grain (Straube & Burnett, 2005). However, the connectedness of the walls between stalks of straw is minimal and the large pores between stalks will minimize this capillary effect. It is expected that there will be minimal water uptake and what straw is capable of absorbing will occur rapidly. There will be some capillary movement after the initial absorption, however, it is expected to be slow in comparison to movement by vapour diffusion.

Assuming an average pore size of 0.45mm in a straw bale specimen (Beck, 2004), the capillary rise would be 65mm, which is not overly significant for the scale of the wall. This distance can be considered the transition from the plaster to the straw; liquid water is not expected to wick considerably into the wall. Rather it will concentrate at the plaster interface.

The effects of water infiltration through the plaster may be more complex as there is a 2-dimensional flow pattern. It may be possible that water infiltrating at upper locations will have more time to move laterally into the wall, as it has further to move vertically by gravity. Therefore, it may be expected that higher concentrations of liquid water will appear in lower sections of the wall and reaching further inward.

Study	Material	Density (kg/m^3)	Water Absorption Coefficient ($kg \cdot m^{-2} \cdot s^{-1/2}$)
Valovirta (2002)	Loose Hemp Insulation	60	0.028

Valovirta (2002)	Mat hemp insulation	45	0.019
Thornton (2004)	Straw Light Clay	645	0.006 (3.4 $kg \cdot m^{-2} \cdot hr^{-1/2}$)

Table 12. Summary of water absorption coefficient testing on related materials.

Material	Water Absorption Capacity ($kg \cdot m^{-2}$)	Water Absorption Coefficient ($kg \cdot m^{-2} \cdot s^{-1/2)}$	Mean Water Content (Weight %, 105°C)
Cellulose-1	39	0.56	550
Cellulose-1	67	0.81	657
Cellulose-3	37	0.27	453
Sheep's Wool	2.5	0.012	79
Flax	2.9	0.016	387
Perlite	66	0.27	314
Perlite SR	0.5	0.005	3.4
Rock Fiber	0.1	0.001	5.8
Glass Fiber	3.0	0.03	394

Table 13. Summary of water uptake study on insulating materials (Hansen et al., 2001).

5.1.6 Specific Heat Capacity

The heat capacity of hemp fibre (1352.3 J/kg·K) and cellulose (1300 J/kg·K) is reported in the *2005 ASHRAE Handbook of Fundamentals*. In addition the heat capacity for softwoods at 12%MC is reported to be 1630 J/kg·K. Therefore, the heat capacity of straw can be approximated at 1400-1500 J/kg·K.

5.2 Plasters

There are various coatings that can be applied to straw bales. They must be applied in a wet and adhering form so that a proper bond will develop with the straw bales. This is necessary for integrity and to eliminate air gaps between the finish and the bale. For this reason it is not a recommended practice to use sheet products to finish bale walls. Instead various types of plasters or stuccos are used. Sheet products could be installed over these finishes, but would be redundant.

The interior and exterior plasters provide several functions. They serve to stop the flow of air through the bales, to stop rodent and insects from entering the wall, give structural support in load bearing applications, provide general structural integrity of in-fill walls, can be used as a vapor retarder when combined with other finishes, and are a rain control layer.

Plasters are of several basic types depending on the bonding agent. They can be made of Portland cement, lime or clay and sometimes a combination of these. In addition to the three primary binders are pozzolans, which can be substituted for parts of the primary binder but are not used on their own. Some examples of pozzolans are fly ash and silica fume, these types of additives are generally used in structural concrete applications and not often in plastering. Gypsum plaster is also used for interior finishes, often only as a final topcoat, but cannot be used for exterior applications due to its poor durability.

Cement and lime are both derived from limestone but differ in their production and use. Cement also uses clay or shale in production. The raw materials are ground to fine particles and heated to 1400-1500^{o}C to form clinker. The clinker then is ground down to finer particles which is the final cement product. Cement particles hydrate when mixed with water to form a solid material. This is a relatively rapid process such that 60% of the final strength is attained within 7 days and most is developed within a month.

Lime is produced through "calcining" of limestone by heating it to 1000^{o}C which drives off CO_2 from the limestone ($CaCO_3$) to leave quick lime (CaO), so called because it will react quickly with water. The quick lime must be hydrated to form calcium hydroxide ($Ca(OH)_2$) before being applied as a plaster, this requires the quicklime to be soaked in water for a period of time (up to years for complete hydration). The result is a lime putty, which is often dried and delivered in powdered form. The process can also be completed by a plasterer but often manufactured hydrated lime is purchased. For plastering, the hydrated lime is mixed with sand and water (if using a powdered hydrated lime) until the desired consistency is reached. It is at this point that the lime starts to react with CO_2 in the atmosphere to convert back to $CaCO_3$ (limestone).

There is no chemical reaction in the use of clay plaster nor in the production of the material. Rather raw clay is combined with water to make a paste that is applied to the wall (other additives such as sand and straw may also be used). The paste then dries and forms a hard plaster. This occurs due to the nature of clay. If the clay is rewetted it can be reformed.

Cement and lime are often combined in plaster applications to benefit from the strength of cement and the workability of lime. The ratios for mixing are typically reported as cement:lime:sand and 1:1:6 is very common, also 1:2:9 in straw bale construction is used. Lime sometimes may be added to clay but this is not as common.

Finish treatments vary depending on desired aesthetics. However, finishes will also affect the moisture properties of the plaster. Water absorption can be reduced by using a

water repellant finish such as siloxane or by topical coatings like paint. Vapor permeability can be reduced by paints

5.2.1 Thermal Conductivity

Some reported thermal conductivities for plasters and similar materials are shown in Table 14. The general range appears to be 0.5-1.0 W/m·K for various types of plasters, for analysis 0.8 W/m·K will be used as representative for all plasters as specific comparisons are not available. It is expected that lightweight plasters would be more insulating than dense plasters, but the variation between 0.5-1.0 W/m·K does not cause a significant change in the temperature profile as the overall R-value of the plaster is less than 5% of the R-value of the straw, see Figure 21 for the change in temperature profile. The greatest change is noticed at the inside of the exterior plaster where it decreases by 0.25^{o}C for a change in thermal conductivity from 1.0 W/m·K to 0.5 W/m·K.

Source	Material	Thermal Conductivity (W/m·K)
Straube and Burnett (2005)	Sand plaster / lath	0.71
	Gypsum plaster / lath	0.16-0.35
	Gypsum plaster w/ sand	0.8
	Sand:cement plaster	0.53
	Concrete	1.4-2.6
Womersley's Ltd (n/d)	Clay one-coat plaster	0.66
Tierrafino (2008)	Tierrafino clay finishing plaster	0.91
Cerny et al. (2003)	Lime plaster	0.73

Table 14. Reported thermal conductivities for plasters and similar materials.

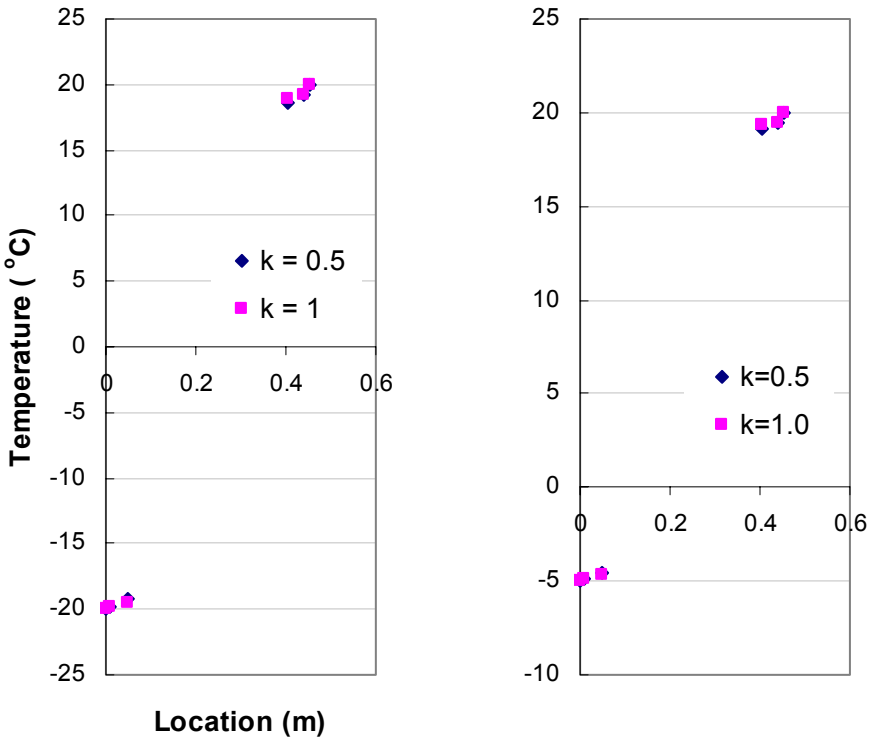

Figure 21. Comparison of variation in plaster conductivity for exterior temperature of -20°C (left) and -5°C (Right). Interior is 20°C.

5.2.2 Permeability

There have been several studies on the permeability of plasters. The results are listed in Table 15.

Study	Plaster Material	Permeability (ng/Pa·s·m)
Straube (2000)	Cement	1.7
	1:1 Cement:Lime	10.3
	1:2 Cement:Lime	14.9
	Lime	18.8
	Lime	18.9
Minke (2001)	Clay soil	25.7
	Clay Earth Plaster	23.3
	Silty Earth Plaster	19.1
	Strawclay (1250 kg/m^3)	41.3
	Strawclay (450 kg/m^3)	82.7
	Lime Plaster	16.9

Study	Plaster Material	Permeability (ng/Pa·s·m)
Straube (2002)	1:0.2 Cement:Lime	13.7
	1:1 Cement:Lime	19
	Lime	30.1
	Earth 1	45.7
	Earth 2	41.2
	Earth 3	40.1
Andersen (2002)	Clay Plaster	25 (wet) 16.7 (dry)
	Lime Coarse	19 (wet) 18.2 (dry)
	Lime Fine	13.3 (wet)
	Clay Plaster w/ Chopped Straw	22.2 (wet)

Table 15. Plaster permeabilities.

5.2.3 Clay Plaster Permeability

Straube (2002) reported a permeability for clay plaster between 40-45 ng/Pa·s·m. Andersen (2002) showed a value 25 ng/Pa·s·m for clay plaster (16 ng/Pa·s·m dry cup) and 22 ng/Pa·s·m for clay plaster mixed with 30% straw. Minke (2001) reported values of 23.3 ng/Pa·s·m and 25.7 ng/Pa·s·m for clay plaster and clay soil respective ely, while 41.3 ng/Pa·s·m for straw-clay at a density of 1250 kg/m3. Thornton (2004) reported a value of 27.4 ng/Pa·s·m for straw light clay in the density range of 880-960 kg/m^3. Higher values were reported by Minke and Thornton for straw-clay mixtures at lower densities up to about 80 ng/Pa·s·m. There is inherent variability due to the type of clay used, if sand was added and the amount of straw added if any. The range of reported values is 22-45 ng/Pa·s·m with values being reported at either end (22-27 ng/Pa·s·m and 40-45 ng/Pa·s·m). These may be results of density variations due to mix proportions and placement procedure. For use in this study Straube's results will be given the greatest weight, but the other values will be considered in parametric studies. Therefore a clay plaster at 42 ng/Pa·s·m and one at 25 ng/Pa·s·m will be used.

5.2.4 Cement-Lime Plaster Permeability

One variable is the ratio of lime to cement. Increasing the lime content was found to increase the permeability. A 1:1:6 mixture had permeability of 10.3 ng/Pa·s·m and a

1:2:9 mixture had a permeability of 14.9 ng/Pa·s·m (Straube, 2000). Again two values will be used: one plaster at 10 ng/Pa·s·m and another at 15 ng/Pa·s·m.

5.2.5 Lime Plaster

Lime plasters have reported values from 13-19 ng/Pa·s·m. A value of 15 ng/Pa·s·m will be used, this will be the same as for one of the cement-lime plasters.

5.2.6 Cement Plaster

Straube (2000) reported a permeability of 1.7 ng/Pa·s·m for a cement:sand mixture of 1:3. Straube and Burnett (2005) reported a range of values for cement stucco from 5-12 ng/Pa·s·m for wet cup and 3-8 ng/Pa·s·m for dry cup. Concrete has a range of 2-6 ng/Pa·s·m. A value of 5 ng/Pa·s·m will be used.

5.2.7 Variation with Humidity

All plaster permeabilities appear to have a dependence on humidity. The permeability increases as the moisture content of the plasters increases. Specific studies were not found and so the permeabilities will be assumed constant over all ranges of moisture content.

5.2.8 Effect of Surface Finishes

Surface finishes are applied to plasters to reduce the water uptake (siloxanes, linseed oil, etc.), to act as a wear layer (lime wash), and as a general finish (paints). Most serve more than one purpose, even if not intended. The effects of some these finishes were studied by Straube (2000) and will vary with each particular product. Some of Straube's findings on 1:1:6 (Cement:Lime:Sand) plaster are shown in Table 16 for reference.

Applied Finish	Thickness (mm)	Permeance (ng/Pa·s·m^2)
None	35	295
Linseed	36	223
Elastomeric	32.5	244
Siloxane	41	203
Latex paint	36.5	203
Oil paint	40	41

Table 16. Effect of surface treatments on plaster permeance for 1:1:6 cement-lime plaster (Straube, 2000).

5.2.9 Sorption Isotherm

Various sorption isotherms are displayed in Figure 22. Stucco, mortar and concrete are found in Straube (2002); lime plaster, two lime-cement plasters, and clay plaster are found in Matiasovsky (2006); three clays are found in Chemkhi (2004); Unfired clay bricks are found in Hansen and Hansen (2002). A sorption isotherm was found for Bentonite Clay but was drastically higher than those shown here, likely due to the expansive nature of Bentonite (Mihoubi, 2006).

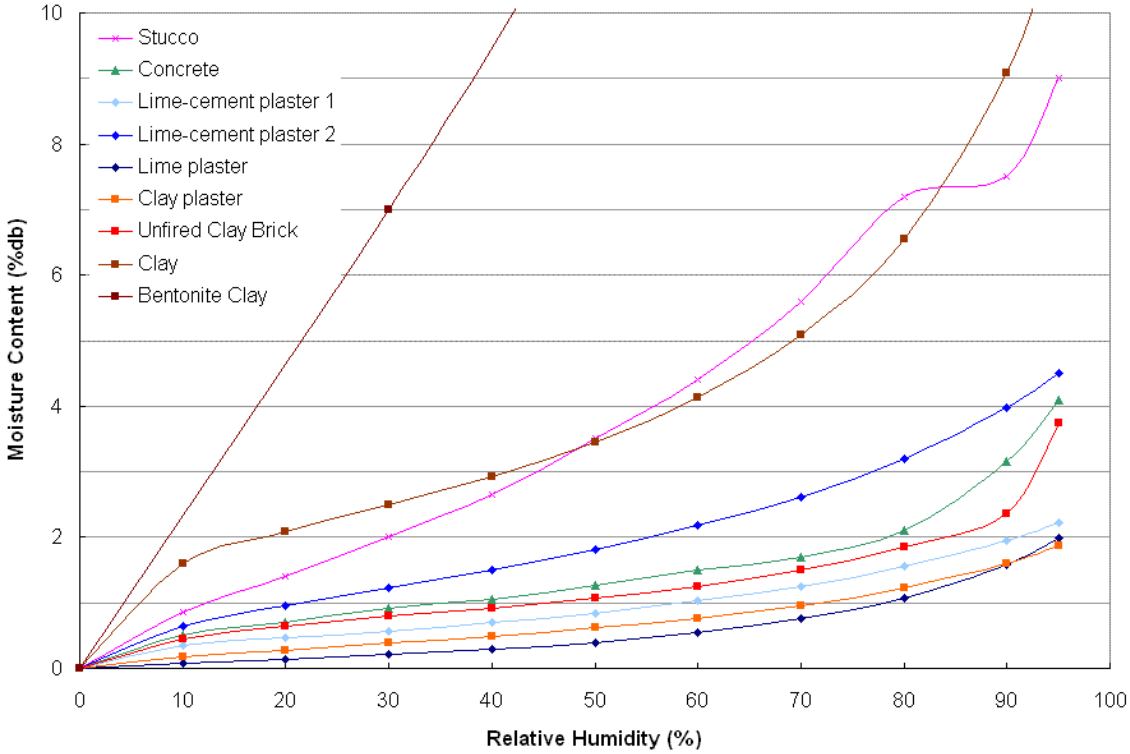

Figure 22. Sorption isotherms for various plasters.

5.2.10 Water Uptake

Results from Straube (2000, 2002) and Minke (2001) are shown in Table 17.

Study	Plaster Material	Water Uptake Coefficient ($kg \cdot m^{-2} \cdot s^{-1/2}$)
Straube (2000)	Cement	0.0378
	1:1 Cement:Lime	0.0917
	1:2 Cement:Lime	0.11
	Lime	0.1273
	Lime	0.1725
Minke (2001)	Earth	0.152
	Strawclay (1150 kg/m^3)	0.052
	Strawclay (450 kg/m^3)	0.04
Straube (2002)	Cement	0.059
	1:1 Cement:Lime	0.083
	Lime	0.164
	Earth 1	0.075
	Earth 2	0.068
	Earth 3	0.067

Table 17. Water uptake coefficients from Straube (2000, 2002) and Minke (2001).

From these results, clay plaster mixed with straw may have a range from 0.04-0.15 $kg/m^2s^{1/2}$ with an expected value of 0.075 $kg/m^2s^{1/2}$. Cement plaster is as low as 0.04 $kg/m^2s^{1/2}$, lime plaster as high as 0.17 $kg/m^2s^{1/2}$, with cement-lime at about 0.08-0.09 $kg/m^2s^{1/2}$.

5.2.11 Heat Capacity

Straube and Burnett (2005) give a range of 800-900 J/kg·K for concrete, brick, rock and minerals. The *ASHRAE Handbook of Fundamentals* (2005) gives a value of 920 J/kg·K for clay.

6 Case Studies on Straw Bale Walls

The majority of current research on moisture in straw ball walls comes in the form of case studies. These are typically a study of the humidity levels within the straw bale walls of an inhabited house. Rarely were the buildings constructed for the testing and often sparse manual readings are the only data collected. As a result these tests are useful to assess the macro-level performance of straw bale walls with respect to moisture and to provide general recommendations on construction techniques, but usually do not provide much detail on the mechanics of moisture movement.

6.1 CMHC (1997-2000)

There have been several studies on various aspects of straw bale buildings sponsored by the Canada Mortgage and Housing Corporation (CMHC). A few of these studies investigated moisture and molding. Gagné (1997) provided a study on houses in Quebec. These were a unique construction in that the bales were plastered on all sides and then assembled; in addition some houses had floor slabs on grade insulated with straw bales.

Wet straw and molded areas were traceable to moisture sources and entrapment where there was net annual wetting. No deterioration was found simply as a result of the straw being in contact with the stucco. Floor insulations showed noticeable rotting with moisture contents above 45% and up to 300% with liquid water visible. An extreme example was a straw insulated swimming pool: in this case only a pile of compost remained at the bottom of the insulation cavity. These findings are not remarkable, but simply act as a reminder that straw will rot when it gets wet. The key is to ensure that through the wetting and drying cycles the net result is drying; in the cases found here the net result was wetting and hence rotting occurred.

Jolly (2000) monitored the walls of eight houses in Alberta and one in Washington State between 1997 and 2000. Sensors were placed in three locations, behind the exterior plaster, middle of the bale, and behind the interior plaster. Initially, only mid bale monitors were used. The first year showed most relative humidities in the mid-bale monitors below 75%RH in July with some occurrences of 75-85% in bathroom walls. Measurements taken in October of the year gave most results between 35-45% with some into 50-60% in wetter locations, such as bathrooms again. North walls were in the range of 20-30% during the second winter and the following summer reached 50-65%.

These results seem promising as the conservative 80%RH limit is not exceeded. However, sensors later located behind the exterior plaster showed readings up to 95%RH. These elevated readings usually followed rain events and the investigator suggested that an earlier idea of quick redistribution of water within a wall is not valid. A house with an exposed north wall showed higher moisture content readings than a covered west wall. The sole effect is reduced precipitation striking the wall. Similar effects were noticed on other houses as well. South side walls showed lower RH readings compared to north walls due to drying caused by solar gains. Jolly noted that two or more of the following design flaws were present at locations where moisture contents were high and thus a potential for mold was present:

1. "Minimal overhangs
2. No capillary break between foundation parging and above grade stucco
3. Extreme interior wetting without drainage
4. Below-grade bales
5. Inadequate backsplash protection
6. Northern exposures" (Jolly, 2000)

Henderson studied houses in Nova Scotia (CMHC, 2000). She found values for the middle of the walls averaging 10% wood MC in May and 12% in July, with some occurrences above 15%. A location of a known leak indicated the highest reading at 19%. Winter readings were 6-8%. North and east walls were 1% higher than south and west walls. No trend within the wall was noticed (high, mid or low).

6.2 Goodhew et al (2004)

Goodhew inserted wood MC probes into lime plastered straw bale walls in a building in Dartmoor, England, which was constructed five years previous. The exterior conditions during the study were 95-100%RH during the winter and dropping as low as 78% in the summer. The interior conditions averaged 95% in the winter and dropped to 75% for the summer.

The south wall was the most exposed and showed the highest moisture content (at the exterior location, during the summer) up to 25%MC, while the east wall reached a maximum of 17% and the west wall 19%.

During the winter the middle-of-wall readings were the same as the outer-edge-of-wall readings but this changed in the summer. The east wall showed higher readings in the middle of the wall compared to the outer location during the summer (15% vs 12%, respectively), the west wall showed similar readings (17-19% vs 19%) and the south wall

showed lower readings (15-17% vs 25%). Although, the south wall readings were noticeably higher than for the other walls, there was no water ingress noted. But degradation of the straw at the bottom of the south wall was noticed when the render was removed.

The seasonal behavior of the south and west wall was similar. They both rose steadily through the spring to 25%MC for the south wall and 19% for the west wall and remained at these levels for the summer. The east wall also rose in the spring but peaked at 17% in April and dried to 12% for the summer.

Straube and Schumacher (2003)

Straube and Schumacher placed temperature and humidity sensors throughout a clay plastered straw bale winery in California. A total of 12 locations were monitored with sensors through the height (lower, middle and upper) and thickness (inner, middle, and outer) of the walls. There were several rooms monitored of various conditions: the barrel room was maintained at 80%RH and 15.5^{o}C, and the tasting room, bathroom, and other rooms were kept at typical occupant conditions (19-23^{o}C).

Rainfall caused a strong response in the moisture of the walls. One event showed a predominant rainfall from the south with an increase in the RH towards the exterior of the south wall rising to nearly 100% and drying to 80% over 6 weeks and finally back to equilibrium at 8-9 weeks. Smaller rain events showed faster drying. Short term changes were noted during rain events; otherwise the RH varied slowly within the walls usually changing over a period of weeks, due to the moisture storage in the straw.

The interior RH of 80% in the barrel room was causing similarly high levels of humidity in the interior of the straw bale walls that enclose the room.

6.3 Wihan (2007)

Wihan monitored a building in Plozevet, France. A house was constructed with lime plaster in late summer of 2005 with the final plaster coat applied in early October of the same year. A large wind driven rain event hit the west wall in early December, enough to cause wet spots on the interior. Wihan installed a sensor in the middle of the wall at one of the wet locations in late January 2006. The conditions at this time were 80%RH and only dried to 75%RH by the summer. Although it appeared to be a major wetting event, only the straw immediately behind the exterior plaster showed any signs of decay. Mold had grown on the stems of the straw up to 50mm inward from the plaster, but at 100mm

inward only a slight darkening of the nodes was noticed. Although sustained relative humidities above 75% were encountered for the 8 months of monitoring in the middle of the wall there was no molding noted at that location.

He also summarized other studies (some mentioned in this paper) and found the cause of failures to be the following, in order of frequency:

- Driving rain
- Sustained high levels of ambient relative humidity
- Rising damp
- Window sill leakage

Wihan also tries to assimilate the vertical variation of humidity that was noted in various studies. Straube and Schumacher show higher humidities at upper levels in wall, whereas other studies show the reverse. Usually where the relative humidity is found to increase vertically it is due to solar radiation drying the lower portion of the wall, while not striking the upper portion. In addition, the natural buoyancy of moist air will cause it to rise within the bales, being slowed by the air-diffusion coefficient of the bales, which is low. Air pockets in the straw bale joints may also increase the air flow. When this does not occur it is expected that the lower portion of the wall is more exposed to rain and splashback and thus should show higher humidity levels.

6.4 Summary

These case studies provided some general insights into straw bale wall behaviour. The wettest conditions are usually towards the exterior of the wall due to rain exposure. However, solar exposure reduces the moisture levels in the walls. Therefore, north walls will generally be wetter than south walls. The middle of wall condition fluctuates slowly with the ambient conditions and are typically below safe levels for mould growth. Some exceptions to this are a result of design flaws or high ambient RH. In a cold climate, the moisture content within the wall rises during the spring and is a minimum during the winter. Last, decomposition of straw will occur in wet conditions, but does require consistently high levels of moisture.

7 Steady State Analysis

Steady state analysis is the most common technique for design professionals to assess the performance of a wall assembly. It is limited by not accounting for temporal fluctuations of temperature, moisture and solar radiation. However, it is used to provide a basis for the understanding of the vapor movement and condensation potentials within straw bale wall. Additionally, it is useful for a parametric study to assess the impacts of different plasters, straw bale permeability, vapor retarders and barriers, and the drying potentials for different saturation conditions.

The physical properties used in the analysis have been discussed in Chapter 4 and a summary of the values used is given in Table 18. Extreme winter conditions used in the analysis were -20^{o}C and 90%RH and the average winter conditions were -5^{o}C and 80%RH. The interior conditions for the winter scenarios were 20^{o}C and 40%RH. The extreme summer conditions were 35^{o}C and 70%RH and the average summer conditions were 27^{o}C and 50%RH. For the summer the interior conditions were 21^{o}C and 60%RH.

Most analyses include several plaster types. The thickness of each plaster is the same at 38mm (1.5”). The resulting permeances therefore give a range of values without any being too similar. In practice different thicknesses may be used; however, if the thickness of the cement-lime plaster is reduced to 25mm (1”) while the lime plaster is maintained at 38mm (1.5”) the resulting permeances for both plasters is 400 ng/sm^{2}Pa, which would be a redundant analysis. Therefore, the following analysis does not necessarily apply to a particular plaster but to the permeance of the plaster layer which may be achieved through the balance of permeability and thickness of the layer.

Steady state analysis of the straw bale walls can be reduced to three layers: the inner plaster, the straw bale layer and the outer plaster layer. The surface films are included but contribute only a small percentage of the overall thermal and vapor resistance, and so do not affect the results considerably. Therefore, analysis of the system only requires the thermal and vapor resistances of the plaster and straw layers. These are determined by the thickness and thermal conductivities and vapor permeabilities, but the resulting resistances are what ultimately affect the performance of the wall. In dynamic analysis, the thermal mass and moisture storage abilities of the plasters and straw bale will be important and then the full dimensions must be utilized.

In order to ignore the thermal resistance of very thin layers, for which the thermal resistance is negligible, a conductance of 1x10^{8}W/m^{2}K was used. This value is not based

on any measured data, but is of a magnitude that eliminates the layer in question from impacting the thermal profile through the wall.

Material	t (m)	k (W/m·K)	μ (ng/s·m·Pa)	U ($W/m^2 K$)	M ($ng/s \cdot m^2 \cdot Pa$)
Cement Plaster	0.038	0.8	5	-	-
Cement-Lime Plaster	0.038	0.8	10		
Clay Plaster 1	0.038	0.8	42	-	-
Clay Plaster 2	0.038	0.8	25	-	-
Exterior Film	-	-	-	34	15000
Interior Film	-	-	-	8.3	75000
Lime Plaster	0.038	0.8	15		
No Surface Finish	-	-	-	$1x10^8$	$1x10^8$
Primer + 1 coat oil paint on plaster	-	-	-	$1x10^8$	120
Six mil poly	-	-	-	$1x10^8$	3.12
Strawbale 1	0.3556	0.065	50	-	-
Strawbale 2	0.3556	0.065	100		
Strawbale 3	0.3556	0.065	150		
Two coats float oil paint	-	-	-	$1x10^8$	250
Vapor Barrier	-	-	-	$1x10^8$	3.12
Vapor Retarder	-	-	-	$1x10^8$	30

Table 18. Material properties for steady state analysis.

7.1 Vapor Diffusion During Winter and Summer

Under extreme winter conditions condensation occurs behind the exterior plaster for all plasters. The rate of condensation increases for higher permeance plasters: $13.9 g/m^2 d$ for Clay 1 and $6.0 g/m^2 d$ for Cement. However, the rate of condensation is reduced with the application of a vapor retarder and results in higher rates for the lower permeance exterior plasters. Therefore, cement plaster has a rate of $1.4 g/m^2 d$ while Clay 1 has a rate of $0.2 g/m^2 d$. With the use of a vapor barrier condensation is eliminated behind all plasters except for the cement plaster, which still shows a relative humidity at 100% but a near zero condensation rate. The relative humidity for the Clay 1 plaster is 87.8%. A summary of these results is shown in Figure 23.

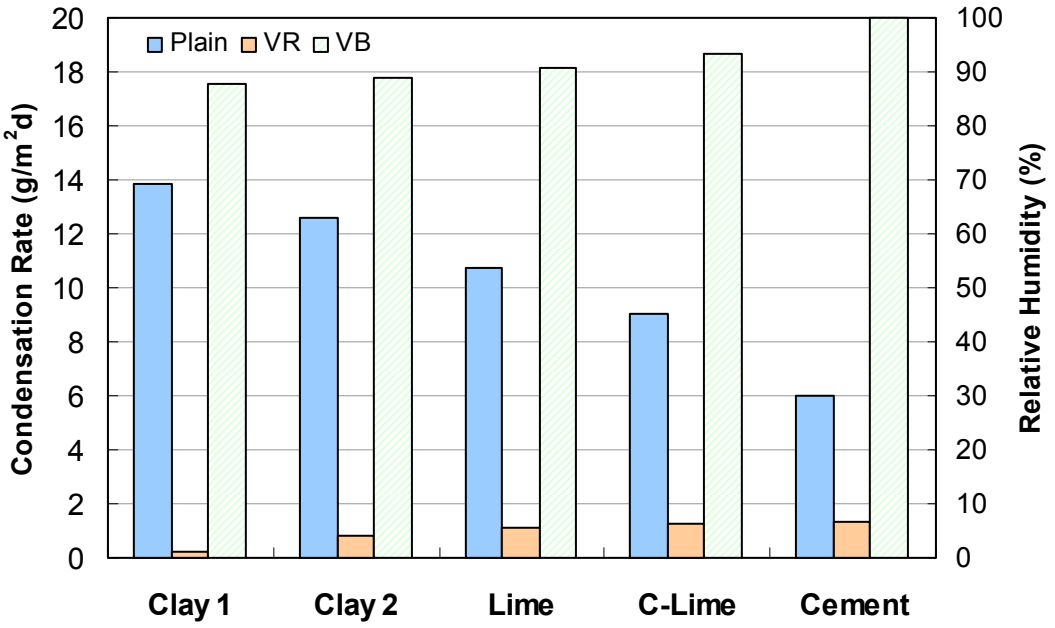

Figure 23. Condensation rates behind the exterior plaster for extreme winter conditions, relative humidity is shown for conditions of no condensation and are indicated with striped fill.

The rate of condensation is a balance between the vapor drive from the interior toward the condensation plane and the drying rate from the condensation plane to the exterior. In the case of bare interior plasters the wetting drive is much greater than the drying flow, as the exterior conditions have a high humidity so there is little driving potential between the condensation plane and the exterior, but the driving potential from the interior to the condensation plane is large. This results in condensation, with increasing condensation for more vapor permeable interior finishes as they allow more outward vapor drive. However, with the application of the vapor retarder and vapor barrier the inner permeance of the walls is nearly the same for all plaster types (Clay 1 29.2 ng/s·m^2·Pa and Cement 24.4 ng/s·m^2·Pa) and decreased considerable (130 ng/s·m^2·Pa for cement to 24 ng/s·m^2·Pa with vapor retarder) so as to significantly reduce the outward vapor drive, and thus condensation is controlled more by the outer permeance. Therefore, vapor permeable plasters allow more drying and have less condensation than less vapor permeable plasters. The vapor retarder still allows enough vapor through to cause condensation, although a significant reduction is noticed compared with no finish, especially for the clay plasters. The vapor barrier eliminates condensation but the relative humidities are still in the range of 90-100%.

Average winter conditions provide more drying potential to the exterior and reduce the wetting potential. This occurs because warmer temperatures cause the vapor pressure between the condensation plane and the exterior to increase, even if the relative humidities are the same as the extreme winter case. This is a result of the exponential increase with temperature of the capacity for air to hold moisture; therefore, a $1^{o}C$ difference will cause a larger saturated vapor pressure increase at higher temperatures than at lower temperatures. The outward wetting drive is reduced because the exterior temperature is closer to the interior temperature and therefore the vapor pressure difference is reduced for a given exterior RH.

Condensation rates for the average winter condition are in the range of $1.2g/m^2d$ (Clay1) to $3.9g/m^2d$ (Lime) for plain construction. Notice that the mid range permeance plasters have the highest rates and the Clay1 plaster and Cement plaster have the lower rates. This is a result of the change in the balance between the wetting and drying vapor flows. As the outside temperature increases and the relative humidity decreases the outward drying will increase, more so for vapor open materials, and the wetting flow will decrease again more for vapor open plasters. Therefore, the decrease in condensation is greatest for open materials and less for closed material. Resulting in the Clay1 plaster showing greatly reduced condensation compared to the extreme winter case but lime only somewhat reduced. Condensation is eliminated with vapor retarders and vapor barriers. The RH ranges from 81-98% with a vapor retarder and 78-81% with a vapor barrier. Vapor open materials produce the lower humidities. These results are summarized in Figure 24.

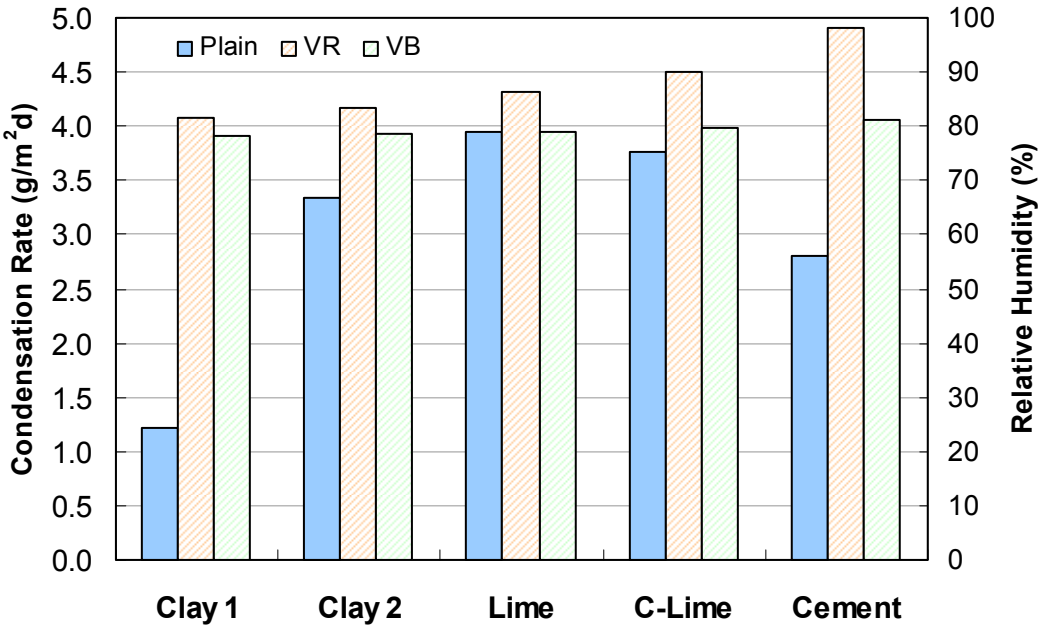

Figure 24. Conditions behind exterior plaster during average winter, condensation rates in solid color, relative humidities in stripes.

The effect of a vapor barrier is not as great for the clay plaster as it is for the cement plaster. Instead the vapor retarder provides nearly the effect of a vapor barrier for a clay plaster, while the vapor barrier improves conditions significantly over the vapor retarder for the cement plaster.

To stay below the 80%RH threshold for mold growth is not possible during the extreme winter conditions even with a vapor barrier. However, these conditions are usually short lived and so the buffering capacity of the materials would need to be accounted for. As well, the cold temperatures preclude the growth of molds. Solar radiation would be required to increase the temperatures into the favourable growth range, but would also aid in drying the accumulated moisture.

For the average winter conditions it is possible to reduce the relative humidity levels to near 80%. A vapor retarder will reduce the clay plasters to 81% and 83%, and a vapor barrier will reduce all walls to below 81%. Again, the negative temperatures preclude mold growth but any solar radiation would increase the temperature into the favourable zone.

The largest uncertainty for mold growth during the winter would be due to the accumulation of condensate during freezing temperatures that may provide a large moisture supply when favourable temperatures for mould growth return. The possibility for mold growth will be reduced by reducing the amount of condensation and increasing the rate of drying during the warm periods.

In addition to using vapor retarders or vapor barriers to reduce the permeance of the interior plaster it may be possible to use a combination of plaster finishes to provide better performance of the wall assembly. For example, a low permeability cement plaster on the interior and a high permeability clay plaster on the exterior will provide better vapor control than a clay plastered wall or a cement plastered wall alone. A combination of plasters was analyzed for the average winter conditions to assess the condensation rates which are shown in Figure 25.

Condensation does not occur for the combination of cement interior with clay2 or clay1 exterior, the RH for these are 97% and 89% respectively. Applying vapor open materials on the interior and vapor resistant materials on the exterior increases condensation rates dramatically. For cement plaster on both the interior and exterior the rate of condensation was 2.8g/m^2d while changing the interior plaster to clay1 will result in a condensation rate of 8.6g/m^2d.

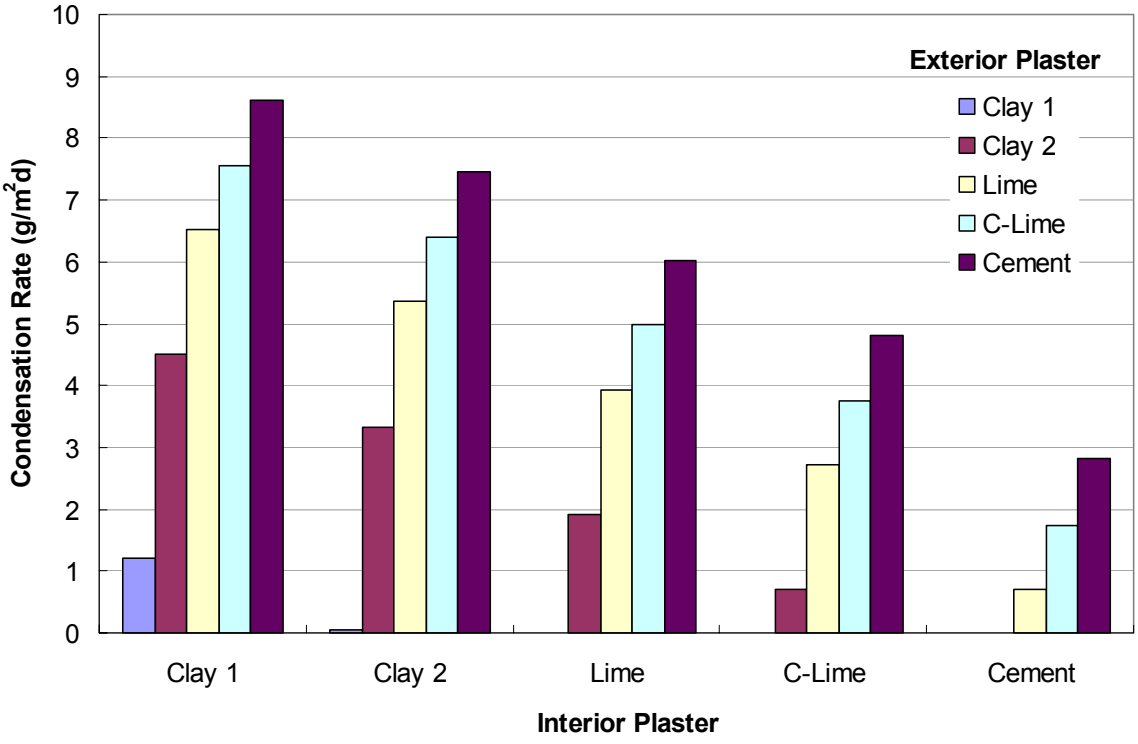

Figure 25. Condensation rates for various plaster combinations during average winter conditions.

In the summer the vapor drive is inward and condensation potential is on the back of the interior plaster. Under extreme summer conditions there is no condensation in the plain finished walls, but relative humidities between 75%(Clay1) and 97%(Cement) are reached. When a vapor retarder or vapor barrier is used there is condensation, with rates from 8.5g/m^{2}d (Cement) to 23.9 g/m^{2}d (Clay 1) for use of vapor retarder and 10.4-26.3 g/m^{2}d with use of vapor barrier. A summary chart is given in Figure 26.

For average summer conditions there is no condensation reached. Instead humidities in the range of 61-64% are achieved with plain finish and 69%-70% for vapor retarder and vapor barrier. These results are shown in Figure 27.

Only during extreme summer conditions may the potential for mould growth be reached. However, as with extreme winter conditions, these are often short lived and so a dynamic analysis would be required to fully assess mould growth potential. With average summer conditions all walls are well below the 80% limit for mould growth.

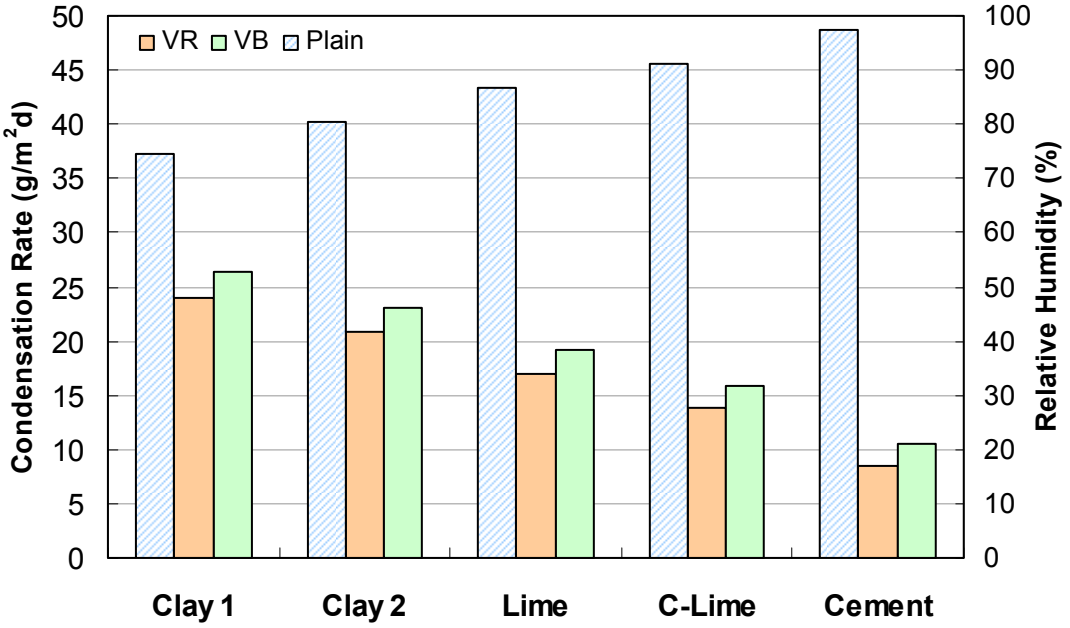

Figure 26. Conditions behind interior plaster during extreme summer, condensation conditions shown with solid colors, relative humidities with stripes.

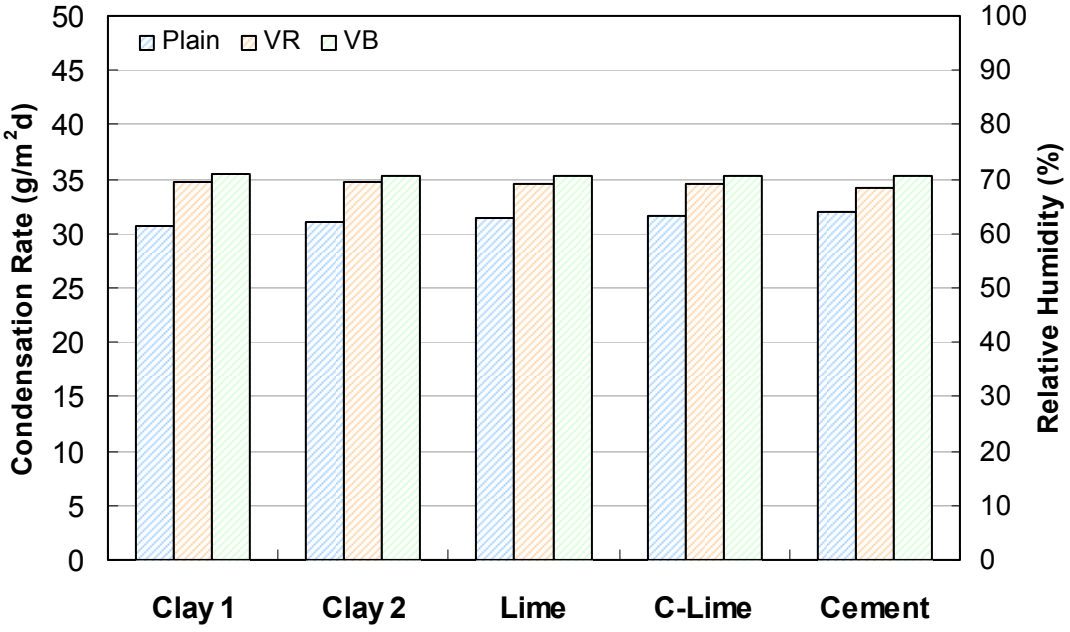

Figure 27. Relative humidities behind interior plaster during average summer conditions.

7.2 Drying of Plaster During Summer

The largest concern for mould growth in summer months is wetting by liquid water due to leaks or driving rain. First, the reduction of the wetting should be achieved, but afterward it is the drying that controls the potential for mould growth. In the case of broken water lines or roof leaks, they may be controlled by good design, and should not occur, but their occurrence is usually not forewarned. Driving rain can be controlled by overhangs and surface finishes, but it is desirable to not have strict requirements for these. Therefore, the analysis of the drying potential may allow for less stringent wetting controls.

Drying may be aided by solar radiation by increasing the temperature of the exterior plaster, potential solar driven drying rates are given in Figure 28. However, this does not apply to north facing walls, nor to cloudy days. Therefore, the drying potential without solar radiation is also required, which is shown in Figure 32.

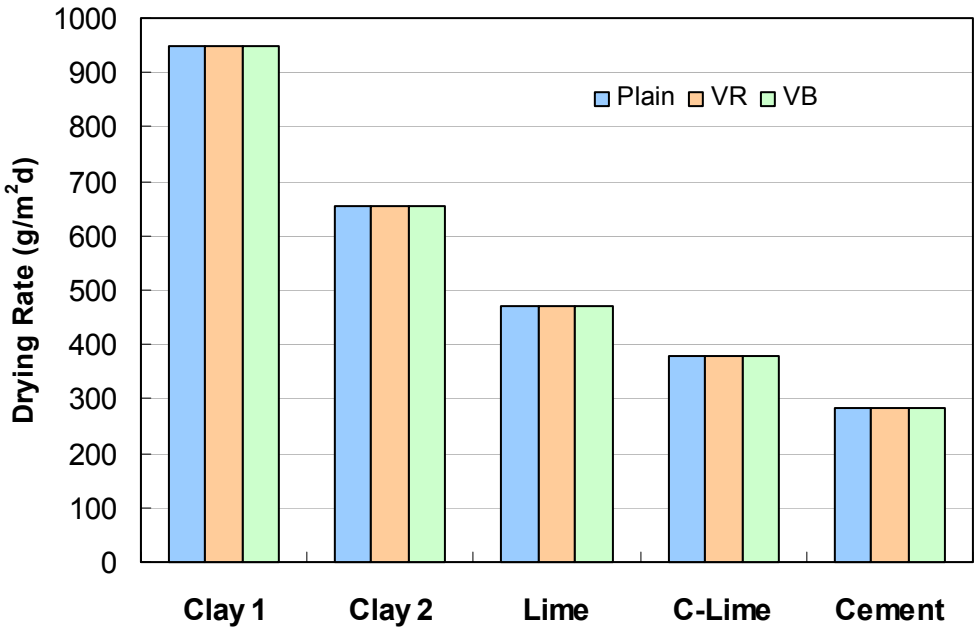

Figure 28. Drying rates of saturated conditions behind exterior plaster with solar radiation during average summer conditions.

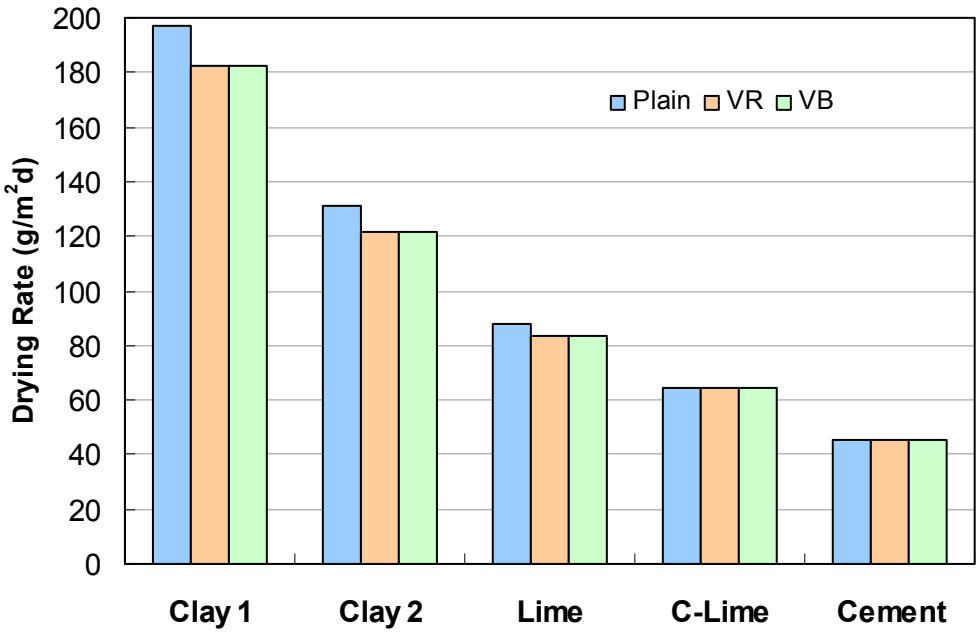

Figure 29. Drying rates of saturated conditions behind exterior plaster without solar radiation during average summer conditions.

Vapor barriers and retarders do not significantly affect the drying rate as it is primarily directed toward the exterior. However, they do increase the condensation of the inward drying vapor. The rates of condensation at the interior plaster due to the inward moving vapor are shown in Figure 30 and Figure 31 for the solar enhanced and normal conditions respectively. Condensation is high as a result of the inward drive from solar radiation it ranges from 83g/m^{2}d to 187g/m^{2}d. Without solar radiation there is no condensation on the plain walls of clay and lime plasters and the relative humidities range from 76% to 94%. With a vapor barrier or retarder the condensation rates are 25g/m^{2}d and 22.7g/m^{2}d respectively.

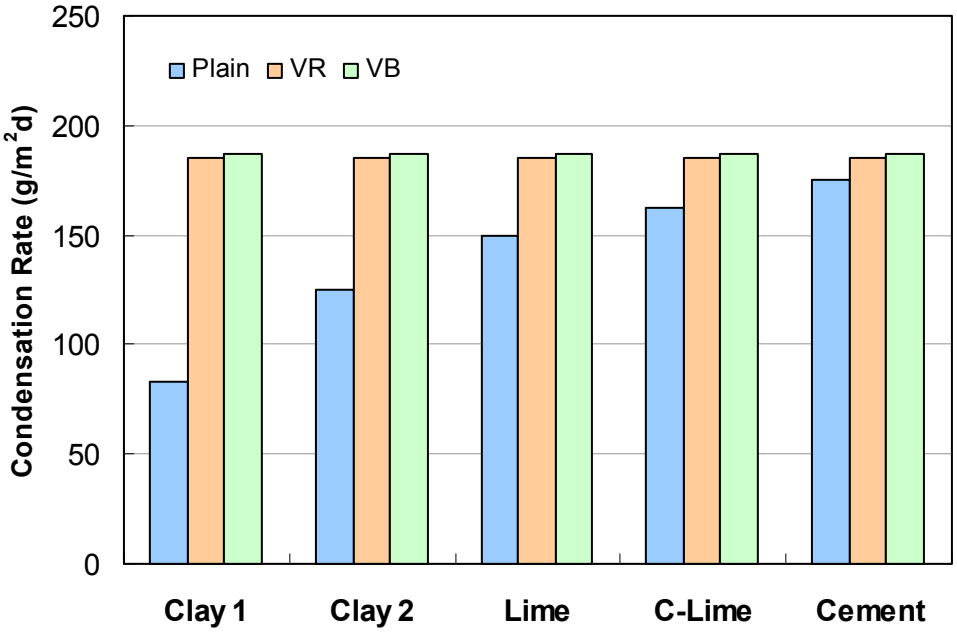

Figure 30. Condensation at interior plaster due to inward drying during the summer with solar radiation.

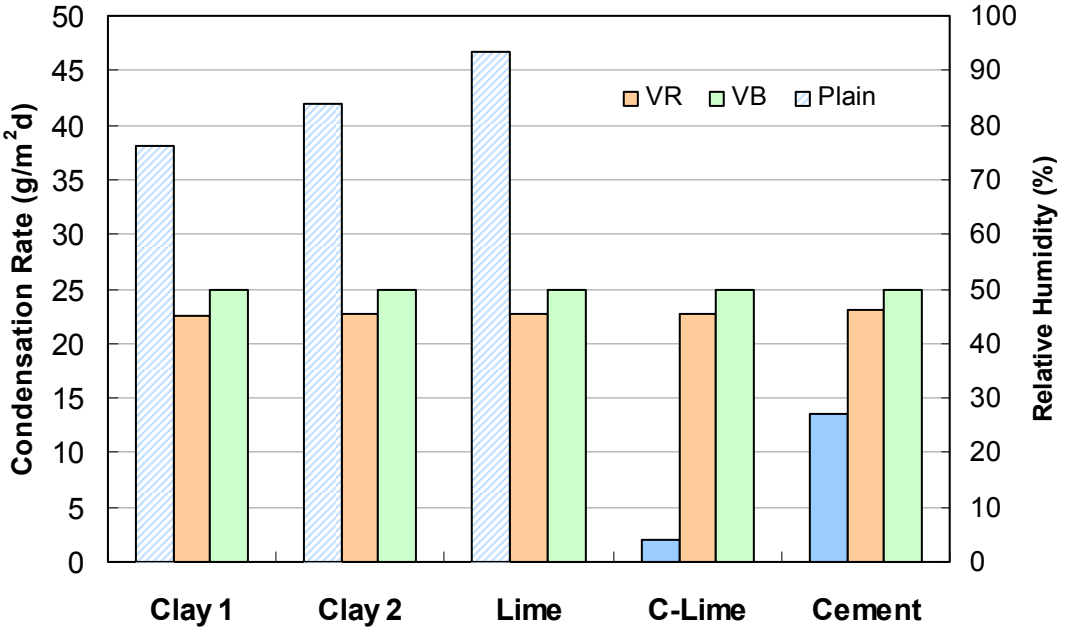

Figure 31. Condensation on interior plaster due to inward drying during average summer conditions without solar radiation, condensation indicated by solid colors, relative humidity with stripes.

Drying of the inward condensation will depend primarily on the permeance of the interior plaster, as it will dry in tandem with the saturated exterior plaster and so will not have much potential to dry to the exterior, if any. Therefore, the rates of drying are given in Table 19 for the different plasters at 38mm thickness.

Plaster	Drying Rate (g/m^2d)
Clay 1	96.1
Clay 2	57.6
Lime	34.7
C-Lime	23.1
Cement	11.6

Table 19. Inward drying rates of condensate behind interior plaster, no vapor flow from or into the straw.

7.3 Drying of Plaster During Winter

South and west facing walls are found to have lower moisture contents than north and east facing walls. This is most likely a result of solar exposure that helps to dry the walls. Therefore, solar drying rates of wintertime condensation were calculated. For extreme conditions the results are shown in Figure 32 and for average conditions in Figure 33.

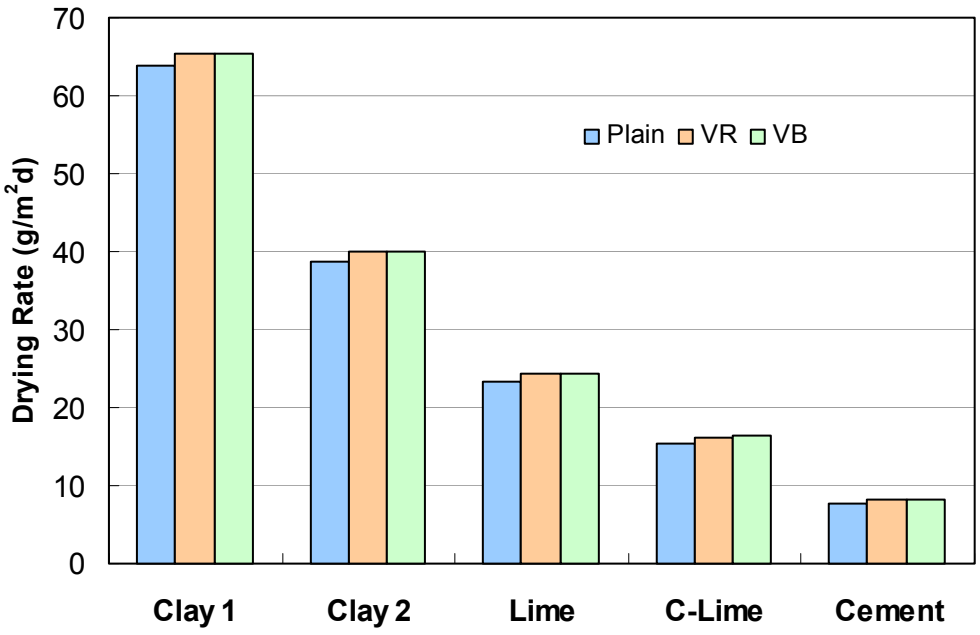

Figure 32. Solar drying rate of condensate during extreme winter conditions.

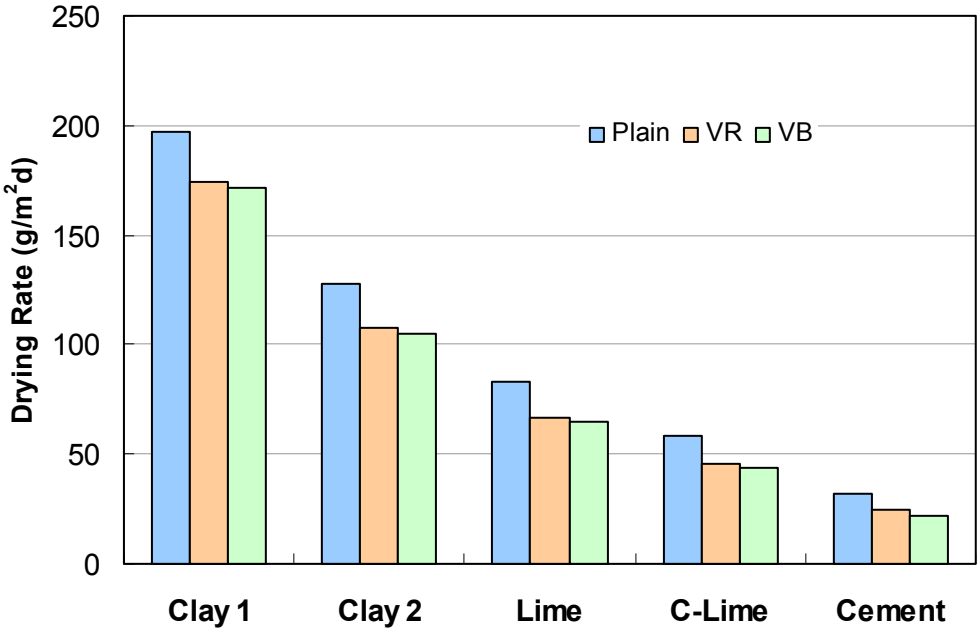

Figure 33. Solar drying rate of condensate during average winter conditions.

The use of vapor barriers or retarders does not significantly affect the drying potential as most vapor drive is towards the exterior.

To balance the rate of condensation their must be a certain fraction of the day that has sunshine. If there is more sun than this balance point the condensate will be completely dried while less sun will not sufficiently dry the condensate. The hours of sunshine required is given in Table 20 for both extreme and average winter conditions.

Plaster	Extreme Winter			Average Winter		
	Plain	VR	VB	Plain	VR	VB
Clay 1	4.3	0.1	-	0.1	-	-
Clay 2	5.9	0.5	-	0.6	-	-
Lime	7.6	1.1	-	1.1	-	-
C-Lime	8.8	1.8	-	1.4	-	-
Cement	10.6	3.4	-	1.9	-	-

Table 20. Number of hours in a day of sunshine required to completely dry condensate that forms during the remaining hours of the day.

7.4 Effect of Variaton of Strawbale Properties

It is expected that the vapor permeability of straw is at least 100ng/Pasm but it may be as low as 50ng/Pasm and higher than 150ng/Pasm. Increased permeability of the straw will result in higher humidities behind the exterior plaster in the winter and behind the interior plaster in the summer as there is less resistance to vapor migration to these locations. The effect of these changes is shown in Figure 34 and Figure 35.

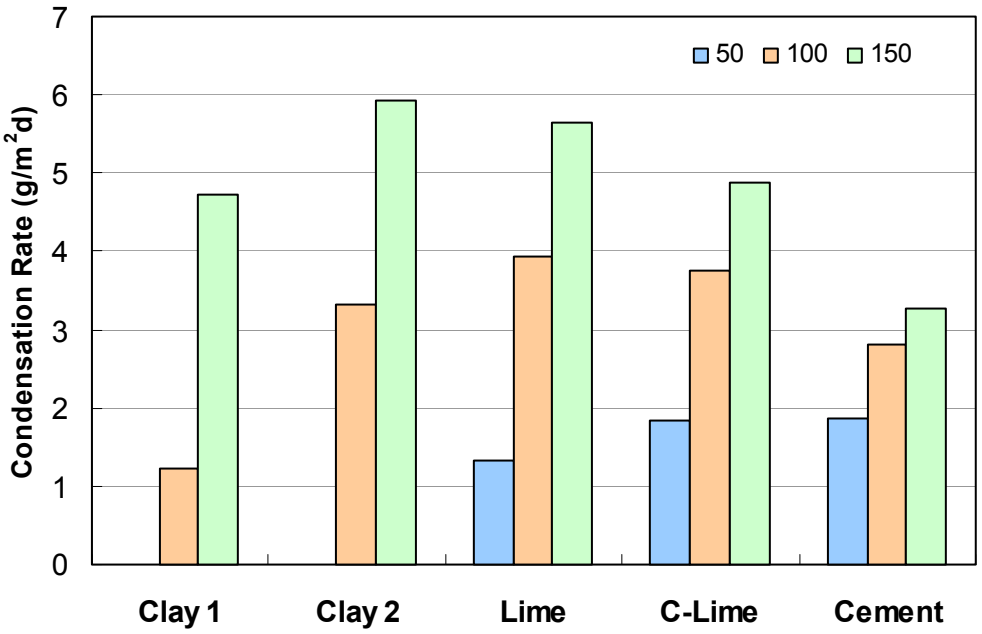

Figure 34. Effect of straw bale permeability on average winter condensation, plain plaster finishes.

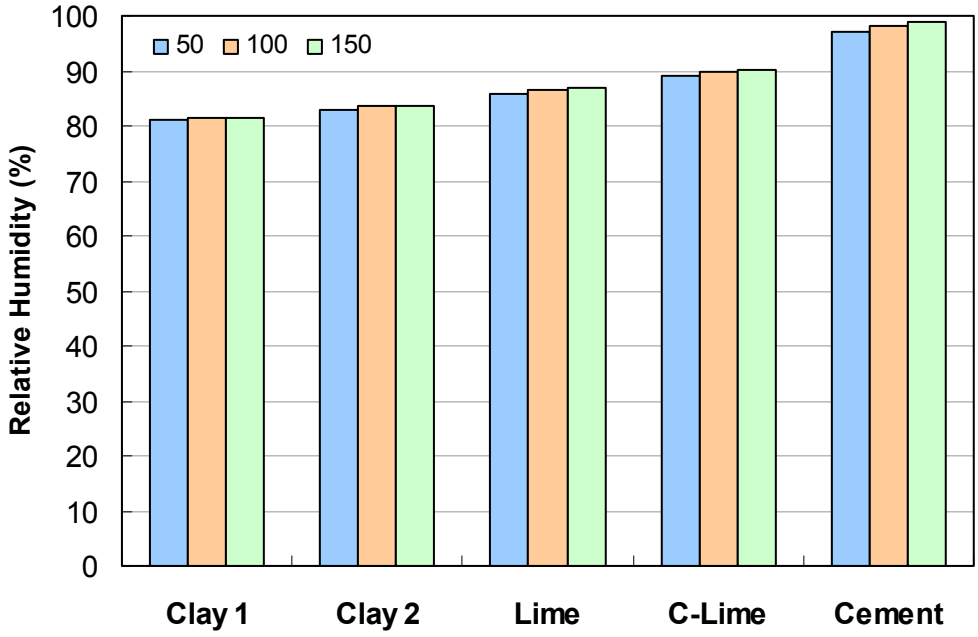

Figure 35. Effect of straw bale permeability on average winter RH behind the exterior plaster when an interior vapor retarder is used.

As can be seen in Figure 34 there is greater impact of varying the straw bale permeability with the clay plaster than with the cement plaster. This is because the straw bale provides a greater percentage of the total vapor resistance with clay plaster than with the cement plaster, therefore a change in the straw bale permeance changes the total vapor resistance of the clay plastered wall by a larger percentage than it does with the cement plastered wall. The effect is minimized for all walls when a vapor retarder is used as the vapor resistance of the straw bale is relatively small compared to the vapor retarder and therefore does not change the total wall vapor resistance very much.

The effect of changing the thermal conductivity is shown in Figure 36. The greatest variability is again in the Clay 1 plaster, with changes of +/-20% occurring for both an increase and decrease of conductivity of +/-0.015 W/mK from 0.065 W/mK. All other plasters vary +/-5% and less, with the cement plaster varying by only +/-1.6%. Decreasing the thermal conductivity increases the rate of condensation by causing the temperature at the exterior plaster to decrease, even though the change is only 0.07^{o}C, from -4.66^{o}C to -4.73^{o}C. But because the exterior temperature is only -5^{o}C the change in the difference of temperature is significant (0.34^{o}C to 0.27^{o}C, or 20%).

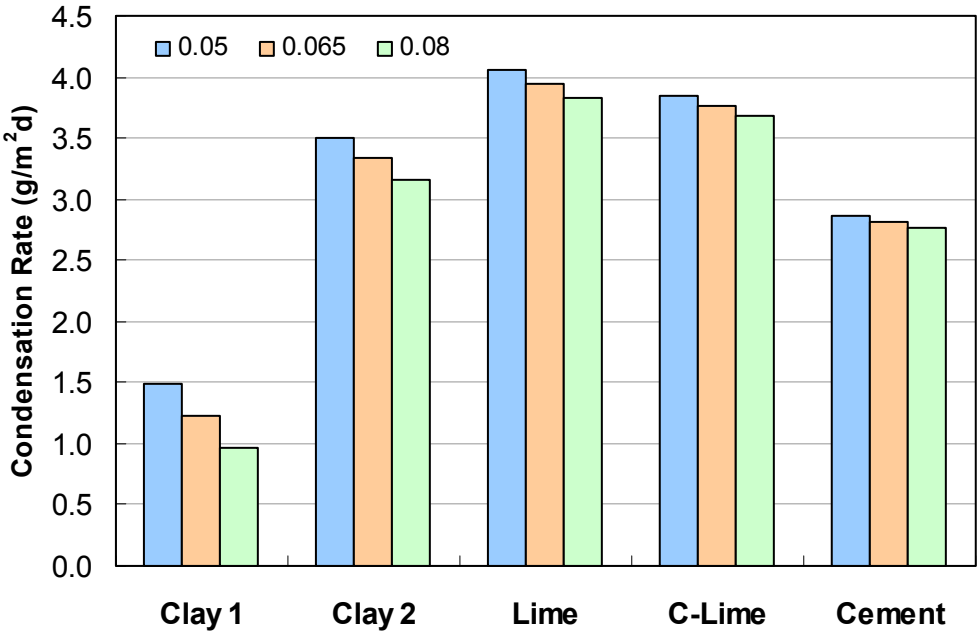

Figure 36. Effect of straw bale thermal conductivity (W/mK) on average winter condensation.

Initially, the variation in thermal conductivity of the plasters was ignored as the change in temperature behind the plaster is relatively small (0.25^{o}C). But it may be significant as seen in by the effects of the previous finding for a change in temperature of only 0.07^{o}C. Therefore, a plot of the change in condensation rate for varying plaster conductivities was produced in Figure 37. Similar changes occur as with the change in straw bale conductivity but the relative changes are bigger for changes to the plaster. A 35% decrease in condensation rate resulted by changing the thermal conductivity from 0.8W/mK to 0.5W/mK for the Clay 1 plaster, with 8.4% for Clay 2 and 2.6% for the cement. Increasing the conductivity to 1.1W/mK had less of an impact, with an increase in condensation of 16% for Clay 1, 3.9% for Clay 2 and 1.2% for cement. Again, the impact is greatest with the most vapor open plasters and decreases significantly for less vapor permeable plasters.

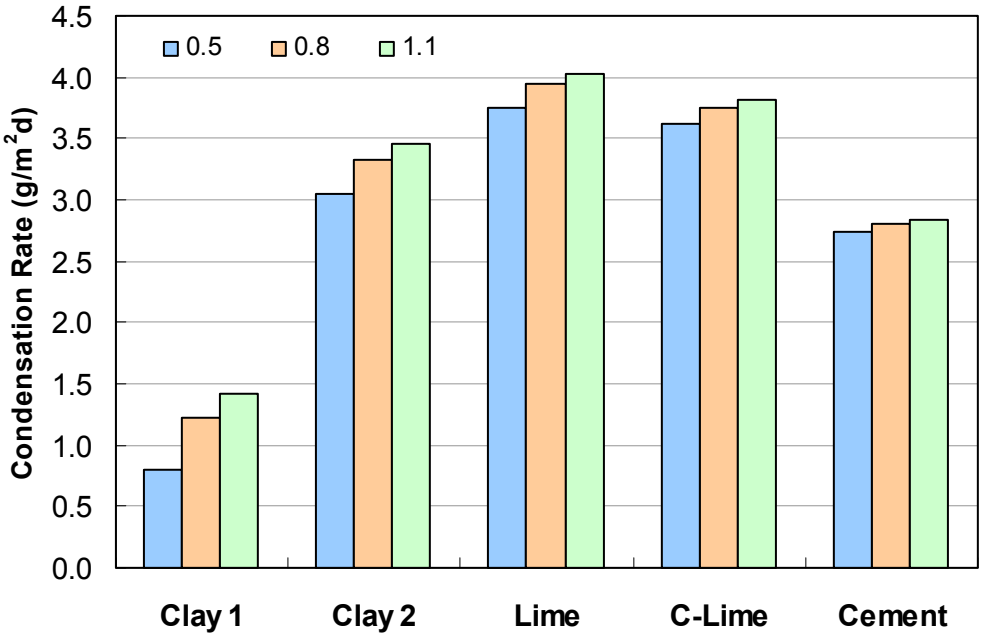

Figure 37. Effect of plaster conductivity (W/mK) on average winter condensation rates.

7.5 Conclusions

The potential for moisture drying is greatly increased with more permeable plasters. This helps to reduce the relative humidity within the wall during all but the extreme winter case. In the extreme winter case it is beneficial to provide a less permeable interior plaster or even a vapor retarder. However, during the summer this layer will trap interior driven moisture and result in high relative humidities during warm temperatures, which are the most favourable conditions to mould growth. A dynamic analysis is required to better assess the extreme conditions as they are typically short lived and the effects of moisture storage will have an impact. It is expected that a high vapor permeance exterior plaster will be best suited to a cold climate when paired with an interior plaster of a slightly lower permeance.

8 Experimental Monitoring

Included in this study is the detailed monitoring of two straw bale walls built in September 2007 at the Building Engineering Group (BEG) test facility at the University of Waterloo. It was constructed to allow test walls to be inserted into the sides of the building in order to expose them to controlled interior conditions and ambient exterior conditions. It is oriented towards the cardinal directions and so each wall faces due North, East, South or West. In this experiment the walls were installed in the east face and the interior conditions were maintained at approximately 20^{o}C and 50%RH for the first winter, with the resulting average vapor pressure being 1050Pa, steady control of the interior conditions was not maintained during the summer or second fall seasons. The exterior conditions are monitored by a weather station that sits atop the test facility. Rainfall, wind-speed, solar radiation, relative humidity and temperature are all recorded.

Overhangs are minimal so that there is no protection from driving rain on any wall. In addition there are no eaves in order to allow rainwater to fall from the roof and splashback on the walls off of 12" concrete tiles that surround the edge of the building. These details are typically the first eliminated in straw bale construction, but were utilized to assess a straw bale wall in the worst case scenario. Further modifications may be made in following years to assess the effect of overhangs and splashback protection.

Figure 38. BEG test facility at the University of Waterloo.

8.1 Wall Construction

Both walls are identical in every way except for their plasters. One wall is constructed with a 1:1:6 cement-lime plaster and the other uses an earth-straw plaster. The walls are approximately six feet wide and eight feet tall. They are divided by an insulated built up column that was wrapped in a waterproof membrane. This provides a hygrothermal barrier between the walls, to minimize edge effects of moisture and heat flows. The same dividers were used to tie the walls into the rest of the building.

Details of the construction were assembled from various builders to attempt to mimic current practice and are shown in Figure 39. This includes a waterproof membrane installed over the foundation, crushed gravel between 2x4 sill plates at the base of the wall, and a 2x4 insulated box beam at the top of the wall. The bales were stacked on edge in running bond to reflect current practice in Ontario, shown in Figure 40. Exactly two bales fit into the wall openings with half sized bales used in every other row to facilitate the running bond. These were retied from the original bales and were slightly oversized to provide a snug fit to the row when laid. Any remaining gaps were filled with loose straw.

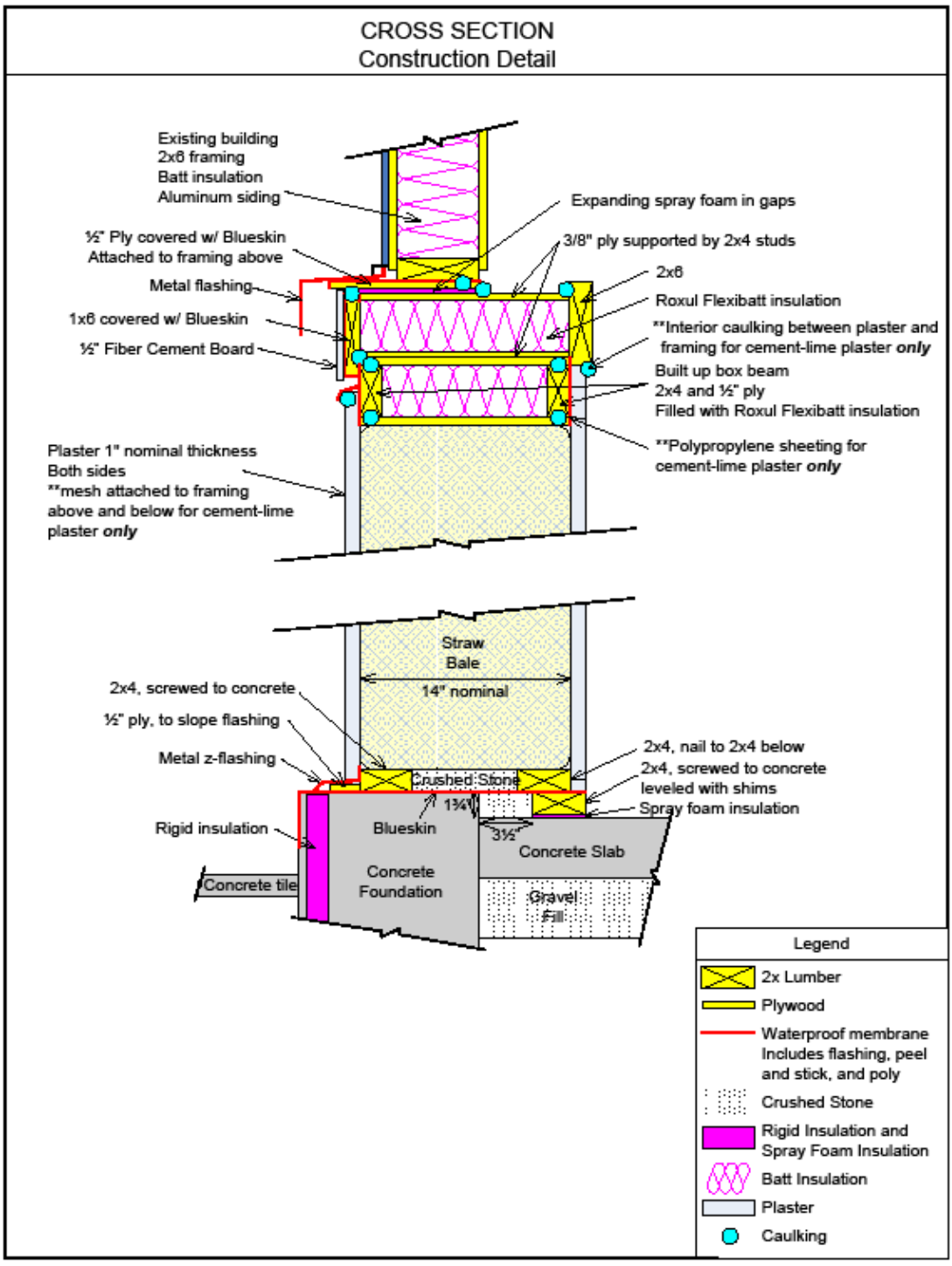

Figure 39. Test walls construction details.

Figure 40. Stacking the straw bales for the test walls.

To aid in applying the plaster Keith Dietrich volunteered his professional services and Harvest Homes supplied the materials. A polypropylene mesh was installed over the wall that was to be covered with cement-lime plaster. It was stapled around the opening and stitched to the bales using twine. This process involves using a "stitching needle" that is a long metal rod capable of pushing the twine through the bales. The twine is then passed back and forth through the wall holding the mesh on either side to the bales.

Cement-lime plaster was mixed on site and applied in two coats, with a day of curing between coats. It was then moistened each day for a week. The clay plaster was mixed previously before construction. Clay slurry was first applied to the bales and then the earth plaster was applied in one coat. Both plasters are nominally one inch thick and are identical on the interior and exterior, except for the surface texture of the cement-lime plaster. It was troweled smooth on the interior and was rubbed to a semi-rough texture on the exterior. After the clay plaster had dried it was wetted down and rubbed to fill any shrinkage cracks that had occurred. However, most shrinkage showed up at the edges of the wall with gaps up to three quarters of an inch. The plaster at these locations was moistened and additional plaster was put into the cracks and smoothed.

Figure 41. Applying the cement plaster.

Figure 42. Applying the clay slip.

Finally all the edges of the plaster were caulked to reduce air infiltration and water penetration. The only exceptions were the bottom exterior, which was not caulked to allow drainage and the interior clay plaster as the additional plaster that was used to fill the shrinkage crack effectively sealed the edges.

There were no finishes applied to any wall face. This has resulted in a slow loss of clay from the exterior side of the clay plastered wall as rain washes it away. This is expected in this type of construction and was anticipated. The degree of wear was of interest to assess the long-term durability of the construction method.

Figure 43. Finished test walls.

8.2 Monitoring

8.2.1 Sensor Layout

During construction relative humidity, moisture content and temperature sensors were placed in the walls. The configuration of these sensors was to allow full monitoring of the walls' behaviors both horizontally and vertically, and also to monitor the wood members that are used in the construction. A map of the layout of the sensors is given in Figure 44 and Figure 45.

The naming convention used has three coordinates. The first is for the type of sensor: R for relative humidity, T for temperature, and M for moisture content. Second, the vertical

location is given: B for bottom, L for lower, M for middle, E for eye-level, U for upper and T for top. The last coordinate is the horizontal location. It is two digits indicating the number of inches the sensor is inward from the exterior plaster. For example, 02 represents a sensor that is 2 inches behind the exterior plaster, that is there are two inches of straw between the exterior plaster and the sensor. Note that the bales are nominally 14 inches deep, thus 07 is the middle of the bale and 12 is 2 inches from the interior plaster. The only exceptions to this coordinate are for sensors that were placed near the exterior face of the plasters, these sensors get "ex" for external conditions and "in" for internal conditions if they are placed in the exterior plaster and interior plaster respectively. They are covered with a small amount of plaster to prevent damage to the sensors. In summary, a sensor with the name RM07 would be a **R**elative humidity sensor at **M**id-height of the wall and **07** inches inward from the exterior plaster. Alternately, a sensor name TB00 represents a **T**emperature sensor at the **B**ottom location at **00** inches from the exterior plaster, which means it is at the plaster-straw interface.

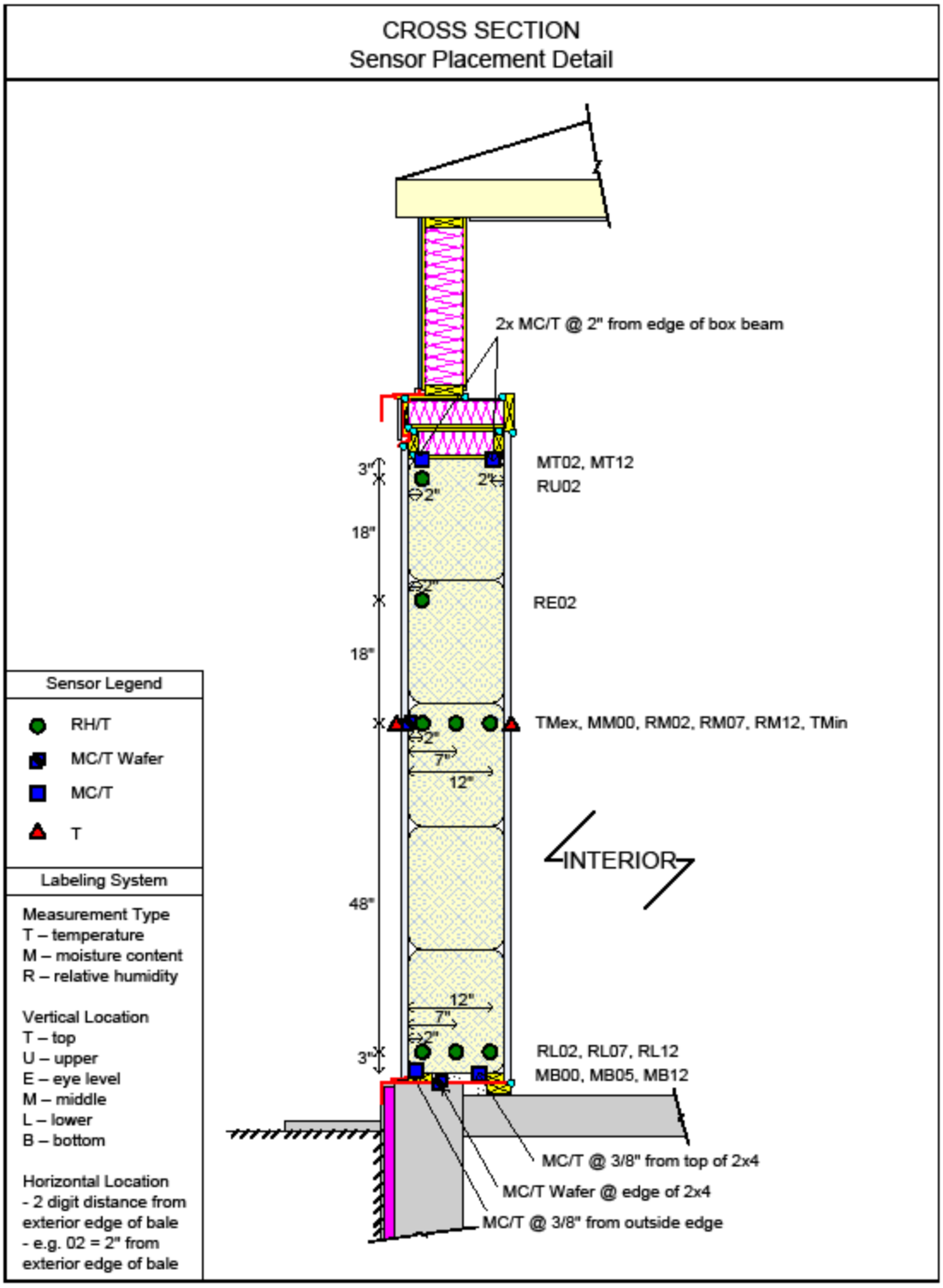

Figure 44. Sensor placement detail, cross sectional view.

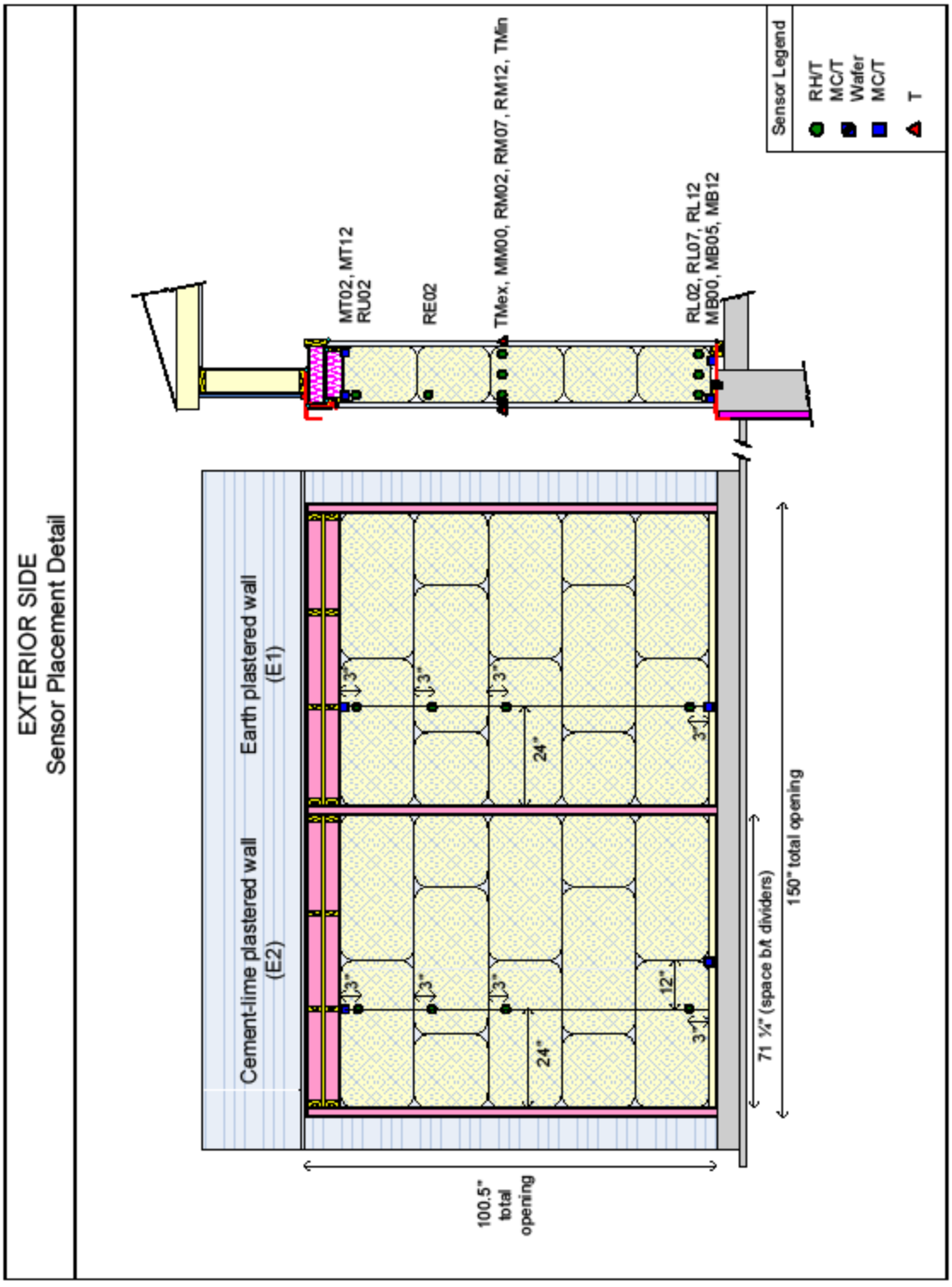

Figure 45. Sensor placement detail, exterior view.

8.3 Interior and Exterior Sensors

The weather station installed on the roof of the BEGHut is capable of measuring rainfall, solar radiation, wind speed, wind direction, temperature and relative humidity. The sensors used for these measurements are described below.

Vaisala™ HMP 35A is used for temperature and relative humidity measurements, with integrated protection from solar radiation and rainfall. Relative humidity is measured by a HUMICAP® sensor and a platinum Pt 100 RTD, with a range and accuracy of 0-100%RH and +/-2%RH. Temperature is measured by a thermistor.

Solar radiation is measured using an Eppley™ pyranometer. It is capable of measuring 105^{o} from the vertical and provides a voltage signal in proportion to the incoming radiation.

Rainfall is recorded by a Rimco™ tipping bucket rain gauge. It is a meteorological standard 8" diameter funnel with gold plating for water repellency. Every 0.2mm of rainfall causes one bucket tip which results in an electrical pulse that is recorded by the datalogger. Wind effects will reduce the catchment of rain because of the height of the gauge from the ground. Van Straaten (2002) references Grey's Handbook of Hydrology to account for this effect which uses a 10% increase in measured rain to represent rainfall at ground level.

The interior conditions are measured by a Vaisala™ HMP 35A RH transducer that is accurate to +/-2%RH and a 3000 Ohm YSI™ thermistor that is accurate to +/-0.2^{o}C. These sensors are located near the middle of the BEGHut at a height of 1.8m from the floor.

8.4 Wall Monitoring Sensors

The sensors used are Honeywell HIH-3610 relative humidity sensor, Fenwal Uni-Curve Series 10k Thermistor, and a wood wafer moisture content sensor. These were assembled by Paul Schumacher. Data from these sensors is measured and collected by a Campbell Scientific CR1000 datalogger in cooperation with an AM16/32A Relay Multiplexer.

8.4.1 Honeywell HIH-3610

This sensor has a +/- 2% accuracy for a range of 0-100%RH, for non-condensing conditions. To prevent damage from condensation the sensors are wrapped with a water repellant building paper of high permeability. Although this will impact the 15 second response capability of the sensor it will not affect the 5 minute readings. The sensor requires 5V input and produces a voltage output that varies linearly (+/-0.5%) with RH. Computing the RH from the voltage reading uses the following equation, for which the generic calibration values (shown) or the measured calibration values (NIST) can be used:

$$RH(\%) = \frac{\left(V_{out} - \text{Zero Offset}\right)}{\text{Slope}} = \frac{\left(V_{out} - 0.958\right)}{0.03068} \qquad 8.1$$

The generic coefficients provide an accuracy of +/-3% while the NIST coefficients provide an accuracy of +/-2%. This study uses the generic coefficients for ease of computation and since the difference in accuracy is not increased beyond that desired.

Temperature correction can be applied to the measured RH by the following equation:

$$\text{True } RH = \frac{\text{Measured } RH}{1.0546 - 0.00216T}, \quad T \text{ in } ^{o}\text{C} \qquad 8.2$$

8.4.2 Fenwal Uni-Curve Series 10k Thermistor

This sensor changes resistance with the inverse of temperature (ie. thermistor), giving a resistance between 1-100kOhm for a temperature range of 80°C to -20°C. Resistance is calculated from a voltage reading on a half bridge circuit using and applied 2.5V and a reference resistance of 1kOhm. The calculated resistance is then converted to temperature by the following equation which has been fit to the calibration data and is accurate to +/-0.03°C for a range of -20 to 60°C.

$$T\left(^{o}C\right) = -0.0937(\ln R)^3 + 4.143(\ln R)^2 - 75.31(\ln R) + 440.385, \qquad 8.3$$

Where R is in Ohms

8.4.3 Wood Moisture Content

Electrical resistance of wood varies with its moisture content. This has been studied and calibrated for various wood species. The lumber used in the construction of the walls and for the wood wafer sensors is white pine. These wafers are approximately 1.5”x1”x0.25”

with metal pins inserted 1" apart in the long and narrow side. The pins are coated with an electrically insulating material, except for the tips to ensure the electrical path is through the core of the wood.

Resistance is calculated by the use of a half bridge circuit, wherein a 12V supply is given and a 100kOhm reference resistor is used. The measured voltage is then converted to the resistance of the wood sensor. Uncorrected moisture content (MC_u) is then found by the following equation and corrected for temperature to get the final moisture content (MC).

$$\log(MC_u) = 2.99 - 2.113\log(\log(R)) \qquad 8.4$$

$$MC = \frac{1}{a} \cdot \frac{MC_u + 0.567 - 0.0260 \cdot T + 0.000051 \cdot T^2}{0.881 \cdot 1.0056^T - b}, \quad T \text{ in } ^{o}\text{C} \qquad 8.5$$

The values a and b are constants depending on the species of wood and for eastern white pine used in this test are 0.821 and 0.556 respectively (Straube, Onysko, & Schumacher, 2002).

8.5 Datalogging

Data from the various sensors is measured and collected by a Campbell Scientific CR1000 datalogger in cooperation with an AM16/32A Relay Multiplexer. The sensor wires connect directly to a Campbell Scientific AM16/32A Relay Multiplexer, which switches between the various sensors to allow for multiple sensor connections to one channel on the datalogger. The Campbell Scientific CR1000 Datalogger is programmed to collect data every 5 minutes and calculates and stores the hourly averages, maximums, or sums as required. A computer connection facilitates uploading the collected data for viewing. Further information on how the datalogger and multiplexer function can be found in their related operator's manuals found on the Campbell Scientific website. Data collection began on November 9, 2007 and is ongoing.

9 Testing Results

9.1 Boundary Conditions (Climate and Interior)

9.1.1 Relative Humidity and Temperature

During the first winter the interior temperature was maintained slightly under 20^{o}C and the humidity slightly below 50%RH. This temperature is below the average household condition but the humidity is greater, resulting in higher outward vapor drives than is typical. However, humidity control was limited during the summer due to failure of a heating element relay in the air handler unit that is part of the dehumidification system. This resulted in conditions that are similar to actual conditions in an air conditioned home. The temperature was maintained around 20^{o}C with interior humidity only being reduced by the temperature conditioning process, thus it fluctuates with the exterior relative humidity. In the second year there was another failed heater, which caused the humidification system to not perform as well as expected. Thus the second winter conditions have lower humidity providing less outward driven moisture from interior humidity, and are a reflection of more typical residential conditions.

The exterior conditions are the ambient weather conditions at the University of Waterloo, in Waterloo, Ontario. Relative humidity and temperature are shown with the plot of the interior RH and T in Figure 46.

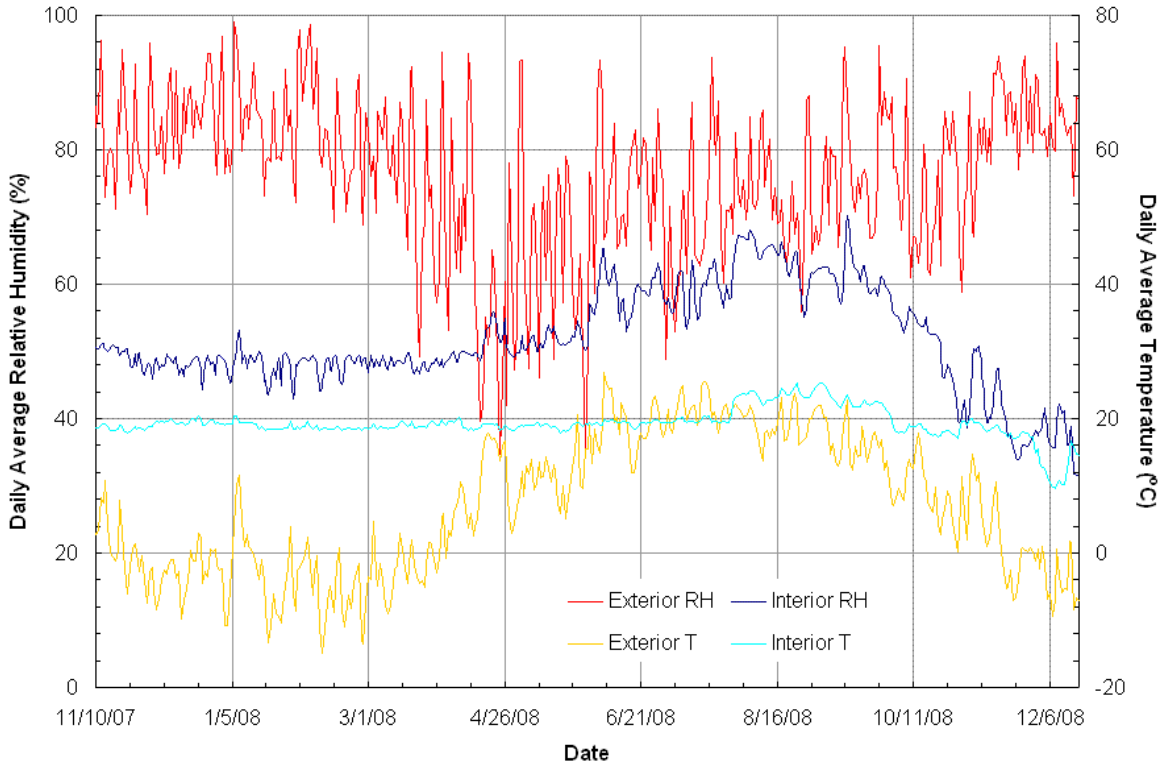

Figure 46. Interior and exterior relative humidity and temperature

9.1.2 Wind and Rain

Wind data from the UW Weather Station was used after finding some errors in the BEGHut wind direction data. Daily average wind and total rain are shown in Figure 47. Wind is primarily westerly as seen in the wind direction frequency chart in Figure 48. However, there were rain events accompanied by easterly winds which are shown in the combined wind direction and rainfall frequency chart in the same figure. The wind direction frequency is the cumulative hours that wind is measured in the various directions (22.5^{o} increments). The driving rain frequency chart is the cumulative hours that wind is measured in a given direction while there is also rainfall measured. To see the temporal variation of driving rain the measured and computed driving rain from the UW Weather Station are shown in Figure 49.

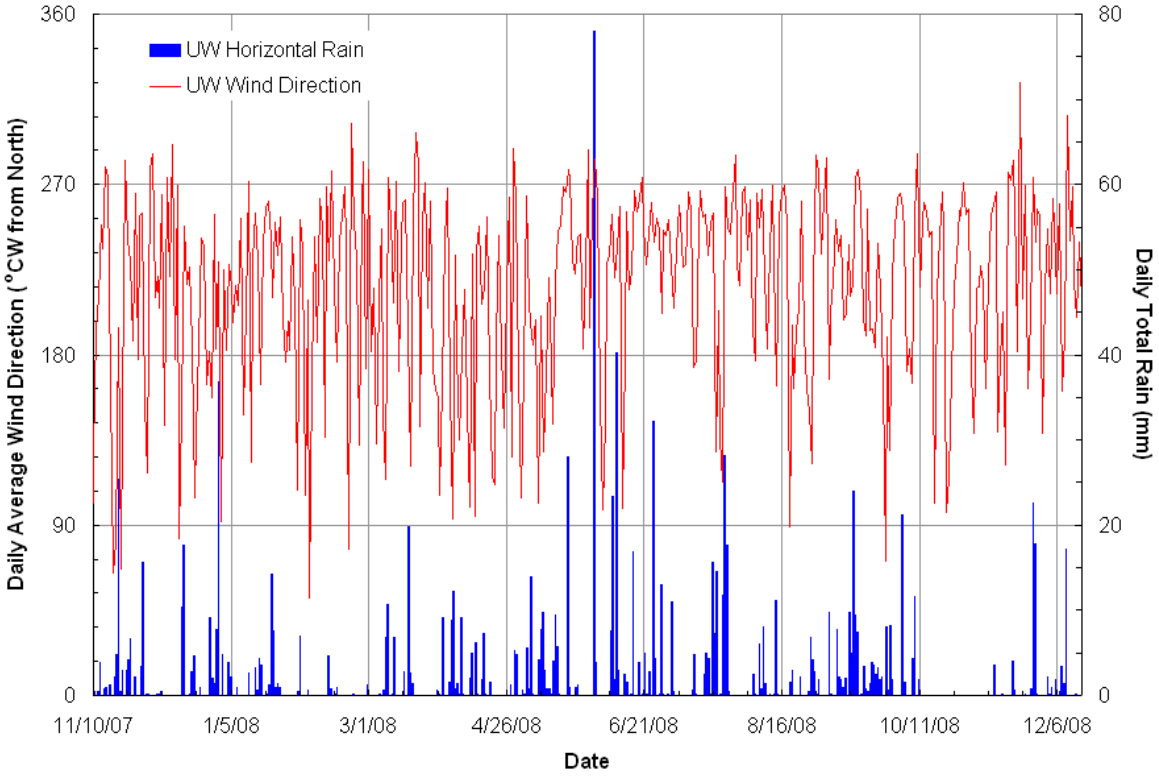

Figure 47. Daily average wind direction and daily total horizontal rain from UW Weather Station.

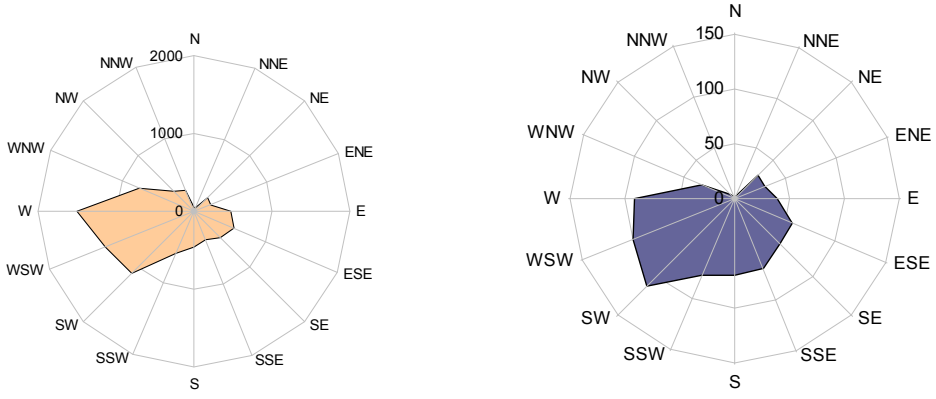

Figure 48. Wind direction frequency in hours (left) and combined wind direction and rainfall frequency (right) for data from the UW Weather Station for Nov 9, 2007 to Nov 9, 2008.

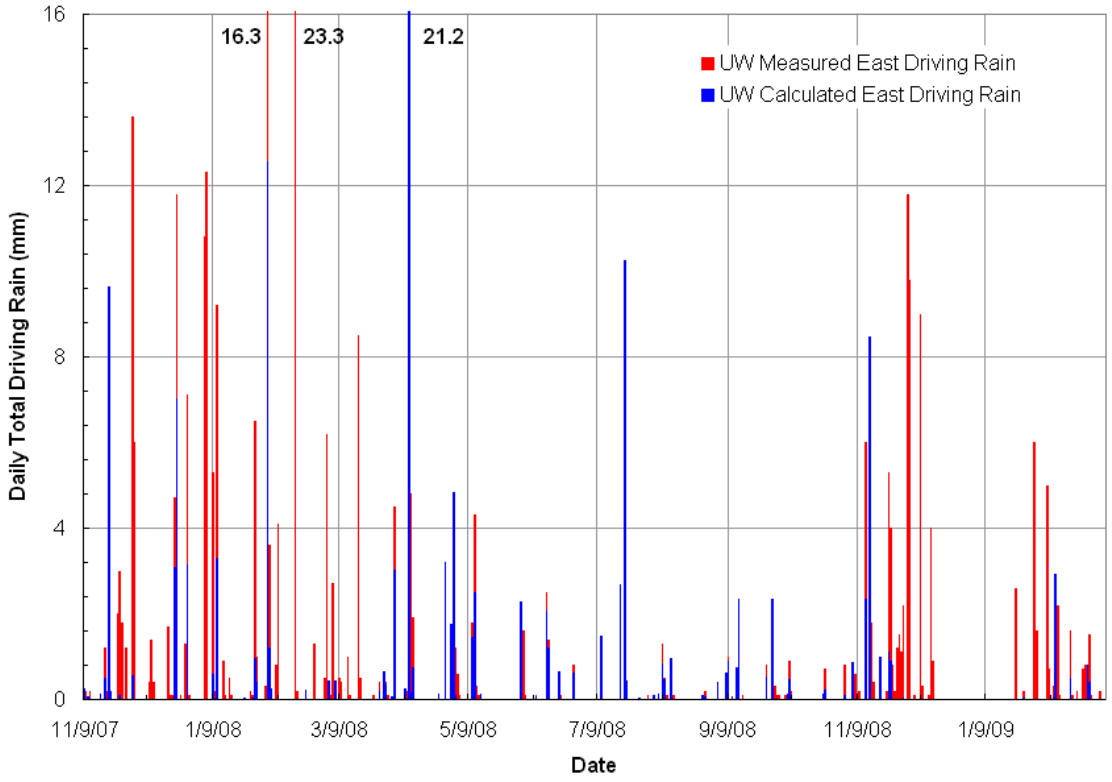

Figure 49. Measured and computed daily total driving rain on east wall from UW Weather Station.

9.1.3 Solar Radiation

Solar radiation was measured on the horizontal. This will give a general indication of the amount of radiation on the east wall (i.e. clear day versus cloudy day). However, for modeling and other computations a conversion of the horizontal radiation to the radiation on the east wall is necessary. The process for this conversion is given in Appendix A. Total daily radiation on the east wall as computed is given in Figure 50 with the total daily radiation on the horizontal.

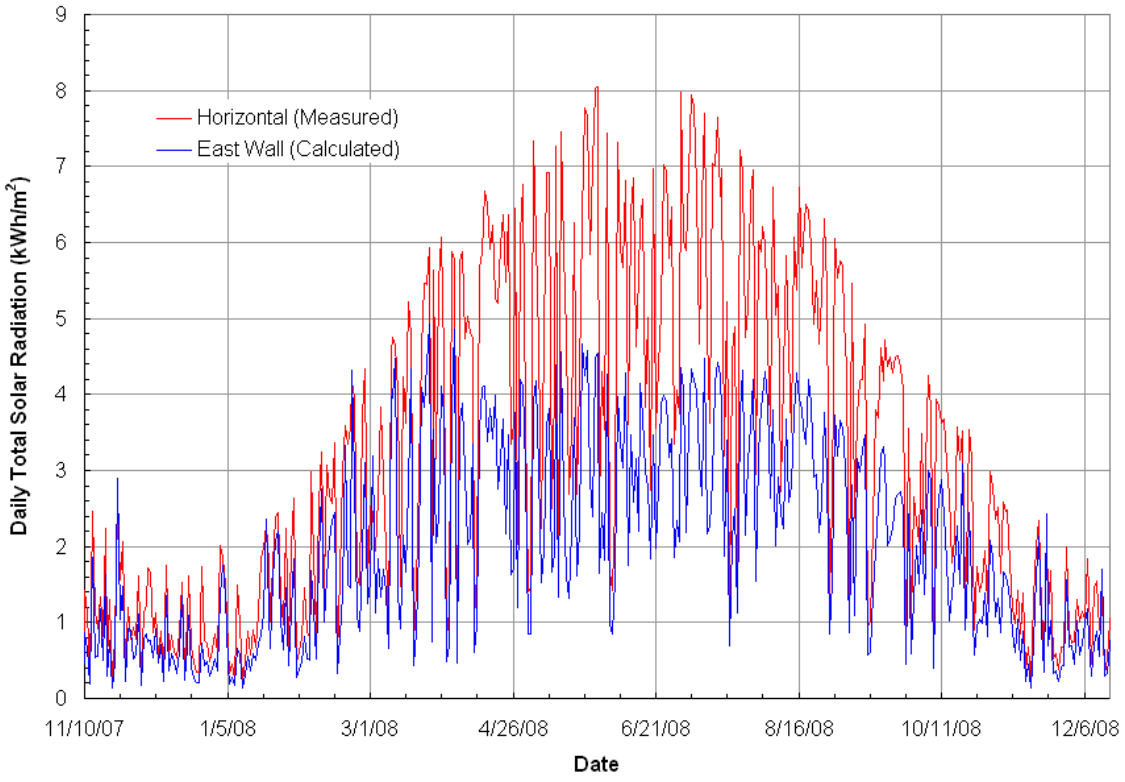

Figure 50. Daily total horizontal solar radiation and computed daily total solar radiation on east wall.

9.2 Temperature

The weekly average temperatures through the mid-height of both walls are shown in Figure 51. Through the winter the weekly average temperatures are between the interior and exterior, whereas they are above the ambient conditions in the summer. Both walls show very similar temperature profiles during the winter on the weekly average plot. Hourly data is shown in Figure 52. The summer data does not appear as similar between walls and is shown in Figure 53.

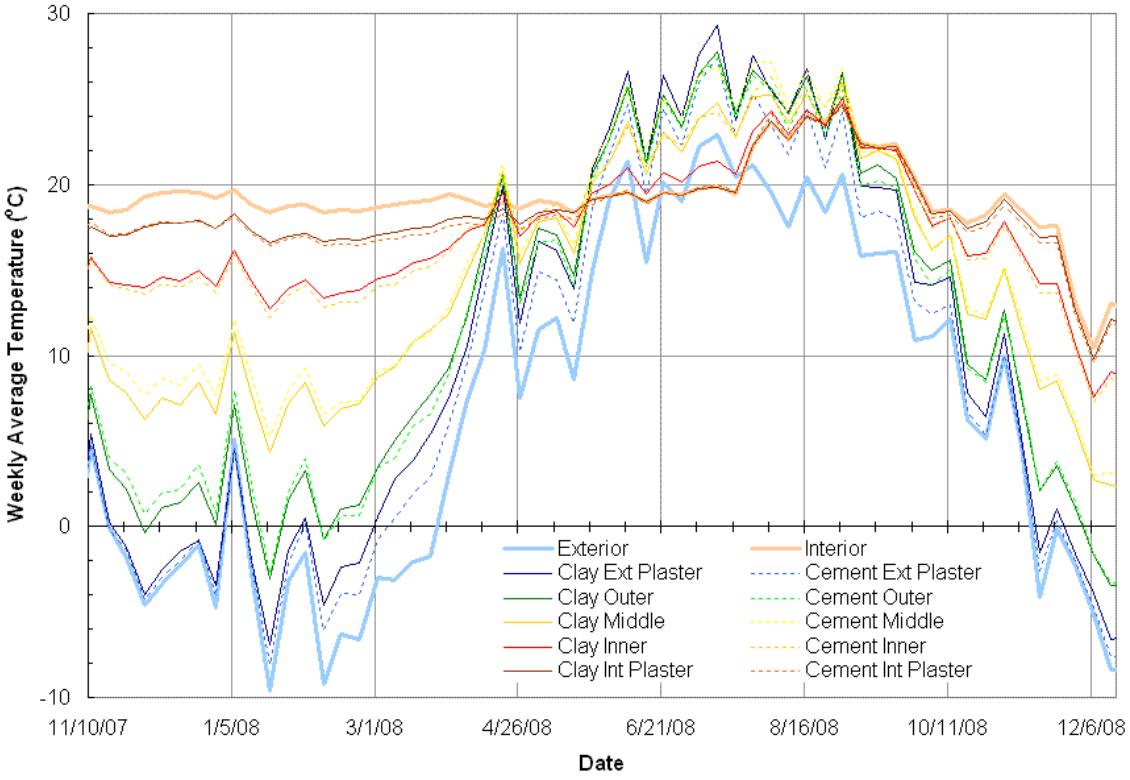

Figure 51. Weekly average temperature for both walls at mid-height.

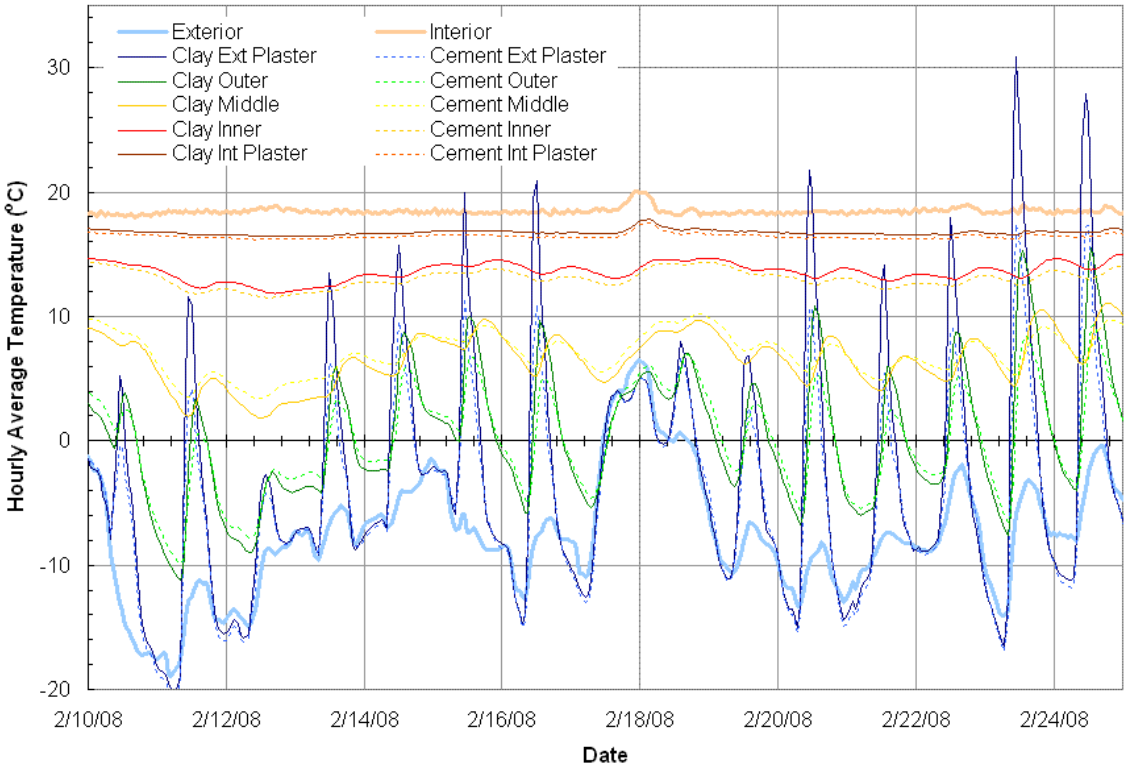

Figure 52. Hourly winter temperatures for both walls at mid-height.

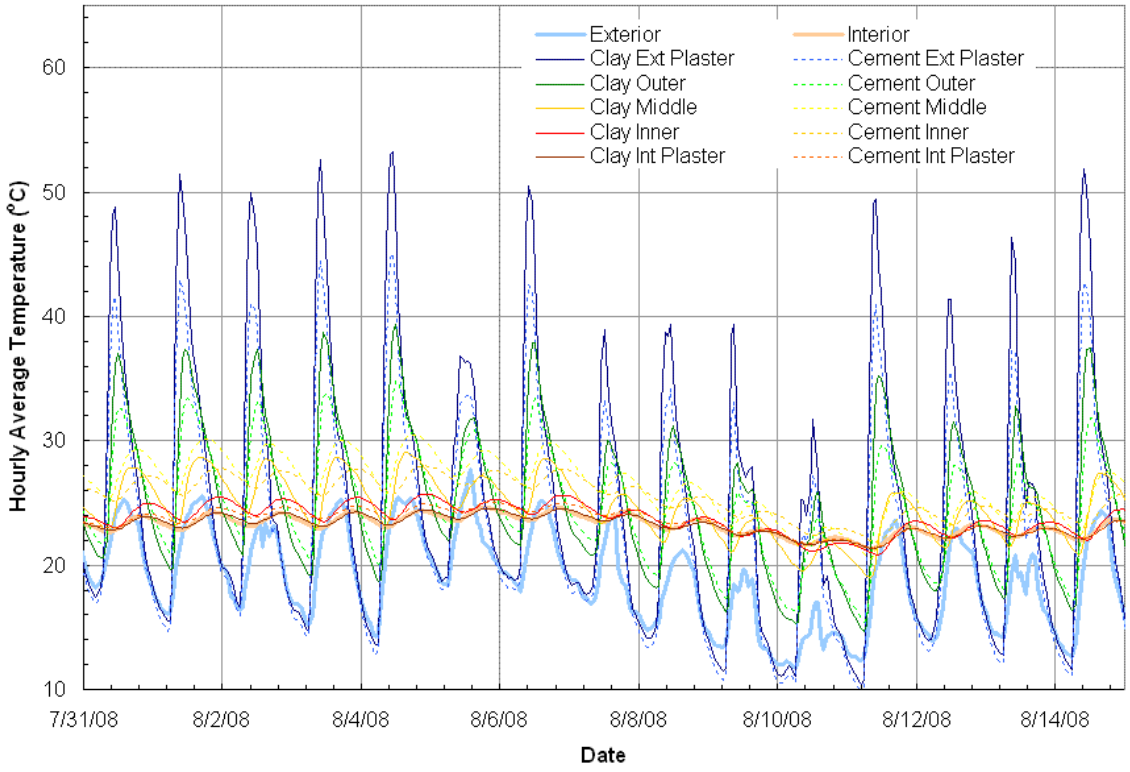

Figure 53. Hourly summer temperatures for both walls at mid-height

The temperatures through both walls are very similar through the first winter as expected. This is due to most of the insulating value coming from the straw which is the same for both walls. The effect of the differences in plaster thermal resistance is negligible on the temperature profile. However, the solar absorptance of the earth plaster is greater than the cement plaster and thus shows a slightly higher temperature (TMex) than the cement plaster during winter. Other differences in temperature may be a result of the placement of the sensors.

The difference in solar absorption is obvious in the hourly temperature plot for the summer: E1 shows noticeably higher plaster temperatures than E2 (53°C vs 45°C). The same trend is shown for the TM02 sensor. However, the inward sensors, TM07 and TM12 show a different behavior. Temperatures inside the cement plastered wall are elevated during the summer in comparison to the earth plastered wall. This behavior is not duplicated at the bottom of the wall but is only found at the mid-height.

Temperatures at the lower height are affected by the foundation at the base of the wall. Comparison of the lower temperature to the mid-height temperatures in the earth plastered wall is shown in figures Figure 54 and Figure 55 for winter and summer

respectively, similar results are found in the cement plastered wall. In the winter this results in the exterior side not being as cold and the interior side not being as warm. Temperatures are reduced at the lower height in the summer in comparison with the mid-height.

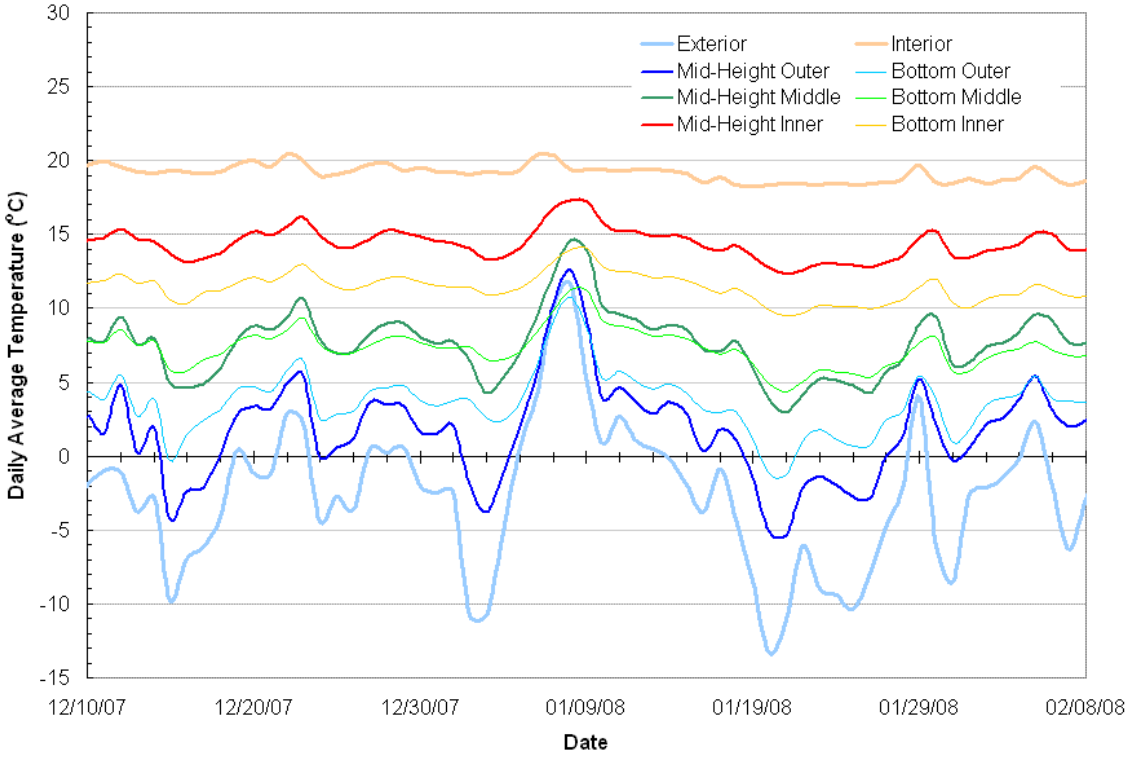

Figure 54. Clay wall lower and mid-height temperature during winter.

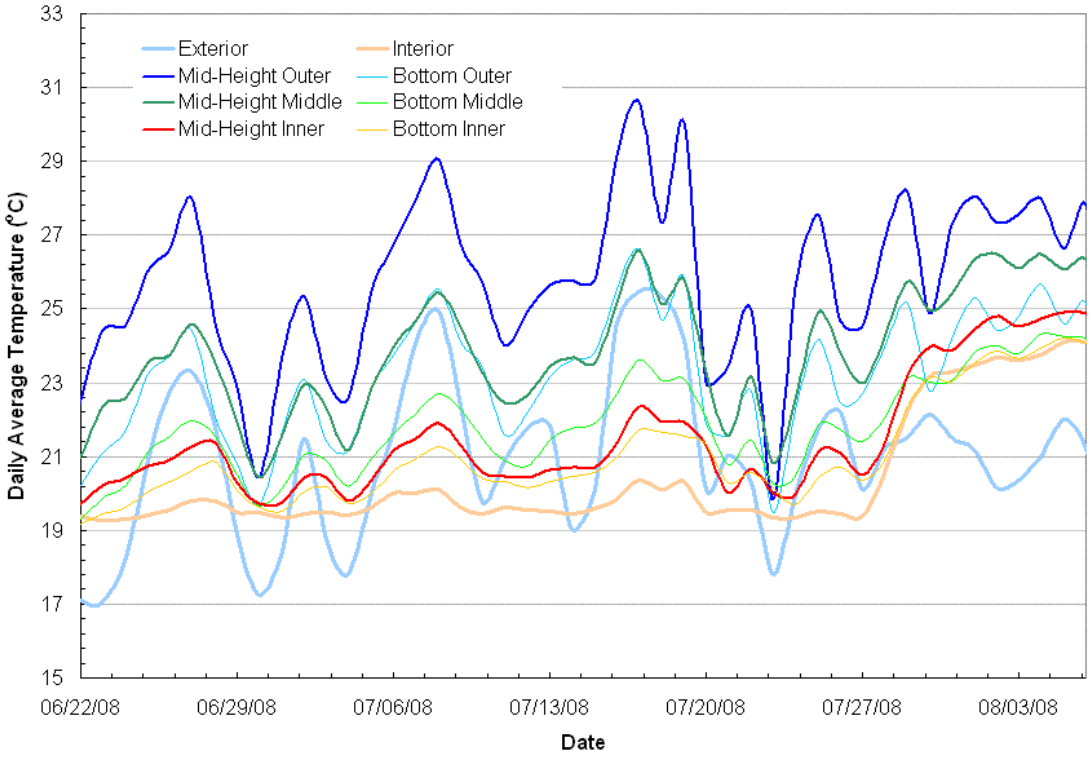

Figure 55. Clay wall lower and mid-height temperature during the summer.

9.3 Relative Humidity

The relative humidity through both walls at mid-height is given in Figure 56. Sine curves were fit to the data by visual inspection to allow for better viewing of the seasonal trends. The same was done for the lower and upper sensors as shown in Figure 57 and Figure 58. Parameters used in the sine curves are summarized in Table 21.

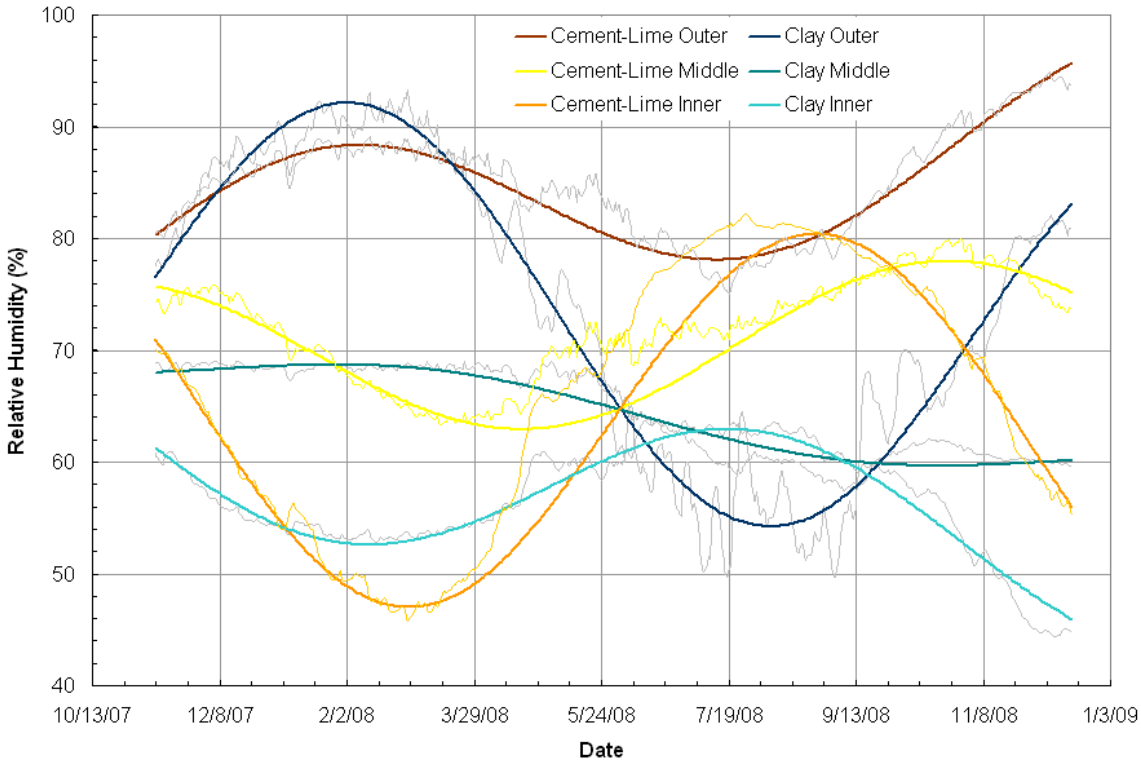

Figure 56. Daily average mid-height RH for both walls.

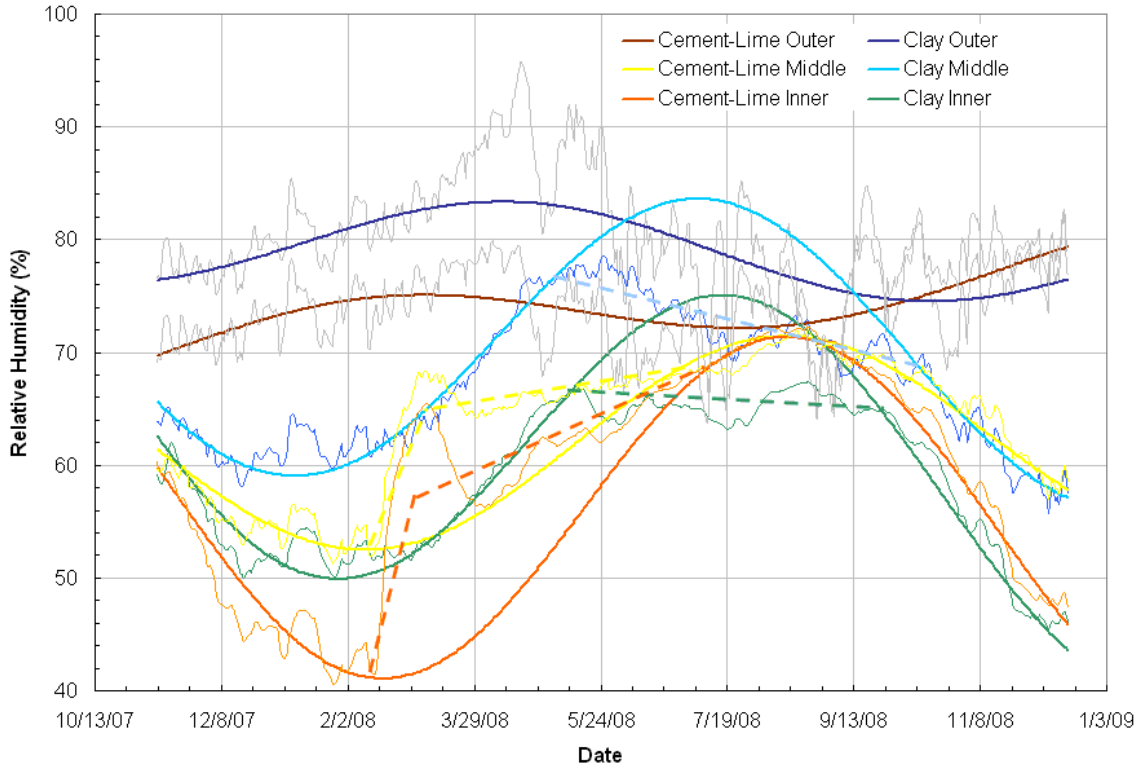

Figure 57. Daily average lower RH for both walls, variances indicated by dashed lines.

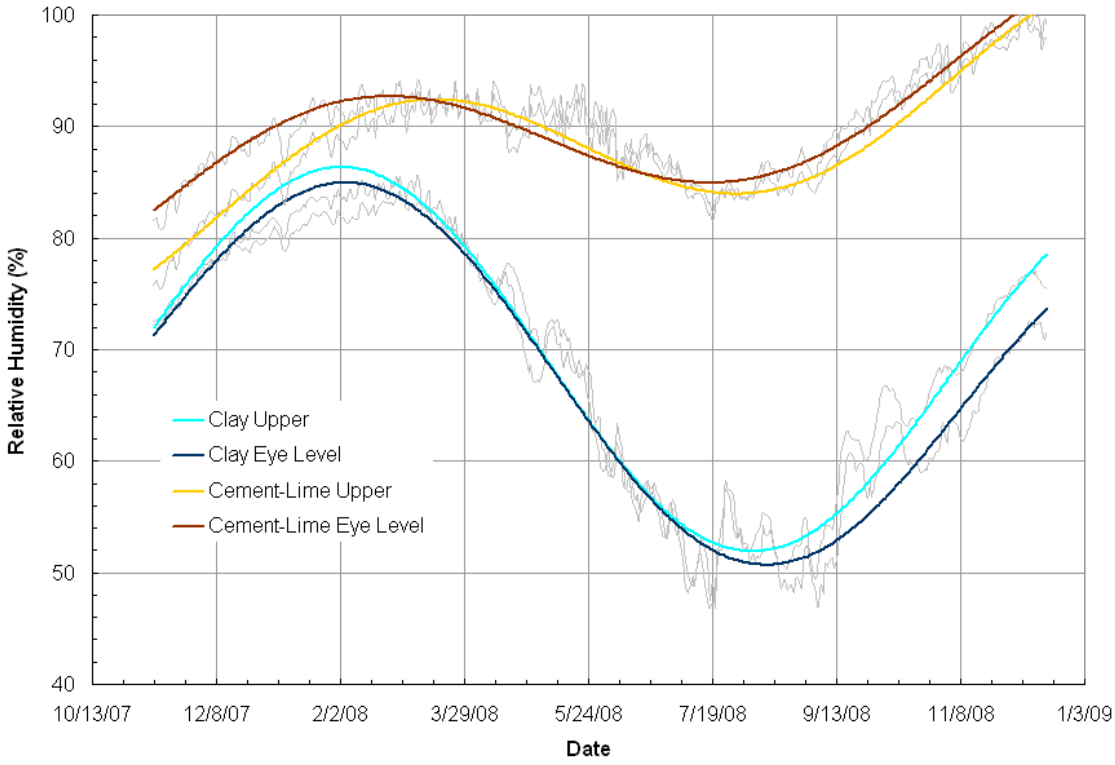

Figure 58. Daily average RH for the upper sensors of both walls, all are outer locations.

Sensor	Period (days)	Avg RH (% RH)	Amplitude (% RH)	Time Offset (days)	Yearly Change (%)
E1-RM02	365	75	18	5	-5
E1-RM07	365	69	2	-30	-12
E1-RM12	365	62.5	7.5	192	-16
E2-RM02	365	78.5	7.5	14	13
E2-RM07	365	69	7	110	3
E2-RM12	365	65.5	17.5	164	-5
E1-RL02	365	80	4	-65	-2
E1-RL07	365	72.5	13	215	-4
E1-RL12	365	67	15	200	-15
E2-RL02	365	70	3	-5	10
E2-RL07	365	61	9	180	3
E2-RL12	365	58	16	176	-6
E1-RE02	365	70.5	16.5	5	-4
E1-RU02	365	71	15.5	1	-9
E2-RE02	365	81	7	-30	15
E2-RU02	365	82	7	4	17

Table 21. Sine curve parameters to fit measured data.

All of these curves were able to use 365 day periods. However some sensors show variances in the data from the sine curves. It was possible to alter the period of the sine curves to attempt to provide a curve that would better follow the variances, but it was thought better to leave the period at 365 since that is the true period and recognize the variances as they are. If different periods were chosen they would not be able to continue into the second year.

The most particular variance is in the cement lime plastered wall, which shows increased RH through the spring for both mid height and lower sensors, most notably at the lower height. These are highlighted in the mid height chart and dashed lines are drawn for the lower height chart. In addition, the earth plastered wall at the lower height shows a plateau of RH in the summer and so diverges from the sine waves. Again this is shown with dotted lines indicating the approximate path of the RH data. Variances are greatest with the lower height as splashback plays a larger role in this location and is not as sinusoidally dependent on the seasons as rainfall is not sinusoidal through the year.

From these trends it is evident that the cement plastered wall is generally showing a slight increase in relative humidity over the year, while the earth plastered wall exhibits considerable decrease. These changes vary through the cross section of the wall. The outward sensors show the least decrease in the earth plastered walls and the largest increase in the cement plastered walls, whereas the inward sensors show the largest decrease and the smallest increase in the earth and cement plastered walls respectively. This is an indication of the concentration of moisture loading at the exterior of the walls. The average between the lower and upper sensors for the outer, middle, and inner locations is a change of 11.5%, 3%, and -5.5% for the cement plastered wall and -3.5%, -8%, and -15.5% for the earth plastered wall, respectively.

There is much more seasonal fluctuation in the exterior location of the earth plaster than for the cement plaster at mid height, but the reverse is true for the inward location. This is likely a result of the difference in permeance of the plasters. They both show a buildup of moisture during the winter, with the earth plastered wall increasing to greater levels than the cement plastered wall. Spring brings warmer temperatures and drying potentials. However, the lower permeance of the cement plastered wall results in a reduced rate of drying compared to the higher permeance of the earth plastered wall. Therefore, instead of primarily drying outward the moisture will also migrate towards the interior side of the cement plastered wall during the spring and summer. Thus the interior sensor in the cement plastered wall shows a significant increase in relative humidity through the summer, whereas the earth plastered wall does not show this increase. This seasonal

moisture movement may best be indicated by the middle sensor. The clay plastered wall shows a general decrease through the spring and summer, whereas the cement plastered wall shows a decrease through the winter when moisture migrates to the exterior, and then an increase through the summer as moisture moves back to the interior side.

The reduced drying potential is also the likely reason for the overall net wetting of the cement plastered wall while there is overall net drying in the earth plastered wall even though it appears more susceptible to rain penetration.

The difference in RH at the outward location is shown well in the plot of the upper sensors in both walls, Figure 58. In addition extremely high levels of humidity are seen in the cement plastered wall as the second winter approaches, upwards of 100%RH. The RH in the cement wall is higher at the upper locations than the mid height and lower height, whereas the earth plastered wall shows lower humidities at the upper locations relative to the lower locations.

In the first winter the relative humidity at the lower location in both walls is generally lower than the relative humidity at the mid height. This may be a result of the difference in temperature, as the foundation at the base of the wall modulates the temperature at the lower height causing the outward temperature to be warmer and the inward temperature to be colder. The cement wall maintains this difference through the year but the earth plastered wall ends up with higher RH at the lower height from the spring onward. The lower sensors peak in the spring and dry somewhat during the summer but not as well as the mid-height sensors due to splashback that affects the lower heights.

Splashback also produces more short term fluctuation in the RH at all locations lower in the wall. The clay wall showed more variation in the mid height compared to the cement wall as previously mentioned, however, they behave similarly at the lower location, in terms of the amount of fluctuation in the RH. The outer sensor of the clay wall fluctuates a little more dramatically in the summer but not significantly more than the cement wall's outer sensor.

Sine curves are more difficult to fit to the lower data. The inward sensors show a better correlation to a sine wave, except for the noted variations. The outer sensors show little correlation, likely due to the large impact of rain and splashback on the humidity in the wall and not the seasonal fluctuations of RH and T. It is currently a mystery as to the large spike in RH in the lower height of the cement wall, this spike is not recorded in any other sensors, but visible dampness was noticed on the interior cement plaster at the

divider that separates both walls on or before Feb 5, 2008, possibly indicating a leak. This occurs before the spike in RH which begins on Feb 15, 2008.

The highest humidities at the lower sensors are found in the spring, when snow cover melts and spring rains occur. In general there is a rise in humidity for all lower sensors through the spring. This is different than the mid height of the wall, which shows differing behavior between the inward and outward sensors.

For better comparison between the mid-height and lower sensors in each wall a combined chart is shown in Figure 59 and Figure 60 for E1 and E2 respectively.

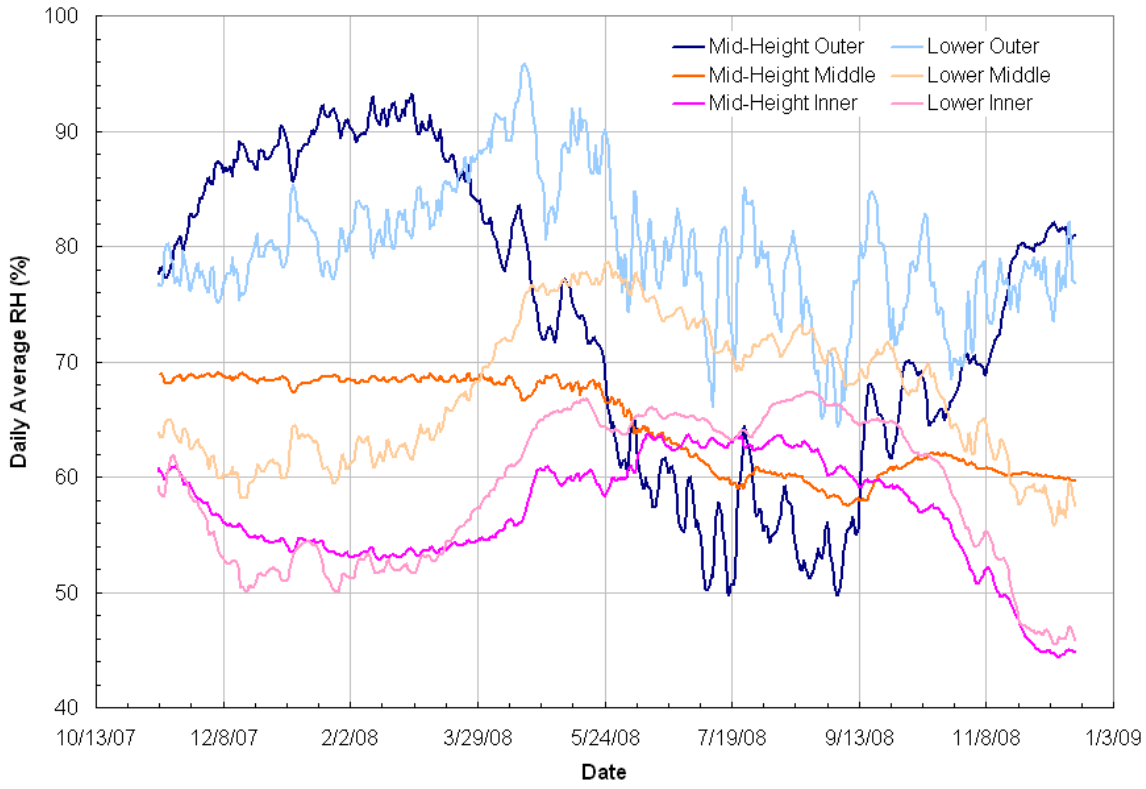

Figure 59. All RH sensors for clay plastered wall (E1).

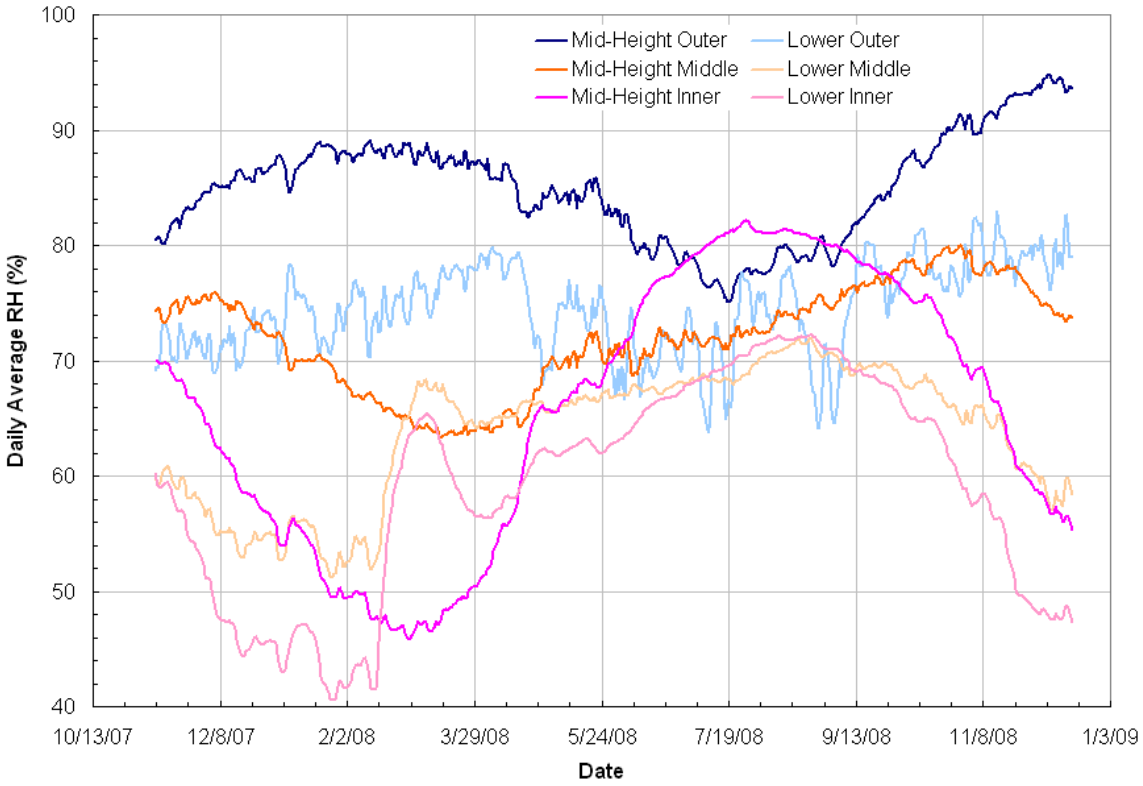

Figure 60. All RH sensors for cement-lime plastered wall (E2).

9.4 Vapor Pressure

The relative humidity gives a good indication of the moisture in the walls; however, to fully understand the vapor drives the vapor pressure is needed. This is determined from the temperature and relative humidity. One reason for the variation of relative humidity at the exterior of the wall is the variation in temperature through the year. At low temperatures (winter) the vapor pressure does not have to be high to cause a high relative humidity but in high temperatures (summer) the vapor pressure has to be much higher to achieve the same relative humidity. This results in some variation of relative humidity due to seasonal temperature fluctuations.

When looking at the vapor pressure at the exterior side of the wall the opposite trend to RH is found. Low vapor pressure occurs during the winter and high vapor pressure during the summer. However, due to the low temperatures in the winter and high temperatures in the summer the relative humidity behaves as it does. The relative humidity is a better measure for mould and health of a wall, while the absolute vapor pressure is required to assess vapor drive potentials.

As is seen in Figure 62, the conditions within the walls are between the interior and exterior during the winter. This results in a net flow of vapor from the interior of the building through the wall to the exterior. The total amount of flow is controlled by the vapor permeance of the assembly as well as the sorption capacity of the straw. In the spring the vapor pressures rise above both interior and exterior pressures and so drying occurs inward and outward. The earth plaster being more vapor permeable will allow more vapor movement. Thus the earth plaster vapor pressures equalize with the interior and exterior by the end of the summer, whereas the cement plastered wall is still 'drying' into December.

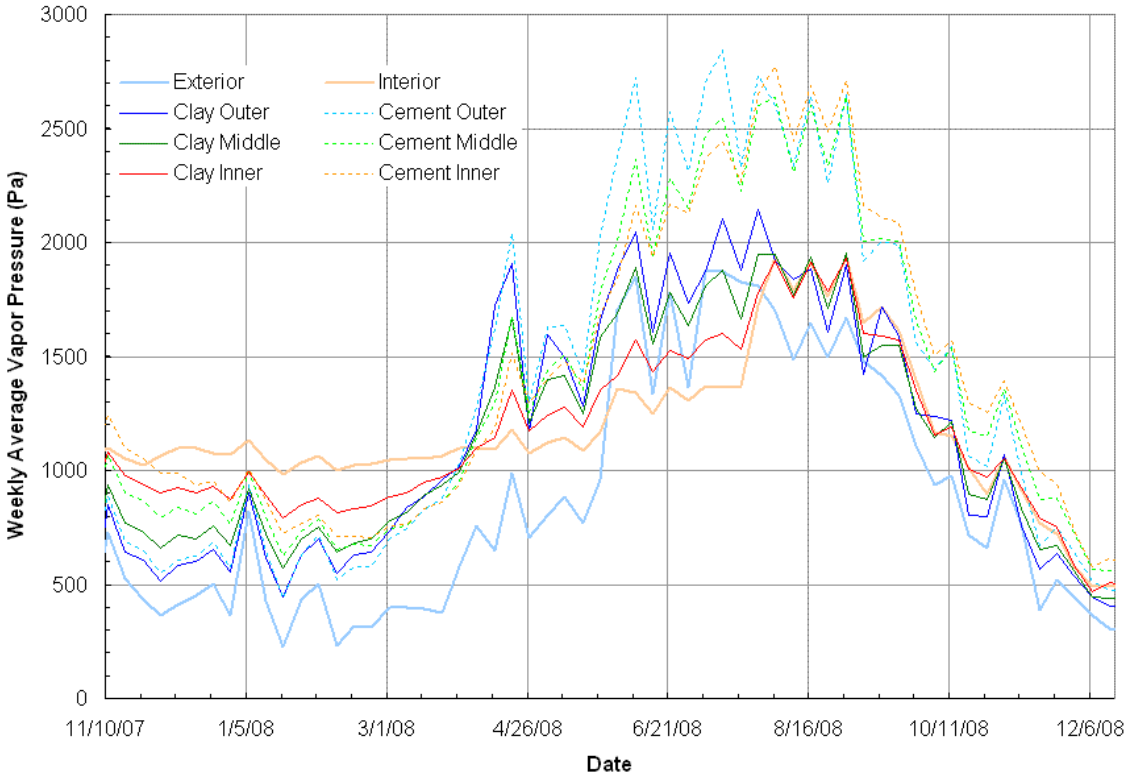

Figure 61. Weekly average mid-height vapor pressure in both walls.

Another phenomenon that arises in both walls is vertical variation in vapor pressure. The cement plastered wall shows the lowest vapor pressure at the bottom of the wall and the highest vapor pressure at the top of the wall. However, the earth plastered wall shows the opposite. It has the highest vapor pressure at the bottom of the wall and the lowest vapor pressure at the top of the wall. This is shown in Figure 62.

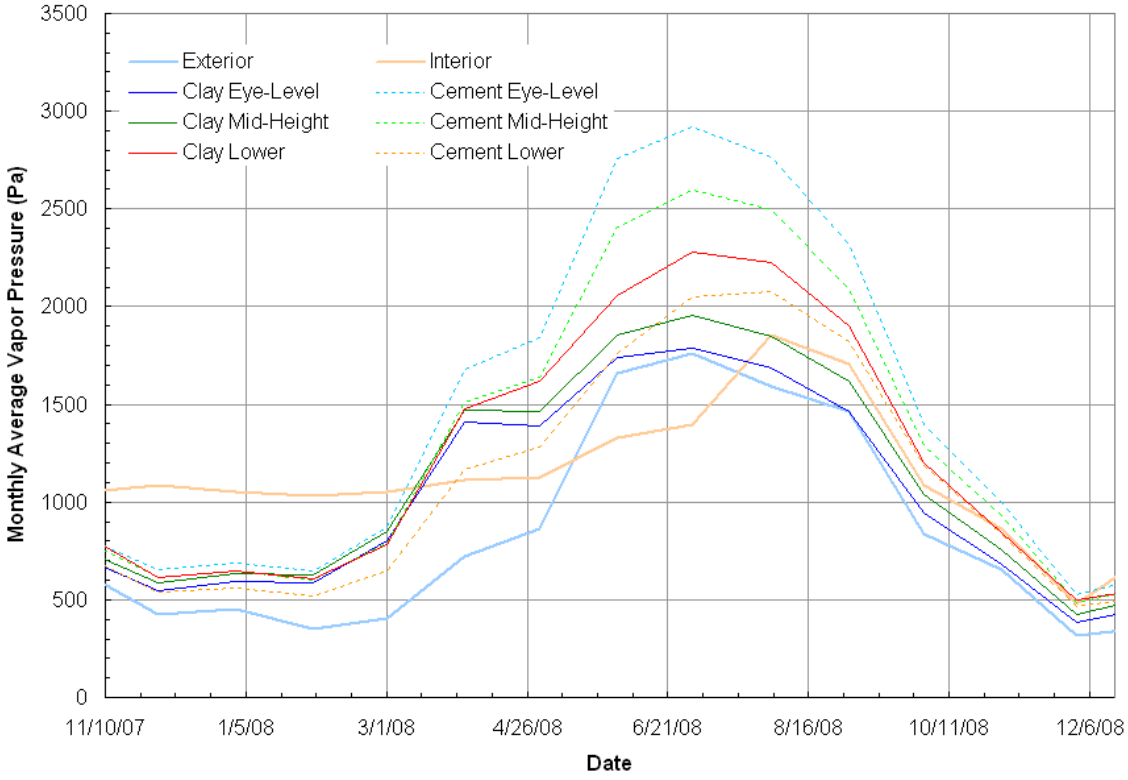

Figure 62. Monthly average vapor pressure at lower, mid-height, and eye-level outer sensors for both walls showing vertical stratification of vapor pressure.

In the one dimensional analysis the flow of vapor was either into or out of the wall, but in reality vapor will also move vertically within the wall. This will be due to differences in pressure, but may also be facilitated by the rising of moist air through the straw bales which is less dense than dry air.

In the cement wall, because it is less vapor permeable the moisture remains in the wall longer and has more time for the stratification to occur. However, in the earth wall, the great permeability of the plaster allows the water vapor to more readily leave the wall and thus stratification due to buoyancy does not occur, although this does not mean the movement of vapor in this manner does not occur, it just means that it occurs at a slower rate than the movement of vapor through the plaster to the exterior or interior.

The reason for the reverse stratification is that the major moisture source in the earth plastered wall is rain, and rain has the greatest impact at the bottom of the wall. This is due to the effect of splashback. This can be seen in Figure 63, where the darkened plaster at the bottom of both walls is indicating wet plaster due to splashback. Also note the

apparent drying of the splashback moisture in the cement plastered wall between March 18, 2008 and March 19, but the earth plastered wall remains saturated.

Figure 63. Splashback wetting, Mar 18, 2008 (left) and Mar 19, 2008 (right).

9.5 Moisture Content

The effect of rain can be seen best in the response of the moisture content wafers that are at the plaster straw interface. Water that penetrates or wicks through the plaster will contact the wafer. The earth plastered wall shows large spikes during wetting events whereas the cement plastered wall shows little variation. The largest events were on November 21, 2007 and April 10, 2008.

A confusing result from this chart is the considerably lower MC at the bottom of the cement plastered wall.

During the winter the outer MC is extremely high and is a cause for concern. However, during the summer the MC drops below 20% which is the generally accepted safety limit for mould growth. The earth plastered wall shows higher MC during the winter but dries more during the spring to result in lower MC readings than the cement plastered wall (at mid height), the bottom sensor is still higher but does dry to about the same level as the mid height in the cement wall by September.

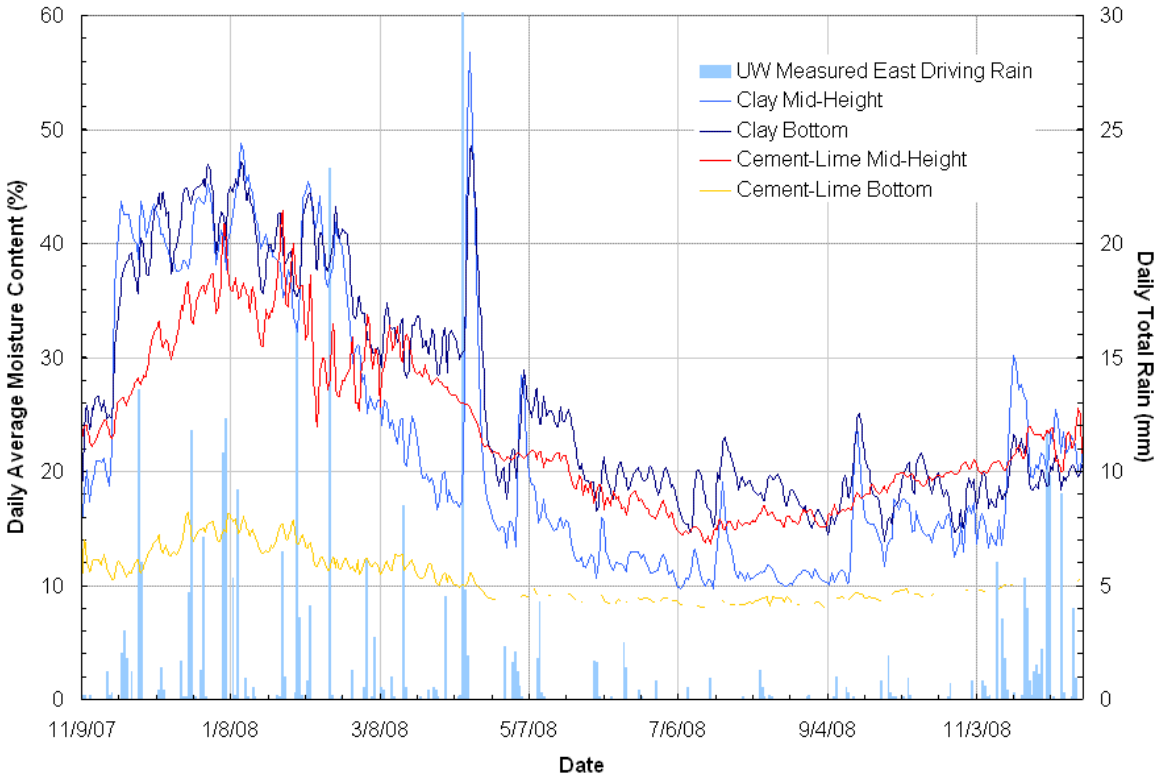

Figure 64. Daily average MC of outer sensors at bottom and mid-height for both walls with driving rain data.

All the MC sensors for the earth plastered wall are shown in Figure 65 with the cement plastered wall sensors shown in light colors for reference. The reverse plot showing the cement plastered wall sensors is in Figure 66.

One note to make is the E2-MB12 sensor that shows 10%MC for the duration of the test except for a small rise of short duration during February. This may be an indication of the leak that was noticed at the beginning of February. This is not noted in the other sensors, which instead drop during this period. However, E2-MT02 remained at a relatively constant level of 26%MC after this event, when it had appeared to be following the drying trend of the mid height sensor.

The wetting event in April appears to have caused the rise in MC at the bottom of the earth plastered wall. Both E1-MB05 and E1-MB12 rise during and shortly after this event and remain elevated during the summer as a slow drying trend occurs. This is not noticed in the cement wall as E2-MB05 and E2-MB12 remain at 10% for the entire year, except for the event in February that elevated the MC at E2-MB12, which was already noted.

Drying of the MC spikes in the earth plaster wall takes up to 10 days. The largest spike occurred on April 10 and returned to the same level by April 20. The ambient conditions will obviously affect the drying.

The bottom of the cement plastered wall remains quite dry all year, always below 16%MC. Even the outer sensor does not show effects from rain. There is some adsorption of the outward vapor drive during the winter, but it remains below 10%MC during the summer. The opposite seems true for the earth plaster wall. It appears to be strongly affected by rain. Winter levels are very high with drying through the spring and lower levels in the summer, but still near 20%MC. The inner bottom sensors appeared to respond to wetting events during the spring and summer, most notably the first large event in April.

The top outward sensors show a surprising response to rain and have quite elevated MC, comparable to the mid-height sensor. E2-MT02 does not dry the same as E1-MT02, this may be due to a leak as mentioned previously. The MT12 sensors behave similarly but E2 shows somewhat higher MC during the summer than E1. This is likely a result of reduced drying potential to the interior.

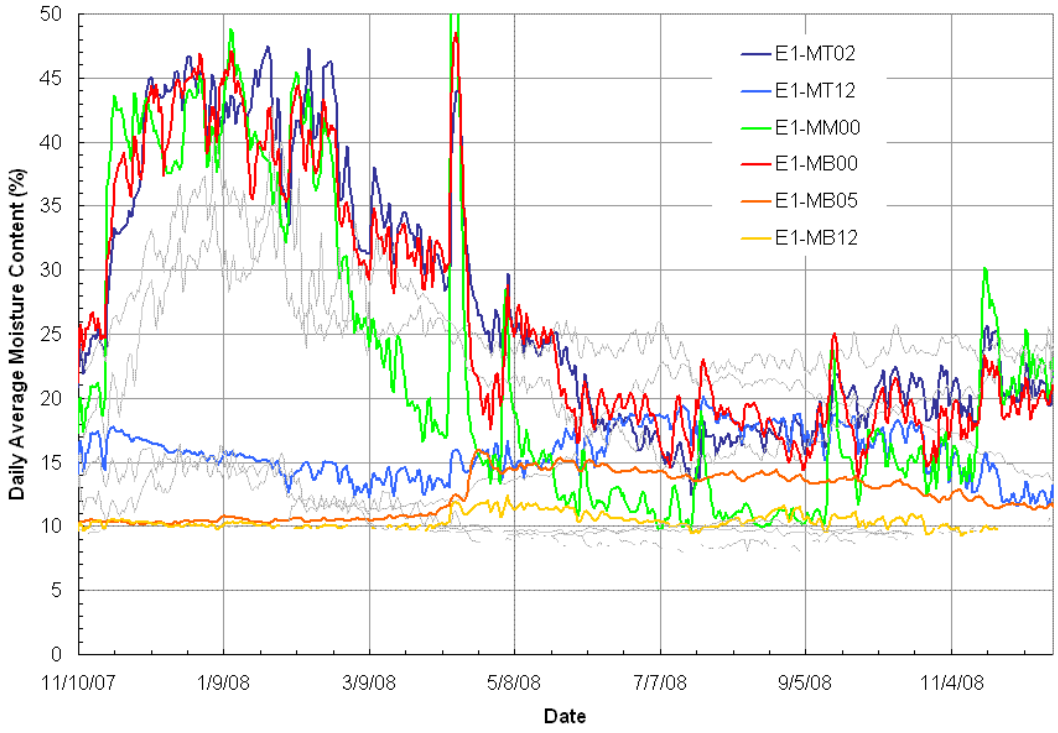

Figure 65. Daily average MC for all MC sensors in clay plastered wall (E1) with cement plastered wall (E2) results in grey for reference.

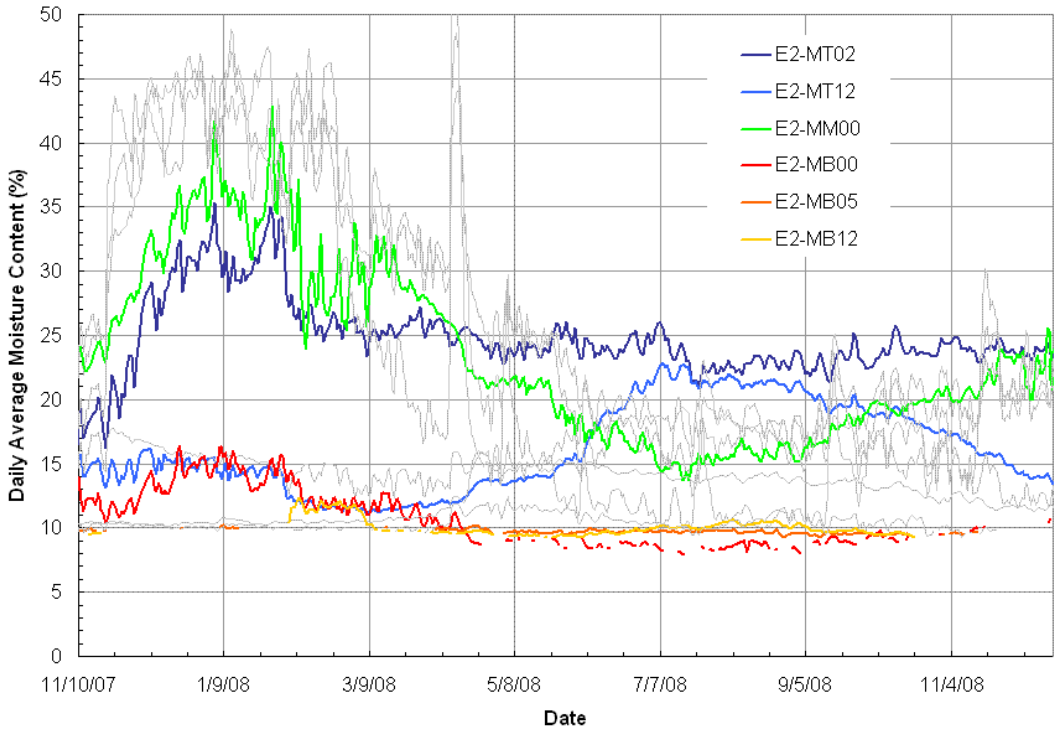

Figure 66. Daily average MC for all MC sensors in cement plastered wall (E2) with earth plastered wall (E1) results in grey for reference.

9.5.1 Rain Wetting

E1 shows large changes in MC with rain events, whereas E2 shows little if any change. This may be partly due to the location of the walls, as E1 is on the edge of the wall which would be more prone to driving rain, but this explanation is not enough to completely explain the differences.

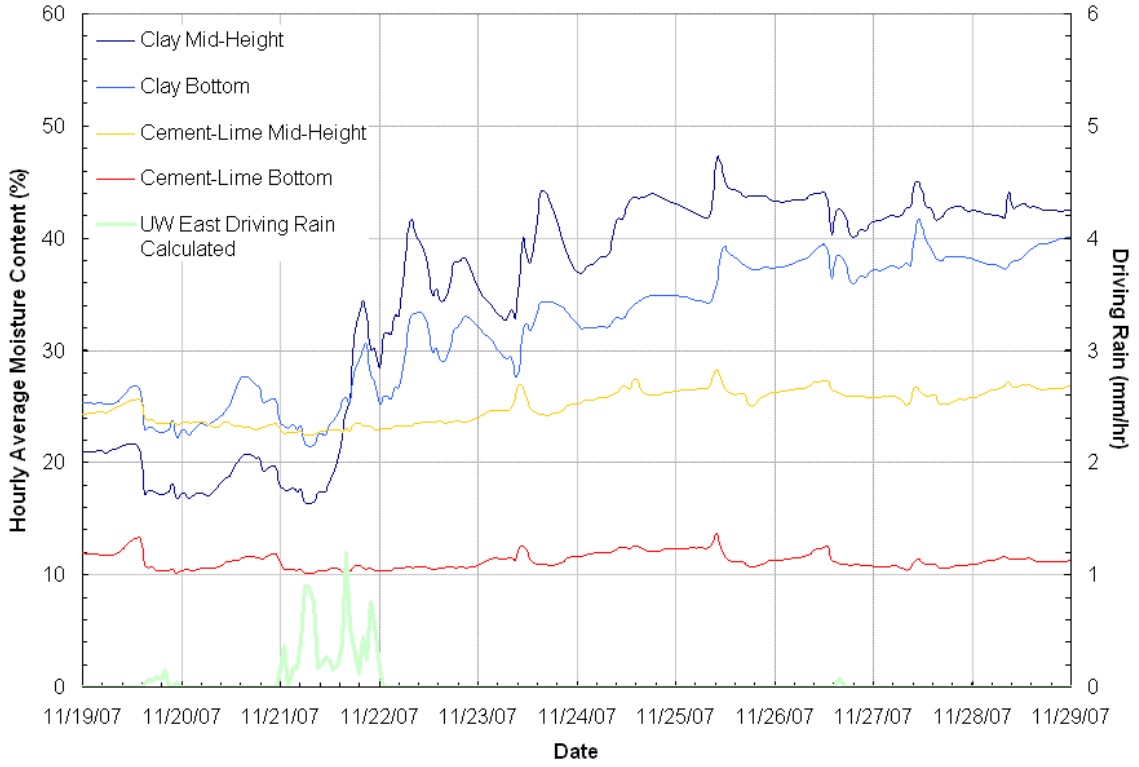

Figure 67. Driving rain event on Nov. 21, 2007, with outer MC sensors for both walls.

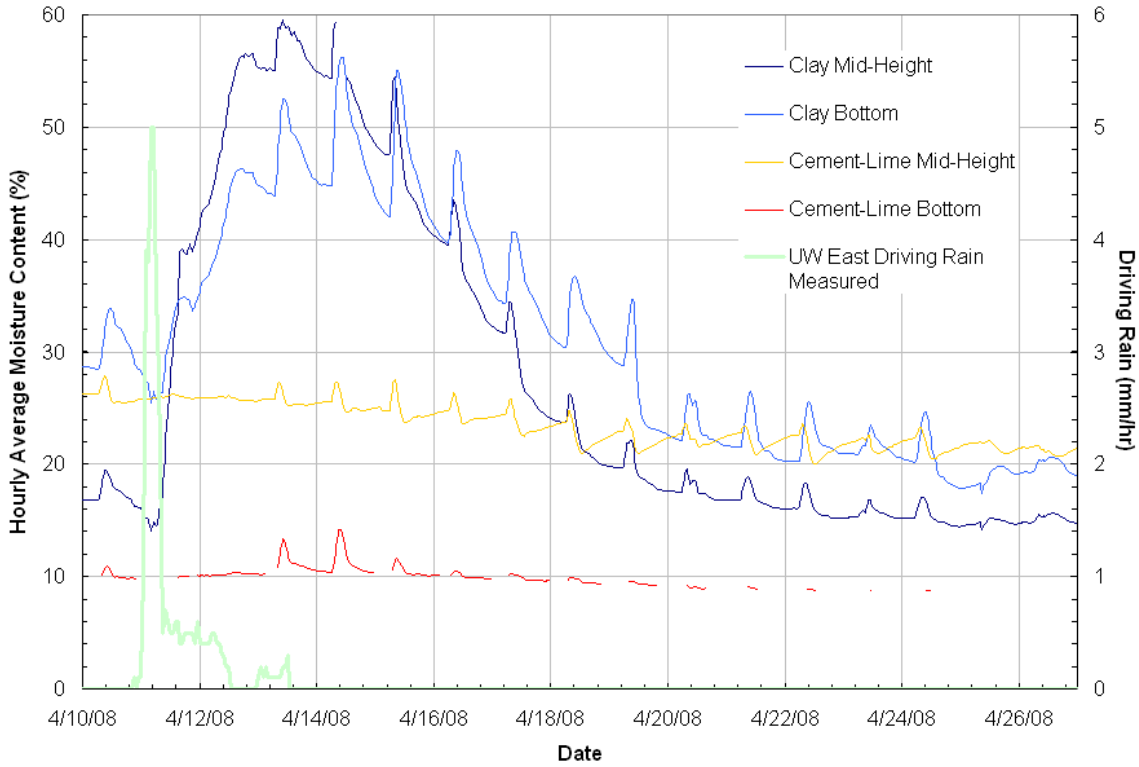

Figure 68. Driving rain event on April 11, 2008 with outer MC sensors for both walls.

9.5.2 Drying

In the previous plot for the rain event in April, there is an obvious drying trend in both walls afterwards. This is due to generally dry sunny conditions. Of interest is the difference in behaviour during the afternoon and evening after drying from solar radiation. E1 continues to dry until the next morning, while E2 stops drying and starts gaining moisture again until next morning. Both show increase in MC with increasing morning temperature as solar driven drying causes moisture to move inward from the plaster. But afterwards, the cement plaster wall increases in MC. This is likely a result of inward driven moisture returning to the sensor, which is not able to exit as readily through the cement plaster as it is able to in the earth plastered wall.

The total drying in the earth plastered wall is tremendous, from 57%MC to a steady 16%MC at mid height over 12 days, where the cement wall goes from 26% to 22%MC over the same period.

9.6 Potential for Mould

The potential for mould was investigated at the exterior locations of the straw bale wall as the inward locations do not show relative humidities above 80%RH. Therefore, the moisture content of the wood MC sensor that contacts the exterior plaster and the relative humidity sensor at 50mm inward from the exterior plaster were investigated.

9.6.1 Static Limit

The total duration of conditions above 80%RH was found. These indicate the most conservative estimate for potential time for mold growth, as they do not account for unfavourable temperature conditions, nor time to germination. However, high relative humidities at temperatures below freezing can usually be ignored. Figures showing the relative humidity over the monitoring period are shown below.

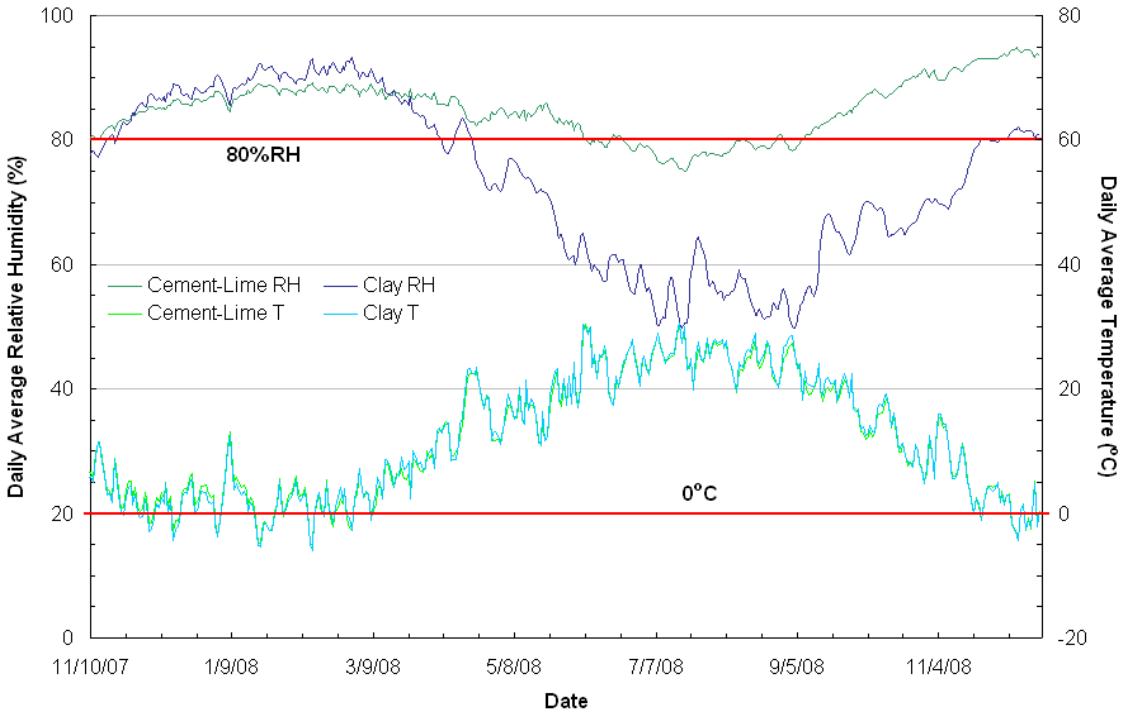

Figure 69. RH of RM02 sensor for both cement-lime and earth plastered walls, conservative mould growth limit is 80%RH, mould growth does not generally occur below 0°C.

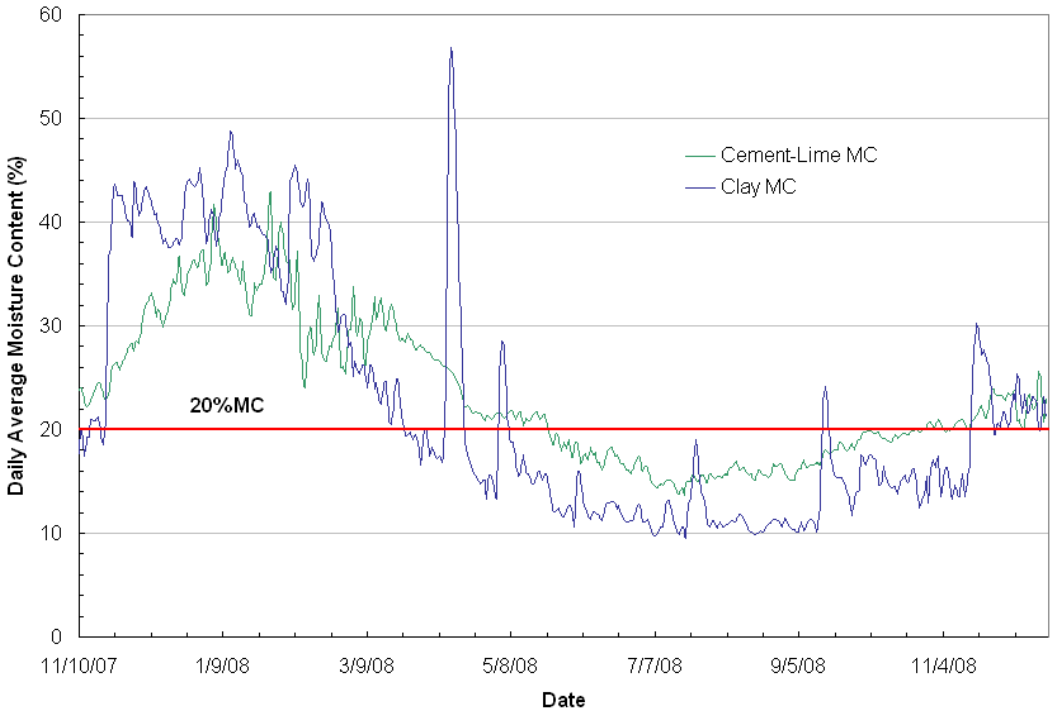

Figure 70. Wood MC of MM00 sensors for both cement-lime and earth plastered walls. Mould growth occurs above 20%MC with substantial growth over 30%MC for wood.

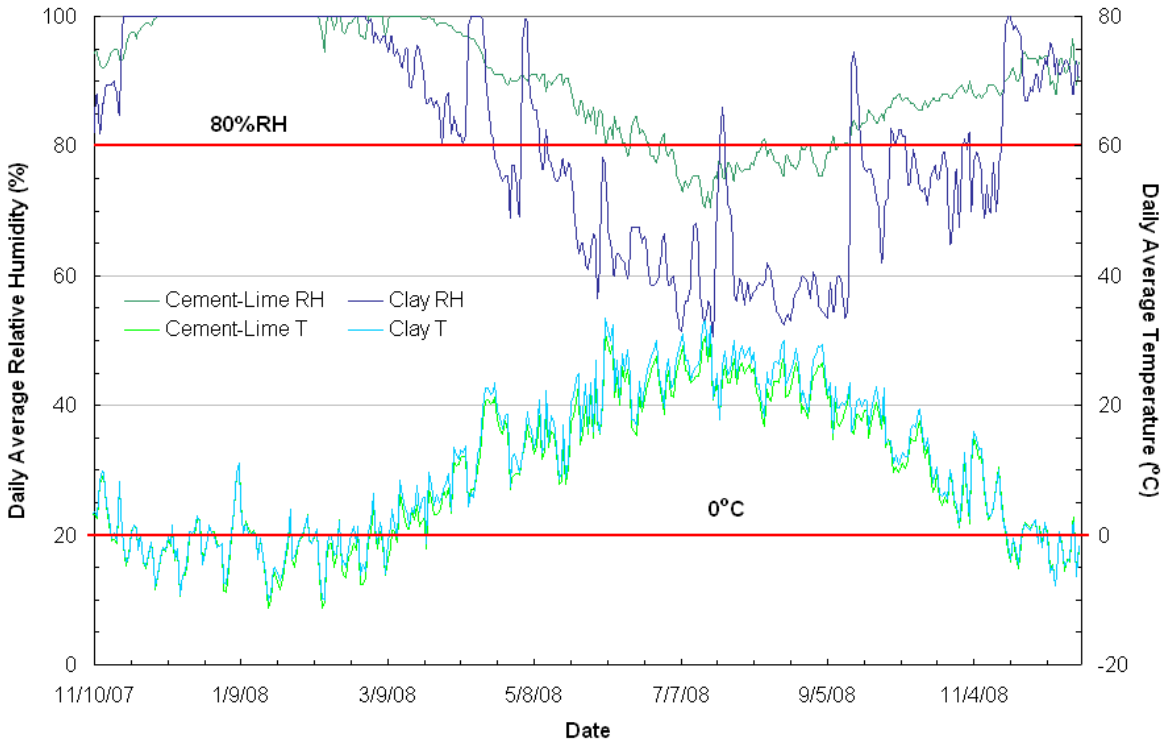

Figure 71. RH calculated from wood MC at MM00 for both walls.

It is evident that during the winter months the relative humidity is well above the 80% threshold for mould growth. Drying occurs through the spring with the lowest RH levels in the summer, for the outer sensors. The total number of hours above 80%RH for each location and wall are shown in Table 22 along with the number of these hours that are above freezing.

Wall	Sensor	Hours above 80%RH	Hours above 80%RH and 0°C
E1 – Earth Plaster	MR02	3975	2807
	MM00	5276	2862
E2 – Cement-lime Plaster	MR02	7798	6757
	MM00	8019	5427

Table 22. Total hours over 80% for outward mid-height sensors, total duration of data is 9699 hours.

Both walls show high levels of humidity in the winter, with the earthen plaster slightly greater than the cement-lime plaster. However, at these humidities the differences would provide little change in the rate of mould growth, in fact liquid water may slow the

growth. But in the spring the earthen plaster dries considerably more than the cement lime plaster the result is that just behind the plaster 54% of the time is above 80%RH for the earth plastered wall and 80% of the time for the cement plastered wall.

The earth plaster shows lower humidity levels during the warmer seasons when temperatures are more favourable to mould growth. However, both walls show a high potential for mould growth based on the 80% threshold, but temperature considerations should be made because much of the high humidities are in the winter season where temperatures may be restrictive.

9.6.2 Lowest Isopleth for Mould

The lowest isopleth for mould (LIM) takes into account the temperatures required for mold. Basic mold potential is the total duration of time that is above the isopleths, which indicates conditions favourable for mould growth. These are shown on graphs for visual inspection. There are a few charts available to use for the lowest isopleths. Those from Sedlbauer (2002) and Clarke at al (1999) will be used here. The average daily conditions were used instead of hourly data as mould growth does not fluctuate within the hour but is better represented by daily data.

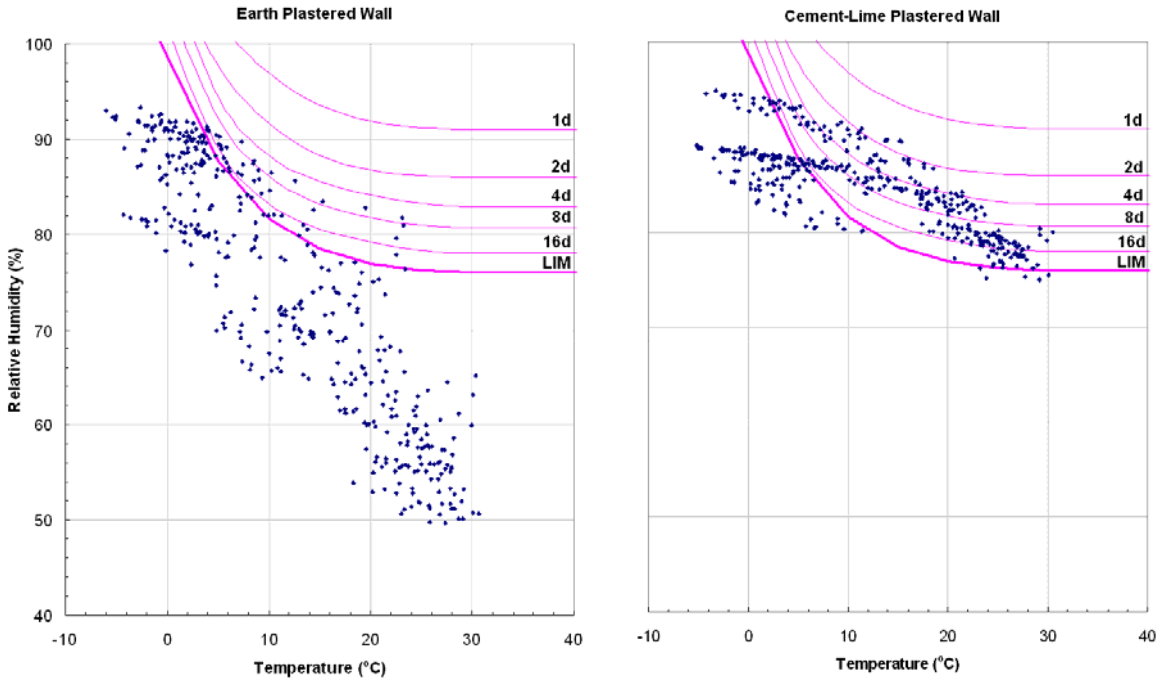

Figure 72. LIM with data from RM02 sensors for both walls.

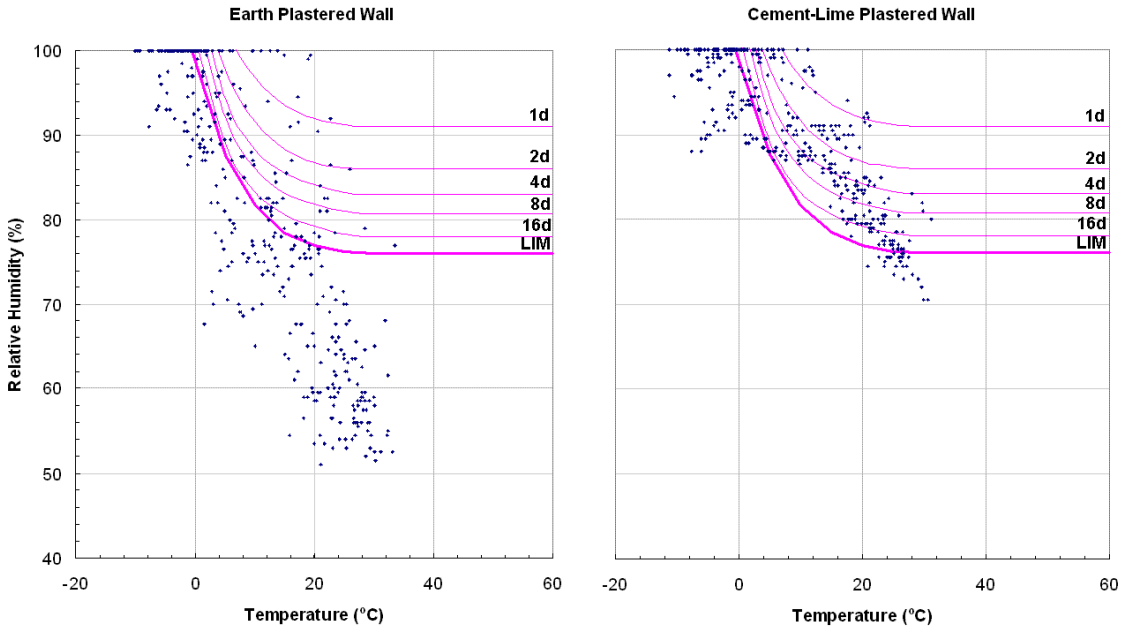

Figure 73. LIM with data from MM00 sensors for both walls.

The previous charts clearly show that the cement-lime plastered wall has more hours above the LIM than the earthen plastered wall for both sensor locations. The total days are listed in Table 23 with the previously tabulated hours for conditions above 80%RH.

Wall	Sensor	Days above 80%RH	Days above 80% and 0°C	Days above LIM
E1 – Earth Plaster	MR02	169	127	44
	MM00	218	120	115
E2 – Cement-lime Plaster	MR02	324	287	266
	MM00	326	222	264

Table 23. Days above the LIM with the days above 80%RH, total days is 405.

Sedlbauer also has isopleths for different times to germination as more favourable conditions require less time to germinate and will have a higher growth rate. The total days above each curve is given in Table 24. Mould germination can be expected if the total days above the given limit exceeds the days required for germination. However, periods of unfavourable conditions are not accounted for which may increase the required time to germination.

			Total Days Above Isopleth				
Wall	Location	LIM	16d	8d	4d	2d	1d
E1	M02	44	***27***	7	0	0	0
	M00	115	***80***	***51***	***31***	***23***	***10***

			Total Days Above Isopleth				
Wall	Location	LIM	16d	8d	4d	2d	1d
E2	M02	266	***225***	***131***	***44***	***5***	0
	M00	264	***216***	***150***	***106***	***55***	***13***

Table 24. Total number of days above each isopleth for spore germination, bold italics indicate potential for mould growth.

Moon (2004) presented a method for predicting mould germination based upon the isopleths developed by Smith (1982). As long as conditions were favourable to mould growth the total days above each isopleths was accumulated. However, when conditions were no longer favourable to mould growth the total days was reset at zero. This should provide a lower bound for mould germination, as dry periods do not completely eradicate the history of the spores or the previous growth of mould. Thus it is expected that there will occur more days with mould growth than Moon's method would suggest.

		Number of Days Favourable to Germination					
Wall	Location	16d	8d	4d	2d	1d	Total
E1	M02	0	0	0	0	0	0
	M00	0	4	11	15	19	19
E2	M02	174	113	40	4	0	174
	M00	114	105	81	50	13	139

Table 25. Number of days for which germination may have occurred by Moon's method, the total is not the sum of the rows as some days overlap.

The previous tables are put into the following figures to help in visualizing the temporal behavior. The cumulative days above the different limits is given. A zero slope indicates conditions are below those favourable for germination, other slopes indicate the ratio of time that is favourable to that which is unfavourable, the TOW as called by Adan (1994), although he used it in on a daily scale. A few slopes are shown for reference.

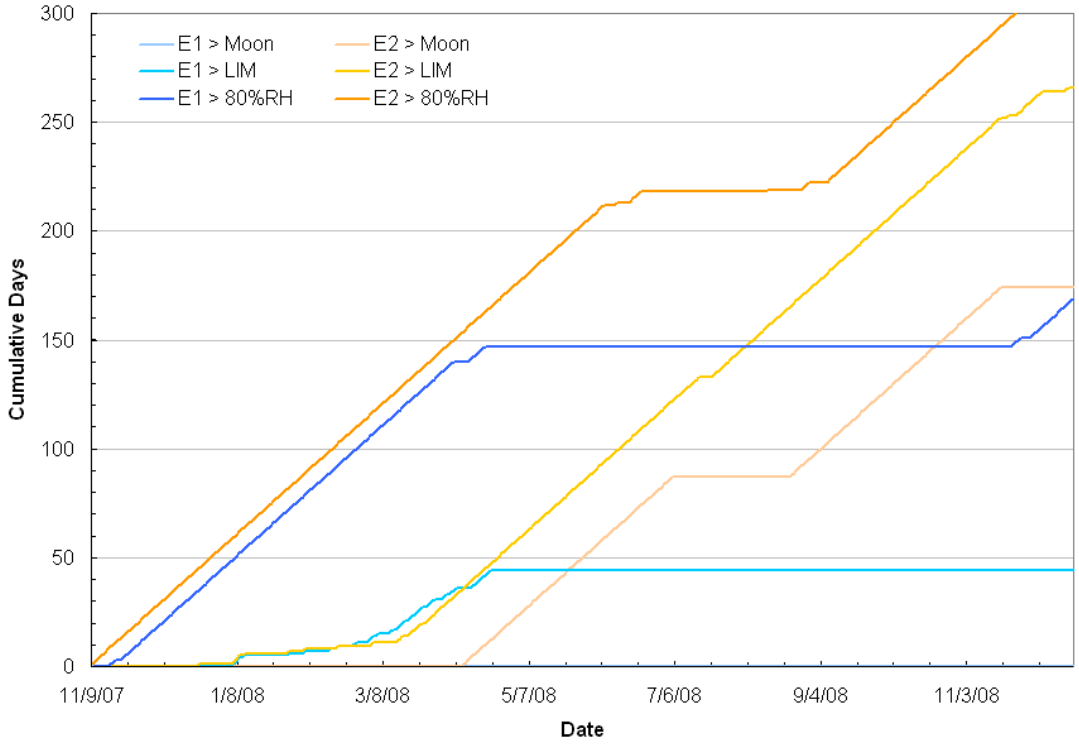

Figure 74. Cumulative days with potential for mould growth for M02 locations.

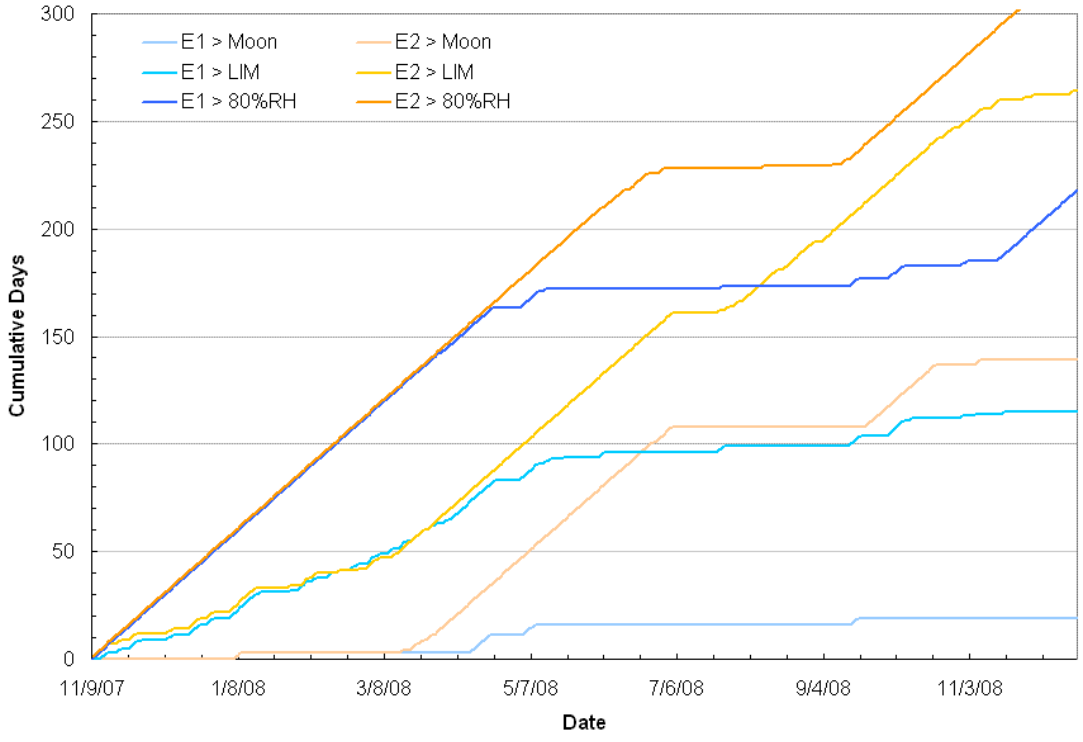

Figure 75. Cumulative days with potential for mould growth for M00 locations.

The previous figures with data indicating a potential for mould growth illustrate the temporal variations. The earth plastered wall shows conditions for mould are greatest in the spring and disappear in the summer as it dries out, but then favourable conditions return in the fall. However, with the cement-lime plastered wall the summer gives the most favourable conditions with continuous periods of days in favourable conditions, indicated by the slope.

From the previous analysis it is expected that mould germination will have occurred in all locations. The only exception is for the earth plastered wall at location M02 which shows a potential for no mould growth.

9.6.3 Mould Growth

The previous figures illustrated the potential for mould germination but did not indicate the total mould growth. While the potential for germination does not have a scale associated with it mould growth does, in terms of the rate of growth. Therefore, the total growth will depend upon the conditions during growth, whereas the prediction of germination just states if growth will occur or not. Using the isopleths from Sedlbauer (2002) the total growth is given in Figure 76.

Effects of TOW were ignored, as the growth occurs during the wet periods, while the effects of TOW are for the same duration of time but fluctuating conditions. Total growth will be less under varying conditions as there is some lag in between occurrence of favourable conditions and the start or continuation of mould growth. Although the numerical result is not precise the relative results between sensors provides a good comparison of the potential total growth. As the rate of mould growth was not given for conditions between the LIM and 1mm/d, a value of 0.1mm/d was used to differentiate it from no mould growth, this value is arbitrary. Predicting mould growth from the hourly data results in different growth rates as the average daily condition will not show spikes in humidity that may lead to excessive growth rates.

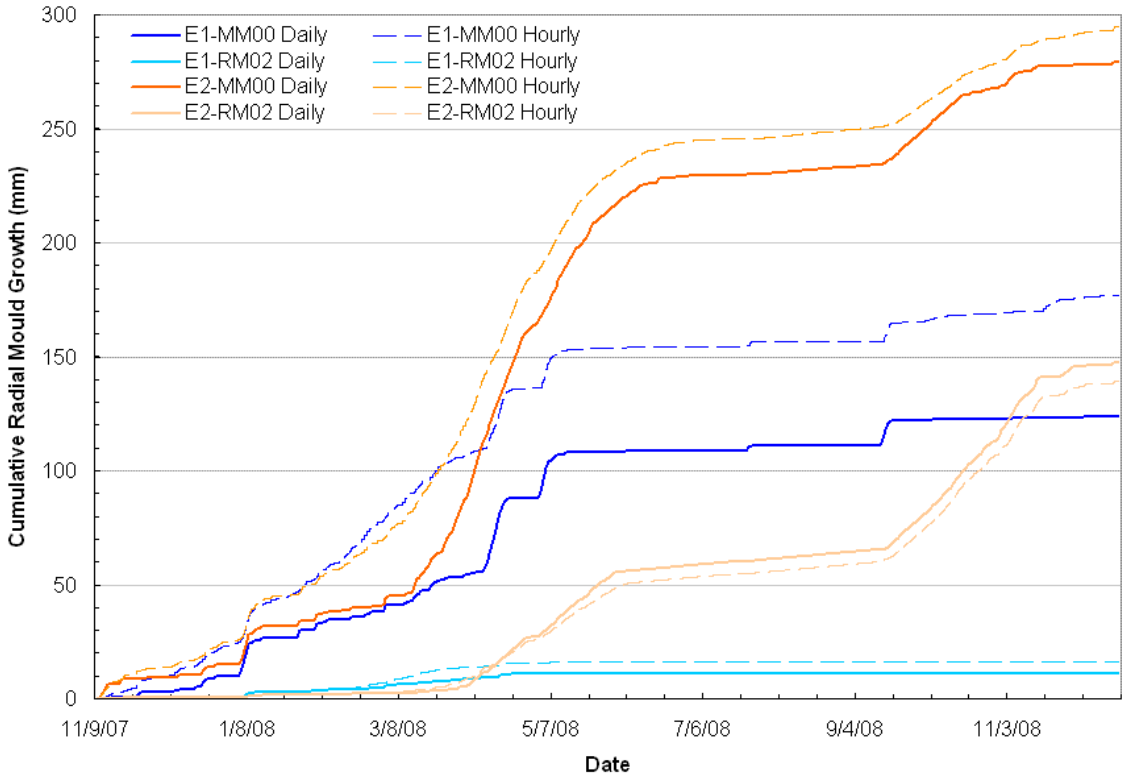

Figure 76. Cumulative radial mould growth for outer sensors of both walls calculated with daily average conditions and hourly average conditions.

9.6.4 Actual Mould Growth

A portion of the exterior plaster on both straw bale walls was removed on June 15, 2010. The openings were located centrally in the wall at the height of the mid-height sensors as shown in Figure 77. A close-up of the 12”x12” openings are shown in Figure 78 and Figure 79 for the cement-lime and clay plaster walls respectively. An opening at the centre-bottom of the clay plaster wall was also made.

Figure 77. Location of cement-lime plaster removed (left) and clay plaster removed (right) on June 15, 2010 for mould inspection.

Figure 78. Cement plaster removal (12”x12”) exposing straw behind.

Figure 79. Clay plaster removal (12”x12”) exposing straw behind.

Both walls had straw on the exterior side with minimal mould growth. In both walls, the straw was yellow, with good structure and did not smell of mould. See Figure 80 for the general appearance of the straw behind the clay plaster. However, there was mould growth on the nodes of the straw stems and within the tubes of the straw, with the worst case of mould growth in the earth plastered wall shown in Figure 81. Mould growth in the cement lime-plastered wall was higher, with the average growth appearing similar to the worst growth in the clay plastered wall. Within two inches of the exterior plaster of both walls the straw was clean and lacking visible mould growth. These findings are better than expected for the exposure conditions of the walls. However, the ultimate goal is no mould growth, which was not achieved.

Figure 80. Photograph showing the straw behind the clay plaster.

Figure 81. Photograph of the highest level of mould growth in the clay plaster wall.

All areas of the clay plastered wall that were investigated showed the same conditions as described above. However, the cement-lime plastered wall had a large section that was considerably decomposed on the exterior side as shown in Figure 82. The decomposing straw was black, moist, soft , it lacked structure and was warm to the touch. The extents of this decomposition are outlined in Figure 83. This pattern indicates the water for the decomposition came from a leak rather than by vapor diffusion, which would have caused a more even level of mould growth as seen in the clay plastered wall. Even though such a large amount of decomposition had occurred it was limited to the first five inches of straw. Beyond five inches into the bale the straw still had structure and was yellow in color, although some mould growth was still visible (Figure 84).

Figure 82. Photograph showing the highly decomposed straw on the right side of the cement-lime plastered wall.

Figure 83. Extent of the highly decomposed straw in the cement-lime plastered wall.

Figure 84. Depth in inches of the highly decomposed straw in the cement-lime plaster wall.

10 Modeling Results

Dynamic one-dimensional computer modeling of a straw bale wall was performed and compared to the measured data. The goal being two-fold: first, to assess the capability for accurate modeling using the hygrothermal properties discussed in Chapter 4; and second, to determine the relative impact of each hygrothermal property on the performance of the wall.

Modeling was performed using WUFI® PRO 4.0, a 1-dimensional transient heat and moisture modeling program (Fraunhofer IBP, 2005). It is capable of modeling the heat and moisture transport through multilayered assemblies for user defined exterior and interior conditions (including temperature, relative humidity, driving rain, and solar radiation). Temperature and relative humidity are the controlling potentials for heat and moisture flows in the software.

Heat transfer is calculated through thermal conduction, enthalpy of moisture movement and phase changes, solar radiation and nighttime radiation. Surface film coefficients are used to calculate heat loss to the surroundings in a manner that is similar to the conduction equations, these films can be constant or wind dependent. Moisture movement is broken into two compounds: vapor and liquid. The vapor movement is computed by vapor diffusion as well as solution diffusion. Liquid transport is characterized by capillary conduction and surface diffusion. Full description of the model assumptions and equations can be found in the doctoral thesis of Künzel (1995), upon which the mathematical model is based.

Straube and Schumacher (2003a) state that the WUFI® software is accurate in predicting hygrothermal behaviour of building enclosures with certain limitations based on their and others' experimental validations. The most important limitation is the input of accurate climate data, particularly sun and rain, which is best measured at the enclosure surface. Another limitation is unintended air and water leakage, which are typically not quantifiable and thus cannot be implemented into the model. From these findings it is assumed that the WUFI software is capable of modeling the straw bale walls, so long as the correct physical properties and boundary conditions are supplied.

Boundary conditions are supplied by the measured data at the BEGHut. Temperature and relative humidity are used directly. However, the driving rain and radiation require conversion from the rain measured on a horizontal surface to the east vertical direction. These conversions are shown in detail in Appendices A and B respectively.

Verification of the BEGHut weather data is made by comparing it with the collected data from the University of Waterloo (UW) Weatherstation. Direct measurements of east driving rain are made at this location and may be used in lieu of or in combination with the calculated driving rain.

Although interior and exterior climate data were measured, they were not measured at the wall surface and therefore errors may result, especially from the conversions for driving rain and solar radiation. The climate data was reviewed for its impact, especially the driving rain and solar radiation, to assess the impact of the errors in the boundary conditions.

As the physical material properties were not directly measured, an initial estimate based on previous studies discussed in Chapter 4 was used and then adjusted for best accuracy. This process also provided the basis for reviewing the effects that each property had on the performance of the wall.

The model results were compared with the measured data from the six sensor locations at the mid-height of the wall. These locations are the exterior surface (Mex), exterior plaster to straw interface (M00), 2"/7"/12" in from the exterior plaster (M02, M07, M12), and the interior surface (Min). The mid-height sensors are the furthest removed from the edges of the wall so as to minimize two-dimensional effects. However, one-dimensional analysis still may not provide an accurate model if there are significant differences in wetting over the height that create lateral moisture transport potentials.

10.1 Thermal Analysis

Investigation into the thermal accuracy of the model led to the following physical parameters providing an adequate model based on visual inspection of the model results in comparison to the measured data for the mid-height of the wall. This was conducted without moisture transport calculations to eliminate potential errors due to moisture effects. However, moisture transport will have an impact on the heat transfer through the wall and will thus be considered afterwards. In fact, it was found that the capacity for moisture storage in the wall can significantly dampen the dynamic fluctuations as energy is absorbed and released by the moisture at high humidity levels (100%RH). It should be noted that the values shown in the table are not definitive but can be varied and still provide a reasonable model.

Material	Thickness t (m)	Density ρ (kg/m^3)	Conductivity k (W/mK)	Heat Capacity c_p, (J/kgK)	Solar Absorptance α (-)
Earth Plaster	0.030	1400	0.6	850	0.90
Cement-lime Plaster	0.025	2000	1.5	850	0.70
Straw bale	0.370	110	0.075	1350	-

Table 26. Physical properties for thermal accuracy.

When exploring the impact of the straw bale conductivity that would result in best fit between the model and the data it was found that the thermal diffusivity was more important. Hence it was found that changing the conductivity and specific heat capacity together was required to maintain the same dynamic behavior as found in the measured data. The result of this exercise is that the conductivity can be adjusted between 0.05-0.15 W/mK and the specific heat capacity between 600-2000 J/kg but the combination of the two should result in a thermal diffusivity between 3-6 x10^{-7} m/s. This is using a dry density of 110 kg/m^3 for the bales. An example of this is shown in Figure 85 where two models are shown each using the limits of straw conductivity as stated, but maintaining the same thermal diffusivity. The expected values from Chapter 4 are a conductivity of 0.070 W/mK and a specific heat capacity of 1400 J/kg, which results in a thermal diffusivity of 4.55x10^{-7} m/s, which is in the middle of the acceptable range.

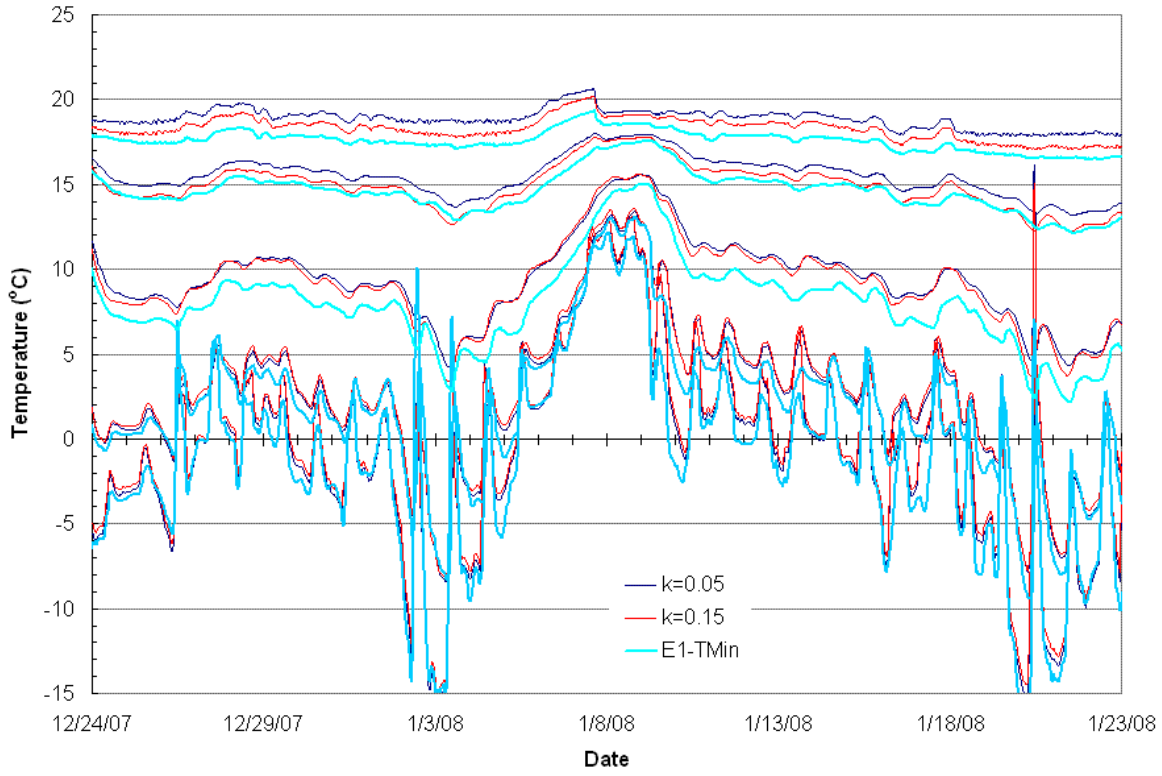

Figure 85. Model results for the limits of straw conductivity in the clay plaster wall while maintaining constant thermal diffusivity. Blue k=0.05W/mK, c_p=800J/kgK. Red k=0.15W/mK, c_p=2400J/kgK. Turqoise, measured results for clay.

The greatest variances between the running average of the modeled and measured data were most easily adjusted by sensor placement in the model, even within 1/2". This can be due to actual sensor placement not being exactly where intended, although precautions were taken to place the sensors vertically into the bales at the correct distance from the front face. However, the sensors may have diverged from vertical and ended up +/-1/4" from the intended location. The location of the tape measure when installing the sensors may have also been +/-1/4" from the true edge of the bale. Even had the sensors been located precisely, the nature of the voids in the straw may cause local temperature irregularities within the bale itself.

Additionally, changing the interior surface film from 0.125 m^2K/W to 0.5 m^2K/W helped to adjust the interior-most temperature readings. This was required to match the modeled winter temperature of the interior plaster to the measured data, since it remains essentially unaffected by the bale width (+/-1") but can be affected by the surface film coefficient. However, it is not likely that 0.5 m^2K/W is reached as this value is only realistically expected at a three-dimensional corner (Straube & Burnett, 2005). Therefore, the

increased surface film coefficient is most likely an adjustment between the measured interior temperature of the BEGHut and the temperature near the wall. The measured temperature may have been consistently low due to two biases: first, the location of the interior temperature sensor is on the opposite side of the test building. Second, the interior temperature sensor is different from those in the test walls and was not calibrated together, which may cause a consistent difference in readings between sensor types.

Although a nominal 14" bale thickness was initially assumed it was found that the inward sensor in the model was consistently warmer than the measured data during the winter. Changing the properties of the materials was not sufficient to correct the difference. However, by increasing the bale thickness by ½" the difference was minimized. The location of the sensors was maintained as measured from the front of the bale, the result of the increase in thickness is thus an increase in the amount of straw between the inward sensor and the interior. This results in a more dramatic change of the inward sensor than the other sensors. See the photograph in Figure 86 taken when installing the sensors to see that the bale width appears somewhat larger than 14" for the installed location. Also projecting straw and the general rough surface may keep the plaster skins separated by more than the nominal bale thickness, although the plaster was thoroughly worked into the straw to eliminate air channels.

Figure 86. Installation of mid-height sensors in the earth plaster wall showing bale thickness greater than 14".

The comparison of the modeled and measured data for the clay plaster wall are shown in the following figures. Figure 87 and Figure 88 show the winter conditions with and without the above mentioned modifications to the sensor locations and surface film coefficient, for which the effect on the interior sensor is considerable. Figure 89 and Figure 90 show the summer conditions. The dynamic behaviour is quite well modeled with when efforts to minimize the effects from the conversion of solar radiation are employed.

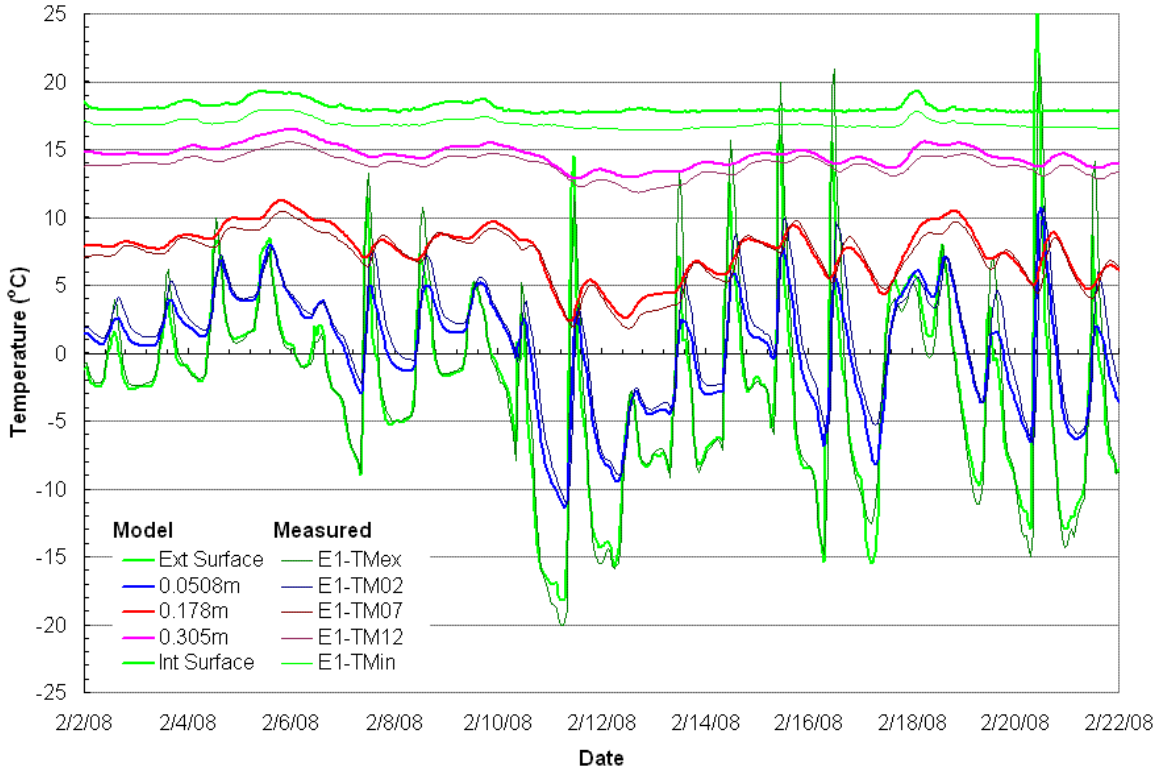

Figure 87. Modeled vs measured winter data for the earth plaster wall using the expected sensor locations and original surface film.

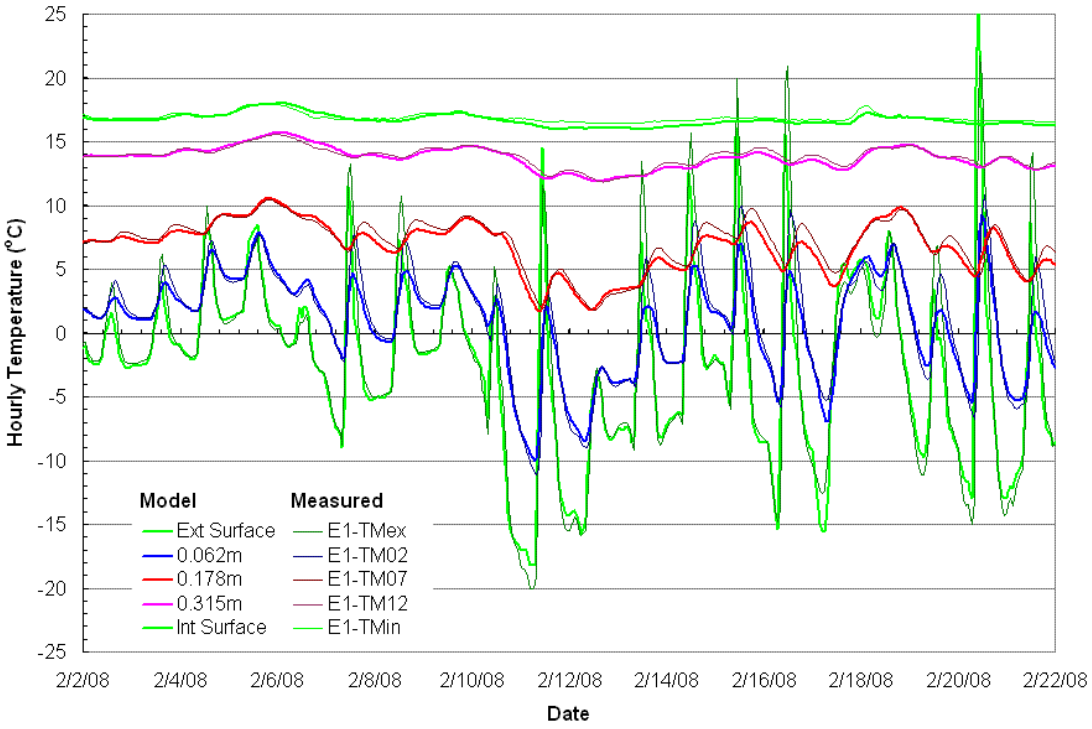

Figure 88. Modeled vs measured winter data for the earth plaster wall using adjusted sensor locations.

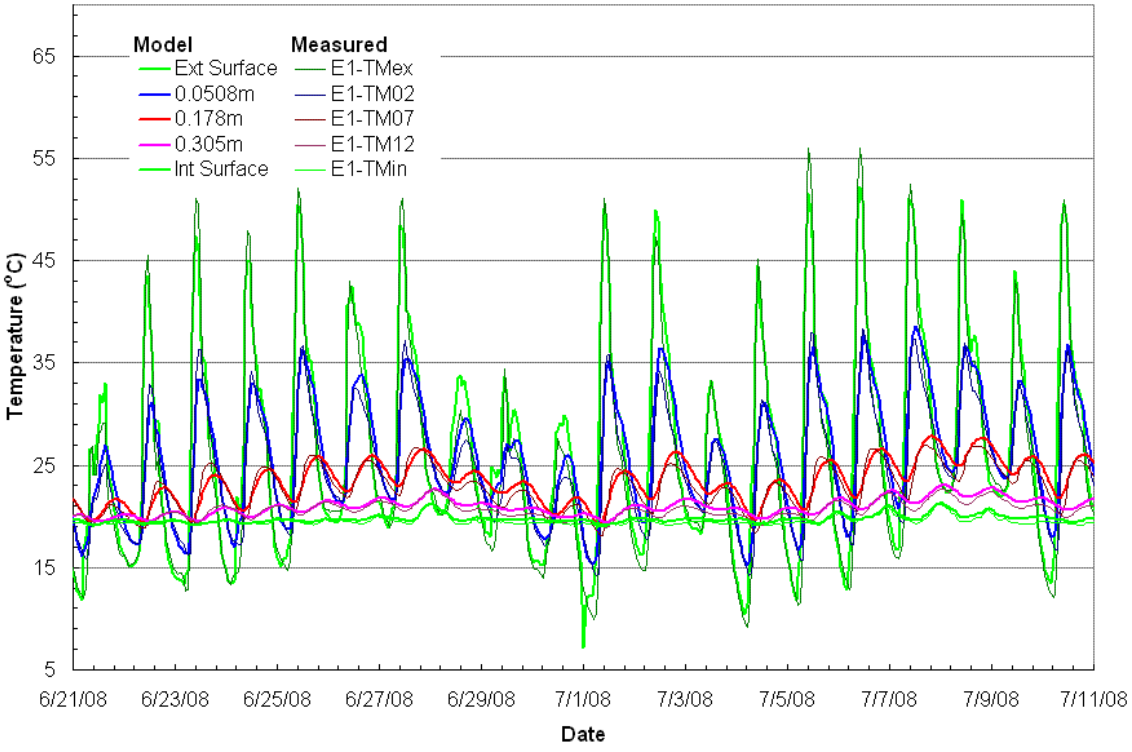

Figure 89. Modeled vs measured summer data for the earth plaster wall using the original surface film coefficient and sensor placement.

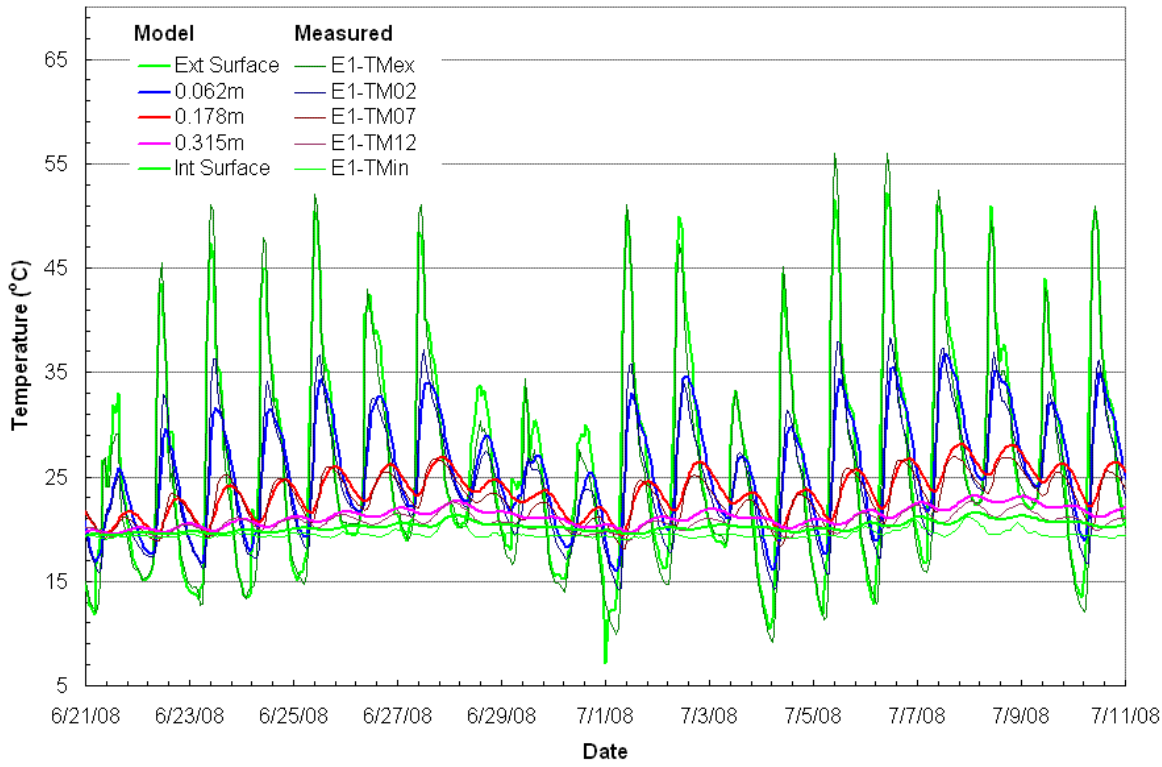

Figure 90. Modeled vs measured summer data for the earth plaster wall using the adjusted sensor locations and surface film.

Histograms of the difference between the model and the measured data for the earth plaster model are given in Figure 91, with bin sizes of 0.5°C. The exterior side sensor shows the largest spread in difference whereas the interior side sensor shows the least spread. The greatest temperature differences occur during periods of solar radiation, which has a larger impact on the exterior side temperatures. Thus, solar radiation is likely the main reason for larger temperature variations between the modeled and the measured data occurring on the exterior side.

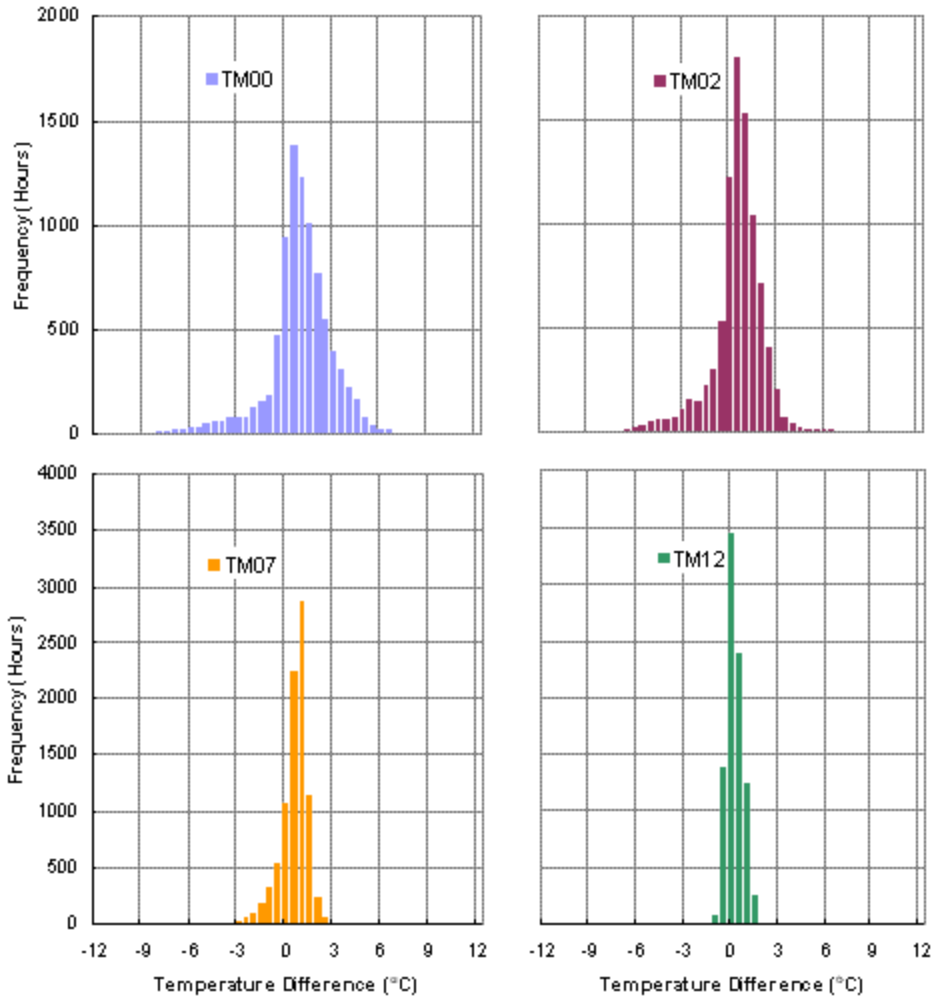

Figure 91. Histograms of the difference between the modeled and measured temperatures in the clay plaster wall, using the original surface film coefficient and sensor placement. Bin size is 0.5°C. Sensor locations at 0", 2", 7" and 12" from the exterior plaster.

It is believed that one of the biggest difficulties in developing an accurate model is the conversion of solar radiation. Discussion of this conversion is in Appendix A. Similar discrepancies were noted in Straube and Schumachers work on the Ridge Winery (2003b). They stated that the main reason for differences between the modeled and measured results in response to solar radiation is the conversion of horizontal radiation to vertical radiation and not the solar absorptance, thermal conductance or heat capacity values.

The differences between the measured temperatures in both walls are primarily due to the solar absorption of the exterior plaster as discussed in the previous chapter. Changes in the thickness, thermal conductivity and heat capacity properties have less effect. This is

shown in Figure 92 with modeled results using the properties for clay and cement-lime plaster given in Table 26 but with both having a solar absorptance of 0.7. It is also expected that other variations in the measured performance are due to the increased moisture levels in the cement-lime plaster wall.

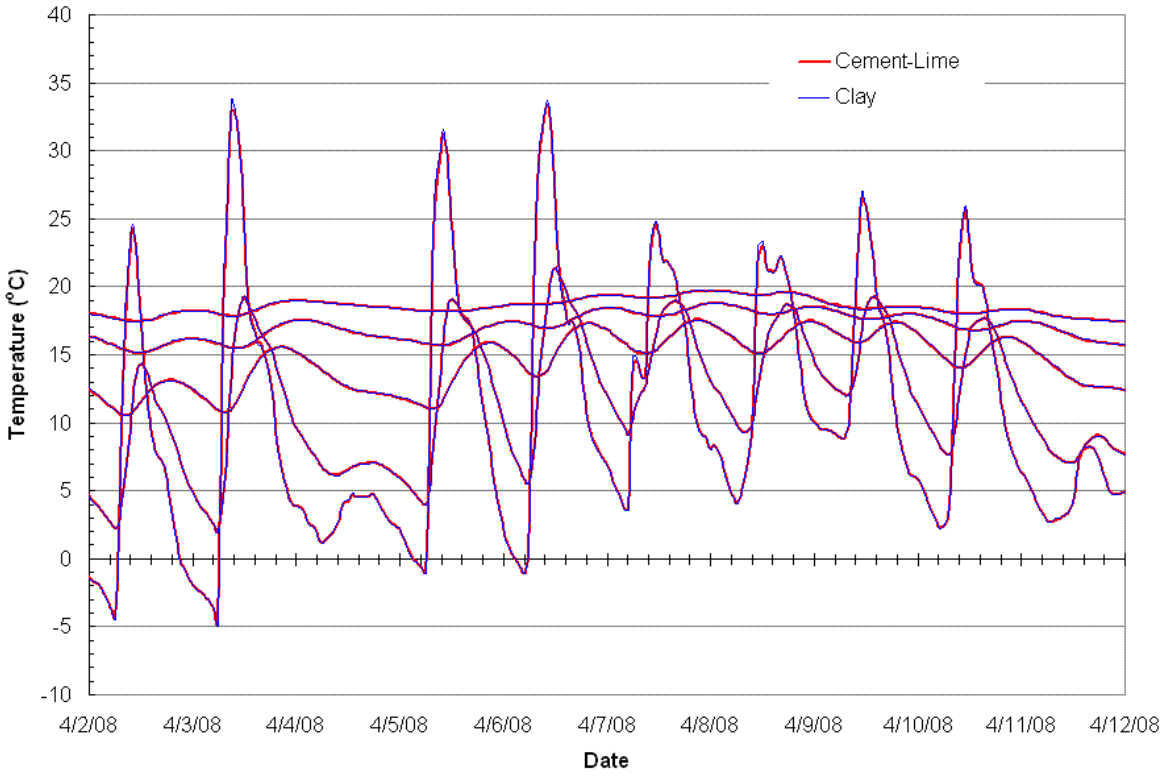

Figure 92. Model results of clay and cement plaster walls both using a solar absorptance of 0.7.

The modeling results for the cement-lime plaster wall are shown in Figure 93 and Figure 94 for winter and summer respectively. A particular phenomenon is the elevated temperatures in the measured data in the middle and interior side of the cement lime wall in the summer when compared to the model data, see Figure 94. The reason is not clear but may be a result of the elevated moisture levels. These levels may lead to moulding which produces heat. Additionally, increased moisture will increase latent heat transfer as solar driven moisture condenses on the interior side of the wall. This increase was noted when moisture transfer was included in the model, however it was still not able to fully predict the noted behavior. This behaviour was not found in the lower sensors.

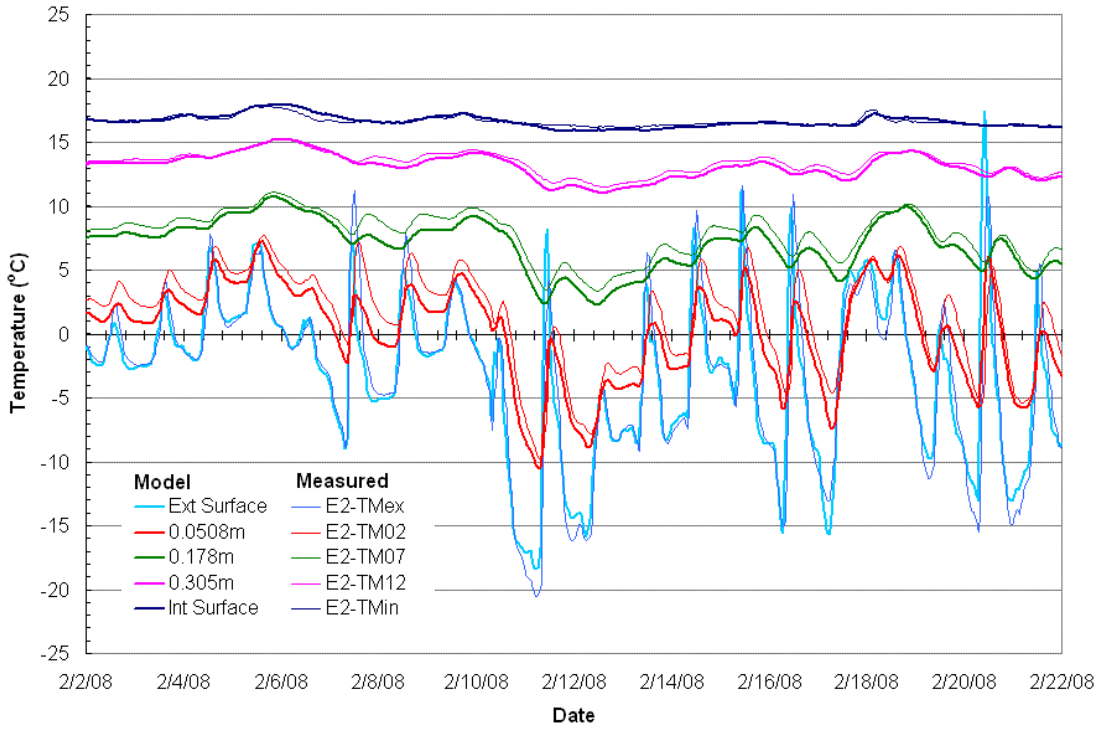

Figure 93. Modeled vs measured winter data for the cement lime plaster wall using the adjusted surface film coefficient.

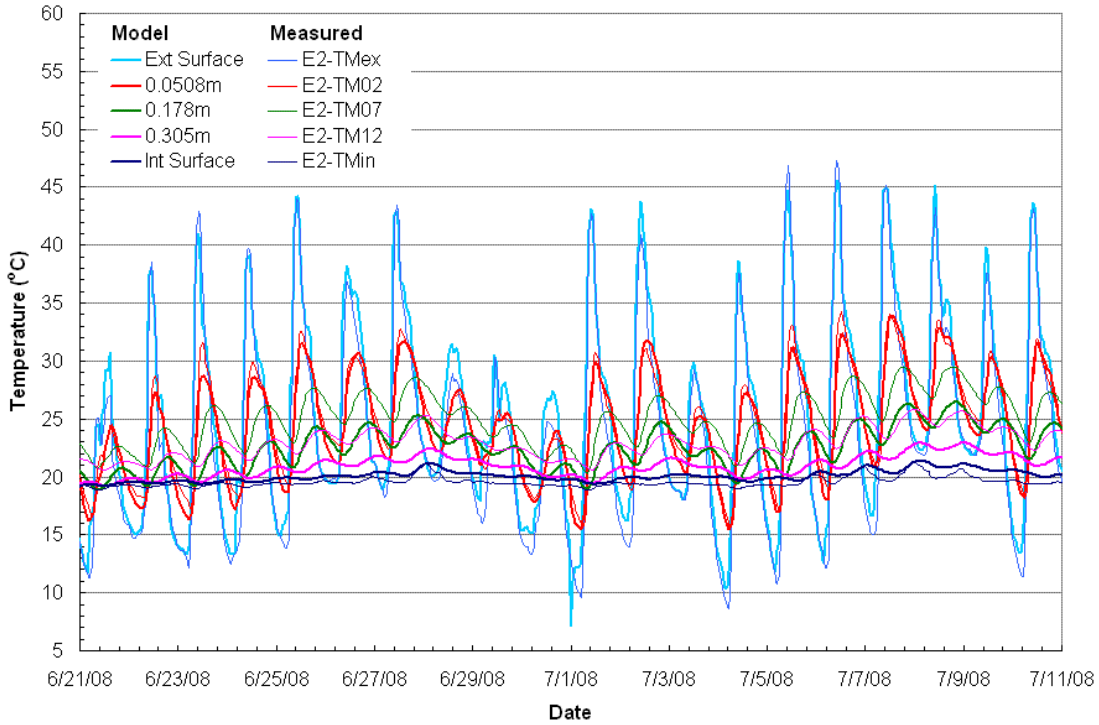

Figure 94. Modeled vs measured summer data for the cement lime plaster wall.

10.2 Moisture Analysis

After deciding on the thermal properties to use in the model, the moisture related properties were investigated. These include the sorption isotherm of the straw and plasters (called the moisture storage function in WUFI), the water uptake coefficients (A-value in WUFI), permeability (diffusion resistance factor is used in WUFI), and the driving rain data.

The precision of the moisture analysis was limited by the rain data and the lack of direct testing of the material properties. Therefore, what follows is discussion on the various parameters and their effects on the model, as opposed to a presentation of the final model. This is done in order to provide the best use of the work that was done.

Moisture modeling was focused primarily on the earth plastered wall as the discrepancies in the model temperatures and the potential leak in the cement plastered wall indicate sources of error that would make the moisture modeling inaccurate for E2. Thus, modeling of E2 was limited and was finished after modeling the earth plaster wall. The parameters that resulted in the best model for E2 until late spring are presented. There was no combination of parameters found that would accurately describe the measured behavior of E2 through the summer into the fall.

Again, the resulting properties used in the WUFI analysis are not definitive but give an approximate value or range for the property that provided a reasonable model. These are listed in Table 27 with moisture storage functions shown in Figure 95. By using the different rain data it is possible to get models that are close to the measured data with different material properties. However, a high plaster storage, a plaster diffusion resistance factor of 5 and a straw diffusion resistance factor of 1.7 are fairly independent of the other factors. The effect of rain is really the difficulty in this modeling as the precision of the rain data is questionable, which results in various modifications and different A-values that each result in reasonable estimates. The rain loading assumed has the biggest impact on moisture results in the model, and can in reality vary significantly.

Plots are given in Figure 96 and Figure 97 of model results compared to measured results to show an example of the better model predictions and give a basis for the following discussion.

Material	Thickness t (m)	Density ρ (kg/m^3)	Diffusion Resistance Factor (-)	Water Absorption Coefficient (kg/m^{2}s$^{1/2}$)	Storage Function
Earth Plaster	0.030	1400	5	0.08-0.3	Figure 95 (High)
Cement-lime Plaster	0.030	2000	20-45	0.06-0.13	Figure 95
Straw bale	0.370	110	1.7	0.001-0.01	Figure 95

Table 27. Moisture properties for best accuracy in dynamic modeling.

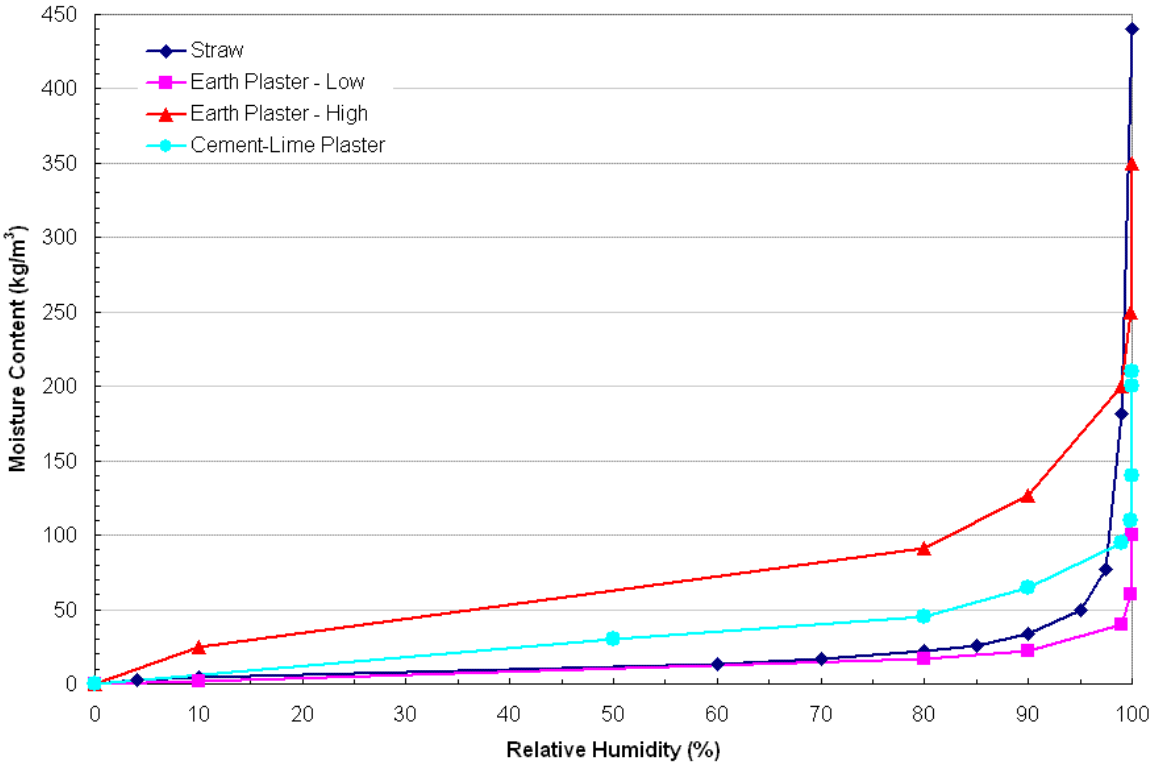

Figure 95. Sorption isotherms for the straw and both plasters as used in the dynamic analysis.

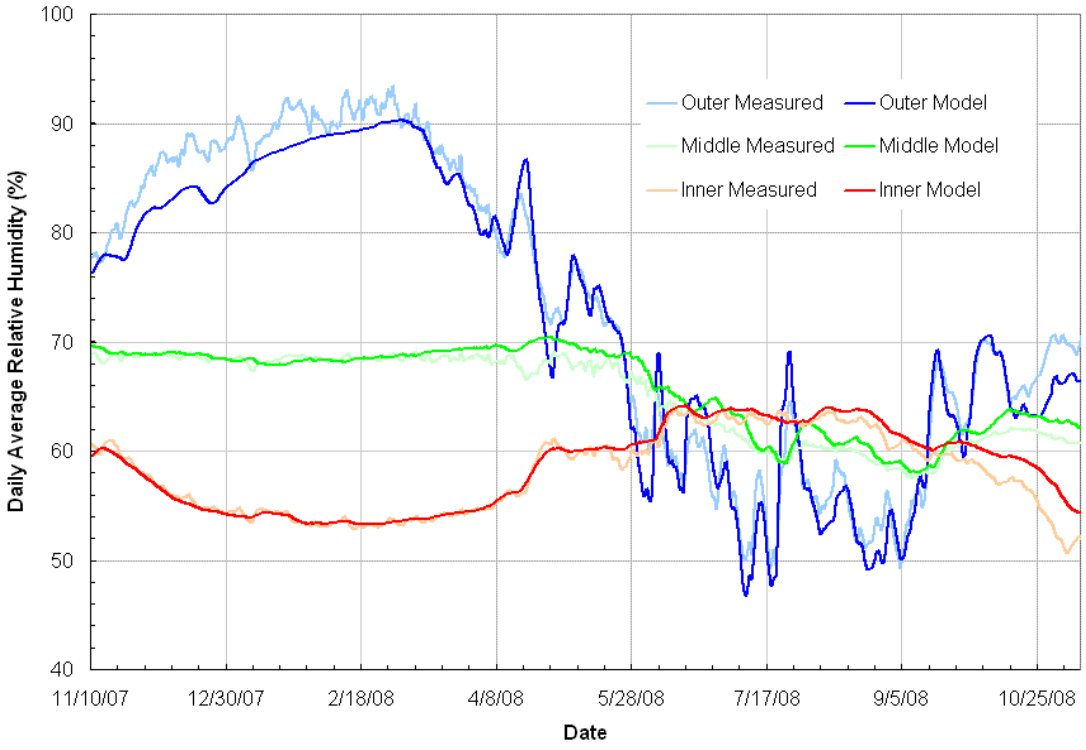

Figure 96. Modeled vs measured data for the earth plaster wall with a combination of calculated and measured rain (Plaster: A-value=0.2, diff. res. factor=5, high moisture storage / Straw: A-value=0.005, diff. res. factor=1.7, initial storage).

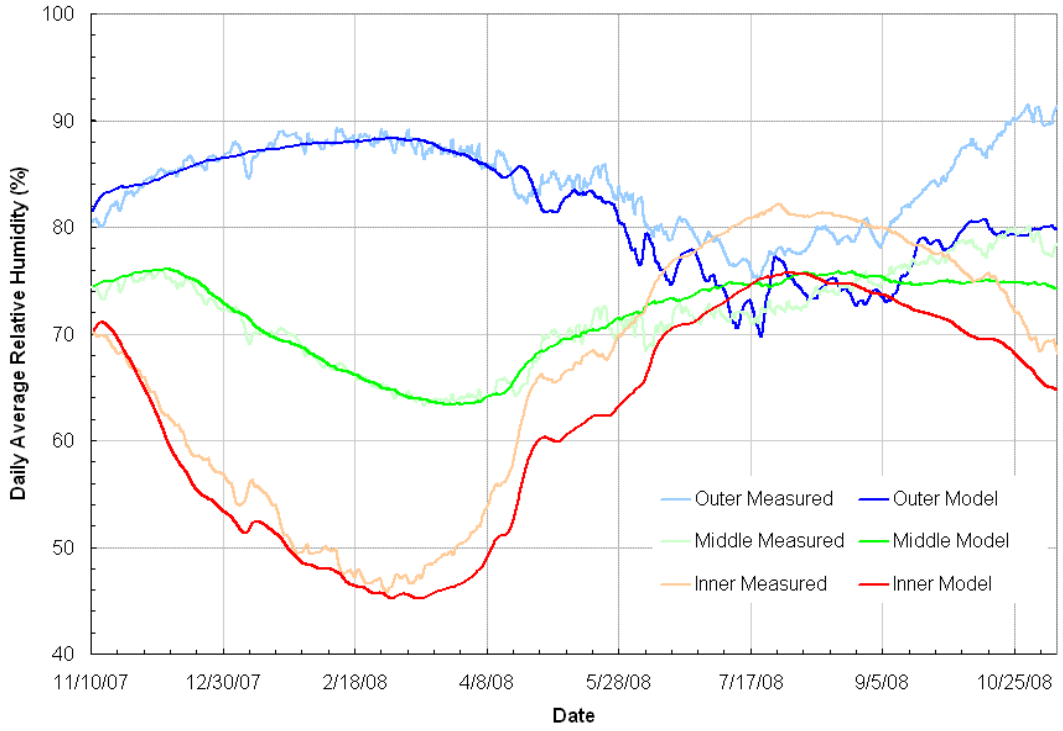

Figure 97. Modeled vs measured data for the cement-lime plaster wall using the average modified rain x 0.9 (Plaster: A-value=0.08, diff. res. factor=35, initial moisture storage / Straw: A-value=0.001, diff. res. factor=1.7, initial moisture storage).

10.2.1 General Measured Trends

Seasonal behaviors are well noted in the measured data for the outward sensor. From November 2007 to March 2008 there was a build up of RH at the outer sensor in both walls, with the earth plaster reaching about 91%RH and the cement-lime plaster 89%. During this time the wood wafer sensors behind the exterior plaster indicate moisture contents between 100%RH and saturation. Through April and May 2008 there is a rapid drying in the earth plastered wall to 55%RH. The cement-lime plastered wall also dries during the spring but only to 76%RH. During the summer and into October the outer sensor is at its lowest levels and fluctuates considerably in the earth plastered wall (by up to 10%RH) but not very much in the cement-lime plastered wall.

The seasonal trends in the middle and inner sensor are evident with minimal short term fluctuations. This data was not analyzed as closely as the outward sensor, but was always checked for accuracy. Therefore, in the following discussions the effects on the outward sensor are discussed more than the effects on middle and inner sensor.

10.2.2 Rain Data

Modeling without rain data showed how rain loading affects the wall performance. For various diffusion resistance factors the outward sensor in the clay plastered wall showed a constant winter level around 80%RH when zero rain was used. The cement-lime plastered wall gave winter levels at 85%RH for the outer sensor, drying to 60% in the summer. These are shown in Figure 98 and Figure 99. Reducing the plaster A-value increased the winter time humidities, potentially indicating reduced outward movement of condensation.

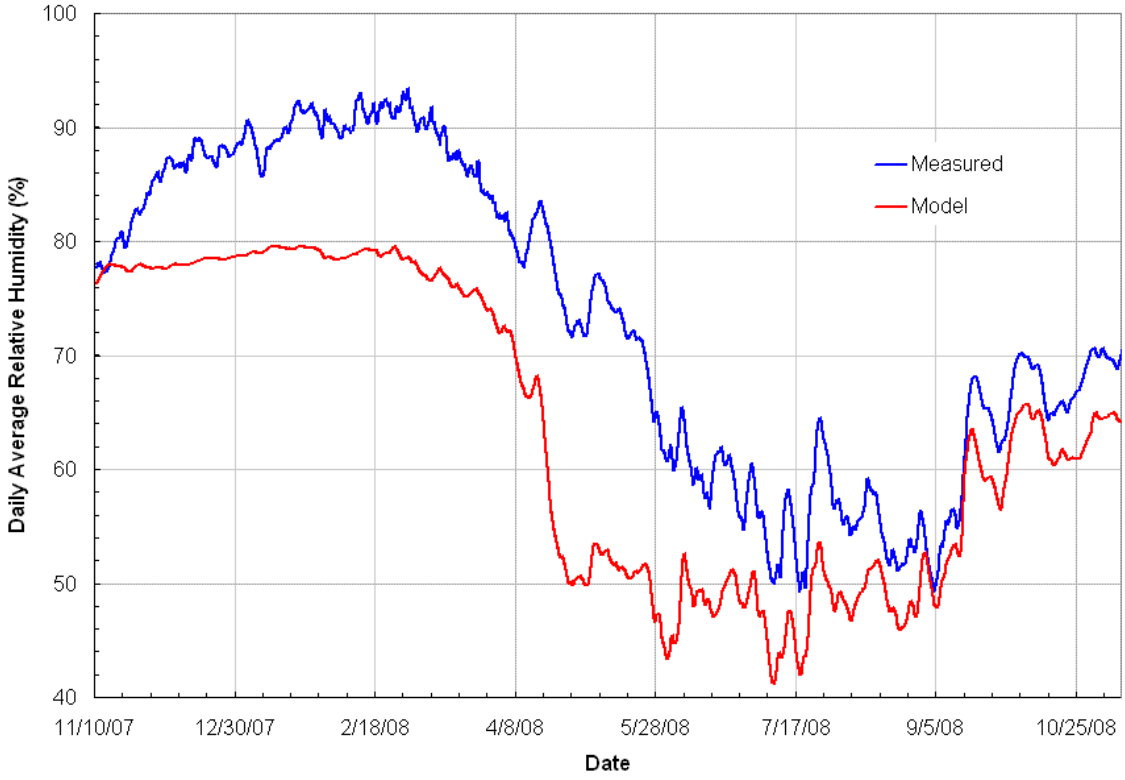

Figure 98. Measured data vs modeled results using zero rain for the clay plaster wall. (Plaster: A-value=0.3, diff. res. factor=5, high moisture storage / Straw: A-value=0.003, diff. res. factor=1.7, initial moisture storage).

Figure 99. Measured data vs modeled results using zero rain for the cement-lime plaster wall. (Plaster: A-value=0.03, diff. res. factor=19, initial moisture storage / Straw: A-value=0.005, diff. res. factor=1.5, initial moisture storage).

From the beginning of March to the beginning of May there was a dramatic drop in the outer sensor humidity when modeling with no rain. From the 80%RH winter level to 45-50% depending on the properties used. For the cement plaster it went from 85% to between 50 and 55%. There is a similar drop in the measured data, although not as dramatic since rain caused the increase in moisture buildup in the winter and there were a few driving rain events during the spring, most notably the large event on April 10, 2008.

The lack of rain causes the summer time levels to be lower than measured, but the trends are similar in the summer for both walls as there is little driving rain during this period, as noted in the UW weather station driving rain gauge. This means the shape of the curves from the model are similar but the absolute values are different. Behavior is primarily a result of vapor movement in response to fluctuating exterior RH. Large fluctuations in the earth plastered wall correspond to rain events, but not necessarily driving rain events, which would cause a spike in exterior RH.

The summer time difference is larger in the cement-lime plastered wall, which is considerably drier than the measured data when modeling without rain (50%RH compared to 76%RH). The earth plastered wall eventually reaches the same level as the measured data by September, whereas the cement-lime plastered wall never reaches the same level as measured after the summer. In fact the cement-lime plastered wall shows a year-to-year drying trend without driving rain and a wetting trend with driving rain.

Driving rain data was computed from the measured horizontal rain with the wind speed and direction at the UW weather station. This was done, as the wind direction as measured at the BEG hut did not appear to be correct and was not giving driving rain amounts as expected. This was confirmed in a quick test where the wind vane was held due west and the measured angle was 290^{o} instead of the expected 270^{o}. Measured driving rain from the UW weather station was also used.

Modifications to the original data were made during modeling to get a better estimate of the actual rain experienced at the walls which would differ from that at the weather station. This ended up with some rain events being increased or added and others decreased or removed.

Introducing rain data brought the outward RH up during all seasons so that it more closely followed the measured data, however short term spikes were too large. The calculated driving rain data appeared at first to give a model with a shape of the outward sensor RH that more closely resembled the shape of the measured data, with a couple of modifications to limit large rain events. This is due primarily to the winter moisture accumulation. However, when investigating the moisture level at the plaster straw interface it was not found to stay near 100% as measured, but was impacted primarily by three driving rain events, between which it dried considerably compared to the measured data.

In contrast the measured driving rain data has more rainfall during the winter, but did not have a high driving rain level for the event on Nov 21, 2007 and had too much rain at the end of February. This caused the winter level to climb more slowing initially and not dry as soon in the spring as was measured. However, by adjusting these events to be closer to the calculated data it was possible to get a better fit than either the calculated data or measured data alone.

Total driving rain was 133mm in the calculated data and 326mm for measured driving rain. These were somewhat closer after modifications, but really indicated the uncertainty in the rain data. However, the true value is likely somewhere in between

these two, as an absorption factor of 0.8 works with the modified calculated data and around 0.5 for the measured data resulting in absorbed moisture levels between 106mm and 163mm. Taking the average of both the modified measured driving rain and modified calculated driving rain after factoring provided a reasonable estimate of absorbed driving rain. A comparison of the different driving rain data is shown in Figure 100.

However, because of this uncertainty the yearly cycle with daily averaged values was visually inspected for accuracy as opposed to diurnal variations.

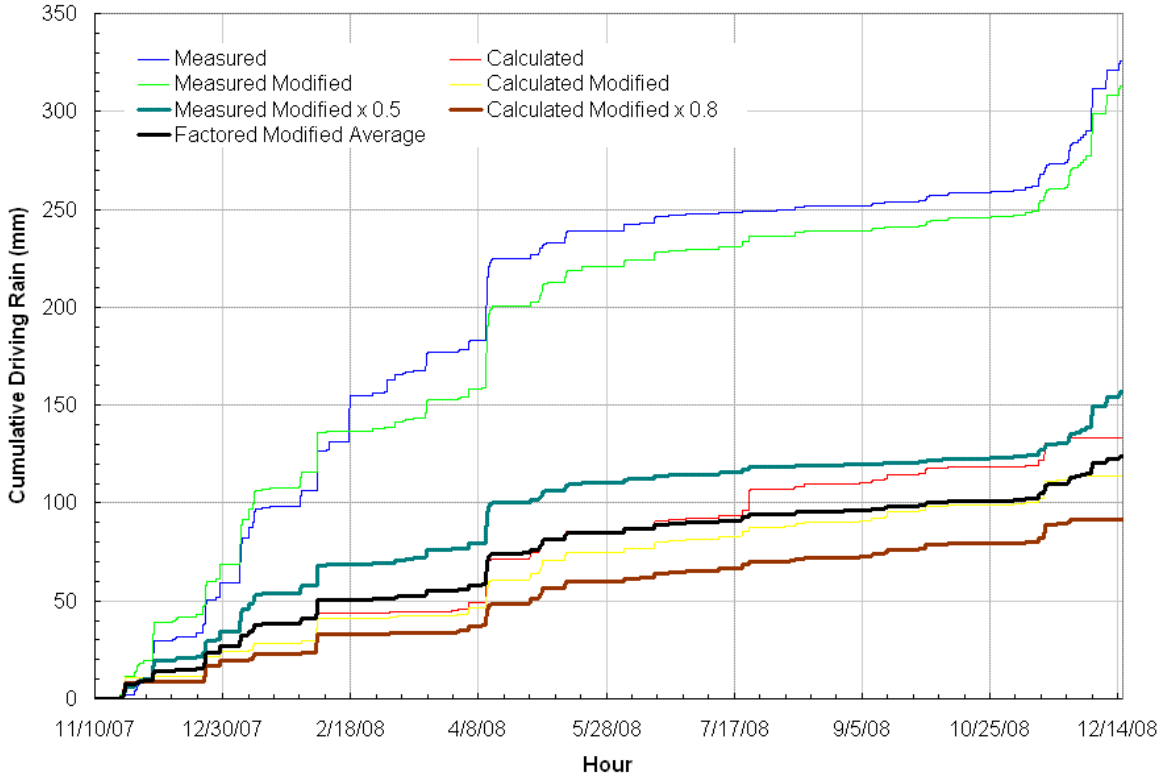

Figure 100. Calculated and measured cumulative driving rain showing the unmodified, modified and factored curves, with the final factored-modified average.

10.2.2.1 Liquid Transport in WUFI

To aid in understanding the relationship between driving rain absorption and the plaster properties the following discussion is given on how the liquid transport coefficient for suction and redistribution were calculated.

Liquid transport coefficients for suction were estimated in WUFI by the following equation, since measured data was not found for all the materials.

$$D_{ws} = 3.8 \cdot \left(\frac{A}{w_f} \right)^2 \cdot 1000^{\left(\frac{w}{w_f} - 1 \right)}$$

Where D_{ws} = water transport coefficient for suction (m^2/s)
A = water uptake coefficient ($kg/m^2s^{1/2}$)
w_f = moisture content at saturation (kg/m^3)
w = actual moisture content (kg/m^3)

WUFI calculates D_{ws} at three points and interpolates between the points during analysis. The first point sets the liquid transport to zero at a moisture content of zero. Liquid transport is assumed zero until the moisture content reaches that which corresponds to 80%RH from the moisture storage function (w_{80}). Therefore, the second point is calculated at w_{80} and is the start of the liquid transport curve, again liquid transport below this level is zero. The last point calculates the liquid water transport at the saturation moisture content (w_f). Interpolation is made for points between w_{80} and w_f. For redistribution the same value at w_{80} is used but the coefficient at w_f is reduced by an order of magnitude, again the values in between are interpolated and redistribution below w_{80} is assumed to be zero.

From the equation it is seen that the water uptake coefficient and saturated moisture content have a direct impact on the liquid transport coefficients, in the A/w_f term. The result is that higher water uptake coefficient and a lower saturation moisture increase liquid transport. Also, a higher moisture storage function means that there is more capability for the material to hold water and thus liquid transport does not occur as soon as for a lower storage material; that is more moisture is required before liquid transport will occur.

10.2.3 Moisture Parameters' Effect on Model

The shape of the data for all sensors was similar regardless of the parameters used, without drastic adjustments. Some modifications cause increased winter moisture levels that last into the spring beyond where the measured data dries and ends with a rapid drying in late spring or summer. This also shows up in the middle sensor as increasing RH at the beginning of spring as the excess outward moisture moves inward. Other changes caused reduced winter buildup, but do not greatly affect the spring drying, although the moisture levels may be somewhat lower. Summer short term fluctuations may be increased or decreased. Amplitudes of the seasonal variations also change, but mostly with the permeances of the materials.

10.2.3.1 Straw Moisture Storage

The sorption isotherm for straw has been documented quite well as discussed in Chapter 4 and thus it is not expected to be considerably different than originally estimated. Likewise, the moisture storage in the cement-lime plaster is expected to be typical.

The straw storage function was set at the expected value for most analyses but increasing or decreasing by 30% was investigated. Overall, the effects are minor in comparison to other parameters. Increased storage causes the winter shape to be flatter while still reaching similar levels but results in increased drying time in the spring. It has a minor effect in reducing short term fluctuations. Reduced storage increases the springtime drying. Also, the effect of the straw A-value is not as pronounced in the winter as with the other storage functions. Short term fluctuations are somewhat increased.

It was found that the assumed moisture storage function is adequate for the model. Adjustments could be made for more precision but are limited by the precision of the other parameters such as rain data.

10.2.3.2 Plaster Moisture Storage

Only one test on the moisture storage for the clay plaster was found and a couple studies on related materials: unfired clay bricks and raw clay. These result in a low, middle and high storage function, each of which was investigated. Some difficulty is also expected in trying to model the behaviour of the clay plaster at near saturation as swelling can change the moisture properties.

Three storage functions were used which were quite different. The shapes were relatively similar with saturation values at 100, 210, and 350kg/m^3 for the low, mid, and high storage functions. Again the shape of the curves with the plaster storage were very similar, but required adjusting the plaster A-value. Low storage needed reduced A-value, between 0.07-0.15kg/m^{2}s$^{1/2}$, while high storage required increased A-value up to 0.3kg/m^{2}s$^{1/2}$. This would be a result of trying to maintain the same rain absorption into the plaster, otherwise the high storage function results in increased winter and reduced summer RH levels at the outer sensor.

Short term fluctuations were the most affected by changes in plaster moisture storage. Low storage resulted in too high of fluctuations in the summer in response to RH variation. Mid storage fluctuations were still a little high. High storage gave a good match to the summer fluctuations. Also, the increased storage gave a better match to the

moisture levels at the plaster straw interface in response to rain events. Low storage resulted in too rapid drying after the rain event, while high storage maintained moisture levels after rain events in a similar fashion to measured.

High storage was chosen as the most accurate storage function because of its better ability to model short term fluctuations (1 week) and especially the response to RH changes. The response to RH changes is also affected by the plaster permeance and straw storage but they were found to not have as much impact and would require adjusting beyond the reasonable range. See Figure 101 for a comparison of summer fluctuations with low and high plaster storage with no driving rain.

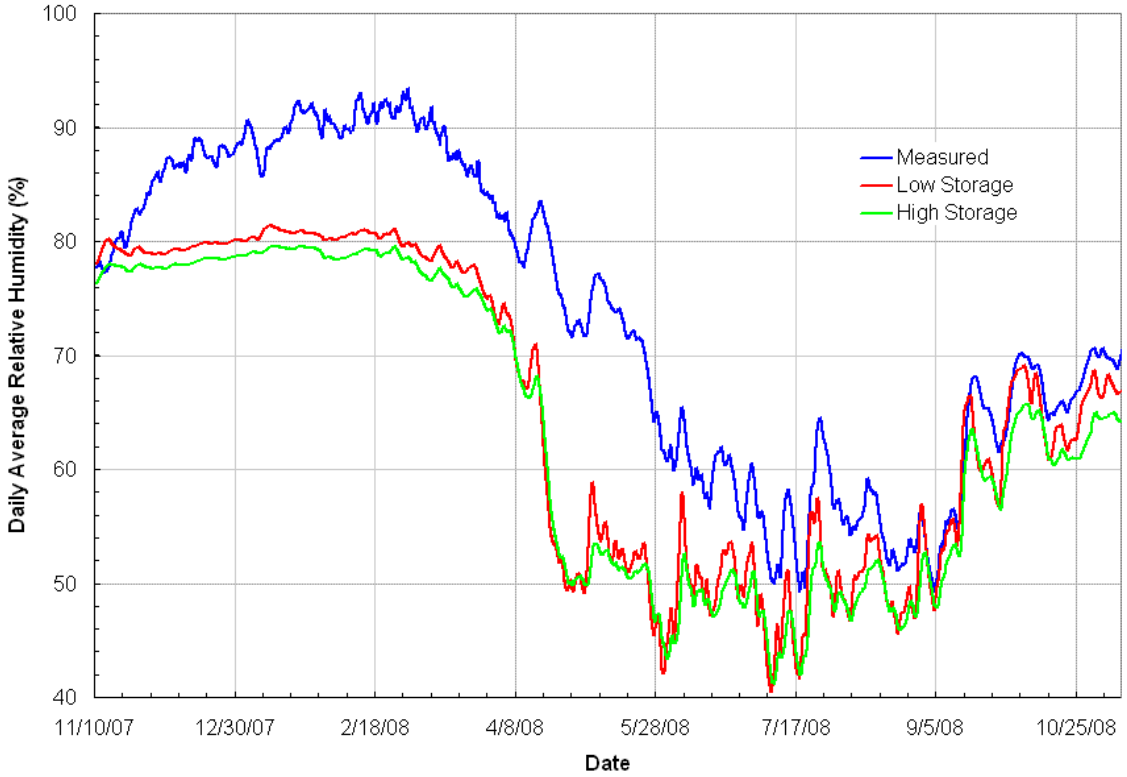

Figure 101. Summer fluctuations modeled with zero rain for the clay plaster with low moisture storage (red) and high moisture storage (green). The measured data is shown in blue.

10.2.3.3 Straw Diffusion Resistance Factor

Straw bale has not been tested directly but, as discussed in Chapter 4, it is expected to be greater than 75ng/Pasm and likely between 100-150ng/Pasm, but may be as high as 190ng/Pasm. These correspond to a range of diffusion resistance factor between 1.0-2.5., with an expected value of 1.8.

The straw diffusion resistance factor was adjusted between 1.2 and 2.2 with minimal effect. Therefore, an average value of 1.7 was used. For plaster diffusion resistances beyond the range of 4-7 it was found that the straw diffusion resistance needed to be adjusted to maintain the shape of the middle and inner sensors.

10.2.3.4 Plaster Diffusion Resistance Factor

The permeability of plasters used in straw bale construction have been tested as noted in Chapter 4. Therefore, the range for earth plaster is between 20-45 ng/Pasm, with an expected value of 40ng/Pasm. This corresponds to a range in diffusion resistance factor of 4-10 with an expected value of 5. For the cement-lime plaster a permeability in the range of 5-15ng/Pasm is expected, with 10ng/Pasm as the initial value. This corresponds to a diffusion resistance factor of 13-40 with 20 as the first estimate.

Confirming the plaster diffusion resistance factor was done without the rain data by checking the inner sensor. Increased diffusion resistance causes low moisture levels in the winter and high levels by the end of the summer. The moisture level should be reasonably well approximated in the winter without rain since vapor drive is outward and the difference between vapor pressures at 80%RH (no rain) and 90%RH (with rain) at 0^{o}C is about 60Pa which is 8.3% of the vapor pressure difference between the interior and exterior around 500Pa. However, summer levels should be lower with no rain as there would be reduced inward driven moisture.

The diffusion resistance as investigated in this manner should be between 4 and 6, corresponding to a permeance between 1000 and 1600 ng/Pasm^2. For further analysis a value of 5 is being used, which gives a permeance around 1300ng/Pasm^2 that matches the testing by Straube (2002).

Using the measured driving rain data gave best results with a diffusion resistance of 7, corresponding to a permeance of 930ng/Pasm^2.

10.2.3.5 Straw A-Value

Straw will be in the range of 0.001-0.03 kg/m^{2}s$^{1/2}$ based on related testing, and most likely towards the low end of the range.

Increasing the straw A-value increases the amount of moisture that moves into the straw, this results in a lot more moisture accumulation through the winter with very high RH maintained into the spring. Therefore, it was found that a low A-value for the straw is

required: 0.001 kg/m^{2}s$^{1/2}$ was used; 0.003 kg/m^{2}s$^{1/2}$ and above was too high. This is expected as straw will not absorb water with much force, but will allow liquid water to move through readily. Therefore, if liquid water is poured onto the straw it will easily enter, but when the moisture is applied to the straw as saturated plaster, there will be minimal suction of that moisture. This may be one of the difficulties in modeling a straw bale wall. In fact, there may be a need to create an additional layer between the plaster and the straw with a combination of properties to account for the moisture storage from rain events.

Low storage plaster showed more rapid drying in the spring than measured but this can be corrected by using a higher straw suction, around 0.01 kg/m^{2}s$^{1/2}$. Also, absorption into the straw also helps to lengthen short term fluctuations due to rain when using low plaster storage. This indicates a lack of understanding in what occurs at the straw-plaster interface. Is the plaster keeping all the moisture or is it moving into the straw? For low plaster storage it is possible to get a reasonable model with moisture moving into the straw (although summer RH fluctuations are not that well predicted), whereas with high plaster storage, little moisture moves into the straw. Since the RH fluctuations in the summer are still better predicted by the higher plaster storage it will be used in the final model.

It is believed that the interaction at the plaster-straw interface is one of the primary difficulties in modeling the moisture behaviour. This difficulty is increased since the moisture storage of the earth plaster and straw at saturation levels is not known precisely. More detailed studies of these properties should be undertaken to get a better understanding of the moisture movement between the plaster and the straw. This is especially important for modeling as the model assumes a clear division between the layers, whereas the plaster is pressed into the straw creating an integrated zone of the materials.

10.2.3.6 Plaster A-Value

As discussed in Chapter 4 the water uptake coefficients are expected to be 0.075 kg/m^{2}s$^{1/2}$ for earth plaster within a range of 0.04-0.15 kg/m^{2}s$^{1/2}$. A value of 0.09 kg/m^{2}s$^{1/2}$ for the cement lime plaster in a range of 0.04-0.17 kg/m^{2}s$^{1/2}$ for the extremes of pure cement and pure lime plaster.

Increasing the plaster A-value does not increase all moisture levels at the outer sensor as was initially expected. Instead, winter levels are decreased by increasing the A-value while summer levels are increased. In the winter, drying due to vapor diffusion is

minimal through the outer plaster and so increasing the A-value helps to increase the drying capacity of condensation and penetrating rainwater. This increase in drying is greater than the increase in wetting due to higher absorption. In the summer when vapor drying is rapid the increased A-value does not impact the drying as much but provides more rain absorption and thus the overall moisture levels increase.

Using the modified measured rain data and for high plaster storage an A-value of 0.3 $kg/m^2s^{1/2}$ was found to be adequate, while for low storage an A-value around 0.1-0.15 $kg/m^2s^{1/2}$ was adequate. When the calculated rain data was used, the A-value was 0.11 $kg/m^2s^{1/2}$ for the high storage and 0.07 $kg/m^2s^{1/2}$ for the low storage. These values are generally higher than expected.

10.2.4 Primary Factors of Seasonal Trends

10.2.4.1 Winter

Initially, the shape in the measured data was best modeled with the UW calculated driving rain. However, this data made it difficult to match the absolute level of RH in the winter without causing high levels in the spring. Therefore, the modified measured data was used which was able to provide increased winter levels without running into the spring.

The trend identified in the measured data was best modeled using the calculated driving rain values from the UW weather station data. However, it is thought that this data does not give sufficient amount of small wetting events as it is difficult to achieve the moisture levels measured without reducing the water uptake coefficient of the plaster considerably. But, this could also be an indication that the assumed water uptake coefficient is incorrect. After modifying the measured driving rain at the UW weather station to include some obvious rain events in the data which were not recorded in the driving rain data, and removing or reducing some events that did not appear in the wall data or the calculated driving rain, it was found that the winter time levels could be reached with the 0.15 $kg/m^2s^{1/2}$ plaster A-value.

The primary causes of the winter moisture are rain and liquid transport in the exterior plaster. Increased rain and reduced water uptake would increase moisture levels. This is first due to more moisture being available from increased rain, and second to reduced drying potential from the low water uptake value. Thus, more liquid moisture is available to penetrate the plaster but it becomes trapped there and is not able to move back through the plaster to exit the wall. Inward drying is not possible as the exterior temperatures are

considerably colder than the interior and thus the vapor pressure drive is outward even under saturated conditions at the exterior. Therefore, varying the behaviour at the exterior has minimal impact on the inward side of the wall. However, the total vapor drive would be slightly reduced by increased humidity at the exterior.

10.2.4.2 Spring

Spring drying was affected by the total amount of moisture accumulation in the straw in the winter. With increased accumulation there was more moisture that required drying and thus high levels increased into the spring with a rapid drying in late spring. This accumulation is determined by the total rain, plaster A-value and straw A-value, as discussed in the section on winter moisture.

Low winter buildup causes a rapid drying at the beginning of the measured spring drying.

Increasing the straw suction will reduce the drying rate by causing more springtime rain to be absorbed into the straw. This was usually done in conjunction with a lower plaster A-value and the lower winter buildup from using the calculated driving rain. A straw A-value of 0.001-0.005 $kg/m^2s^{1/2}$ was required for almost all runs with the measured rain data.

10.2.4.3 Summer

The level of RH at the outer sensor during the summer depends upon how much rain is absorbed and how readily it can dry. With more rain absorbed and lower permeances of the plaster the average summer RH is increased. However, these do not drastically affect the short term fluctuations due to exterior RH changes.

Fluctuations due to RH changes can be adjusted by the moisture storage of the plaster and the straw, in cooperation with the diffusion resistance factor of both. Adjusting the moisture storage of the plaster gave the greatest effect, while moisture storage of the straw gave a minor effect. Since the realistic range of the plaster permeance is not too great it did not contribute a significant effect in the range of 4-7 diffusion resistance factor for the earth plastered wall.

Summer levels in cement-lime plaster were difficult to model. This may be a result of the potential leak in February, 2008. However, the summer trends are similar, but the levels are much lower. The inner sensor could be matched but only at the expense of excess outward humidities due to increased rain absorption. This does indicate the effect

of the leak, as excess rain absorption is required to cause the inner sensor to reach the levels it does.

10.3 Conclusions

The modeling showed that temperature behaviour can be reasonably predicted. The most important parameter in the thermal model is the absorbed solar radiation, which depends on the solar radiation from the climate data and the solar absorptance of the plaster. The other physical properties of the plasters can be adjusted within the range of tested values discussed in Chapter 4 with minimal effects. Similarly the straw bale thermal conductivity and heat capacity can be adjusted considerably with minimal impact, so long as the thermal diffusivity is in the range of 3-6 $x10^{-7}$ m/s.

Moisture modeling was found to be not nearly as precise as the thermal modeling due to the more varied nature of driving rain and the less precise capability for converting horizontal measured rain to driving rain. It is suggested that driving rain be measured at the wall surface for precise modeling. However, a reasonably accurate model for the clay plaster wall was developed after modifying the measured rain data that was available. A potential leak in the cement-lime plaster wall is the likely cause for the inability to accurately model that wall.

It was found that driving rain has the greatest impact on the moisture performance of the straw bale walls. Without driving rain the moisture levels within both walls are reduced. Most notably, the cement-lime plaster wall without rain shows a year-to-year drying trend, whereas with rain it shows a wetting trend. The earth plastered wall in both cases shows a drying trend and ends the year at a similar condition, with the no rain case only 5%RH lower at the exterior side.

As driving rain had the largest impact on the model it was found that the plaster properties were more crucial than the straw bale properties. The straw bale moisture storage function and permeability as described in Chapter 4 were adequate for the model. However, the water uptake coefficient required adjustment alongside the plaster properties due to its impact on the amount of driving rain absorbed into the straw. This property was the most critical of the straw bale properties due to its effect on the interface with the plaster.

It was found that the interface between the straw and the plaster has a large impact on the wall performance. Modeling gave the best results when the earth plaster had a high storage function so that the amount of rain penetrating the interface was limited.

However, a low moisture storage plaster could model the measured results with an increase to the straw bale water uptake coefficient. These two situations indicate the uncertainty as to how much driving rain is stored in plaster compared to the amount that penetrates the plaster and is stored in the straw bale. It is expected that the straw will not absorb moisture at a high rate from saturated plaster, but that any liquid moisture that penetrates the plaster will easily enter the straw. Due to this uncertainty, testing of the interaction between the straw and the plaster under driving rain conditions is suggested.

11 General Conclusions

There is a growing interest in straw bale construction for its low embodied energy and insulation value. Early questions of its structural behaviour and fire resistance have been generally answered through a variety of research projects. These studies have shown that straw bale construction as a viable alternative to traditional techniques. However, the biggest remaining obstacle to widespread acceptance is the moisture behaviour within the straw bale walls, especially as it concerns mould growth. The uncertainty of this behaviour leads to the hesitation of building officials and insurance providers to freely accept straw bale construction. Therefore, this study investigated the moisture, temperature and mould growth in straw bale walls, through a combination of analysis, dynamic modeling and field studies.

Simple steady state vapour diffusion analysis indicates that a vapour barrier may not be required on the interior side of a cold-climate to control outward vapour diffusion during the winter. Additionally, a low permeance vapor barrier may be detrimental during the summer when temperatures are more favourable to mould growth. Decreasing the vapour permeance of the interior plaster relative to the exterior plaster may be beneficial but requires further investigation. Increasing the vapor permeance of the exterior side plaster is always beneficial in a cold-climate to promote the drying of rain absorbed moisture and to reduce the accumulation of outward driven vapour during the winter.

Two straw bale walls (14"thick x 6' wide x 8' high) were successfully constructed and instrumented throughout for moisture and temperature. Both walls were identical except for the plaster. One wall used a common earth plaster and the other a typical cement-lime plaster. Data was collected and analyzed over more than a year. Failure of the wall in terms of high moisture levels that could lead to mould growth and deterioration of the straw was expected due to the highly exposed exterior condition (no overhangs or eavestroughs) and the high interior relative humidity during the winter (50%RH).

The earth plaster wall performed better than the cement-lime plaster wall; however, it is likely that a leak occurred in the cement-plaster wall, which impairs a direct comparison. The earth plaster wall showed generally lower humidities at the mid and upper locations, especially in the spring and summer when temperatures are more favourable to mould growth. However, neither wall showed consistently low humidities and both experienced relative humidities above the 85%RH throughout the winter on the exterior side.

The location most challenged by high humidities was the exterior side of the wall. This was a combined result of outward winter vapour diffusion and rain absorption. The only exception was the inward sensor of the cement-lime wall, which rose to 80%RH during the summer as a result of inward solar-driven vapour diffusion. The earth plaster wall experienced larger spikes in MC behind the exterior plaster due to rain events, but dried much faster than the cement-lime plaster and therefore showed more favourable conditions during the summer. However, the bottom of the earth plaster wall was more affected by rain splashback and showed higher moisture levels than the cement-lime plaster wall.

The straw bale test walls were also modeled using WUFI® software. It was found that modeling the hygrothermal behaviour of straw bale walls is highly dependent on the driving rain data input. Therefore, not having a driving rain gauge directly on the wall surface reduces the ability to accurately model the moisture performance of the walls. Additionally, the physical properties that were found to have the greatest impact on the model were those affecting the rain absorption, namely the plaster water uptake coefficient and moisture storage function as well as the straw water uptake coefficient. The behaviour of a straw bale wall in absorbing rain has a strong impact on its performance and should be studied in more detail.

Thermal modeling was able to predict the temperatures in the walls well when due care was taken to calculate solar radiation, as the sun had the largest impact on the short term fluctuations of temperature within the walls. Therefore, the most critical properties for developing an accurate thermal model were found to be the solar absorptance of the plaster and the thermal diffusivity of the straw. A parametric study of other variables showed that they did not have a significant impact over reasonable ranges of values.

The test walls would both be considered failures according to the 80%RH upper limit. However, the extent of mould growth found within the walls after two years was not as significant as this limit would suggest, with the exception of the highly decomposed portion of the cement-lime plastered wall, which did not occur at the sensor locations. The mould predictions that included temperature and time to germination appear to give a better prediction of the actual mould growth. However, these methods require further validation before they can be relied upon to accurately predict mould growth in straw bale walls.

Although the general extent of mould growth in both walls did not affect the wall's structure, it is not desirous for health reasons and long term durability and therefore these

walls are considered to have failed. This was the expectation from the beginning due to the high level of rain exposure; however, the level of failure is lower than expected and should eliminate any concern for moisture in a rain sheltered straw bale wall. Further work will aid to determine the minimum required shelter. The portion of highly decomposed straw in the cement-lime plastered wall indicates the sensitivity of the construction to water leaks. Therefore, great care must be taken to eliminate leaks.

References

Adan, O.C.G. (1994) *On the fungal defacement of interior finishes*. PhD Thesis, Eindhoven University of Technology.

Agriculture. (n.d.). Retrieved July 14, 2009, from Wikipedia: http://en.wikipedia.org/wiki/Cereal

Andersen, B.M. and Munch-Andersen, J. (2001). *Halmballer og muslinger som isoleringsmaterialer*, Report 2001-06-21, (electronic copy)

Andersen, B.M., and Nicolajsen, A. (2002). Report 423-8/A. Statens Byggeforskningsinstitut. (Electronic Copy.)

ASHRAE. (2005). *2005 Handbook Fundamentals.* Atlanta: ASHRAE Inc.

Beck, A., Heinemann, U., Reidinger, M., and Fricke, J. (2004). "Thermal Transport in Straw Insulation." *Journal of Thermal Envelope and Building Science*, 27(3), 227-234.

Black, C.D. (2006). *Mould Resistance of Full Scale Wood Frame Wall Assemblies*. Masters Thesis, University of Waterloo.

Brown, W.C., Bomberg, M.T., Ullett, J.M., & Rasmussen, J. (1993). "Measured thermal resistance of frame walls with defects in the installation of mineral fibre insulation." *Journal of Building Physics*, 16(4), 318-339.

Campbell Scientific. (2000). *CR1000 Measurement and Control System – Operator's Manual*. Retrieved September 20, 2007 from Campbell Scientific's website: http://www.campbellsci.ca/Catalogue/CR1000_Man.pdf

CBC. (2008). *Canadian magazine makes history using special paper.* Retrieved July 14, 2009 from http://www.cbc.ca/canada/story/2008/05/21/magazine-wheat.html

Cereal. (n.d.). Retrieved July 14, 2009, from Wikipedia: http://en.wikipedia.org/wiki/Cereal

Cerny, R., Drchalova, J., Kunca, A., Tydlitat, V., and Rovnanikova, P. (2003). "Thermal and hygric properties of lime plasters with pozzolonic admixture for historical buildings."

In Carmeliet, Hens and Vermeir (Eds), *Research in Building Physics* (pp.27-34). Lisse, The Netherlands: Swets & Zeitlinger.

Clarke, J.A. et al. (1999). "A technique for the prediction of the conditions leading to mould growth in buildings." *Building and Environment*, 34, 515-521.

CMHC. (2000). *Research Highlights – Straw Bale House Moisture Research*. Canada Mortgage and Housing Corporation, Ottawa, Canada.

Cochrane, V.W. (1974). "Dormancy in spores of fungi." *Trans. Amer. Micros. Soc*., 93(4), 599-609.

Coggins, C.R. (1980). *Decay of Timber in Buildings: Dry rot, wet rot and other fungi.* East Grinstead, W. Sussex: Rentokil Ltd.

Colbeck, S. C. (1993). "The vapor diffusion coefficient for snow." *Water Resour. Res*., 29(1), 109–115.

Corum, N. (2004). *Building One House: A Handbook for Straw Bale Construction*. Bozeman: Red Feather Development Group.

Dexter, S.T. (1947). "The moisture content of various hays in equilibrium with atmospheres at various relative humidities." *Agron J*, 39, 697–701.

Duggal, A.K. and Muir, W.E. (1981). "Adsorption equilibrium moisture content of wheat straw." *J. Agric. Engng Res*, 26(3), 15-320.

Dyrbol, S., Svendsen, S, & Elmroth, A. (2002). "Experimental Investigation of the Effect of Natural Convection on Heat Transfer in Mineral Wool." *Journal of Thermal Envelope and Building Science*, 26(2), 153-164.

Elizabeth, L., & Adams, C. (2000). *Alternative Construction: Contemporary Natural Building Methods*. New York: John Wiley & Sons.

Erbs, Klein, and Duffie. (1982). *Estimation of the diffuse radiation fraction for hourly, daily and monthly-average global radiation.* Solar Energy, 28(4), 293-302.

Finch, G. (2007). *The Performance of Rainscreen Walls in Coastal British Columbia.* MASc Thesis, University of Waterloo.

Findlay, W.P.K. (1950). "The resistance of wood-rotting fungi to desiccation." *Forestry*, 23(2), 112-115.

Fraunhofer Institut Bauphysik. (2005). *WUFI® PRO Ver. 4.0 Release 4.0.1.208.DB.23.13* [computer software]. Germany: Fraunhofer IBP.

Gagne, L. (1997). *Pilot study of moisture control in stuccoed straw bale walls.* Report for Canada Mortgage and Housing Corporation, Ottawa, Canada.

Galbraith, G.H., Guo, J.S., & McLean, R.C. (2000). "The effect of temperature on the moisture permeability of building materials." *Building Research and Information*, 28(4), 245-259.

Gonzalez, H.J. (2002). "Energy use in straw bale houses." *CMHC Technical Series 02-115.* Ottawa, ON: CMHC.

Goodhew, S. and Griffiths, R. (2004). "Analysis of thermal-probe measurements using an iterative method to give sample conductivity and diffusivity data." *Applied Energy*, 77(2), 205-223.

Goodhew, S., Griffiths, R., and Woolley, T. (2004). "An investigation of the moisture content in the walls of a straw-bale building." *Building and Environment*, 39, 1443-1451.

Goodhew, S and Griffiths, R. (2005). "Sustainable earth walls to meet the building regulations." *Energy and Buildings*, 37, 451–459.

Gottlieb, D. (1978). *The Germination of Fungus Spores*. Shildon, England: Meadowfield Press Ltd.

Gow, N.A.R, and Gadd, G.M. (1995). *The Growing Fungus*. New York, NY: Chapman & Hall.

Grant et al. (1989). "The moisture requirements of moulds isolated from domestic dwellings." *Int'l Biodeterioration*, 25, 259-284.

Hammett, J., & Hammett, K. (1998). *The Strawbale Search*. Retrieved February 18, 2008, from The Last Straw: A History of the Strawbale Resurgence Web site: http://www.thelaststraw.org/history/roots.html

Hansen, K. K., Rode, C., and Hansen, E. (2001). "Experimental investigation of the hygrothermal performance of insulation materials." *Proceedings for Performance of Exterior Envelopes of Whole Buildings VIII: Integration of Building Envelopes*, December 2-7, Clearwater Beach, Florida

Harmathy, T.Z. (1967). *Moisture sorption of building materials.* National Research Council, Technical Paper 242. Ottawa, ON: NRC.

Hedlin, C.P. (1967). "Sorption isotherms of five types of grain straw at 70^{o}F." *Canadian Agricultural Engineering*: 9(1), 37.

Helwig, J., Jannasch, R., Samson, R., DeMaio, A., & Caumartin, D. (2002). *Agricultural Biomass Residue Inventories and Conversion Systems for Energy Production in Eastern Canada.* Retrieved July 14, 2009 from R.E.A.P. Canada On-Line Library Web site: http://www.reap-canada.com/library.htm

Hens, H. (2000). "Minimizing fungal defacement." *ASHRAE Journal*, 42(10), 30-38.

Hukka A. and Viitanen H.A. (1999). "A mathematical model of mould growth on wooden material." *Wood Science and Technology*, 33, 475-485.

James, M. (1999). "Refining straw bale R-values." *Home Energy Magazine Online*. Retrieved July 12, 2008 from Home Energy Magazine's website: http://www.homeenergy.org/archive/hem.dis.anl.gov/eehem/99/990306.html

Johansson, C.H. and Persson, G. (1958). *Moisture absorption curves for building materials.* National Research Council, Technical Translation 747. Ottawa, ON: NRC.

Jolly, R. (2000). *Strawbale moisture monitoring report*. Report for Canada Mortgage and Housing Corporation, Ottawa, Canada.

Karoglou, M., Moropoulou, A., Maroulis, Z. B. and Krokida, M. K. (2005). "Water sorption isotherms of some building materials." *Drying Technology*, 23(1), 289-303.

Kehrer, M; Kunzel, H.; and Sedlbauer, K. (2003) "Ecological insulation materials – does sorption moisture affect their insulation performance?" *Journal of Thermal Envelope and Building Science*, 26(3), 207-212.

King, B. (2003). *Load Bearing Straw Bale Construction: A summary of worldwide testing and experience.* Retrieved July 12, 2008 from the Ecological Building Network website: http://www.ecobuildnetwork.org/pdfs/Load-Bearing_SB_Const.pdf

King, B. (2006). *Design of Straw Bale Buildings: The State of the Art*. San Rafael: Green Building Press.

Künzel, H.M. (1995). *Simultaneous Heat and Moisture Transport in Building Components One- and two-dimensional calculation using simple parameters.* Stuttgart: IRB Verlag.

Kymäläinen, H. and Pasila, A. (2000). "Equilibrium moisture content of flax/linseed and fibre hemp straw fractions." *Agric and Food Sci in Finland*, 9, 259-268.

Lacinski, P., & Bergeron, M. (2000). *Serious Straw Bale: A Home Construction Guide for All Climates*. White River Junction: Chelsea Green Publishing Company.

Lackey, J.C., Marchand, R.G., and Kumaran, M.K. (1997). "A logical extension of the ASTM Standard E96 to determine the dependence of water vapour transmission on relative humidity." In R.S. Graves and R.R. Zarr (Eds), *Insulation materials: Testing and Applications: Third Volume, ASTM STP 1320* (pp. 456-472). West Conshohocken, PA: ASTM.

Lamond, W.J., and Graham, R. (1993). "The relationship between the equilibrium moisture content of grass mixtures and the temperature and humidity of the air." *J. Agric. Engng Res*, 56, 327-335.

Larmour, Judy. (1992). *Making Hay While the Sun Shone: Haying in Alberta Before 1955.* Retrieved February 18, 2008, from Heritage Community Foundation Presents Alberta Online Encyclopedia Web site: http://www.abheritage.ca/abresources/history/history_technology_soil_ag_haying_horse_bail.html

Magwood, C., Mack, P., & Therrien, T. (2005). *More Straw Bale Building: How to Plan, Design and Build with Straw*. Gabriola Island: New Society Publishers.

Manohar, K., Rmroopsingh, J., and Yarbrough, D. (2002). "Use of sugarcane fiber as building insulation." In Desjarlais, A.O., and Zarr, R.R. (Eds) *Insulation Materials: Testing and Applications: 4th Volume, ASTM STP 1426* (pp. 299-313), West Conshohocken, PA: ASTM International.

Matiasovsky, P; Takacsova, Z. (2006). "Sorption isotherms of interior finish materials." In *Proceedings of 4th Slovak/Czech symposium. Theoretical and experimental research in structural engineering* (pp. 191-197), Bratislavia, SV: ICA SAS. Retrieved July 12, 2008 from Katholieke Universiteit Leuven's website: http://www.kuleuven.ac.be/bwf/projects/annex41/protected/data/SAS%20Oct%202006%20BGinf%20A41-T2-Sl-06-1.pdf

Moon, H.J. and Augenbroe, G. (2003). *Evaluation of hygrothermal models for mold growth avoidance prediction.* Eindhoven, Netherlands: Eighth International IBPSA Conference.

Moon, H.J. and Augenbroe, G.L.M. (2004). "Towards a practical mould growth risk indicator." *Building Ser Eng Res Technol*, 25(4), 317-326.

Mordant, N. (2009, June 10). "Shell Canada gas station sells wheat-straw biofuel." *Reuters*. Retrieved from http://www.reuters.com

Morris, P.I. and Winandy, J.E. (2002). *Limiting conditions for decay in wood systems*. 33rd Annual Meeting, The Int'l Research Group on Wood Preservation, Section 1, 1-11.

Nielsen, K.F. (2002). *Mould Growth on Building Materials.* PhD Thesis, By og Byg, Statens Byggeforskningsinstitut.

Nilsson, D., Svennerstedt, B., and Wretfors, C. (2005). "Adsorption equilibrium moisture contents of flax straw, hemp stalks and reed canary grass." *Biosystems Engineering*, 91(1), 35–43.

Nikolaisen, L. (Ed.) (1998). *Straw for Energy Production, 2nd Ed*. Retrieved July 14, 2009 from The Centre for Biomass Technology Web site: http://www.videncenter.dk/uk/index.htm

O'Sullivan, C.T. (1990*).* "Newton's law of cooling – A critical assessment." *American Journal of Physics*. 58(10), 956-960.

Rissanen, R and Viljanen, M. (1998). *Bio-fibre based building materials; properties and utilisation - Report 77.* Helsinki University of Technology, Laboratory of Structural Engineering and Building Physics. http://www.tkk.fi/Yksikot/Talo/abstract/abs77.htm

Rowan, N.J, et al. (1999). "Prediction of toxigenic fungal growth in buildings by using a novel modeling system." *Applied and Environmental Microbiology*, 65(11), 4814-4821.

Sain, P., and Broadbent, F.E. (1975). "Moisture absorption, mold growth, and decomposition of rice straw at different relative humidities." *Agron J,* 67, 759–762.

Sedlbauer, K., Krus, M. and Breuer, K. (2001). *A new model for mould prediction and its application on a test roof.* Cracow, Poland: 2nd Int'l Scientific Conference on "The Current Problems of Building-Physics in the Rural Building",

Sedlbauer, K. (2002) "Prediction of mould growth by hygrothermal calculation." *Journal of Thermal Env. & Bldg. Sci*., 25(4), 321-336.

Silberstein, A. (1990). "Natural convection in light fibrous insulating materials with permeable interfaces: onset criteria and its effect on the thermal performances of the product." *Journal of Building Physics*, 14(1), 22-42.

Smith, S.L., and Hill, S.T. (1982). "Influence of temperature and water activity on germination and growth of aspergillus restrictus and aspergillus versicolor." *Transactions of the British Mycological Society*, 79(3), 558-560.

Snow, D., Crichton, M.H.G., and Wright, N.C. (1944) "Mould deteriation of feeding-stuffs in relation to humidity of storage: Part I. The growth of moulds at low humidities." *The Annals of Applied Biology*, 31(2), 102-110.

Snow, D., Crichton, M.H.G., Wright, N.C. (1944). "Mould deteriation of feeding-stuffs in relation to humidity of storage: Part II. The water uptake of feeding stuffs at different humidities." *The Annals of Applied Biology*, 31(2), 111-116.

Snow, D. (1949). "Germination of mould spores at controlled humidities." *Applied Biology*, 36(1), 1-13.

Southam Business Communications, Inc. (1997). "Manitoba gains particle board mill (Elie plant to make panels from straw)." *Pulp & Paper Canada*, 98(2), 7.

Steen, A.W., Steen, B., & Bainbridge, D. (1994). *The Straw Bale House*. White River Junction: Chelsea Green Publishing Company.

Stone, N. (2003). *Thermal Performance of Straw Bale Walls*. Retrieved November 18, 2007 from Ecological Building Network website: www.ecobuildnetwork.org

Straube, J.F. (2000). *Moisture properties of plaster and stucco for straw bale buildings.* CMHC, Ottawa.

Straube, J.F. (2002). *Moisture properties of plaster and stucco for straw bale buildings.* Retrieved November 1, 2007, from the Ecological Building Network website: http://www.ecobuildnetwork.org/pdfs/Straube_Moisture_Tests.pdf

Straube, J.F., Onysko, D, & Schumacher, C. (2002). "Methodology and design of field experiments for monitoring the hygrothermal performance of wood frame enclosures." *Journal of Thermal Env. & Bldg Sci*., 26(2), 123-151.

Straube, J.F., & Schumacher, C. (2003a). "Hygrothermal Enclosure Models: Comparison with Field Data." *Proceedings of 2nd Int'l Conference on Building Physics: Research in Building Physics*, Sept 14-18 2003, Leuven, Belgium.

Straube, J.F., and Schumacher, C. (2003b) *Monitoring the hygrothermal performance of straw bale walls.* Retrieved July 12, 2008 from the Ecological Building Network's website: http://www.ecobuildnetwork.org/pdfs/Winery_Monitoring.pdf

Straube, J.F., & Burnett, E.F.P. (2005). *Building Science for Building Enclosures*. Westford: Building Science Press, Inc.

Summers, M.D., Blunk, S.L., and Jenkins, B.M. (2002). "Moisture and thermal conditions for degradation of rice straw." *Chicago, Illinois: ASAE Annual International Meeting/CIGR XVth World Congress.*

Theis, B. (2006). "Fire." In B. King (Ed.), *Design of Straw Bale Buildings: The State of the Art* (pp.173-183). San Rafael: Green Building Press.

Tierrafino. (2008). *Clay Finishing Plaster: Technical Data Sheet.* Retrieved July 12, 2008 from Tierrafino's website: http://www.tierrafino.com/pdf/Tierrafino%20Finish%20TDS.pdf.

Thornton, J. (2004). *Initial material characterization of straw light clay.* CMHC, Ottawa.

Ueno, K. and Straube, J. (2008). *Laboratory Calibration and Field Results of Wood Resistance Humidity Sensors*. Proceedings of Building Enclosure Science & Technology Conference, Minneapolis.

Valovirta, I., and Vinha, J. (2002). "Hemp as insulation material in wooden houses." In Gustavsen, A., and Thue, J.V. (Eds), *Proceedings of the 6th Symposium on Building Physics in the Nordic Countries* (pp. 469-475). Trondheim, Norway: Norwegian University of Science and Technology.

Van Straaten, R., Jeong, J., and Straube, J. (2002) *Development of Design Strategies for Rainscreen and Sheathing Membrane Performance in Wood Framed Walls – Construction and Instrumentation Report*. Building Engineering Group, University of Waterloo.

Waite, R. (1949). "The relation between moisture content and moulding in cured hay." *Applied Biology*, 36(4), 496-503.

Wallentén, P. (2001). "Convective heat transfer coefficients in a full-scale room with and without furniture." *Building and Environment*, 36(6), 743-751.

Washburn, E.W. (1921). "The dynamics of capillary flow." *The Physical Review,* 17(3), 273-283.

West, L.A. (1967). *Agriculture: Hand Tools to Mechanization*. London: H.M.S.O.

Wihan, J. (2007). *Humidity in straw bale walls and its effect on the decomposition of straw.* Master's Thesis, University of East London School of Computing and Technology. Retrieved July 12, 2008, from Jakub Wihan's website: http://www.jakubwihan.com/pdf/thesis.pdf

Wilson, A. (1995). *Straw: The Next Great Building Material?* Environmental Building News, 4(3). From Building Green Web site: http://www.buildinggreen.com/auth/article.cfm/1995/5/1/Straw-The-Next-Great-Building-Material

Womersley's Ltd. *Clay One-Coat Plaster: Technical Information Sheet.* Retrieved July 12, 2008 from Womersley's website: www.womersleys.co.uk/pdfs/onecoatclayplaster.pdf Last accessed December 29, 2009.

Zabel, R.A. and Morrell, J.J. (1992) *Wood Microbiology: Decay and Its Prevention.* Toronto: Academic Press Inc.

Appendix A - Solar Radiation Conversion

It is necessary to know the incident solar radiation (short wave radiation) on the study wall to account for solar heating. In lieu of directly measuring the radiation on the wall, it is possible to convert radiation measured at a different orientation.

Typical weather stations take measurements of total short wave radiation incident on a horizontal surface. This is the case at the BEGHut, with measurements taken every 5 minutes and the hourly average recorded. It is also measured at the UW Weather Station, along with ground reflected short wave radiation, and recorded every 15 minutes.

In order to convert the measured data it is necessary to know the fraction of the total that is beam radiation, which is dependent upon orientation, and diffuse radiation, which is assumed isotropic and thus independent of orientation. Correlations have been developed by Erbs et al. (1982) to relate the diffuse fraction of the total radiation to the clearness index. This index is a ratio of the measured total horizontal radiation to the computed extraterrestrial radiation at the same orientation. This radiation is found from the following equation.

$$G_{OH} = G_{sc} e_n \cos(\theta_z) \qquad A.1$$

where :

G_{OH} = extraterrestrial radiation on horizontal

G_{sc} = solar constant = 1367 W/m^2

e_n = eccentricty factor $= 1 + 0.033 \cos\left(\frac{2\pi n}{365}\right)$

n = day of the year

θ_z = solar zenith angle

The solar zenith angle can be computed from knowledge of the date and time. However, it is first necessary to compute the solar declination and hour angle. Solar declination is found from the day of the year (n) through the following equation:

$$\delta = 0.4093 \sin\left(2\pi \frac{284 + n}{365}\right) \quad [rad] \qquad A.2$$

Or more precisely,

$$\delta = 0.006918 - 0.399912\cos\gamma + 0.070257\sin\gamma - 0.006758\cos 2\gamma + 0.00907\sin 2\gamma - 0.002697\cos 3\gamma + 0.00148\sin 3\gamma \quad [rad] \qquad A.3$$

where:

$$\gamma = 2\pi\left(\frac{n-1}{365}\right) \qquad A.4$$

Solar noon for a given location is defined as the time that the sun is at its highest location in the sky and is due south. Since collected data is measured in local standard time, it is necessary to convert it to solar time by the following equation.

$$LST = ST + 4(L_{st} - L_{loc}) + EOT \qquad A.5$$

where :

LST = local solar time

ST = standard time

L_{st} = standard longitude of time zone (deg)

L_{loc} = local longitude (deg)

EOT = equation of time (min)

$$= 229.2(0.000074 + 0.001868\cos B - 0.032077\sin B - 0.014615\cos 2B - 0.04089\sin 2B)$$

$$B = 2\pi\left(\frac{(n-1)}{365}\right)$$

Note that the time added to standard time is in minutes and there may be a correction for daylight savings time in the summer. The calculated solar time can then be converted to a solar hour angle (ω). This is defined as 0^o at solar noon, when the sun is due south, with negative hour angles to the east of south (morning) and positive angles to the west of south (afternoon). A total of 2π radians is passed in 24 hours, which defines the conversion. It is formulated as follows:

$$\omega = \frac{\pi}{12}(LST - 12) \qquad A.6$$

where :

ω = solar hour angle $[rad]$

LST = local solar time $[hr]$

Finally, solar zenith (θ_z) can be calculated from latitude (φ), declination (δ), and hour angle (ω) by the following equation.

$$\cos\theta_z = \cos\phi\cos\delta\cos\omega + \sin\phi\sin\delta \qquad A.7$$

In addition the solar azimuth (γ_s) is found from

$$\cos\gamma_s = \frac{\cos\theta_z \sin\phi - \sin\delta}{\sin\theta_z \cos\phi} \qquad A.8$$

With knowledge of the solar zenith the clearness index can be computed. G_{OH} can be computed as shown earlier and the ratio of G_{tH}/G_{oH} is defined as the clearness index and is given the notation of k_t' for instantaneous, k_t for hourly, K_T for daily, and $\overline{K}_T$ for monthly-averaged daily. Erbs et al. (1982) developed a correlation between the clearness index and the diffuse fraction (k', k, K, and $\overline{K}$).

For hourly data the correlation is

$$\begin{aligned}
&\text{For } k_t \le 0.22 \\
&\quad k = 1 - 0.09k_t \\
&\text{For } 0.22 < k_t < 0.8 \\
&\quad k = 0.9511 - 0.1604k_t + 4.388k_t^2 - 16.638k_t^3 + 12.336k_t^4 \\
&\text{For } k_t \ge 0.88 \\
&\quad k = 0.165
\end{aligned} \qquad A.9$$

This correlation is the weakest point in converting the solar radiation. It is based on numerous measurements and is a good average correlation but the nature of weather over a single hour varies dramatically and thus cannot be simplified to a single correlation such as this while maintaining precision. Therefore, the computed diffuse fraction is only a good estimate as opposed to a true correlation.

From the previously computed angles and diffuse fraction it is possible to convert the total radiation on a surface of arbitrary orientation defined by the surface azimuth (γ) and surface tilt (β). Surface azimuth is the angle from south at which the surface faces, with positive angles to the west, e.g due west is 90°. Surface tilt is the angle the surface is tilted from the horizontal, thus flat is 0° and vertical is 90°. In order to convert the beam radiation it is necessary to know the angle of incidence of beam radiation on the surface. This is found by the following:

$$\cos\theta = \cos\theta_z \cos\beta + \sin\theta_{zH} \sin\beta \sin(\gamma_s - \gamma) \qquad A.10$$

The beam radiation can then be converted based on the ratio of the angle of incidence to the surface to the solar zenith.

$$I_{bT} = (1-k) I_{tH} \frac{\cos\theta}{\cos\theta_z} \qquad A.11$$

Hours during which the sun rises or sets will have a solar azimuth near 90°. This results in a near zero denominator when calculating $\cos\theta_z$. Errors will arise and will be indicated by spikes in the beam radiation on the surface. In order to minimize these errors, hours with less than 3 minutes of sunshine were ignored and a filter was also applied to the converted data to eliminate any early morning spikes that were not eliminated by the first method. Early morning conversion is important for the east walls since the greatest solar radiation occurs at this time for these walls. However, the difficulty in converting at these angles is apparent and shorter time periods for measurements may result in increased accuracy.

The diffuse component does not depend on the surface azimuth but rather the tilt of the surface, which determines how much sky is 'visible' to the surface. This results in the following equation:

$$I_{dT} = k I_{tH} \left(\frac{1+\cos\beta}{2} \right) \qquad A.12$$

Ground reflected radiation often uses the following simple equation, using the ground reflectance (ρ), and the ground view factor of (1-cosβ)/2:

$$I_{gT} = \rho I_{tH}\left(\frac{1-\cos\beta}{2}\right) \qquad A.13$$

This assumes that there is no shadow in front of the surface by using I_{tH}. However, for the test walls a shadow from the building develops as the sun moves past south and it elongates into the evening. This would affect the ground reflected radiation on the wall. Therefore, a shadow view factor was developed to account for how much ground reflected radiation is only reflecting diffuse radiation. The view factor is found by:

$$ShadowViewFactor = \frac{1}{2}\left(1 + A + \sqrt{1 + A^2}\right) \qquad A.14$$

where :

$$A = -1.25\tan\theta_z \cos(\gamma_s - \gamma) \qquad A.15$$

Therefore, the ground reflected radiation is computed by from two components: the radiation reflected from the shadow, which only sees diffuse radiation, and the radiation reflected from the rest of the ground which sees the total horizontal radiation. This is written

$$I_{gT} = \rho\left(I_{tH}\left(GroundViewFactor - ShadowViewFactor\right) + kI_{tH}\left(ShadowViewFactor\right)\right) \qquad A.16$$

The ground reflectance used in the previous equation was determined from the ratio of ground reflected radiation to total horizontal radiation from UW Weather Station data. Three reflectances were used (0.2, 0.5 and 0.8) to represent bare ground, mixed snow, and fresh snow. In addition at low solar zenith angles the ground reflectance increases, a condition that east walls experience every morning. Therefore, the ground reflectance was increased to 0.3, 0.6, and 0.9 for solar zeniths greater than 65^o. This method is a simple attempt to account for this behaviour and indicates another source of error in converting the solar radiation.

Total radiation on the surface (I_{tT}) is found by summing the beam, diffuse and ground reflected radiation.

$$I_{tT} = I_{bT} + I_{dT} + I_{gT} \qquad A.17$$

Appendix B - Driving Rain Calculations

Driving rain is calculated from the rate of rainfall, wind speed and wind direction. Rainfall intensity indicates the size of the rain droplets. There is a distribution of droplet size, but an average size (mm) can be found from the following equation with horizontal rainfall (r_h in mm/m^2/h),:

$$\phi = 1.1042 r_h^{\,0.232} \qquad B.1$$

Terminal velocity (V_{term} in m/s) of the rain droplet is found by

$$V_{term} = -0.166033 + 4.91844\phi - 0.888016\phi^2 + 0.054888\phi^3 \le 9.2 \qquad B.2$$

This is used to determine the DRF (driving rain factor)

$$DRF = \frac{1}{V_{term}} \qquad B.3$$

Where V_{term} = terminal velocity in m/s.

Then the amount of driving rain (r_v in mm) can be calculated from the horizontal rain (r_h in mm) using the DRF (s/m), the wind velocity (V_{wind} in m/s) and angle of the wind from the normal to the wall (θ).

$$r_v = DRF \cdot V_{wind} \cdot \cos\theta \cdot r_h \qquad B.4$$